Tide-Induced Currents in Harbors of Arbitrary Shape

by

Wen-Li Chiang

and

Jiin-Jen Lee

USCSG-TR-01-81

SEA GRANT

TECHNICAL REPORT SERIES

Institute for Marine and Coastal Studies
University of Southern California
Los Angeles, California 90007

The **Institute for Marine and Coastal Studies** was founded by the University of Southern California in 1975 to be the institutional framework for its marine programs, many of which had been in operation since the early 1900s. The Institute promotes basic and applied research as well as training in marine studies; sponsors workshops, conferences, and extension courses; and produces reports and publications based on Institute-sponsored research. The work of the institute takes place throughout the southern California region—at USC's University Park campus, on several research vessels, at the research facilities located at the Port of Los Angeles, and at the Catalina Marine Science Center on Santa Catalina Island.

For additional copies of this paper, or for more information about the Institute for Marine and Coastal Studies, write to:

The Institute for Marine and Coastal Studies
University of Southern California
Los Angeles, California 90007
Telephone: (213) 743-6840

Tide-Induced Currents in Harbors of Arbitrary Shape

by

Wen-Li Chiang

and

Jiin-Jen Lee

USCSG-TR-01-81

This work is the result of research sponsored by the NOAA Office of Sea Grant, Department of Commerce, under Grant No. 04-8M01-186. The U.S. government is authorized to produce and distribute reprints for governmental purposes, notwithstanding any copyright notation that may appear hereon.

Published by:

Sea Grant Institutional Program
Institute for Marine and Coastal Studies
University of Southern California
University Park
Los Angeles, CA 90007

ACKNOWLEDGEMENTS

This report is a minor modification of a Ph.D. thesis by Wen-Li Chiang, submitted to the Graduate School of the University of Southern California in November 1979. The research is made under the supervision of Jiin-Jen Lee, Associate Professor of Civil Engineering, University of Southern California. This research is supported by NOAA Sea Grant, grant No. 04-8M01-186.

The writers appreciate the helpful comments made by Drs. L. C. Wellford and B. A. Troesch. Thanks are also due to Dr. H. L. Wong for help provided on computer plotting.

TABLE OF CONTENTS

LIST OF TABLES

LIST OF FIGURES

CHAPTER 1

INTRODUCTION

1.1 Background

With the increase in the perception of the importance of the natural environment, the maintenance of water quality has become as important as safety considerations in harbor construction and modifications. The water quality in a harbor depends strongly on its circulation patterns. As a result, it is of primary importance to find an efficient method to study and predict the harbor circulation.

Both field measurements (Robinson & Porath 1974) and physical experiments (McAnally 1975) have revealed that there exists a large scale gyre inside outer Los Angeles Harbor. This gyre acts as an natural oxidation pond to increase mixing and reaeration rates. The numerical model used by Raney (1976) was not able to reproduce this gyre.

The presence of tidal forces is the major cause of harbor circulation. The goal of the present study is to find an efficient way of predicting tide-induced currents in harbors of arbitrary shape and apply this general technique to various configurations (present and future) of

Los Angeles-Long Beach Harbor. In order to achieve this goal a numerical model for the harbor circulation problem is proposed. The numerical method developed in this study is capable of reproducing the gyre structure in the harbor.

1.2 Objectives

The objectives of this study were:

1. To develop an efficient numerical model for simulating tide-induced currents in a harbor of arbitrary shape;
2. To demonstrate the use of the model by simulating the circulations in Los Angeles-Long Beach Harbor;
3. To verify the proposed model by comparing the results of the numerical circulation with the results obtained by U.S. Army Waterways Experiment Station using a hydraulic model test;
4. To predict the extent of changes in the circulation pattern when the harbor geometry is modified, through constructions of moles, fills, or piers in the harbor;
5. To test the sensitivity of the model due to changes of various parameters.

1.3 Scope of Study

This research studies the tide-induced currents in a harbor of arbitrary shape. The principles and method used in the present study are applicable to most two-dimensional shallow-water problems. The thermodynamic effects have been neglected. The water is assumed to be homogeneous and incompressible. The pressure distribution is assumed to be hydrostatic. The velocities studied are vertically averaged ones. Modeled fluid motions include the planar flow and the fluctuation of the water surface. Effects of nonlinear advection, bottom friction, eddy viscosity, and Coriolis force were considered. Effects of molecular viscosity were included in the eddy viscosity. Wind stress was included in the model, but the tests were performed with a still-wind condition, in order to better understand the circulation under the effect of tidal motion. Surface inflows were excluded from the model. Water-land interfaces were modeled as fixed, vertical, solid boundaries. Breakwaters were assumed to be impervious.

The numerical model uses an implicit finite difference method in conjunction with an alternating-direction-iteration technique and a space-staggered mesh. Central-difference in both the time and the spatial domains were used to a large extent with only a few exceptions.

In summary, the research work involves the development, testing, and verification of a numerical model for the study of the tide-induced currents in Los Angeles-

Long Beach Harbor.

1.4 Outline of Report

In Chapter 2, a literature review is provided. The literature reviewed includes certain studies of the circulation in Los Angeles-Long Beach Harbor, applicable numerical modeling techniques, coefficients of roughness, wind stress, eddy viscosity, and other miscellaneous topics.

In Chapter 3 the theoretical model and the numerical method, for solving the finite difference equations are described. The derivation of the finite difference equations is included.

In Chapter 4, a description of the geometrical study area is presented. The source, evaluation, and selection of various input data are discussed.

In Chapter 5, the results of numerical simulations are presented. Also, in this chapter, an analysis and discussion of the results is included.

In Chapter 6, overall conclusions and recommendations for future research are presented.

The detailed derivations of the partial differential equations for shallow water flows are arranged in Appendix A. Computer programs used in this study are listed in Appendix B. A sample input to run the basic test in the present study is also included.

CHAPTER 2

PREVIOUS STUDIES

2.1 Existence of Gyre Structure

Current speeds in the Los Angeles Harbor have been measured by Soule & Oguri (1972) and Robinson & Porath (1974). A large gyre was found to exist in the harbor. This large gyre serves as a natural oxidation pond which supplies dissolved oxygen to satisfy the heavy biological and chemical oxygen demand caused by the Terminal Island effluents and the dumping of fish cannery wastes into outer Los Angeles Harbor (Soule & Oguri 1976). Robinson & Porath (1974) proposed that the configuration of Los Angeles Harbor was the main factor in producing the large gyre.

During 1973-1975, a hydraulic model of Los Angeles and Long Beach Harbors was built at the U.S. Army Engineer Waterways Experiment Station at Vicksburg, Mississippi. This hydraulic model was designed to allow the observation of the tide-induced currents in the harbor (McAnally 1975). The results of the tests demonstrated the existence of the large-scale gyre. At the same experiment station, the overall circulation pattern was studied using a two-dimensional, depth-averaged, numerical model (Raney 1976). The gyre-strength reproduced by this numerical model was very small compared to that found in the hydraulic experiment. The numerical simulation required approximately 90-minute of CDC-7600 computer time to define the circulation in a diurnal tidal cycle. A more efficient numerical model, which can at the same time produce more satisfactory results, is clearly needed.

2.2 Modeling Techniques

The contents of this section are limited to the discussion of the existing literature which is related to the numerical simulation of nonlinear, shallow-water flows.

The differential equations describing the dynamics of water movement can not be solved analytically for field problems, unless the field conditions are over simplified through the use of various assumptions. Either a physical model or a numerical model must be used to find the approximate solution. Physical models are usually associated with scaling problems, and are not easy to adapt to the modification of field geometry. Numerical models are usually more flexible than physical models.

So far, most of the numerical models for tidal behavior have used finite difference approximations. Models using the finite element technique are developing at a fast pace. Grotkop (1973) calculated the oscillation of the

North Sea due to the semi-diurnal tide. This analysis employed a finite element Galerkin technique in both space and time. This method has been found to be quite time-consuming (Nihoul 1976). Implicit finite element schemes for nonlinear models have been applied by Wang & Connor (1975) and by Taylor & Davis (1975). Reichard & Celikkol (1978) adapted the model of Wang & Connor (1975) to study the behavior of the Great Bay Estuary, New Hampshire. The main advantage of the finite element technique over the finite difference technique is the ability to describe bathymetry and lateral topography more accurately. Yet the technique is still inefficient for transient problems (Pinder & Gray 1977). For a steady state problem, the efficiency of the finite element technique is comparable to the finite difference technique. Hence, some investigators have used the Fourier transform method to transform the transient equations into time-independent forms and then apply the finite element technique.

The finite difference techniques can be classified in two categories: (1) direct methods and (2) characteristic methods (Amein & Fang 1969). Both of these categories are further classified into explicit and implicit methods. Each method has many variations depending on exactly how the partial differential equations are transformed into the finite difference analogues. Explicit direct and implicit direct methods are most common ones to be used in tidal simulations. For the sake of convenience, they are referred to as explicit and implicit methods, respectively, in this report.

A characteristic method is suitable in tracing the disturbance of waves or the movement of fluid constituents. It requires some form of intermediate transformation when the solutions are required at fixed locations.

The explicit method has been used quite often for shallow water computations (e.g., Fischer 1965; Gates 1966; Reid & Bodine 1968; Matthews & Mungall 1972). Heaps (1969) gave a review of various versions of the explicit method. The computations involved in this method are straightforward in that the unknown at every grid point is solved explicitly in terms of known data. The solution of a system of simultaneous equations is not required. However, the time step in this method is limited by the Courant-Friedrichs-Lewy stability criterion. No combination of signals from one grid point may travel over another grid point during a time step (Crowley 1970). For a linearized, two-dimensional, invicid flow, the stability criterion is

$$\Delta t \leqslant \Delta s/(2gH)^{1/2} \tag{2.1}$$

where Δt is the allowable time step, Δs is the minimum grid-spacing, g is the gravitational acceleration, and H is the maximum water depth. The ratio $(\Delta t)(2gH)^{1/2}/(\Delta s)$ is termed the Courant number.

By using an implicit method, unknowns in the finite difference equations are expressed in terms of other unknown values. Together with boundary conditions, a set of simultaneous algebraic equations is solved to evaluate those related unknowns at one time. The time step is limited not by the stringent Courant stability criterion, but by accuracy considerations. An implicit method requires more computer storage than an explicit method. The computation time, per time step, is also longer for the implicit method, if the same time step is used in the two methods. However, the implicit method allows a larger time step to be used in the computations. Consequently, the total computation time can often be reduced by using an implicit method with a large time step. In this case, the phase error associated with the use of a large time step should be taken into account (Leendertse 1967).

According to the experience obtained from the present study and from other investigators (e.g., DiPrima & Rogers 1969; Weare 1976), the implicit method, when applied to a nonlinear system, is not, in general, free of stability problems.

Whether to choose an explicit method or an implicit method depends on the nature of the problem, on the availability of numerical methods or computer program, and possibly on the limits of computer core and time.

Numerical models simulating three-dimensional unsteady flows in estuaries have been developed (e.g., Leendertse, Alexander & Liu 1973; Forristall 1974; Heaps 1976; Cooper, Nelson & Pearce 1978). They can be called quasi-three-dimensional models because they are actually layered two-dimensional models. The cost of simulations with a three-dimensional model is very high. Two-dimensional models are more practical tools whenever the flow in the third dimension can be neglected. Sometimes, a three-dimensional model yields much more accurate result. For example, a three-dimensional model is preferable when the vertical movement and the stratification of water flow are important. This may be due to the existence of wind stresses, salinity gradient, or temperature gradient. Also it may be due to large amount of influent fresh water into a saline water body. The requirement of such accurate results for the third dimensional flow arises usually in water quality problems. To calculate the tide-induced currents in Los angeles-Long Beach Harbor, a two-dimensional model is sufficient because wind stresses are not considered in the model, surface inflow can be neglected, and the water body can be assumed homogeneous in the study area.

A two-dimensional model can be either vertically integrated or transversely integrated. A vertically integrated model calculates water movements in x- and y-directions. The currents in ocean or coastal areas are usually calculated through this kind of model. A vertically two-dimensional flow model calculates the flows in x- and z-directions. It can be applied to the calculation of flows in a long, simple estuary. The velocities in both x- and y-directions have to be considered when the geometry of the study area is complex.

When the implicit method is applied to a one-dimensional flow with N grid points, a set of N simultaneous arithmetic equations has to be solved at every time step. For a two-dimensional flow with M by N grid points, a set of (MXN) simultaneous equations must be solved at every time step. In a real problem, a significant number of computer core is required to store several (MXN) by (MXN) matrices wherein M and N are on the order of a hundred. Clearly, it is a monumental task to solve such a set of equations. In order to overcome this problem, Peaceman & Rachford (1955) proposed the alternating-direction-implicit (ADI) method. This method is related to a method developed by Douglas (1955) to solve the two-dimensional heat equation

$$\partial \emptyset / \partial t = \partial^2 \emptyset / \partial x^2 + \partial^2 \emptyset / \partial y^2 \qquad (2.2)$$

By ADI, a time interval is divided into two half-time-steps. In one of the two half-time-steps, computations are carried out row by row. A set of N simultaneous arithmetic equations is solved to evaluate N unknown values in each row. All unknowns are limited to the same row. Those unknown terms on the other rows are substituted by their corresponding known values obtained at the previous time step. In the next half time-step, similar operations are carried out column by column. A set of M simultaneous equations are solved for each column operation. Gustafsson (1971) applied the ADI method to solve the equations of a shallow water problem.

Many vertically integrated, two-dimensional, numerical models have been developed. Some of them have simplified the problem by neglecting one or more terms in the governing equations. Some models have used linearized equations (e.g., Heaps 1969). If the advective terms are included, the momentum equation is nonlinear and the computation becomes more troublesome. The role of nonlinear terms on the numerical instability has been of great interest to many investigators (e.g., Moe, Mathisen & Hodgins 1978). The nonlinear terms can not be neglected in studying the gyre structures in a harbor such as that in the present study.

The work of Leendertse (1967) constituted an important landmark for the modeling of two-dimensional flows due to the fact that the model allowed a relatively large time-step for simulations by using an implicit method. The author's statement claiming that the model was unconditionally stable has attracted much attention. Leendertse (1972) extended it to a water-quality model. Hess & White (1974) applied it to Narragansett Bay. Blumberg (1977a) applied a similar model to Chesapeake Bay. Tee (1976) used a similar model including the effect of eddy viscosity. The three-dimensional finite-element model of Wang & Connor (1975) is also a similar model with eddy-viscosity terms included.

Very few numerical experiments have been carried out on the unsteady circulations in a harbor area where the scale of motion of interest is relatively small. A small grid spacing is required to study small scale motions. The grid spacing should also be small enough to better represent a complex geometry. For example, a grid spacing greater than 1,000 ft is too large for the flow in a navigation channel of which the width is typically between 500 ft and 800 ft. By referring to the Courant criterion in equation (2.1), one can see that a smaller grid spacing requires a smaller time-step. That means it takes thousands or more time-steps to simulate the circulation of just one diurnal tidal cycle, when the Courant number is less than unity. In a nonlinear model, numerical instability is likely to occur when the simulation time is long.

In some cases, a high-density network is required at local areas either to supply detailed results or to include important information, while a coarse network may be sufficient in the other areas. A model with varied grid-spacings (Bryan 1966; Abbott, Damsgaard & Rodenhuis 1973) may save computation costs without losing important features at local areas. Butler (1978b; 1978c) used a coordinate transformation in the form of a piecewise exponential stretch to obtain a smoothly varied grid system. The grid spacing varied from 150 ft to 900 ft for the Coos Bay Inlets/South Slough model and from 604 m to 2,583 m for the Galveston Bay model. Pinder & Gray (1977) pointed out that the finite difference approximation is correct to the first order for a model with irregular grid spacing and to second order for one with an equally spaced grid.

Most numerical models use fixed, vertical boundaries for the coastal line. Water is not allowed to pass over the boundary. In a storm surge problem, the movement of the shoreline might be significant. Some models (e.g., Reid & Bodine 1968; Damsguaard & Dinsmore 1975) used a fixed boundary yet allowed the flow to pass the water-land interface when the surface elevation exceeds the elevation of the adjacent dry land. The error due to assuming a solid boundary is then decreased. There are also some models (e.g., Matthews & Mungall 1970; Leendertse 1970; Yeh & Yeh 1976; Yeh & Chou 1979) which allow the solid boundary to move backward and forward depending on the water depth on the ocean side of the boundary. One should be aware of the fact that this type of moving-boundary model, when associated with large grid spacing, produces fast expansion or reduction of large surface areas. The error may be significant. Other treatments of the closed boundary included having sloping boundaries (Sielecki & Wurtele 1970) and having the irregular shorelines mapped into rectangular computational regions by a coordinate transformation (Boericke & Hall 1974).

The circulation pattern will be more definite if the strength of local vorticity can be found. The vorticity can be calculated from the velocity data which are obtained from a numerical model. A more direct approach for finding the gyre structure is to calculate vorticity directly through the continuity and vorticity equations. This approach is still not available for free-surface shallow water problems. Difficulties exist in establishing surface and bottom boundary conditions. Chorin (1973) used a statistical method to evaluate the vorticity generated or dissipated through solid boundaries, in the case of flow past a circular cylinder. The practical application of the vorticity equation is still limited to two-dimensional flows without the effects of outer boundaries (e.g., Thomson & Meng 1975; Wu, Spring & Sanker 1975).

In the present study, the numerical model uses the implicit finite difference method to compute the time-dependent velocities and surface elevations based on the depth-integrated continuity and momentum equations. The ADI technique is used. The network has equally spaced grid for both x- and y-directions. The coastline is assumed to be a fixed, vertical, solid boundary.

2.3 Eddy Viscosity

The concept of eddy viscosity was introduced for atmospheric motions in 1876 when Goldberg and Mohn assumed that the internal frictions per unit mass of turbulent flow is proportional to the current velocity (Neumann 1968):

$$I_x = k\ U\ /\rho \tag{2.3}$$

where k is an eddy viscosity coefficient and ρ is the density of the fluid.

In the case of turbulent flow, Reynolds stresses are used instead of shearing stresses and the kinematic molecular coefficient is replaced by an eddy viscosity. This concept has been used in the work of Durst (1924), Sverdrup (1942), Munk (1950), Neumann (1954), Bowden (1962), Liggett

(1969), Bye (1970), Deardorff (1971), Fischer (1973), Hseuh & Peng (1973), Nihoul (1975a), Fischer (1976a), Holland (1977), Madsen (1977), Stolzenbach et al. (1977), and Liu & Leendertse (1978), with various synonyms for the eddy viscosity.

The internal friction per unit mass of turbulent flow in the x-direction can be expressed as (Neumann 1968)

$$I_x = [\partial(A_{xx}\partial u/\partial x)/\partial x+\partial(A_{xy}\partial u/\partial y)/\partial y+\partial(A_{xy}\partial u/\partial z)/\partial z]/\rho \quad (2.4)$$

in which A_{xx} and A_{xy} are horizontal eddy viscosities and A_{xz} is a vertical eddy viscosity.

The eddy viscosity can be assumed constant, for simplicity, to yield a linear viscosity as what has been used in many numerical models (e.g. Liggett & Hadjitheodorou 1969; Allender 1975) or it can be a nonlinear viscosity (see Smagorinsky 1963) in which it is related directly to the gradient of either velocity or vorticity.

A linear eddy viscosity coefficient large enough to suppress small-scale vorticities might at the same time dampen large-scale eddies. Crowley (1970) indicated that some mechanism is needed to remove small-scale vorticities and that a nonlinear eddy viscosity, which usually depends on local flow conditions, is a better choice than a linear eddy viscosity. For two-dimensional turbulences, Crowley (1968, 1970) used the nonlinear eddy viscosity in the form of (see also Leith 1969; Haney & Wright 1975; Leendertse & Liu 1977)

$$A_{xy} = C^{3/2} (\Delta s) |\nabla\omega| \tag{2.5}$$

where C is a dimensionless coefficient, s is the grid spacing, and $\nabla\omega$ is the finite-difference approximation to the magnitude of gradient of vorticity. For a one-dimensional flow, Reynolds (1976) used an assumption of the form

$$A_{xy} = K (\Delta U) b \tag{2.6}$$

where ΔU is some appropriate velocity difference associated with the flow (for example, the difference between the velocity of the centerline of a jet and the velocity of the external field), b is a length scale characterizing the width of the jet, and the constant K may vary from flow to flow with a typical range of 0.05 to 0.1. For a boundary layer flow, the viscosity can be expressed as written in the following way (Reynolds 1976):

$$A_{xy} = L^2 | \partial U / \partial y | \tag{2.7}$$

where L is the Prandtl's mixing length. This relation is based on Prandtl's theory (see Sverdrup, Johnson & Fleming 1942).

Von Neumann & Richtmyer (1950) introduced the artificial viscosity for computing one-dimensional shock propagations in an inviscid flow field, in order to smooth out the discontinuity at the front of the shock wave. This artificial viscosity has only a mathematical meaning and not physical one. Lax & Wendroff (1960) used the same idea in their work.

The value of eddy viscosity coefficient is discussed and determined in Section 4.2.

2.4 Bottom Friction

The x-direction bottom stress which is defined in equation (A.57) of Appendix A, can be expressed by (Boericke & Hall 1974)

$$s_{bx} = f'' \rho q U/8 \tag{2.8}$$

where f" is the Darcy-Weisbach friction coefficient, ρ is the fluid density, and q is defined as

$$q = (U^2+V^2)^{1/2} \tag{2.9}$$

Equation (2.8), when substituted with the relation between the Darcy-Weisbach coefficient, f", and the Chezy coefficient, C, (cf. Giles 1962)

$$f'' = 8g/C^2 \tag{2.10}$$

becomes

$$s_{bx} = \rho g q U/C^2 \tag{2.11}$$

A similar expression was given by Heaps (1976).

Combining the above equation and equation (A.60) in Appendix A, one obtains

$$F_x = gqU/(HC^2) \qquad (2.12)$$

Gauckler in 1868 and Hagen in 1881 arrived independently at the conclusion that the Chezy coefficient C varies as the sixth root of the hydraulic radius R (see Henderson 1966). In 1891, Flamant wrongly attributed this conclusion to I. R. Manning and expressed it as

$$C = R^{1/6}/n \qquad (2.13)$$

which later led to the Manning equation which is also known as Strickler's equation on the continent of Europe (Henderson 1965). To be used with U.S. Customary units instead of the International System units, the above equation should be converted to

$$C = 1.486R^{1/6}/n \qquad (2.14)$$

where n is the Manning coefficient.

Other expressions of the bottom friction can be found in Welander (1965) and Cheng, Powell & Dillon (1976). An expression similar to that of the wind stress, equation (2.20), is (see Allender 1975)

$$s_{bx} = \rho C_d U^2 \qquad (2.15)$$

where C_d is a drag coefficient.

A linearized form of the bottom friction is (Bowden 1953; Heaps 1969, 1973)

$$F_x = c'U \tag{2.16}$$

where the coefficient c' can be expressed by (Groen & Groves 1962)

$$c' = r/h \tag{2.17}$$

in which r is a friction parameter of the dimension of a velocity, to be determined empirically (cf. Bowden 1956; Reid 1956).

The value of bottom friction coefficient is discussed in Section 4.3.

2.5 Wind Stress

Based on Prandtl's mixing length theory (see Sverdrup 1942), the wind stress can be expressed as (cf. Dorn 1953)

$$s_a = \rho_a K U_z^2 \tag{2.18}$$

where s_a is the wind stress acting on the water surface, ρ_a is the density of air, K is a nondimensional drag coefficient, and U_z is the wind velocity at a certain elevation. Strictly speaking, the wind velocity related to the surface fluid velocity should be used to replace U_z (Groen & Groves 1962).

Defining

$$K' = \rho_a K/\rho \tag{2.19}$$

where ρ is the density of water, equation (2.18) becomes (see Silvester 1974b)

$$s_a = \rho K' U_z^2 \tag{2.20}$$

The drag coefficient is an empirical coefficient, depending on the wind velocity (see Sheppard 1958), on the vertical stability of the air mass (Groen & Groves 1962), on the surface roughness (Yeh & Chou 1979), and possibly on distant storm conditions (Fischer 1976). It can be obtained by calibrating the simulated storm surge against the measured values. Sverdrup, Johnson & Fleming (1942) cited K = 0.0026 and 0.0024 from different sources. Von Arx (1962) stated that K varies with wind speed from 0.0001 to around 0.005. Values of the drag coefficient for

$$s_a = \rho_a K U_{10}^2 \tag{2.21}$$

where all units are in MKS system and U_{10} is the wind velocity at 10 m above sea surface, are collected and discussed by Deacon & Webb (1962). Based on the data of thirty oceanic observations, Wu (1969) concluded

$$K = \begin{cases} 0.00125/U_{10}^{1/5} & (U_{10} \leqslant 1 \text{ m/sec}) \\ 0.0005U_{10}^{1/2} & (1 < U_{10} < 15 \text{ m/sec}) \\ 0.0026 & (U_{10} \geqslant 15 \text{ m/sec}) \end{cases} \quad (2.22)$$

in which there are two discontinuities in the function. Heaps (1969) gave

$$K = \begin{cases} 0.000577 & (U_{10} \leqslant 4.9 \text{ m/sec}) \\ -0.000125 + 0.0001427U_{10} & \\ & (4.9 < U_{10} \leqslant 19.2 \text{ m/sec}) \\ 0.00262 & (U_{10} > 19.2 \text{ m/sec}) \end{cases} \quad (2.23)$$

Sheppard, Tribble & Garratt (1972) gave

$$K = 0.00036+0.0001U_{10} \qquad (3 \leqslant U_{10} \leqslant 16 \text{ m/sec}) \quad (2.24)$$

Based on observed data, Denman & Miyake (1973) gave a constant value $K = 0.00163 \pm 0.00028$ for $U_{10} < 17$ m/sec. Tsai & Chang (1974) proposed

$$K = \begin{cases} 0.00125 & (U_{10} \leqslant 5.1 \text{ m/sec}) \\ 0.00125 + 0.00175 \sin[\pi (U_{10}-5.1)/19.8] & \\ & (5.1 < U_{10} < 15 \text{ m/sec}) \\ 0.0030 & (U_{10} \geqslant 15 \text{ m/sec}) \end{cases} \quad (2.25)$$

Silvester (1974b) preferred

$$K = \begin{cases} 0.00065U_{10}^{1/2} & (U_{10} < 15 \text{ m/sec}) \\ 0.0026 & (U_{10} > 15 \text{ m/sec}) \end{cases} \quad (2.26)$$

Fischer (1976b) mentioned that the value ranges from 0.0007 to 0.003.

All values of drag coefficient cited above were derived from oceanic observations. Different values would be obtained for near shore areas. For air-water interaction above ponds, Dorn (1953) gave the experimental formula

$$K = \begin{cases} 0.001 & (U_{10} < 5.6 \text{ m/sec}) \\ 0.001+0.0019(1-5.6/U_{10})^2 & (U_{10} > 5.6 \text{ m/sec}) \end{cases} \quad (2.27)$$

The application of wind stress to estuary areas can be found in Wilson (1960) and Reid & Bodine (1968). Li (1977) took 0.0012 for the value in his Kiel Bay model. Based on several data sets from different sources, Wang & Connor (1975) suggested a linear equation for cases of both open ocean and closed basin as

$$K = 0.0011 + 0.0000536U_{10} \quad (2.28)$$

for all wind speeds.

All the formulas cited above are derived on the base of using a fixed-boundary model. The coefficient calibrated from a moving-boundary model would yield a higher value than that obtained from a fixed-boundary model.

Sometimes wind velocities are measured at elevations different from 10 m. To convert this kind of data into the equivalent U_{10}, the wind distribution near the sea surface should be available. Pierson (1964) suggested the relationship

$$U_z/U_{10} = 1 + [\ K^{1/2}\ \ln(z/10)\ ]/k \qquad (2.29)$$

where U_z is the wind velocity at the elevation of z meters and k=0.4 is Karman's constant. Based on this equation, Silvester (1974a) presented a figure and a table in order to perform the conversion.

For a two-dimensional problem, the square terms in equations (2.18), (2.20), and (2.21) should be replaced by suitable products of velocities. For example, equation (2.21) should be replaced by

$$s_{ax} = \rho_a K U_{10}(U_{10}^2+V_{10}^2)^{1/2} \qquad (2.30)$$

and

$$s_{ay} = \rho_a K U_{10}(U_{10}^2+V_{10}^2)^{1/2} \qquad (2.31)$$

The wind stress is included in the finite difference equations which are derived in Chapter 3. However, the numerical tests in the present study assume the windless condition in order to obtain a clearer picture of the circulation induced by tidal motions.

CHAPTER 3

MATHEMATICAL MODEL

3.1 Partial Differential Equations

A rotating right handed Cartesian x-y-z coordinates system fixed on the earth with the z-axis vertical upwards is used in this report. For a homogeneous, incompressible, isothermal, Newtonian fluid, the continuity equation and the Navier-Stokes equations are equations (A.4) and (A.16) to (A.18) as derived in Appendix A. Based on these equations, a set of depth-integrated equations are also derived in Appendix A and are used in this chapter as the governing equations for the present study.

In general, partial differential equations may be solved either analytically or numerically. A practical problem has to be simplified by assigning some assumptions before the analytical solution can be evaluated. As far as the tide-induced currents in a real harbor is concerned, analytical solutions from a set of highly simplified equations are generally far from the field measurement because many factors are either ignored or over-simplified in the theoretical analysis. In order to observe details of the currents, both physical models and numerical models can be used. Numerical models are more flexible when the harbor geometry is modified. They can be used for different projects by just changing the input data.

It takes tremendous computer storage and computation time to run a three-dimensional model. In a harbor area, the shallow water is usually not stratified and both vertical velocity and vertical acceleration can generally be neglected. Hence a vertically integrated two-dimensional model is used here and is expected to be able to produce satisfactory solutions. Three-dimensional models are not considered in the present study.

Assuming hydrostatic pressure, the depth-averaged continuity equation and equations of motion are

$$\partial E/\partial t + \partial(HU)/\partial x + \partial(HV)/\partial x = 0 \tag{3.1}$$

$$\partial U/\partial t+U\partial U/\partial x+V\partial U/\partial y-fV+g\partial E/\partial x=\nu(\partial^2U/\partial x^2+\partial^2U/\partial y^2)-F_x+W_x \quad (3.2)$$

and

$$\partial V/\partial t+U\partial V/\partial x+V\partial V/\partial y+fU+g\partial E/\partial y=\nu(\partial^2V/\partial x^2+\partial^2V/\partial y^2)-F_y+W_y \quad (3.2)$$

where E is the surface elevation related to mean water level; H=E+h is the total depth; h is the distance between the mean water surface and bottom; U and V are the vertically averaged velocities along x- and y-axes, respectively; f is the Coriolis parameter as defined in equation (A.83); g is the gravitational acceleration; ν is the kinematic viscosity; and, from equations (A.59) and (A.60),

$$F = s_b \; / \; (\rho H) \tag{3.4}$$

and

$$W = s_a \; / \; (\rho H) \tag{3.5}$$

are the bottom friction and wind forces per unit mass, respectively, while s_b and s_a denote bottom stress and surface stress, respectively. Equation (3.1) is based on the conservation of mass and equations (3.2) and (3.3) are based on the conservation of momentum in x- and y-directions. In the momentum equations, the first term is called the local acceleration term; the second and the third, the convective-inertia terms; the fourth, the Coriolis force term; and the fifth, the pressure gradient term. On the right hand side of the momentum equations, there are three terms representing the internal friction, bottom friction, and wind force, respectively.

The wind force term indicates the input of momentum from the relative wind motion through the air-sea interface. Wind stresses can be expressed as shown in equations (2.30) and (2.31) in Chapter 2.

The bottom friction term shows the momentum dissipation due to the presence of sea bottom. The x-direction bottom stress is expressed by equation (2.11).

The relation between the Chezy coefficient, C, and the Manning coefficient, n, has been expressed in equation

(2.14). In the numerical calculation of the two-dimensional flow in harbors or larger areas, the friction effect of side walls is not included in the bottom friction term and the water depth is used to replace the hydraulic radius. Thus equation (2.14) becomes

$$C = 1.486\ H^{1/6}\ /\ n \tag{3.6}$$

where H denotes the total water depth. Substituting into equation (2.11) gives

$$s_{bx} = n^2 \rho g q U/(1.486^2 H^{1/3}) \tag{3.7}$$

By combining equations (3.4) and (3.7), one obtains:

$$F_x = n^2 g q U/(1.486^2 H^{4/3}) = C' q U/H \tag{3.8}$$

where C' is a dimensionless friction coefficient and can be defined as

$$C' = g/C^2 = n^2 g/(1.486^2 H^{1/3}) \tag{3.9}$$

(see also Wang & Connor 1975). If equations (2.9) and (2.11) are used, equation (3.4) gives

$$F_x = g q U(HC^2) = gU(\ U^2+V^2\ )^{1/2}/(HC^2) \tag{3.10}$$

In the equations of motion (3.2) and (3.3), those terms with the kinematic molecular viscosity ν represent a process in which the momentum of high velocity fluid particles is exchanged with that of low velocity particles. This process is termed the diffusion of momentum.

The fluid motions in the ocean and atmosphere are usually turbulent flows in which there are small-scale eddies and where interchanges of momentum between adjacent portions of fluid appear (Lamb 1924). The rate of diffusion of momentum due to the turbulent motion is much higher than that due to the molecular viscosity. The concept of eddy viscosity has been introduced and used by many investigators (see Section 2.3) to describe this type of momentum diffusion in turbulent flows.

For tidal flows, the vertical velocity as well as its derivatives are negligible. Only shearing stresses resulting from the horizontal motion of fluid are of importance. Neglecting the term with vertical eddy viscosity in equation (2.4), equations (3.2) and (3.3) become

$$\partial U/\partial t+U\partial U/\partial x+V\partial U/\partial y-fV+g\partial E/\partial x = A(\partial^2U/\partial x^2+\partial^2U/\partial y^2)-F_x+W_x \tag{3.11}$$

and

$$\partial V/\partial t+U\partial V/\partial x+V\partial V/\partial y+fU+g\partial E/\partial y = A(\partial^2V/\partial x^2+\partial^2V/\partial y^2)-F_y+W_y \tag{3.12}$$

where the eddy viscosity, A, is assumed constant.

As the model applied to a study area of complex geometry, there might be some local areas where the velocity is so small at a certain time period that the Reynolds number is small and the flow is laminar instead of turbulent. In this case, the eddy viscosity is too large and the molecular viscosity should be used instead. However, since the velocity is very small in these local areas, an extremely high viscosity will not give any noticeable error to the macropicture.

Equations (3.1), (3.11), and (3.12) form the governing equations for a two-dimensional, homogeneous, viscous, unsteady flow. These equations contain the nonlinear terms. In general, the presence of nonlinearity makes it more difficult to obtain the numerical solution to a given problem. A linear system can be obtained by neglecting the advective terms, assuming that the total depth H is equal to the mean depth h, and assuming that both bottom friction and wind force are linearly proportional to the velocity. For a harbor circulation problem, none of the above three assumptions can be accepted. Thus, the nonlinearity has to be retained and a suitable numerical method must be developed to solve this nonlinear system. A numerical approach is presented in the following section.

3.2 Numerical Method

A numerical method of some type is necessary to find the circulation pattern in a harbor of arbitrary topography. The finite difference method and the finite element method are two possible choices in solving this kind of problem numerically. The former is used in the present study. Which particular method is superior, of course, depends on the specific problem under consideration, the available information, the user's knowledge and skill of the methods, and possibly the available computer core and computation time.

The finite element method uses a more flexible network which can fit much better the irregular solid boundary of the study areas such as harbors. In the present study, which uses the finite difference method, the coastline is approximated by a zigzag boundary. However, the resultant error is negligible as long as the grid spacing has been reasonably chosen. The details of the solution near the boundary is not important in this study. The error in the computation of total volume of water in the study area is small and can be minimized by carefully aligning the boundary lines.

Another advantage of the finite element method is that all elements are involved in the computation. Due to the nature of the finite difference method (in the case of using Cartesian coordinates), a rectangular network is used to cover the usually non-rectangular study area. The variables for the grid points outside the study area do nothing but occupy the computer storage. To overcome this disadvantage in the finite difference method, a mapping technique is designed in the present study such that variables are assigned only to the computational points. In the present study, the simulation of flows in the Los Angeles-Long Beach Harbor requires a network of 108X69 (=7425) points while the number of grid points involved in the computation is only 4695. Without the designed mapping technique, 37% of the grid points will be wasted. The mapping technique involves an additional transformation; yet the computer time can be reduced by proper coding.

The advantages of the finite element method are not significant in the present study, as mentioned above. Furthermore, the finite difference method provides elegant computation, since the matrix of the simultaneous equations is a tri-diagonal matrix. There exist special techniques to treat this type of simultaneous equations (see Chiang 1977). Neither matrix inversion nor Gaussian elimination is required.

For the present study, which pertains to the simulation of gyre structures in Los Angeles-Long Beach Harbor, it is deemed appropriate to use the finite difference method, especially with the aid of a mapping technique for making all grid points active points.

Governing equations (3.1), (3.11), and (3.12) are converted into finite difference equations in implicit form to constitute a set of simultaneous algebraic equations. The simultaneous equations are then solved to yield the numerical solution to the problem.

To transform the partial differential equations into the finite difference equations, a central-difference formulation is used in formulating both the time and spatial differentiations in order to give more accurate results than those from either a forward-difference or backward-difference method. A space-staggered scheme is adapted to increase the efficiency of programming and to automatically fit the boundary condition which requires that the normal velocity be zero at a closed boundary. Depth, velocities, and surface elevation are described at different grid points as indicated in Figure 3.1. Two possible schemes are shown in the figure. The upper scheme in the figure will yield a clearer representation of the finite difference equations than that from the lower one. The lower one is used in the present study because the field data of water depth was collected on the basis of this scheme. Since the indices in a computer program have to be integers, all variables in the small squares surrounded by the dotted lines in Figure 3.1 are assigned the same indices. For example, $V_{i,j+1/2}$ becomes V(i,j) and $H_{i+1/2,j-1/2}$

(A)

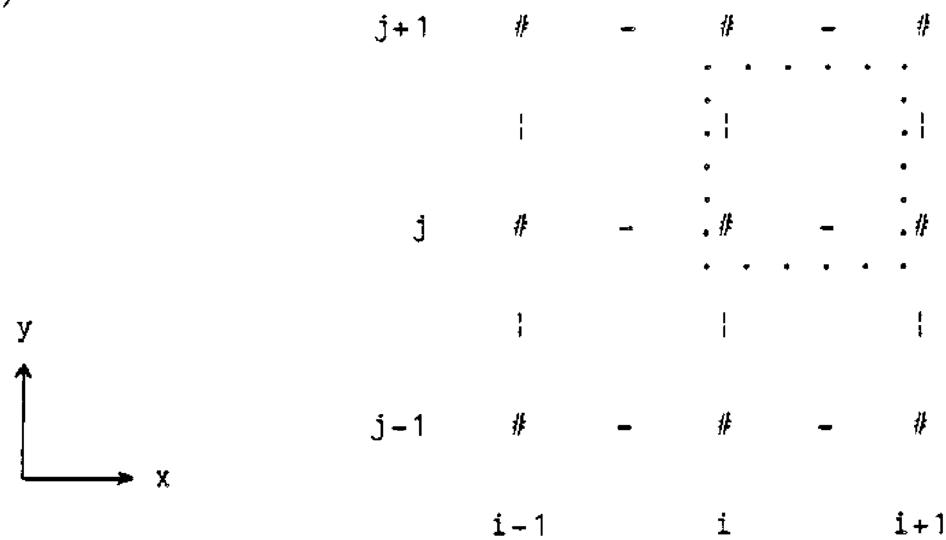

(B)

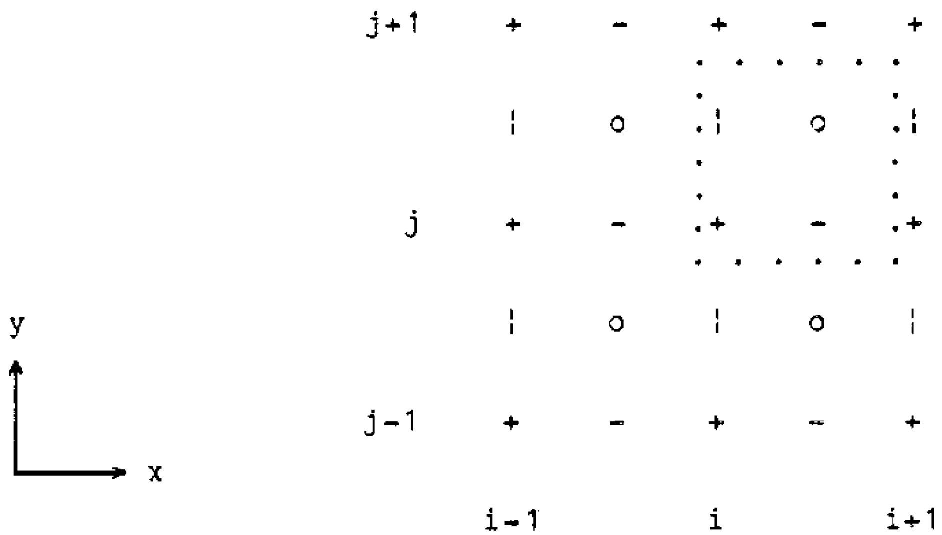

\+ Surface elevation (E)
\- U velocity (U)
¦ V velocity (V)
o Depth & friction coefficient (h,C)
\# Surface elevation, depth, & friction coefficient (E,h,C)

Figure 3.1. Definition sketch of the space-staggered schem.

becomes H(i,j-1) in the computer program.

A time-step consists of two half time-steps:

$$\Delta T = 2\Delta t \tag{3.13}$$

A uniform grid-spacing is used for both directions:

$$\Delta x = \Delta y = \Delta s \tag{3.14}$$

With Ø denoting an arbitrary dependent variable, n the sequential number of time-steps, and i and j the x- and y-direction indices, respectively, as shown in Figure 3.1, the following notations are used in deriving the finite difference equations:

$$\emptyset^{n}_{i,j} \equiv \emptyset(i\Delta s, j\Delta s, n\Delta t) \tag{3.15}$$

$$\emptyset^{n} \equiv \emptyset^{n}_{i,j} \tag{3.16}$$

$$\emptyset^{+} \equiv \emptyset^{n+1/2} \tag{3.17}$$

$$\emptyset^{-} \equiv \emptyset^{n-1/2} \tag{3.18}$$

$$\emptyset_{i,j} \equiv \emptyset^{n}_{i,j} \tag{3.19}$$

$$\emptyset_{+,j} \equiv \emptyset_{i+1/2,j} \tag{3.20}$$

$$\emptyset_{-,j} \equiv \emptyset_{i-1/2,j} \tag{3.21}$$

$$\emptyset_{i,+} \equiv \emptyset_{i,j+1/2} \tag{3.22}$$

$$\emptyset_{i,-} \equiv \emptyset_{i,j-1/2} \tag{3.23}$$

$$\delta_t \emptyset^n \equiv (\emptyset^+ - \emptyset^-)/(2\Delta t) \tag{3.24}$$

$$\delta_t' \emptyset^n \equiv (\emptyset^{n+1/4} - \emptyset^{n-1/4})/\Delta t \tag{3.25}$$

$$\delta_x \emptyset_{i,j} \equiv (\emptyset_{i+1,j} - \emptyset_{i-1,j})/(2\Delta s) \tag{3.26}$$

$$\delta_y \emptyset_{i,j} \equiv (\emptyset_{i,j+1} - \emptyset_{i,j-1})/(2\Delta s) \tag{3.27}$$

$$\delta_x' \emptyset_{i,j} \equiv (\emptyset_{+,j} - \emptyset_{-,j})/\Delta s \tag{3.28}$$

$$\delta_x^2 \emptyset_{i,j} \equiv {}_x({}_x\emptyset_{i,j})$$

$$= {}_x(\emptyset_{+,j} - \emptyset_{-,j})/\Delta s$$

$$= ({}_x\emptyset_{+,j} - {}_x\emptyset_{-,j})/\Delta s$$

$$= [(\emptyset_{i+1,j} - \emptyset_{i,j}) - (\emptyset_{i,j} - \emptyset_{i-1,j})]/(\Delta s)^2$$

$$= (\emptyset_{i+1,j} + \emptyset_{i-1,j} - 2\emptyset_{i,j})/(\Delta s)^2 \tag{3.29}$$

$$\delta_u^2 \emptyset_{i,j} \equiv (\emptyset_{i,j+1} + \emptyset_{i,j-1} - 2\emptyset_{i,j})/(\Delta s) \tag{3.30}$$

$$\bar{C}^x_{i,+} \equiv (C_{+,+} + C_{-,+})/2 \tag{3.31}$$

$$\bar{C}^y_{+,j} \equiv (C_{+,+} + C_{+,-})/2 \tag{3.32}$$

$$\bar{H}^x_{+,j} \equiv \bar{E}^x_{+,j} + \bar{h}^y_{+,j} \equiv (E_{i+1,j} + E_{i,j} + h_{+,+} + h_{+,-})/2 \tag{3.33}$$

$$\bar{H}^y_{i,+} \equiv \bar{E}^y_{i,+} + \bar{h}^x_{i,+} \equiv (E_{i,j+1} + E_{i,j} + h_{+,+} + h_{-,+})/2 \tag{3.34}$$

$$\bar{\bar{U}}_{+,j} \equiv (U_{i+3/2,j} + U_{-,j} + U_{+,j+1} + U_{+,j-1})/4 \tag{3.35}$$

$$\bar{\bar{V}}_{+,j} \equiv (V_{i+1,j} + V_{i,+} + V_{i+1,-} + V_{i,-})/4 \tag{3.36}$$

$$\bar{\bar{U}}_{i,+} \equiv (U_{+,j+1} + U_{+,j} + U_{-,j+1} + U_{-,j})/4 \tag{3.37}$$

$$\bar{\bar{V}}_{i,+} \equiv (V_{i,j+3/2} + V_{i,-} + V_{i+1,+} + V_{i-1,+})/4 \tag{3.38}$$

$$k \equiv 2g(\Delta t)/(\Delta s) \tag{3.39}$$

$$E^{+*} \begin{cases} \equiv E^n & \text{(before iteration)} \quad (3.40) \\ \equiv E^+ & \text{(when } E^+ \text{ is available)} \quad (3.41) \end{cases}$$

$$E^{(n+1)*} \begin{cases} \equiv E^+ & \text{(before iteration)} \quad (3.42) \\ \equiv E^{n+1} & \text{(when } E^{n+1} \text{ is available)} \quad (3.43) \end{cases}$$

$$U^{+*} \begin{cases} \equiv U^{-} & \text{(before iteration)} \quad (3.44) \\ \equiv U^{+} & \text{(when } U^{+} \text{ is available)} \quad (3.45) \end{cases}$$

$$V^{(n+1)*} \begin{cases} \equiv V^{n} & \text{(before iteration)} \quad (3.46) \\ \equiv V^{n+1} & \text{(when } V^{n+1} \text{ is available)} \quad (3.47) \end{cases}$$

$$H^{+*} \equiv E^{+*} + h_{i,j} \qquad (3.48)$$

For equations (3.1), (3.11), and (3.12), the finite difference equations at the point (i,j,n) can be written as

$$\delta_t E^n + \delta_x (HU)_{i,j} + \delta_y (HV)_{i,j} = 0 \qquad (3.49)$$

$$\delta_t U^n + U_{i,j}\delta_x U_{i,j} + V_{i,j}\delta_y U_{i,j} - fV_{i,j} + g\delta_x E_{i,j}$$

$$= A(\ \delta^2_x U_{i,j} + \delta^2_y U_{i,j}\ ) - (F_x)_{i,j} + (W_x)_{i,j} \qquad (3.50)$$

and $$\delta_t V^n + U_{i,j}\delta_x V_{i,j} + V_{i,j}\delta_y V_{i,j} + fU_{i,j} + g\delta_y E_{i,j}$$

$$= A(\ \delta^2_x V_{i,j} + \delta^2_y V_{i,j}\ ) - (F_y)_{i,j} + (W_y)_{i,j} \qquad (3.51)$$

With the difference operators defined in equations (3.24) to (3.30), equations (3.49) to (3.51) form a set of arithmetic equations. Unknowns at the time level n+1/2 can be solved from the known values at the time levels n-1/2 and n. If the boundary conditions are available, starting from initial values of two time levels, the problem can be solved step by step. The unknowns at every grid point would be solved explicitly.

The explicit method is associated with the Courant-Friedrichs-Lewy stability condition as shown in equation (2.1). If the maximum water depth is 110 ft and the grid size is chosen to be 500 ft, the time step should be about 5 sec or less. Thus it takes about 18,000 or more time-steps to simulate the flow for a diurnal tidal cycle. It requires a tremendous amount of computer time to simulate the circulation pattern for a few tidal cycles. Alternatively, an implicit method can be used. This method is not restricted by the Courant stability condition and the size of its time step can be larger than the critical time step for an explicit method.

The principle of the alternating-direction-iteration (ADI) method in solving heat equations has been applied to two-dimensional flow problems (e.g., Leendertse 1967). Unlike the heat equation which contains only one variable, there are three variables for the present governing equations. These three variables are surface elevation, E, and two velocity components, U and V. In the first half-time-step, the continuity equation and the x-direction momentum equation are coupled to solve for E and U at every grid point, having the terms with x-direction gradient expressed implicitly and the terms with y-direction gradient expressed explicitly. In the second half-time-step, the continuity equation and y-direction momentum equation are used to find E and V.

In the algorithm used by Leendertse (1967), V and U are solved explicitly in the first and second half-time-steps, respectively. From the experiments of the present study, it was found that these two sub-steps, which solve V and U explicitly, were the main source of the generation of numerical oscillations. This oscillation could eventually lead to divergent solutions. Hence these sub-steps are discarded for the present study. Since those two parts of explicit calculations were removed from the model, oscillations have totally disappeared from the simulation results.

In solving for E and U at time-step n+1/2, the finite difference equations from equations (3.1) and (3.11) can be written as

$$\delta_t E^n + [\, \delta_x (HU)^+ + \delta_x (HU)^- \,]/2 + \delta_y (HV) = 0 \qquad (3.52)$$

and

$$\delta_t U_{+,j} + (U^{+}_{+,j} \delta_x U^{+}_{+,j} + U^{-}_{+,j} \delta_x U^{-}_{+,j})/2$$

$$+ V_{+,j}(\delta_y U^{+}_{+,j} + \delta_y U^{-}_{+,j})/2 - fV_{+,j} + g(\delta'_x E^{+}_{+,j} + \delta'_x E^{-}_{+,j})/2$$

$$= A(\delta^2_x U^{+}_{+,j} + \delta^2_y U^{+}_{+,j} + \delta^2_x U^{-}_{+,j} + \delta^2_y U^{-}_{+,j})/2 - (F_x)_{+,j} + (W_x)_{+,j} \tag{3.53}$$

where notations (3.15) to (3.30) are used and, based on equation (3.10),

$$(F_x)_{+,j} = g(U^{+}_{+,j} + U^{-}_{+,j})[(U^{+}_{+,j} + U^{-}_{+,j})^2/4 + (V_{+,j})^2]^{1/2}$$

$$/ [2H_{+,j}(C_{+,j})^2] \tag{3.54}$$

For the second half-time-step, similar equations can be written to solve for E and V at time-step n+1.

The above formulations use the central-difference scheme for both time and spatial differentiations. The difference equations are consistent with the partial differential equations. However, the computation involves both velocity components U and V in two time levels and the water surface elevation E in three time levels. This means that computer storage of the seven matrices for E, U, and V are required.

In order to save the computer memory of one matrix such that only two time levels of E are needed in the computation, the following modified formulation is used for this study.

For the first half time-step, to solve for E and U at time-step n+1/2, the finite difference equation at (i,j,n+1/4) for the continuity equation (3.1) is written as (Leendertse 1967),

$$\delta_t' E^{n+1/4} + \delta_x (HU)^+ + \delta_y (HV)^n = 0 \tag{3.55}$$

where the difference operators are defined in equations (3.25) to (3.27). For x-direction momentum equation (3.11), the difference equation at (i+1/2,j,n) is written as

$$\delta_t U_{+,j} + U_{+,j}\, \delta_x U_{+,j} + V_{+,j}\, \delta_y U_{+,j} - fV_{+,j} + g\delta_x' E^+_{+,j}$$

$$= A(\delta_x^2 U^-_{+,j} + \delta_y^2 U^-_{+,j})$$

$$- gU^-_{+,j}[(U^-_{+,j})^2+(V_{+,j})^2]^{1/2}/[H_{+,j}(C_{+,j})^2] + (W_x)_{+,j} \tag{3.56}$$

where the difference operators have been defined in equations (3.24) to (3.30). The elevation term (pressure term) is raised a half time-level in order to have the unknown E^t expressed implicitly. The bottom friction term is assigned to the lower time-level as was done by Leendertse (1967). The eddy viscous term, which is not included by Leendertse, is also assigned to the lower time-level according to Tee (1976). The main difference of this formulation from that of Leendertse is that the first four terms of equation (3.56) are on exactly the same time level. The acceleration term and the advective terms are fully centered in time. This arrangement may be the main reason to have this model maintain much longer simulation time than other models.

Expanding the difference operators in equations (3.55) and (3.56) gives

$$(E^{+}-E^{n})/\Delta t$$

$$+ [(\bar{H}^{x})^{+}_{+,j}U^{+}_{+,j}-(\bar{H}^{x})^{+}_{-,j}U^{+}_{-,j}+(\bar{H}^{y})_{i,+}V_{i,+}-(\bar{H}^{y})_{i,-}V_{i,-}]/\Delta s$$

$$= 0 \tag{3.57}$$

and $(U^{+}_{+,j}-U^{-}_{+,j})/(2\Delta t) + U^{+}_{+,j}\ {}_{x}U^{+}_{+,j} /2 + U^{\mp}{}_{,j}\ {}_{x}U^{-}_{+,j} /2$

$$+ \bar{\bar{V}}_{+,j}[\ {}_{y}U^{+}_{+,j}+ {}_{y}U^{-}_{+,j}]/2 - f\bar{\bar{V}}_{+,j} + g(E^{+}_{i+1,j}-E^{+})/\Delta s$$

$$= 4A(\bar{\bar{U}}^{-}_{+,j}-U^{-}_{+,j})/(\Delta s)^{2}$$

$$- gU^{-}_{+,j}[(U^{-}_{+,j})^{2}+(\bar{\bar{V}}_{+,j})^{2}]^{1/2}/[(\bar{H}^{x})_{+,j}(\bar{C}^{x}_{+,j})^{2}]$$

$$+ (W_x)_{+,j} \tag{3.58}$$

where notations (3.31) to (3.36) are used to simplify the expressions. Care has been taken such that all terms are available as defined in Figure 3.1.

The above two equations can be rewritten as

$$-r_- U^+_{-,j} + E^+ + r_+ U^+_{+,j} = a_i \tag{3.59}$$

and
$$-kE^+ + d_+ U^+_{+,j} + kE^+_{i+1,j} = b_+ \tag{3.60}$$

where

$$a_i \equiv E^n - \Delta t[\ (\overline{H}^y)_{i,+} V_{i,+} - (\overline{H}^y)_{i,-} V_{i,-}]/\Delta s \tag{3.61}$$

$$b_+ \equiv U^-_{+,j}\{\ 1 - \Delta t(\delta_x U^-_{+,j}\ )$$

$$-2g(\Delta t)[(U^-_{+,j})^2 + (\overset{=}{V}_{+,j})^2]^{1/2}/[(\overline{H}^x)_{+,j}(\overline{C}^x_{+,j})^2]\ \}$$

$$+ (\Delta t)\overset{=}{V}_{+,j}(\ 2f - \delta_y U^{+*}_{+,j} - \delta_y U^-_{+,j}\ )$$

$$+ 8(\Delta t)A(\ \overset{=}{U}^-_{+,j} - U^-_{+,j}\ )/(\Delta s)^2 + 2(\Delta t)(W_x)_{+,j} \tag{3.62}$$

$$d_+ \equiv 1 + \Delta t(\delta_x U^{+*}_{+,j}) \tag{3.63}$$

$$k \equiv 2g(\Delta t)/(\Delta s) \tag{3.64}$$

$$r_{-} \equiv \Delta t(\overline{H}^{x})^{+*}_{-,j}/\Delta s \tag{3.65}$$

and

$$r_{+} \equiv \Delta t(\overline{H}^{x})^{+*}_{+,j}/\Delta s \tag{3.66}$$

Those terms marked with an asterisk indicate unknown terms to be substituted with known values. During the first iteration in every half time-step, those terms, as shown in equations (3.40) to (3.48), are substituted with their corresponding terms obtained from the previous half time-step or previous time-step. During the successive iterations in the same half time-step, they are substituted with their corresponding terms obtained from the previous iteration. With this arrangement, coefficients a, b, d, k, and r are all known values in calculating E and U at time level n+1/2. It is found that, in general, no more than one iteration is necessary.

All the equations derived so far are applicable to points inside the field of computation. More consideration is required for the boundary points. A boundary can be a coastal boundary, which is considered a solid boundary in the present study, an open boundary with elevations specified, or an open boundary across which the discharges or velocities are given. The solid boundary is considered to be a high, impervious wall such that no flooding is allowed. Water depths should be such that no negative values appear due to the fluctuation of the surface elevation.

A sketch of the field of computation can be drawn as the first step in preparing input data. An example showing the layout of boundary lines is given in Figure 3.2. The open boundary passes through the locations at which the boundary values (any of elevation, discharge, and velocity), are given. The solid boundary passes through the locations at which the velocities are described. By this arrangement, the boundary condition which requires that the normal velocity vanish is satisfied implicitly.

The breakwaters are assumed to be impervious. The effects of the porosity of breakwater on the circulation pattern in harbors are left to the future research. A submodel such as the Darcy equation can be employed to estimate the discharge through breakwaters.

Consider a row of computational points (i,j; i=I,I+1, ...,M) with boundary conditions given beyond the two end points I and M. If the boundary with the lower index, I, is a solid boundary, the normal velocity is zero

$$U^{+}_{I-1/2,j} = 0 \tag{3.67}$$

If the boundary is an open boundary, either discharge or

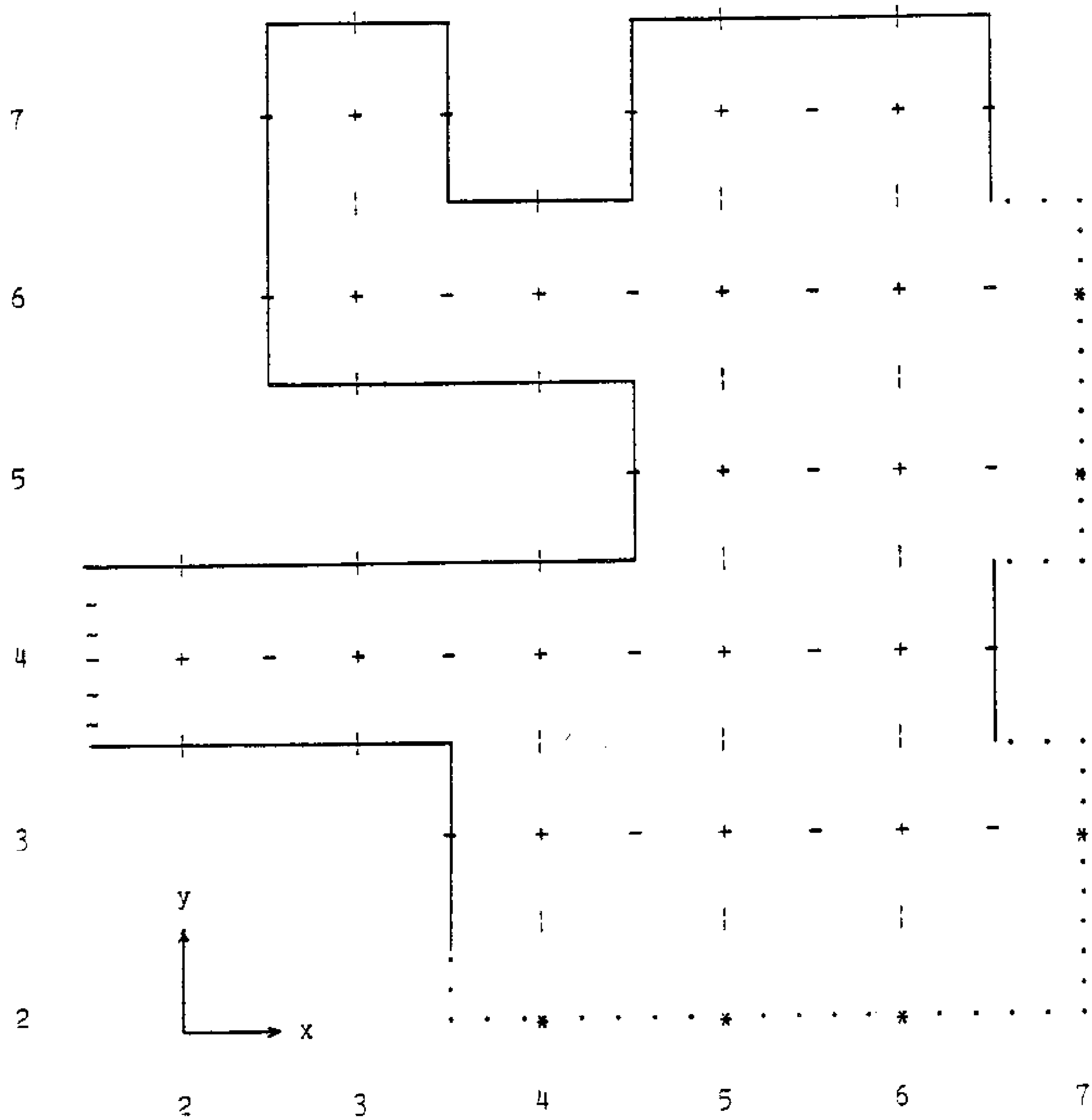

\+ Surface elevation to be computed
* Surface elevation given on open boundary
\- U velocity
¦ V velocity
——— Solid boundary
..... Open boundary with given elevations
~ Open boundary with given discharge

Figure 3.2. Definition sketch for the location of open and solid boundaries.

elevation is available. If the discharge is given, the velocity can be easily estimated. If the elevation is given, equation (3.60) can be written as

$$U^{+}_{I-1/2,j} = -R_{I-1}E^{+}_{I} + S_{I-1} \tag{3.68}$$

where $R_{I-1} \equiv k/d_{I-1/2}$ (3.69)

and $S_{I-1} \equiv (b_{I-1/2}+kE_{I-1})/d_{I-1/2}$ (3.70)

in which $b_{I-1/2}$ and $d_{I-1/2}$ can be evaluated from equations (3.62) and (3.63), having $U_{I-3/2,j}$ estimated through extrapolation. For either a solid boundary or an open boundary with a given discharge,

$$R_{I-1} = 0 \tag{3.71}$$

and $S_{I-1} = U^{+}_{I-1/2,j}$ (3.72)

For the first point (I,j) in a computational segment of row j, equation (3.59) gives

$$E^{+}_{I} = -P_{I}U^{+}_{I+1/2,j} + Q_{I} \tag{3.73}$$

where $P_{I} \equiv r_{I+1/2}/(1+r_{I-1/2}R_{I-1})$ (3.74) and $$Q_I \equiv (a_I+r_{I-1/2}S_{I-1})/(1+r_{I-1/2}R_{I-1}) \tag{3.75}$$

At location (I+1/2,j), equation (3.60) gives

$$U^+_{I+1/2,j} = -R_I E^+_{I-1} + S_I \tag{3.76}$$

where $$R_I \equiv k/(d_{I+1/2}+kP_I) \tag{3.77}$$

and $$S_I \equiv (b_{I+1/2}+kQ_I)/(d_{I+1/2}+kP_I) \tag{3.78}$$

In general, the following recursion formulas can be written:

$$E^+ = -P_i U^+_{+,j} + Q_i \qquad (i=I,I+1,...,M) \tag{3.79}$$

and $$U^+_{-,j} = -R_{i-1}E^+ + S_{i-1} \qquad (i=I,I+1,...,M) \tag{3.80}$$

where $$P_i \equiv r_+/(1+r_-R_{i-1}) \qquad (i=I,I+1,...,M) \tag{3.81}$$

$$Q_i \equiv (a_i+r_-S_{i-1})/(1+r_-R_{i-1}) \qquad (i=I,I+1,...,M) \tag{3.82}$$

$$R_i \equiv k/(d_++kP_i) \qquad (i=I,I+1,...,M-1) \tag{3.83}$$

$$S_i \equiv (b_++kQ_i)/(d_++kP_i) \qquad (i=I,I+1,...,M-1) \tag{3.84}$$

and if the boundary is either closed or open with discharge given,

$$R_{I-1} = 0 \tag{3.85}$$

$$R_M = 0 \tag{3.86}$$

$$S_{I-1} = U^{+}_{I-1/2,j} \tag{3.87}$$

$$S_M = U^{+}_{M+1/2,j} \tag{3.88}$$

if the boundary is open with elevation given,

$$R_{I-1} = k/d_{I-1/2} \tag{3.89}$$

$$R_M = k/(\ d_{M+1/2}+kP_M\ ) \tag{3.90}$$

$$S_{I-1} = (\ b_{I-1/2}+kE^{+}_{I-1}\ )/d_{I-1/2} \tag{3.91}$$

$$S_M = (\ b_{M+1/2}+kQ_M\ )/(\ d_{M+1/2}+kP_M\ ) \tag{3.92}$$

where a, b, d, k, and r are defined in equations (3.61) to (3.66).

For the points (i,j; i=I,I+1,...,M) in the computational field, equations (3.59) and (3.60) form a set of

2(M-I+1) simultaneous equations to solve for (M-I+1) sets of E's and U's. Since they form a tri-diagonal matrix, the computation is quite simple. No matrix inversion or Gaussian elimination is required. First, the coefficients P, Q, R, and S are evaluated forward from I to M by using equations (3.81) to (3.92). Then E and U are found backward from M+1 to I, based on equations (3.79) and (3.80).

Similarly, for the second half-time-step, the recursion formulas are

$$E^{n+1} = -P_j V^{n+1}_{i,+} + Q_j \qquad (j=J,J+1,...,N) \quad (3.93)$$

$$V^{n+1}_{i,-} = -R_{j-1} E^{n+1} + S_{j-1} \qquad (j=J,J+1,...,N) \quad (3.94)$$

with

$$P_j \equiv r_+/(\ 1+r_- R_{j-1}\ ) \qquad (j=J,J+1,...,N) \quad (3.95)$$

$$Q_j \equiv (\ a_j + r_- S_{j-1}\ )/(\ 1+r_- R_{j-1}\ ) \qquad (j=J,J+1,...,N) \quad (3.96)$$

$$R_j \equiv k/(\ d_+ + kP_j\ ) \qquad (j=J,J+1,...,N-1) \quad (3.97)$$

$$S_j \equiv (\ b_+ + kQ_j\ )/(\ d_+ + kP_j\ ) \qquad (j=J,J+1,...,N-1) \quad (3.98)$$

$$k \equiv 2g(\Delta t)/(\Delta s) \quad (3.99)$$

$$r_{+} \equiv \Delta t(\overline{H}^{y})_{i,+}^{(n+1)*}/\Delta s \qquad (j=J,J+1,\ldots,N) \quad (3.100)$$

$$d_{+} \equiv 1+\Delta t(\delta_{y}V_{i,+}^{(n+1)*}) \qquad (j=J,J+1,\ldots,N-1) \quad (3.101)$$

$$a_{j} \equiv E^{+} - \Delta t[\ (\overline{H}^{x})_{+,j}^{+}U_{+,j}^{+}-(\overline{H}^{x})_{-,j}^{+}U_{-,j}^{+}\ ]/\Delta s$$

$$(j=J,J+1,\ldots,N) \quad (3.102)$$

$$b_{+} \equiv V_{i,+}\{\ 1-\Delta t(\delta_{y}V_{i,+})$$

$$-2g(\Delta t)[(\overset{=}{U}{}_{i,+}^{+})^{2}+V_{i,+}^{2}]^{1/2}/[(\overline{H}^{y})_{i,+}^{+}(\overline{C}^{y}{}_{i,+})^{2}]\ \}$$

$$-\ (\Delta t)\overset{=}{U}{}_{i,+}^{+}(2f+\delta_{x}V_{i,+}^{(n+1)*}+\delta_{x}V_{i,+})$$

$$+\ 8(\Delta t)A(\overset{=}{V}_{i,+}-V_{i,+})/(\Delta s)^{2}$$

$$+\ 2(\Delta t)(W_{y})_{i,+} \qquad (j=J,J+1,\ldots,N-1) \quad (3.103)$$

If the formulation (3.52) to (3.54) were used, the recursion formulas and most of the coefficients would have been the same, and equations (3.79) to (3.92) and (3.65) to (3.66) would have remained to be effective, and equations (3.61) to (3.64) should have been replaced by

$$a_i \equiv E - (\Delta t)[\ (\overline{H}^x)^-_{+,j}U^-_{+,j} - (\overline{H}^x)^-_{-,j}U^-_{-,j}\ ]/\Delta s$$

$$- 2(\Delta t)[\ (\overline{H}^y)_{i,+}V_{i,+} - (\overline{H}^y)_{i,-}V_{i,-}\ )/\Delta s \qquad (3.104)$$

$$b_+ \equiv U^-_{+,j}\{\ 1-\Delta t(\delta_x U^-_{+,j})$$

$$-g(\Delta t)U^-_{+,j}\quad [\ (U^{+*}_{+,j}+U^-_{+,j})^2/\overline{\overline{4}}+(V_{+,j})^2\ ]^{1/2}$$

$$/\ [(\overline{H}^x)_{+,j}(\overline{C}^x_{+,j})^2]\ \}$$

$$+ (\Delta t)\overline{\overline{V}}_{+,j}(\ 2f-\delta_y U^{+*}_{+,j}-\delta_y U^-_{+,j}\quad)$$

$$+ 4(\Delta t)A(\overline{\overline{U}}^{+*}_{+,j}+\overline{\overline{U}}^-_j-2U^-_{+,j})/(\Delta s)^2+2(\Delta t)(W_x)_{+,j} \qquad (3.105)$$

$$d_+ \equiv 1 + \Delta t\, \delta_x U^{+*}_{+,j} + 4(\Delta t)A/(\Delta s)^2$$

$$+g(\Delta t)[\ (U^{+*}_{+,j}+U^-_{+,j})^2/4+(\overline{\overline{V}}_{+,j})^2\ ]^{1/2}/[\overline{H}^x_{+,j}(\overline{C}^x_{+,j})^2]$$

$$(3.106)$$

$$k \equiv g(\Delta t)/(\Delta s) \qquad (3.107)$$

This formulation requires extra computer storage for the third E matrix, because of the existence of E^- in equation (3.104).

Based on equations (3.61) to (3.66) and (3.79) to

(3.103), a computer program is developed for the numerical calculation. The program is listed in Appendix B.1.

CHAPTER 4

NUMERICAL EXPERIMENTS

4.1 Description of Study Area

A number of numerical experiments were performed during the development of the algorithm based on the finite-difference equations derived in Chapter 3. The computations were made for the tide-induced flow in Los Angeles-Long Beach Harbor (Figure 4.1). The Los Angeles-Long Beach Harbor is chosen for the verification of the model because the circulation patterns in this area have previously been studied through both physical and numerical models by U.S. Army Corps of Engineers (McAnally 1975; Raney 1976).

Los Angeles-Long Beach Harbor (Figure 4.2) consists of two adjacent ports, Los Angeles Harbor and Long Beach Harbor, in San Pedro Bay, California. Separate authorities constitute the administration of the two ports. San Pedro Bay was originally fully open to the south and southeast. Now the Los Angeles-Long Beach Harbor in the bay is protected by an 8-mile-long breakwater extending from Point Fermin eastward to near Seal Beach. The breakwater consists of three sections: the San Pedro breakwater, the

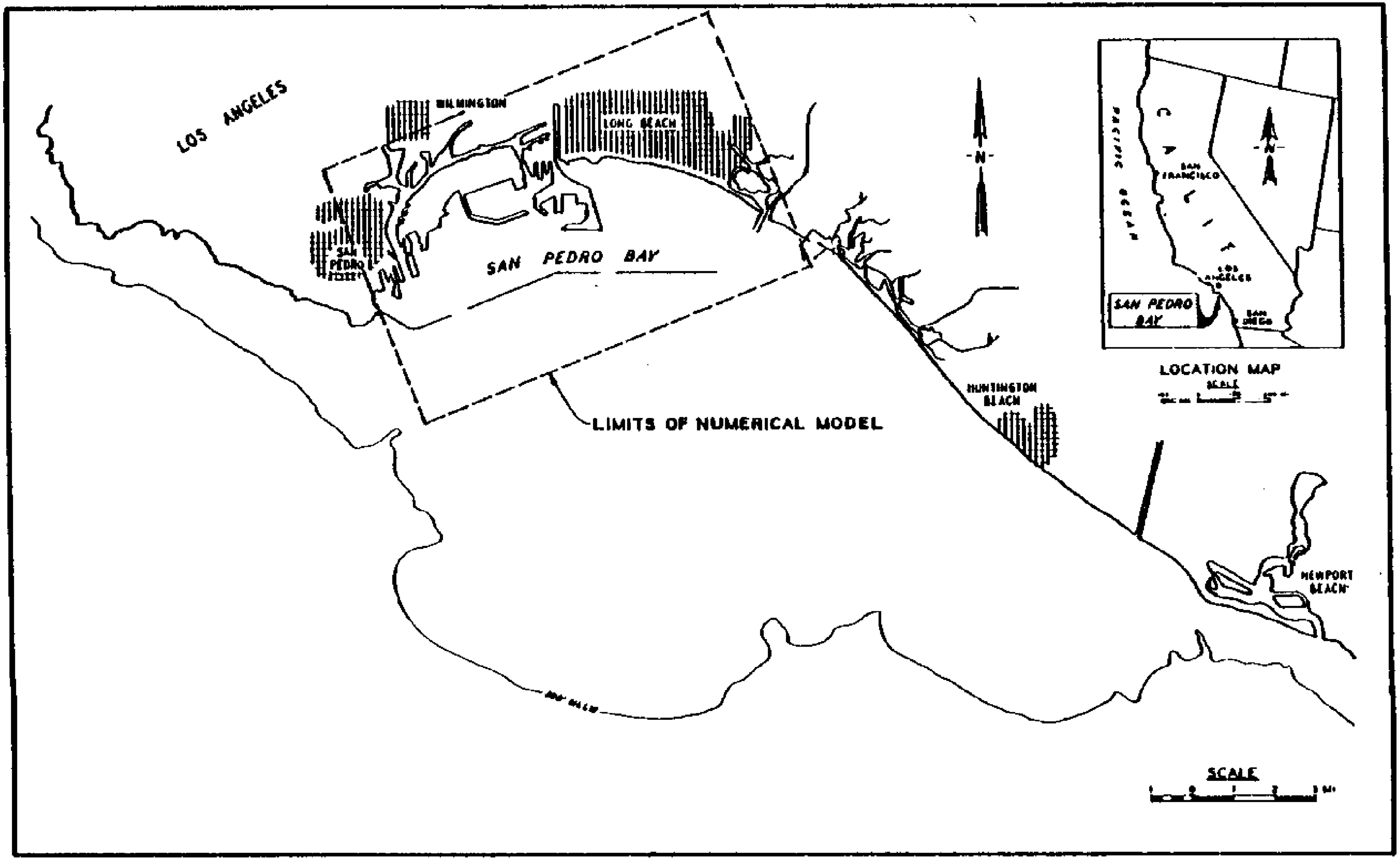

Figure 4.1 Site Map and Limits of Numerical Model.

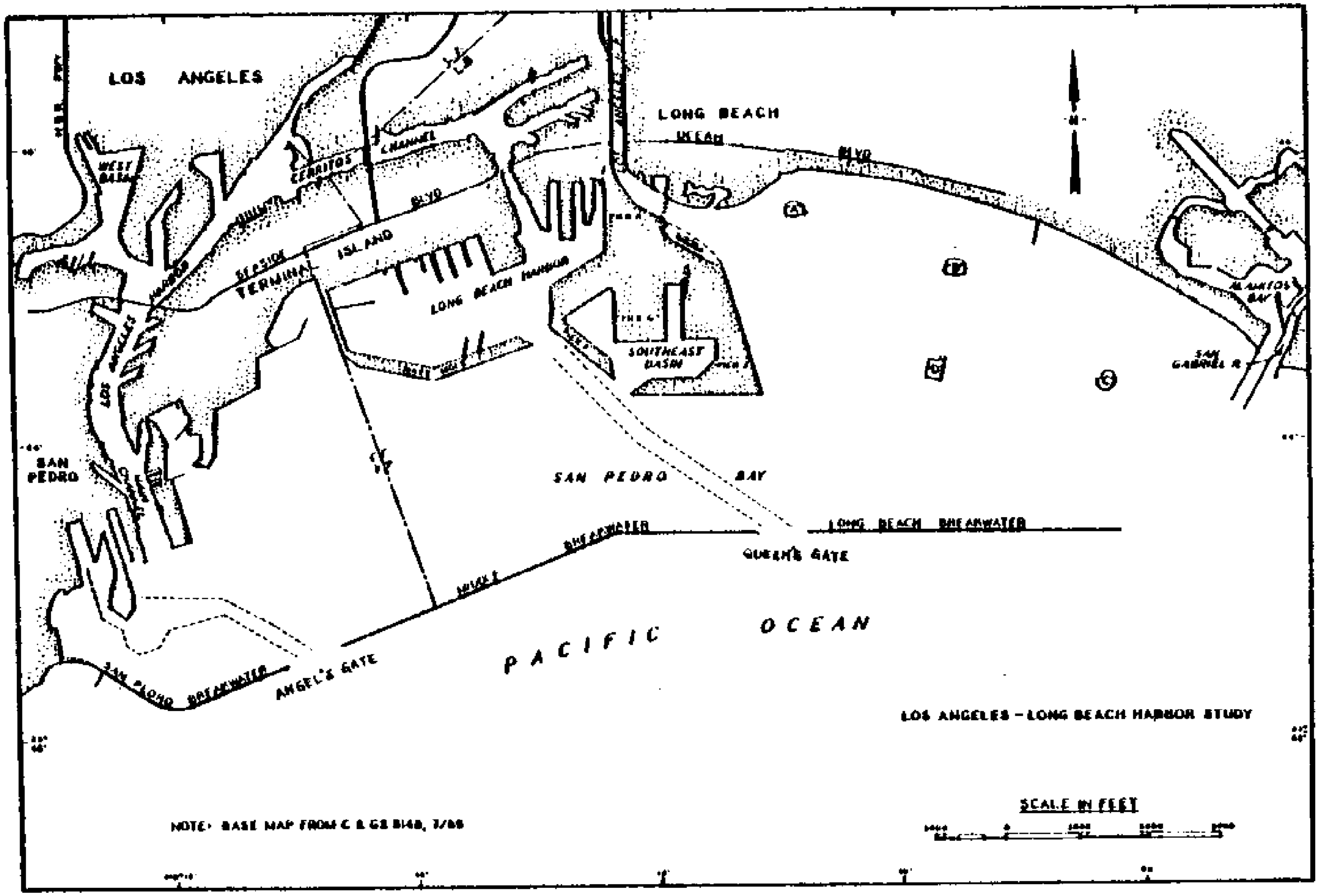

Figure 4.2 Base Map of Los Angeles-Long Beach Harbor.

Middle breakwater, and the Long Beach breakwater. The San Pedro breakwater is 11,000-ft long (McAnally 1975). It extends from the shoreline east of Point Fermin to Angel's Gate. The Middle breakwater extends northeasterly from Angel's Gate for 12,500 ft before it turns eastward for another 6,000 ft to Queen's Gate. The Long Beach breakwater extends 13,350 ft eastward from Queen's Gate. Angel's Gate, which is 2,100-ft wide, is the navigation opening for the port of Los Angeles. Queen's Gate, which is 1,800-ft wide, is the navigation opening for the port of Long Beach. To the east end of the Long Beach breakwater, the width of opening for the ship entrance is about 1 mile (see U.S. Department of the Army 1974).

The port of Los Angeles consists of Outer Harbor, Fish Harbor, Main Channel, West Channel, East Channel, Turning Basin, West Basin, East Basin Channel, East Basin, and some slips. The port of Long Beach consists of Outer Harbor, Middle Harbor, West Basin, Southeast Basin, East Basin, Inner Harbor, Cerritos Channel, and some small channels. Some basin characteristics summarized by McAnally (1975) are listed in Table 4.1 for reference. Four small islands inside the east bay are named (from west to east respectively) Island Grissom, Island Freeman, Island White, and Island Chaffee. Terminal Island is a relatively larger island located inside the Los Angeles-Long Beach Harbor.

Basin loaction	Surface area	Average depth below mllw	Low-water volume	Ratio of tidal prism to low-water volume in %		
	10^6 in sq ft	in ft	10^9 in cu ft	Neap tide (3.5 ft)	Mean tide (5.4 ft)	Spring tide (7.1 ft)
LA outer harbor	139	29	4.0	12	19	24
LA main channel	35	31	1.1	11	17	23
LA west basin	10	33	0.3	11	16	22
Eastern bay	250	35	8.8	10	15	20
LB outer harbor	123	46	5.7	8	12	15
LB SE basin	11	43	0.5	8	13	16
LB west basin	27	40	1.1	9	14	18
LB east basin	15	44	0.7	8	12	16
LB inner harbor	13	45	0.6	8	12	16
Total	623		22.7			
Average		36		10	15	20

Table 4.1. Basin Characteristics. (After McAnally 1975)

The boundary between the City of Los Angeles and the City of Long Beach cuts through this island. As one can see, such a complicated harbor layout makes it an ideal area to test the numerical model. In studying the circulation pattern, the flows in two perpendicular directions are of equal importance in this area. Therefore, it is clear that the grid spacings for two directions may be set equal to each other.

There are two sources of surface inflow into the harbor area. The Los Angeles River (los Angeles County Flood Control Channel), which drains an 832-square-miles basin, flows into Long Beach Outer Harbor (the east bay) and the Dominguez Channel, which is 8.5-miles long and collects runoff from an 80-square-miles area west of the Los Angeles River basin and flows into the East Basin of Los Angeles Harbor. The maximum discharge at the mouth of Los Angeles River is 110,000 cfs. The mean annual discharge is 5,240 million cubic-feet (see Southern California Coastal Water Research Project 1973). Most of the 16,000 acre-ft mean annual runoff that passes through the Dominguez Channel occurs during relative short intermittent periods during the winter months (see U.S. Department of the Army 1974). Comparing to the water volume in the harbor (see Table 4.1) and to the tidal discharge of more than one billion cubic-feet (see McAnally 1975, Table 2), these surface inflows can be neglected.

In the port of Los Angeles, the maximum mean-lower-low water depth is 46 ft inside its Outer Harbor; in the port of Long Beach, the maximum depth is 73 ft inside its Outer Harbor. The base of breakwaters is about 50-ft deep. Los Angeles Main Channel is 47 ft for width of 500 ft. Long Beach Channel is 60 ft for width of 700 ft (see U.S. Department of Commerce 1977a,b). The mean depth of water around the area where the large gyre appears occasionally is about 30 ft. The depth at Angel's Gate ranges between 44 and 50 ft. The water outside the breakwaters are deeper than 50 ft. The maximum depth in the study area is 109 ft at the southwest corner. The average value of a set of sampled depth data for the whole study area is 48 ft.

The study area is bounded by the latitude of 33°41'N and 33°47'N and the longitude of 118°06'W and 118°17'W (see Figure 4.2). In calculating the Coriolis parameter, 33.72° was used to represent the latitude of the study area.

The climate in this area is of the subtropic Mediterranean type. Precipitation occurs predominantly from November through April. The mean yearly rainfall observed at the Long Beach Weather Service Office is 25.1 cm (see Southern California Coastal Water Research Project 1973). The rainfall, if any, is too small to be considered as an input source to the numerical model.

During the daytime, southwest sea-breezes commonly blow with less than 10 fps. During summer afternoons, this velocity sometimes reaches 25 to 35 fps (see U.S. Department of the Army 1974). If the wind force were included into the model, at least one extra coefficient would have to be adjusted during hindcast runs. This extra variable would increase the difficulty in adjusting the coefficients of bottom friction and eddy viscosity. Since this research is focused on the tide-induced currents, the wind force terms were removed from the numerical model.

U.S. Department of Commerce (1977c) predicted that the mean range of tide in San Pedro Harbor (during 1978) would be 3.7 ft; the diurnal range, 5.3 ft; and the mean lower low water, 2.7 ft below mean sea level. In this area, the higher high always precedes the lower low.

Tidal currents play an important role in flushing the harbor. Without these currents, the effects of discharged waste would be greatly magnified and the variety of life forms would be severely restricted (U.S. Department of the Army 1974). Through a drogue study, Soule & Oguri (1972) obtained the circulation patterns in the Los Angeles Harbor area. In the later measurements, current speeds were found to be 0.1 to 0.2 knots (0.17 to 0.33 fps) at the surface (Robinson & Porath 1974). A current speed as high as 1.4 to 1.7 fps has been measured near the Angel's Gate (U.S.

Department of the Army 1974).

Winter storm waves and high summer swells are largely reflected or dissipated by the breakwater (U.S. Department of the Army 1974), but significant amounts of wave energy do penetrate directly through the breakwater (Lee & Walther 1974). However, the breakwaters are assumed impervious in this study. The effects of the porosity of breakwaters on the circulation pattern inside the harbor is left for future research.

4.2 Eddy Viscosity

The momentum equations (3.11) and (3.12) in Chapter 3 include eddy viscosity terms. Only horizontal eddy viscosity is considered in this research which studies two-dimensional planar flows. The value of the eddy viscosity coefficient depends on the type and scale of motion under consideration. It is time dependent and often varies considerably from one part of the fluid to another. In a numerical model, it should be adjusted to the grid spacings, the time step, and the particular numerical scheme used for realistic results. While there are many factors affecting this value, Sverdrup (1942) stated that no relation appeared between the value and the average current velocity. While it is not a physical constant characteristic of the fluid in motion, it can be determined from observed ocean currents (Durst 1924). In order to have an accurate numerical model, the value of the eddy viscosity coefficient should be determined from the hindcast runs of the particular numerical model of certain time step and grid spacings, for the specified area.

Only one single variable or one relationship among variables can be adjusted through hindcast tests. By hindcast, one can not determine a variable as a function of either time or space, unless the function is a mathematical function in which there is just one coefficient to be determined. So, in practical cases, the value of eddy viscosity is usually assumed to be either a constant value, or a one-coefficient function which depends on either (or both) grid spacing or flow conditions. The constant or coefficient can then be determined by trial and error until the differences between the calculated results and field data are acceptable. The function thus determined is valid for that particular degree of turbulence under the circumstances considered when that numerical model is used. However, it can well be used as an approximate value for similar flow conditions. Usually, a certain degree of error on this value would not cause much difference to the simulated results. Therefore, the data from other experiments can sometimes be used as a rough estimation. The eddy viscosity used in this study was assumed to be a constant value.

Proudman (1953) gave some methods to determine the eddy viscosity from field observations. Montgomery & Palmén (1940) determined the coefficient of horizontal eddy viscosity $A = 7\times10^{7}$ cm^2/sec = 7.5×10^{4} ft^2/sec for a stable Atlantic equatorial countercurrent. Based on dynamical principles, Munk (1950) obtained $A = 5\times10^{7}$ cm^2/sec = 5.4×10^{4} ft^2/sec for the western currents. This value compares favorably with the value of 4×10^{7} cm^2/sec and 7×10^{7} cm^2/sec which are determined from the diffusion of salt and from dynamical principles, respectively, for the Atlantic equatorial countercurrent (Munk 1950). Stommel (1955) found $A = 10^{6}$ cm^2/sec = 1.1×10^{3} ft^2/sec from the current measurements in the Straights of Florida. Holland (1977) proposed the same value based on dynamical principles. Tee (1976, 1977) used this value in his numerical model of Minas Channel and Minas Basin. Crean (1978) used the same value in a numerical model and indicated that, in view of the grid spacing of 2 km and the time step of 23 sec, this value implied a relatively small degree of lateral averaging. For the length scale in the order of 20 to 30 km, Fofonoff (1962) found that the value ranges from 10^{6} cm^2/sec for a small current system to 10^{10} cm^2/sec for the Antarctic circumpolar current (see also Hidaka & Tsuchiya 1953). Von Arx (1962) showed the value ranging from the order of 10 through 10^{9} cm^2/sec, depending on the scale of fluid motion. The smaller values were obtained from the rate of spread of dye spots; the larger values from studies of horizontal motion on an oceanic scale such as the diffusion of mass or momentum associated with the meandering flow of the Gulf Stream. Bowden (1962) cited the values of 5×10^7 cm^2/sec and 10^8 to 10^9 cm^2/sec. Both Neumann (1968) and Nihoul (1975b) cited a value of the coefficient as 10^8 cm^2/sec, or 1.1×10^5 ft^2/sec. Crowley (1970) termed this value a standard linear eddy viscosity. By comparing the computed results against the field data, Bowman (1978) determined the same value for the Hudson River effluent, and stated that the value was two orders of magnitude larger than values often taken for open ocean viscosities, due to the large surface slopes found within the effluent. Marchuk et al. (1973) used the same value for their North Sea model but another value of 8.5×10^8 cm^2/sec for their Arctic Seas model. Both of these two values were obtained through calibration. Liggett (1970) tested his lake circulation model with various values of eddy viscosity coefficient range from 0 to 1.56×10^8 cm^2/sec and found that the lower values might be more realistic. Nihoul (1975a) gave the value in the order of 10^3 cm^2/sec for the length scale of 5 m and in the order of 10^6 cm^2/sec for the scale of about 5000 m.

It seems that the coefficient of eddy viscosity can vary within a great range, depending on many factors. It is especially difficult to choose a suitable one for a particular model. In addition, nearly all of the values cited above are obtained from large scale motions. No study on the coefficient for the circulation in harbors are found in the literature.

However, from the dimensional arguments based on the two-dimensional turbulence, Crowley (1968, 1970) and Leith (1969) proposed that the coefficient of eddy viscosity is linearly proportional to the grid spacing, as shown in equation (2.5) in Chapter 2. Therefore, the value for the circulations in a harbor should be small compared to those obtained from the large scale oceanic motion. With this assumption of the linear relationship, the interpolation of the data given by Nihoul (1975a) yields the coefficient of horizontal eddy viscosity on the order of 30 ft^2/sec for the numerical model with a grid spacing of 500 ft.

The following discussions in this section are presented in order to point out how a constant coefficient of eddy viscosity is affected by a particular numerical model.

In the present model, the finite difference form of the x-direction momentum equation is, as shown in equation (3.60) in Chapter 3,

$$-kE^{+} + d_{+}U^{+}_{+,j} + kE^{+}_{i+1,j} = b^{+} \qquad (4.1)$$

where both k and d_+, which have been defined in equation (3.63) and (3.64), are independent of $U^-_{+,j}$, and b_+, defined previously in equation (3.62), can be written as

$$b_+ = U^-_{+,j} + 8(\Delta t)A(\bar{\bar{U}}^-_{+,j} - U^-_{+,j})/(\Delta s)^2$$

$$- (\Delta t)U^-_{+,j}\{ (U^-_{i+3/2,j} - U^-_{-,j})/(2\Delta s) + 2g[(U^-_{+,j})^2 + (\bar{\bar{V}}^-_{+,j})^2]$$

$$/[(\bar{H}^x)_{+,j}(\bar{C}^x_{+,j})^2] \}$$

$$+ (\Delta t)\bar{\bar{V}}_{+,j}[2f - \delta_y U^{+*}_{+,j} - (U^-_{+,j+1} - U^-_{+,j-1})/(2\Delta s)]$$

$$+ 2(\Delta t)(W_x)_{+,j} \tag{4.2}$$

The eddy viscosity term acts as a modifier to U in the acceleration term. The first two terms can be rewritten as

$$b' \equiv U^-_{+,j}[1 + 8(\Delta t)A(\bar{\bar{U}}^-_{+,j}/U^-_{+,j} - 1)/(\Delta s)^2] \tag{4.3}$$

which can be considered as the value of $U^-_{+,j}$ in the acceleration term modified through the smoothing effect due to the eddy viscosity. There are two remarkable values of the coefficient A. The first is

$$A = 0 \tag{4.4}$$

such that $b' = U^{-}_{+,j}$ (4.5)

which means that there is no effect from the eddy viscosity. The second is

$$A = (\Delta s)^2/(8\Delta t) \tag{4.6}$$

such that $b' = \overline{\overline{U}}^{-}_{+,j}$

$$= (U^{-}_{i+3/2,j}+U^{-}_{-,j}+U^{-}_{+,j+1}+U^{-}_{+,j-1})/4 \tag{4.7}$$

which indicates that $U^{-}_{+,j}$ in the acceleration term is totally smoothed out and is replaced by the average value of the four surrounding points.

The value of A should normally be bounded by those of equations (4.4) and (4.6) such that the value of b' lies between equations (4.5) and (4.7). Any value of A beyond those two limits would cause a kind of "negative smoothing" effect. In view of a practical application, the value of A should lie in an even smaller range between those two limits.

Therefore, if the grid spacing is 500 ft and the half-time-step is 180 sec, the value of eddy viscosity in this model should not exceed 173 ft^2/sec, according to equation (4.6). This limit is proportional to the square of grid spacing and is inversely proportional to the time step used in simulations. In simulating circulation patterns in a harbor area, the grid size is relatively small, and the coefficient of eddy viscosity should be carefully chosen such that it does not exceed the higher limit. The value should be lower when the time step is larger.

Different values of eddy viscosity coefficient range from 0 to 10,000 ft^2/sec were tested in the present study to see the effects of this parameter.

4.3 Roughness Coefficient

In this numerical model, the Chezy coefficient is determined through equation (3.6):

$$C = 1.486H^{1/6}/n \tag{4.8}$$

where H denotes the total depth and n denotes the Manning's roughness coefficient which is assumed to have a constant value. The mean water depth was used to determine C in equation (4.8) and hence C is independent of time in this study. Although the actual total depth may be used to correct C at every half-time-step, it is time-consuming and it is doubted whether there is any visible improvements over the simulation results.

The value of Manning's n for flows in pipes, lined canals, or natural channels have been tabulated in many textbooks and handbooks of hydraulics or fluid mechanics (e.g., Chow 1959). Yet there are very few studies which focus on the bottom friction coefficient for flows in the coastal area. Usually a value is picked from the one for the natural channel of comparative condition. The value so chosen may be improved during the trial and error process.

In order to make the discussion clearer, the following two equations are repeated from equations (3.8) to (3.10):

$$F_x = C'qU/H$$

$$= gqU/(HC^2) \tag{4.9}$$

$$C' = g/C^2$$

$$= n^2 \; g/(1.486^2 H^{1/3}) \tag{4.10}$$

where C' is a dimensionless roughness coefficient.

Hansen (1962) gave C' = 0.003 and expected this value to be applicable to both estuaries and open oceans. Marchuk et al. (1973) followed this value to calculate the water movements in North Sea and in Arctic Seas. Tee (1976, 1977) used the same value in his numerical model of Minas Channel and Minas Basin. Crean (1978) used the same value in the Strait of Georgia and in Juan de Fuca Strait, between Vancouver Island and the mainland coast. In the region of the channels between the San Juan and Gulf Islands, the value was increased to an unusually high value of 0.030. This high value in the island region was derived from calibration (Crean 1978). Dronkers (1964) stated that C' lies between 0.002 and 0.003 in tidal computations. It follows from equation (4.10) that the Chezy coefficient, C, lies in the range of 103 to 127 $ft^{1/2}$/sec. Patridge & Brebbia (1976) indicated that C' in shallow water problems is usually less than 0.004 which is corresponding to C > 90 $ft^{1/2}$/sec. Li (1977) took C' = 0.0025 for his Kiel Bay model, which is equivalent to have C = 113 $ft^{1/2}$/sec. Blumberg (1977a) found that the best simulation of the circulation in Chesapeake Bay is produced by using a constant value of 0.0025. The author also stated that the coefficient is a sensitive parameter in a long, shallow bay.

Leendertse (1967) used C = 50 $m^{1/2}$/sec = 91 $ft^{1/2}$/sec for his Tokyo Bay model. The same author obtained the following expression experimentally from computations of his Haringvliet model:

$$C = 19.4 \ln(0.9H) \qquad (4.11)$$

in which all units are in MKS system and H denotes the total depth. Apparently, this equation does not apply to the cases of H lower than 1.1 m. The input data of the Chezy coefficient ranges from 40 to 145 $ft^{1/2}$/sec in his Haringvliet model. Prandle (1972) used 90 to 160 $ft^{1/2}$/sec for C in his one-dimensional model and C = 100 $ft^{1/2}$/sec for his two-dimensional model of the St. Lawrence River. Based on a simplified momentum equation, Reichard &

Celikkol (1978) developed a method for fast selection of the bottom friction coefficient in the calibration process.

Wang & Connor (1975) indicated that normal values of Manning's n for a two-dimensional unsteady circulation ranges from 0.025 for stony bottoms, 0.030 for bottoms with small rocks, to 0.035 and 0.040 for sandy bottoms. Blumberg (1977b) cited n = 0.022 as the value to produce the best result in the prediction of the tidal characteristics of the Potomac River Estuary.

This study used n=0.020 in the basic run. Cases of n=0 and n=0.040 were also tested to check the sensitivity of the model. Values of C and C' corresponding to n=0.020 and n=0.040, calculated from equations (4.8) and (4.10), are plotted in Figure 4.3, for the range of water depths in this study area. It can be seen that n=0.040 may be too large as te corresponding C' in Figure 4.3 is larger than 0.005 for the whole range of water-depth used.

4.4 Boundary Conditions

Two kinds of boundaries were used in this study. The first is called the solid boundary which can be considered as a high, impervious wall. This was used for the coastline and breakwaters. The velocity normal to the solid boundary vanishes at every grid point along the solid boundary.

The second kind of the boundary is called the open

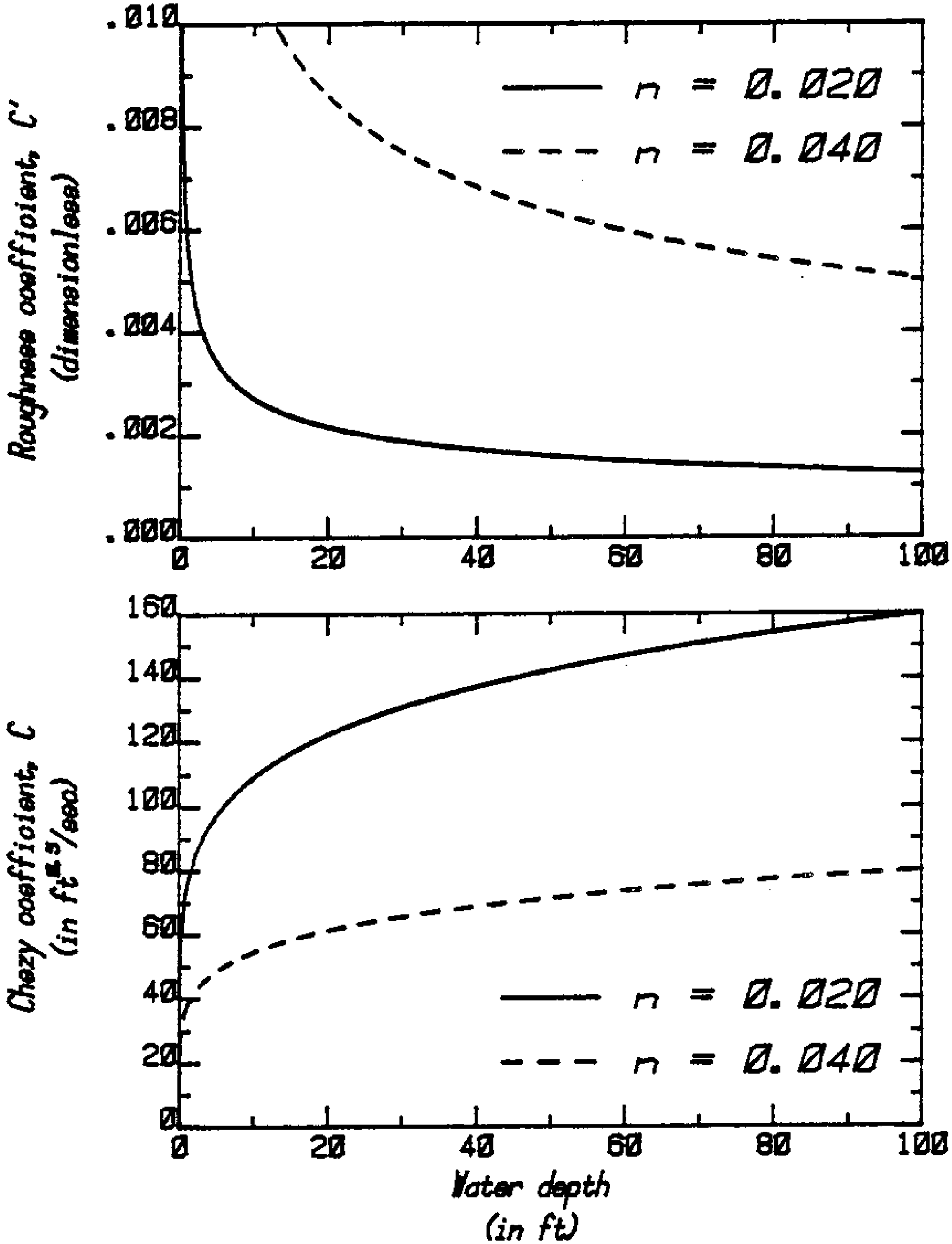

Figure 4.3 Roughness Coefficients corresponding to the Manning's n Used in this Study.

boundary which represents the limit of the study area to the open ocean. Tidal elevation as a function of time was specified along the open boundary.

The numerical model can be modified slightly to allow for other kinds of boundary conditions such as a pervious boundary or an open boundary specifying with either discharge or velocity. The former boundary can be associated with the conditions of pervious breakwater; the latter can be used for surface inflows.

In the Los Angeles-Long Beach model, the open boundary is composed of two sections. The length of the section on the east side is 13,500 ft. The section on the south side is 53,500-ft long and meets the West Jetty outside of the Anaheim Bay at the southeast corner of the study area. Since these two sections are relatively short and they are inside the open-ocean area, the difference of tidal elevations of any two points on these two sections can be neglected. A single tidal function was applied to all points along the open boundary.

Three sets of tidal data were used in the numerical tests. For the basic run, a cosine function was assumed for an M_2 tide (which is an ideal tide induced by only the lunar force) with the range of 5.6 ft and period of 12.5 hr. The other two sets of tidal data were those of spring tide and neap tide used for the hydraulic model of Los

Angeles and Long Beach Harbors studied by the U.S. Army Engineer Waterways Experiment Station (McAnally 1975). The digital data of these two kinds of tide were obtained from the Waterways Experiment Station (Outlaw 1979). Discrete data was recorded at 30-min interval for a 25-hr tidal cycle (marked with solid circles in Figure 4.4). The elevations were expressed in feet above the mean lower low water.

At the first trial of using tidal data, the digital data were read into the computer directly. Since the original data were taken at 30-min intervals, a linear interpolation was applied to obtain the boundary condition data at the interval of a half-time-step which was 3 min in the base run. The results (see details in Chapter 5) showed that both the picture of circulation pattern and the time history of elevation appeared normal. Yet the time history of velocities showed a small oscillation with a period of 30 min. A second-order polynomial interpolation was then used to supply the boundary condition for every half-time-step. It gave results similar to those obtained from the linear interpolation.

The oscillation appeared because the original data were not smooth and the differences of tidal elevations between successive half-time-steps were not smooth in time. The abrupt change of $\Delta E/\Delta t$, which is the forcing function

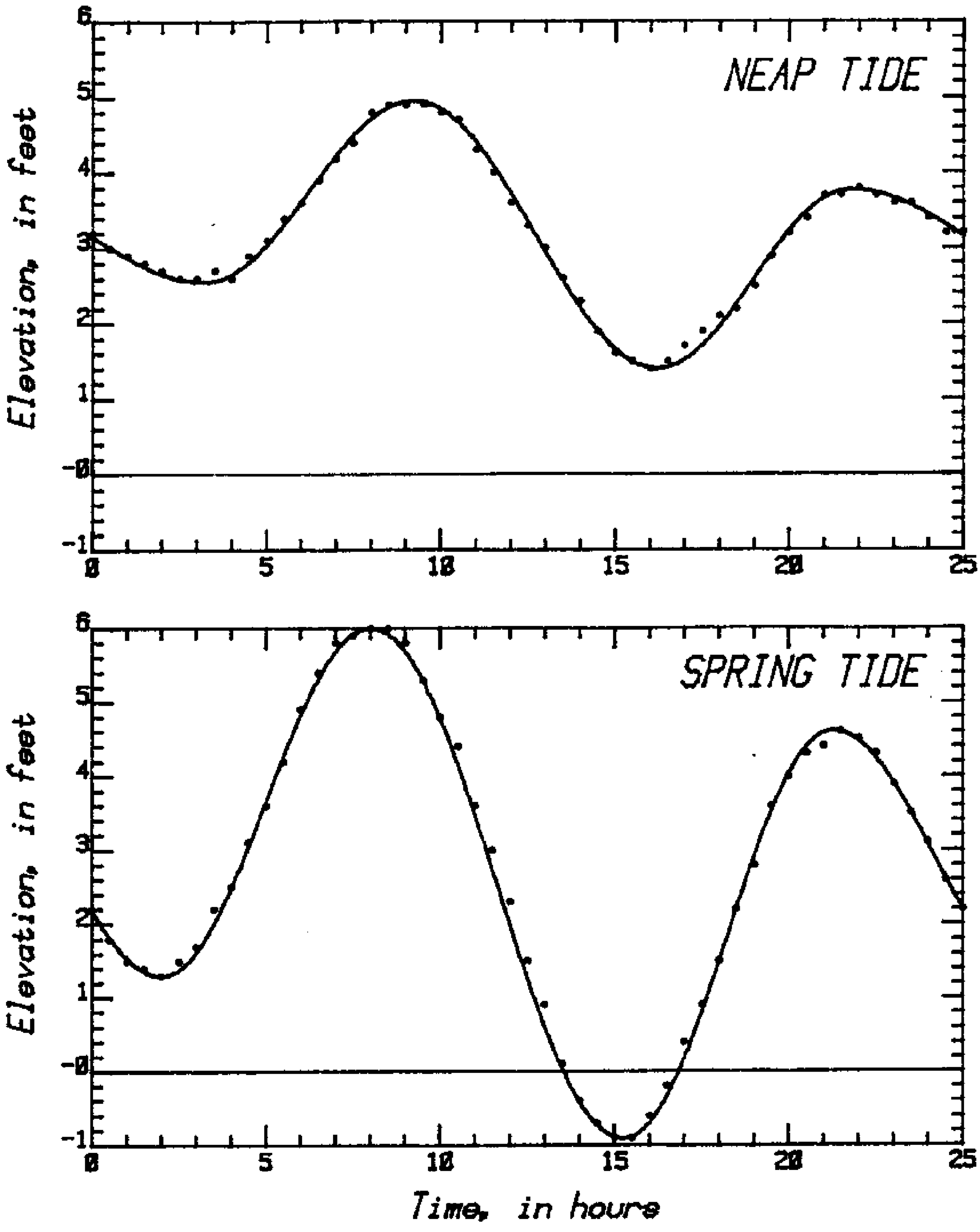

Figure 4.4 Comparison of Inputted Tidal Elevations (Shown in Solid Curve) and Original Data (Marked with Solid Circles) for Spring and Neap Tides.

of the tidal flows, would make the velocity change rapidly. When this abrupt change of $\Delta E/\Delta t$ occurs every 30 min, the time history of velocities would show dramatic change of amplitude every 30-min.

In the third and fourth trials, the data obtained through the second-order polynomial interpolation were smoothed once and twenty times, respectively, by a filter

$$E'_j = (E_{j-2}+4E_{j-1}+6E_j+4E_{j+1}+E_{j+2})/16 \qquad (4.12)$$

Both trials showed similar results as before although the time history of velocities appeared much smoother.

It seems that the digital tidal data can not be used directly as the boundary condition data, unless the first-order derivative of the data is relatively smooth. Yet there are still exceptions. Leendertse (1967) used digital tidal data as input data for his Haringvliet model. One could not tell whether the author had any of the similar problems, because the time histories of transport in that memorandum were plotted at 60-min intervals although the time histories of surface elevation were plotted at 6-min intervals. However, the experiments of Leendertse may not show this kind of oscillation because of two possible reasons. First, due to the large study area, Leendertse had five sets of tidal input (which were of different characteristics for the first-order derivative) at five locations. Along the open boundary, at every grid point in a section between two of those five locations, the boundary condition was obtained through linear interpolation of the data at two ends of the section. At any point inside the field, the velocity changes due to the effects of unsmoothed data from every open-boundary point could possibly cancel each other. Secondly, the tidal data were inputted every half-time-step. The data did not have any characteristic pattern for any time period. As a result, the oscillation of velocity curve, if any, would be of the period of one half-time-step and would disappear from a figure in which the data were plotted at a half-time-step or larger interval.

If only one set of data is applied to the whole open boundary, the best approach is to have the data represented by a mathematical function which is smooth in the first-order derivative.

Different methods of curve fitting have been tried. It was found that due to limited number of observed data, a harmonic analysis of tides with periods of a few (for example, eight) important constituents specified (Dean 1966)

$$E_t = a_o + \sum_i^N [a_i \sin(2\pi t/T_i + d_i)] \tag{4.13}$$

can not be used to determine the phases and amplitudes in a tidal function, unless the function describes only an M_2 tide which has a single tidal-period of around 12.42 hr.

If the periods are not specified, the general harmonic analysis

$$E_t = a_o + \sum_i^N [a_i \cos(it) + b_i \sin(it)] \qquad (4.14)$$

gives quite satisfactory results if a proper number of constitutes, N, is chosen. However, it was considered too time-consuming to use equation (4.14) to calculate the tidal elevations for every point along the open boundary at every half-time-step, because N is usually large.

Finally, it was determined to pick up four extreme points, i.e., higher low, higher high, lower low, and lower high, from the 25-hr tidal data and construct four cosine functions in between these four extreme points. For illustration, let the four extreme points be (E_k, t_k; k=1,2,3,4). Let

$$E_5 = E_1 \qquad (4.15)$$

$$t_5 = t_1 \qquad (4.16)$$

Then the tidal elevation at any time between t_k (k=1,2,3,4) and t_{k+1} can be assumed to be

$$E_t' = 0.5(E_k - E_{k+1}) \cos[\pi(t-t_k)/(t_{k+1}-t_k)] \quad (k=1,2,3,4) \quad (4.17)$$

The first-order derivative of the elevations thus determined is smooth in between extreme points and approaches zero when a data point shifts toward any extreme point. Figure 4.4 compares the original data and the tidal data calculated from equation (4.17). The original data were marked with closed circles. The calculated data were plotted at 3-min interval while the neighboring points were connected by straight line segments. The figure indicates that the curve represented by equation (4.17), which composed of four cosine functions, is a good approximation of the original data. Having used these four cosine functions, the simulation results showed normal time-history of velocities, thus, the undesirable oscillations in the velocity history described previously are eliminated.

4.5 Other Input Data

Navigation charts for the study area, published by the National Ocean Survey (U.S. Department of Commerce 1977a, 1977b), were used to design the grid network, to locate boundaries, and to estimate water depths.

Due to the natural property of the alternating direction implicit technique used in numerical models, the simulation results may depend on the orientation of the coordinate system, especially if the time step is large. The flow is easier to go straight forward along either the x- or y-direction than go through in a zigzag fashion. To study the gyre structure in the Los Angeles Outer Harbor, the y-axis was set about 23.5 degrees west from north, such that the x-axis is parallel to the east half of the San Pedro breakwater and the west two-third of the Middle breakwater. The y-direction flow through Angeles Gate is normal to the opening between breakwaters. Most of the flow directions in Los Angeles Main Channel is parallel to the y-axis. Cerritos Channel is almost parallel to the x-axis.

As to choosing the grid spacings, several factors were considered. First, based on the consideration of geometry of the study area, the x- and y-direction grid spacings were taken to be constant and equal to each other. Secondly, in order to reveal the true structure of the interested gyre in the outer Los Angeles Harbor (which is of the dimension of about 10000 ft), the grid spacing should not exceed 1000 ft.

The third factor considered was the widths of navigation spacing for the harbor. With a moderate change in an opening, there will be little effect on the tidal prism in the Harbor as well as the discharge through the opening. If the discharge is constant, the velocity is inversely proportional to the width of the opening. In this numerical model, which has constant grid spacing, the width has to be represented by an integral multiplication of the spacing. The widths of Angel's Gate and Queen's Gate are 2100 and 1800 ft, respectively. Since this study focuses on the gyre structure to the north and northeast of Angel's Gate, the width of this gate is the more important factor to be considered. The spacing was finally set to be 500 ft. When the x-axis is set parallel to the east half of the San Pedro breakwater and the west two-third of the Middle breakwater, the width of Angel's Gate in the numerical model is represented by four grids or 2000 ft. The width of Queen's Gate in the model is $500 \times 4 \times \sec[\arctan(2/4)] = 2236$ ft(cf. input map in Appendix B.1). The width of the opening to the east of the Long Beach breakwater is so large compared to the grid spacing that diferent grid spacing has little effect on the computed velocity during simulations.

The fourth factor considered was the width of the inner channels. The width of Los Angles Main Channel is about 1,000 ft which can be represented by two 500-ft grid spacings. Cerritos Channel west of the Heim lift bridge is 500-ft wide and its east part has a width that varies from 700 to 1000 ft. It was considered appropriate to choose 500 ft as the grid spacing although a smaller one like 300 or 250 ft would give a better representation of those narrow channels.

The grid spacing used in this study area was finally decided to be a constant value of 500 ft, comparing to 300 ft used by Raney (1976) for the same study area. Using a smaller grid spacing would have the network fit the harbor geometry better. Yet it would cost more computer storage and computation time, since a smaller grid spacing is usually accompanied by proportionally smaller time step.

With the grid size and the orientation of net work chosen as outlined above, this Los Angeles-Long Beach Harbor model consists of 108x69=7425 grid points, among which 4695 points are actually involved in the computation.

In this implicit finite-difference model, the time step is not limited by the Courant-Friedrichs-Lewy stability criterion, equation (2.1). Dronkers (1975) indicated that the grid spacing for the implicit method can be several times larger than that for the explicit method depending on the particular problem. It implied that when the grid spacing is fixed, the time step for implicit methods can be several times larger than that for explicit methods. Peaceman & Rachford (1955) stated that the alternating-direction-implicit method is stable for any size of time step. Nevertheless, the size of time step does affect the accuracy of simulation results. Leendertse (1967) proved that the higher the Courant number, the larger the wave deformation. However, due to the long wave-length and small grid-spacings in this study, the wave deformation is negligible, as can be seen from the figures provided by Leendertse (1967).

Patridge & Brebbia (1976) gave an accuracy criterion as

$$t < T/20 \tag{4.18}$$

based on the argument that 20 points may reasonably well represent a smooth sine curve. That is, if T is taken to be 12.42 hrs for an M_2 tide, the half-time-step, which is the time interval to yield a data point, should be no larger than 2236 sec. Hinwood & Wallis (1975) stated that the time step for models of tidal waters usually ranges from 300 to 1200 sec, depending on the grid spacing and the numerical formulation.

In calculating the tidal oscillations of the North Sea by using an explicit finite element technique, Grotkop (1973) simulated seven semidiurnal tidal cycles, the first four with time step of 1800 sec and the last three with a time step of 900 sec. Marchuk et al. (1973) used a time step of 7200 sec to calculate the water movements in the North Sea and the Arctic Seas by using an implicit finite difference technique. Baltzer & Schaffransk (1978) used 90 sec as the time step to calculate the circulation in the Port Royal Sound; and Butler (1978) used 180 sec for the Balvestor Bay.

The basic run in this study selected 360 sec for a full time-step. With a grid spacing of 500 ft and a maximum depth of 109 ft, the dimensionless parameter $\Delta T(2gH)^{1/2}/(\Delta s)$ reaches 60 for the basic run. To see the effect of different time steps, computer runs with the step size ranges from 5.625 to 720 seconds were tested.

Simulation results from computer runs of different tidal inputs and from some sensitivity tests are presented in the next chapter. For every computer run, part of the data obtained from the major program which performs the simulation process were fed into the auxiliary program listed in Appendix B.2 to plot the time histories of surface elevations and velocity components at two arbitrary chosen points (22,20) and (22,60). Point (22,20) is located just inside Angel's Gate of Los Angeles Harbor. The velocity in the y-direction is relatively large at this point. Point (22,60) is located north to Queen's Gate inside the Long Beach Outer Harbor. A relatively strong x-direction current passes through this point. The time histories were used to check the stability and to see if the results showed repeating cycles after a certain simulation time.

Part of the output from the major program were fed into the auxiliary program listed in Appendix B.3 to have flow patterns plotted by an electromechanical plotter. Two kinds of flow patterns were plotted. One of them shows the velocity vectors for every grid point at a time instant.

It serves as if a snap shot of the velocity distribution in the study area. The velocities plotted are the depth-averaged ones instead of the bird's-eye view of surface velocities.

The second kind of plots show residual velocities. Residual velocity is the velocity of the corresponding residual current. The term "residual current" is defined here as that part of the current that is left after removal of the diurnal, semidiurnal and higher frequency signals (see Tee 1977). It can be either an Eulerian or a Lagrangian residual currents. The former is the residual current at a fixed point in space, whereas the latter is that of a water particle. In this report, the term "residual" refers to the Eulerian residual. The residual values may be produced by the existence of nonlinear bottom-friction, nonlinear eddy-viscosity terms, the nonlinear advective terms in momentum equations, and the nonlinear terms in continuity equation (see also Tee 1976).

The residual velocity can be considered as the mean velocity averaged over a long period. It is the net direction and amplitude of the motion of water particles. If the only forcing function in a model is a tide of which the integration of any component over a cycle is zero, then the residual velocity at any point in the study area is the local velocity averaged over the tidal cycle. Nihoul *et al.* (1978) defined the residual current as the mean current over one or several tidal cycles.

At a fixed point, if the arithmetic mean of the velocity over a tidal cycle is zero, the residual velocity is zero. This occurs when the oscillation of velocity is symmetry with respect to zero-line. If the tidal motion is the only forcing function, the residual velocity should be very small at a small single-entrance of a harbor, where the flow is essentially one-dimensional.

If the velocity is a constant value (for example, when a gyre stays at a position with a constant angular velocity), the residual velocity is the same as that value.

The residual velocity is studied here to help one understand gyre structures in the Los Angeles Harbor.

Results of computer runs are presented and discussed in Chapter 5.

CHAPTER 5

DISCUSSION OF RESULTS OF NUMERICAL EXPERIMENTS

5.1 Basic Numerical Test

The basic run simulated the tide-induced circulations in Los Angeles-Long Beach Harbor. The forcing function was a sinusoidal-type tide with a period of 12.5 hr and tidal range of 5.6 ft. The bathymetry was determined from the navigation charts published by the National Ocean Survey (U.S. Department of Commerce 1977a, 1977b). The network consists of 108x69 grid points. The grid size was 500 ft for both x- and y-directions; the time step 360 sec; and the Manning coefficient 0.020. The coefficient of eddy viscosity was set equal to zero in order to find out the stability without the influence from momentum diffusions. Momentum input from wind stress was excluded. The computer program and its input data used to run this basic test is listed in Appendix B.1. When the program was run in a VAX 11/780, the basic run took less than 50min of computer time to simulate 1,000 time steps, or eight semi-diurnal tidal cycles. The storage required to run the program listed in Appendix B.1 is 251 k (1 k = 1024 words) in a DEC-system computer.

Shown in Figure 5.1 to 5.4 are the velocity distributions at four stages during the ninth tidal cycle of the simulation in the basic run. Similar to all other figures of circulation pattern and residual velocity in this report, the solid lines in these figures represent the solid boundary of the harbor and the dashed lines represent the open boundary of the study area. Velocities shown in the figures are all depth-averaged velocities obtained from the computer output. For most of the figures concerning velocity pattern in this report, the velocity vectors smaller than 0.12 fps were not plotted in order to save the plotting time. In the figures of circulation pattern in this report, the term "peak" or "high tide" indicates the state the data were taken at the time when the tidal elevation along the open boundary reaches higher high water; "trough" or "low tide" indicates lower low water; "rising" or "flooding tide" indicates the tidal state of being midway between higher low water and higher high water; and "falling" or "ebbing tide" indicates the state of being midway between higher high water and lower low water.

Figures 5.1 to 5.4 indicate that a large clockwise gyre appears in the outer Los Angeles Harbor. The center of this gyre is north-northeast of Angel's Gate and is midway between the Middle breakwater and the Navy Mole on the Los Angeles-Long Beach city boundary. The current velocity of the gyre can be higher than 0.2 fps. During flood tide,

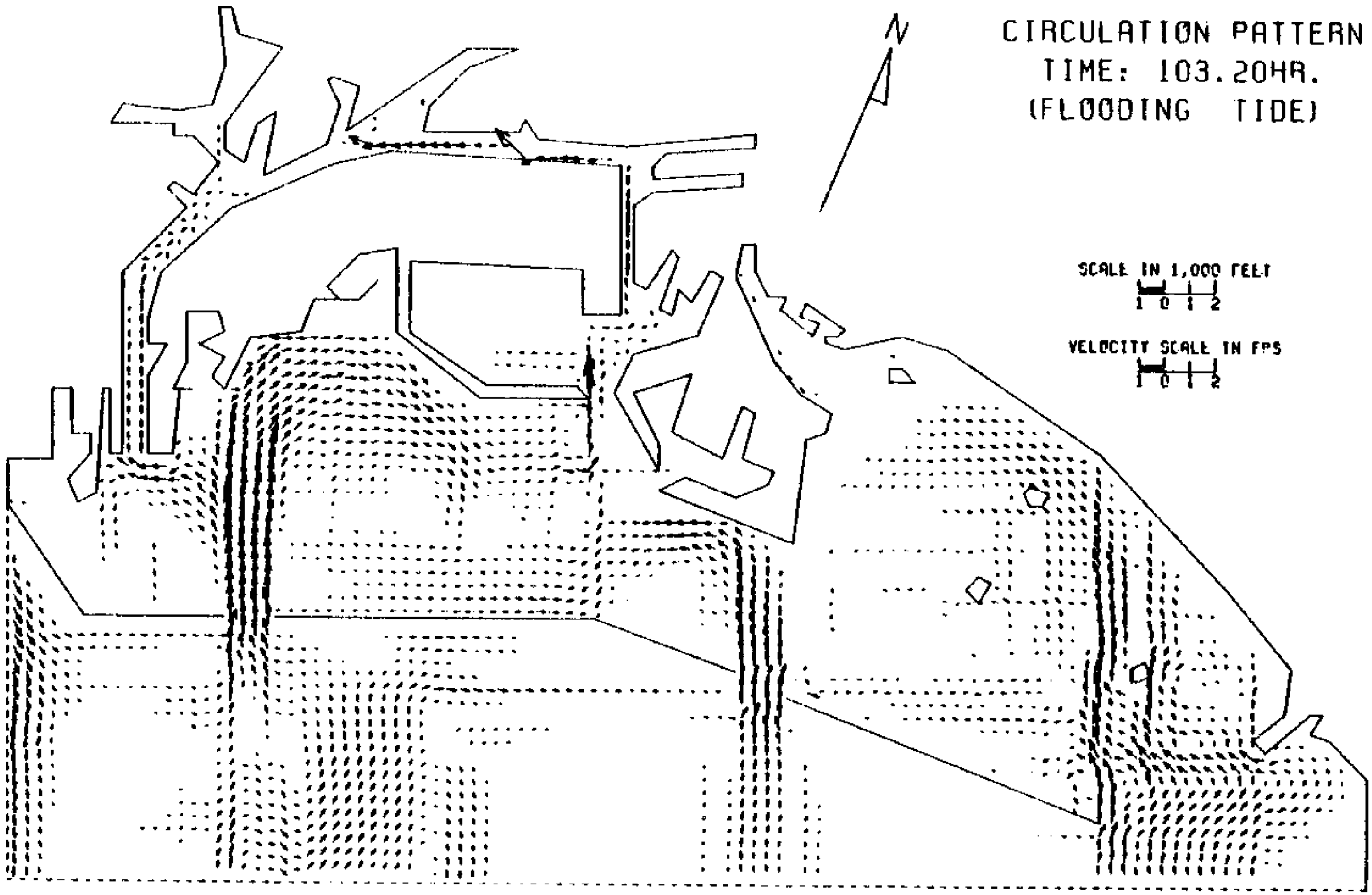

Figure 5.1 Circulation Pattern at t = 103.2 hr (Flooding Tide) for the Basic Test (Run #1).

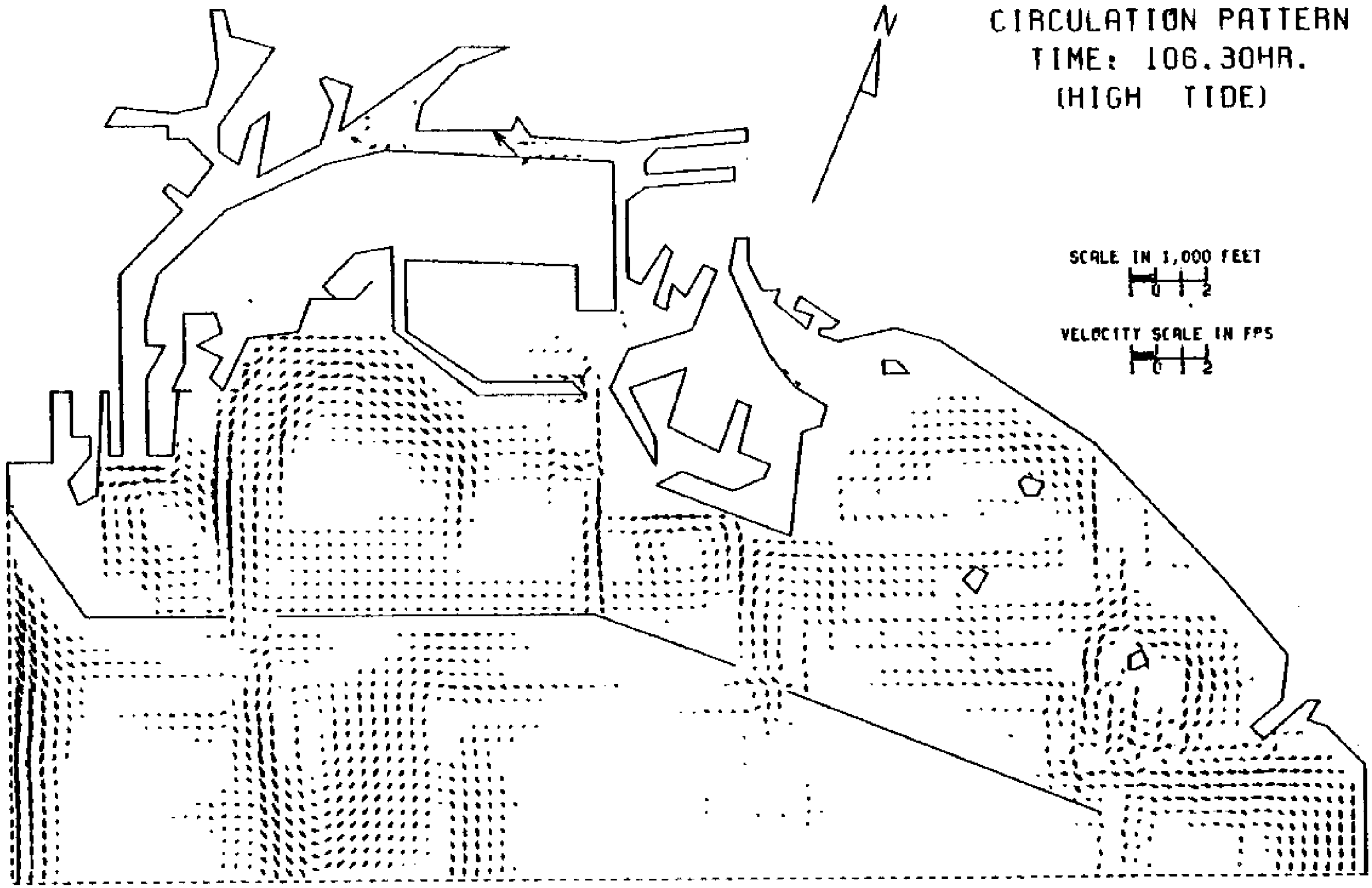

Figure 5.2 Circulation Pattern at t = 106.3 hr (High Tide) for the Basic Test (Run #1).

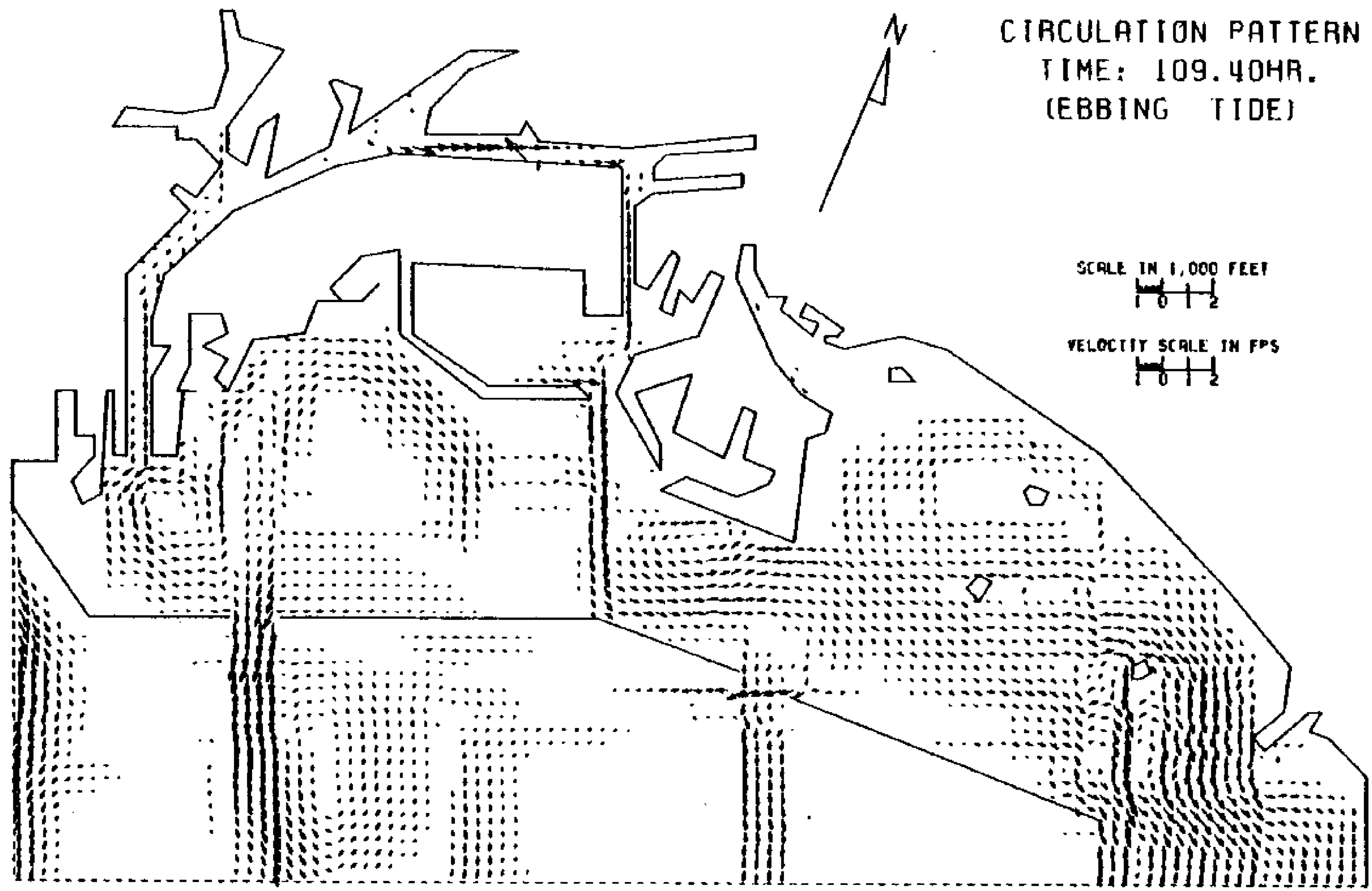

Figure 5.3 Circulation Pattern at t = 109.4 hr (Ebbing Tide) for the Basic Test (Run #1).

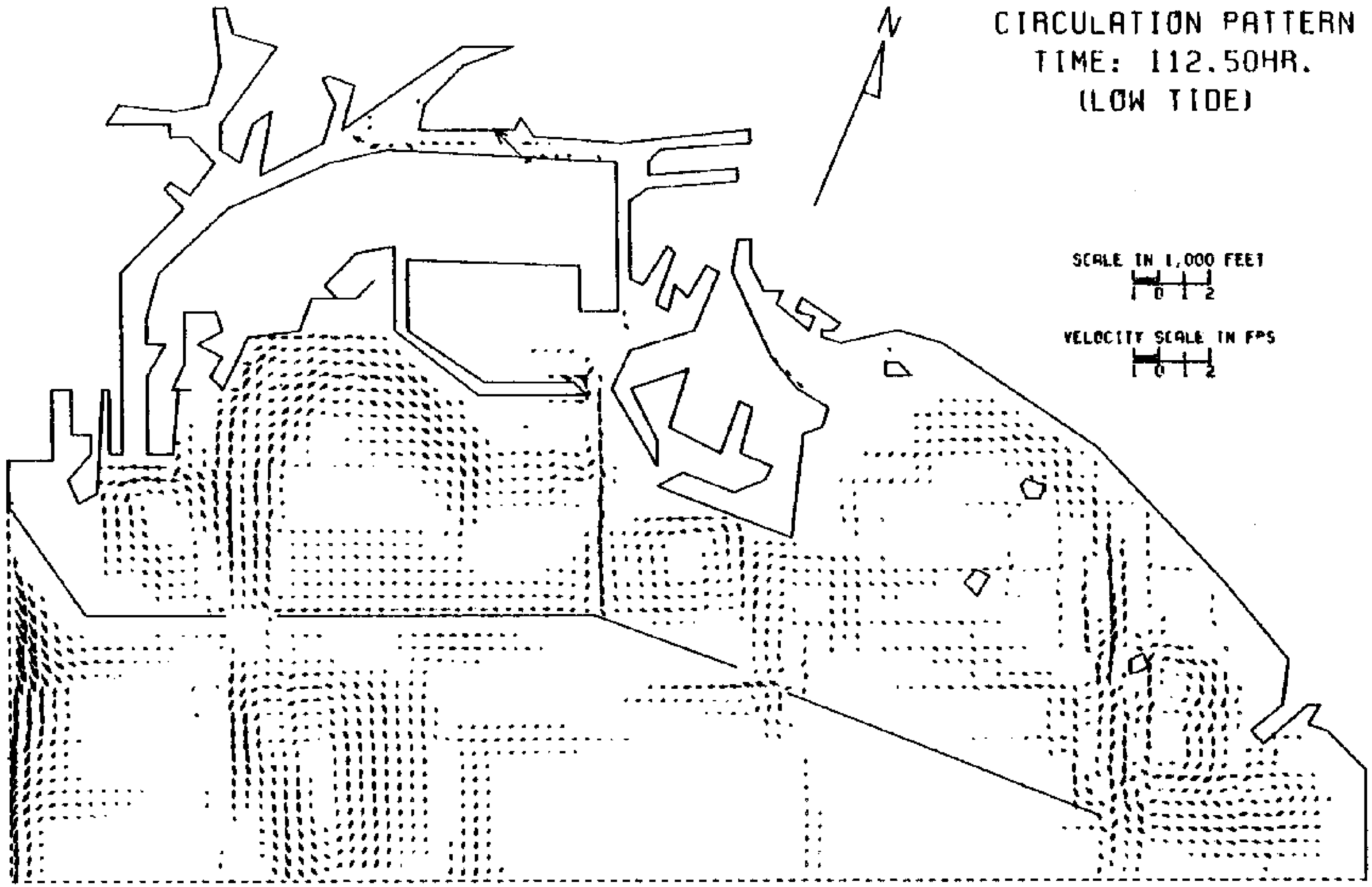

Figure 5.4 Circulation Pattern at t = 112.5 hr (Low Tide) for the Basic Test (Run #1).

currents from Angel's Gate and Queen's Gate are joined together giving recharge to this strong gyre. During ebb tide, most of the water in this gyre flows toward Angel's gate. The clockwise motion of this gyre persists throughout the whole tidal cycle. Two smaller counterclockwise gyres appear to the west of Angel's Gate and to the west of Queen's Gate. They disappear during the flood tide and show their strongest motion when the water flows outward from the Los Angeles Main Channel and Cerritos Channel during the ebb tide. A small clockwise gyre appears to the north of Queen's Gate when the current passing through the gate is weak. The circulation pattern to the north of the Long Beach breakwater is not simple due to the existence of small islands. Although the inputted tidal data are different, the circulation patterns from this test show the same basic features as those from the hydraulic model shown in McAnally (1975).

Figure 5.5 depicts the distribution of residual velocities in the study area. The data were obtained by taking the mean velocities in the tidal cycle which ended at the time shown on the figure, 112.5 hr. Backward and forward motions cancel each other out during the integration process. The remainder of what was left as residual velocities are the net velocities in that tidal cycle. A clockwise or counterclockwise residual-velocity pattern indicates that the flow there represents the fluctuation of

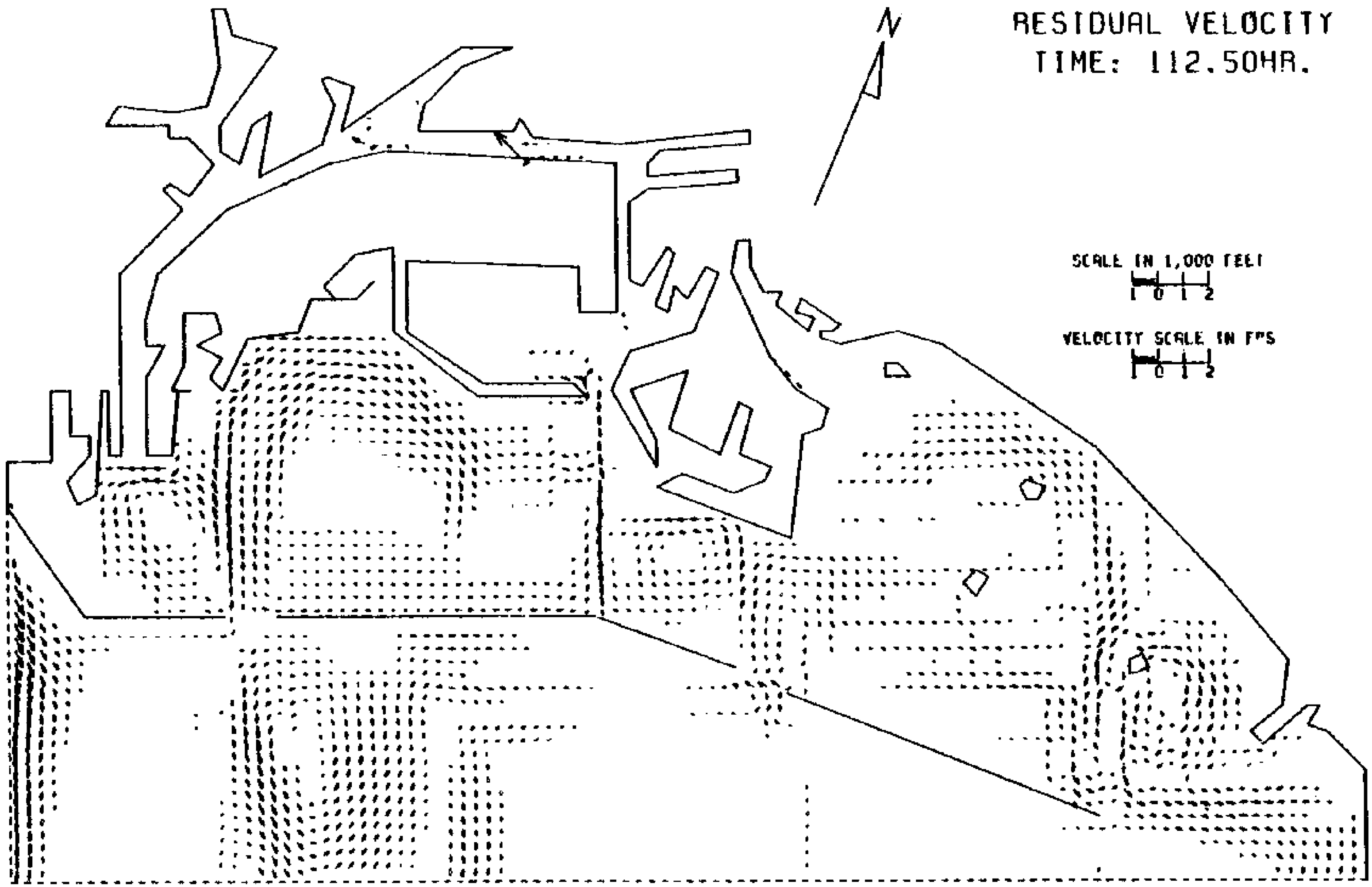

Figure 5.5 Distribution of Residual Velocities for the Basic Test (Run #1).

that circular motion. Since this study pertains to the circulation pattern in the Los Angeles Harbor, the figure of residual velocities is employed to identify the gyre structures. It is noticed that (for all different runs) after the flow is warmed up from the motionless initial state, the differences among the figure of residual velocity and the circulation pattern taken at high tide and low tide are very small.

Figure 5.6 shares the same velocity data with Figure 5.5. It has all velocity vectors plotted while Figure 5.5 (like most of other plots of circulation in this report) does not show velocity vectors with magnitude less than 0.12 fps. Figure 5.5 and 5.6 support the conclusions obtained previously from figures 5.1 to 5.4 about the gyre structures.

One can notice that there is higher recharge through Queen's Gate during the flood tide than discharge during the ebb tide. During ebb tide, as shown in Figure 5.3, the current coming out of the Cerritos Channel flows toward the eastern part of Long Beach Outer Harbor and increases the discharge through the opening east of the Long Beach breakwater. Figures 5.5 and 5.6 show net inflow through Queen's Gate and net outflow through the opening to the east of the Long Beach breakwater. There is also a small net inflow passing through Angel's Gate.

Figure 5.7 depicts a sequence of circulation patterns

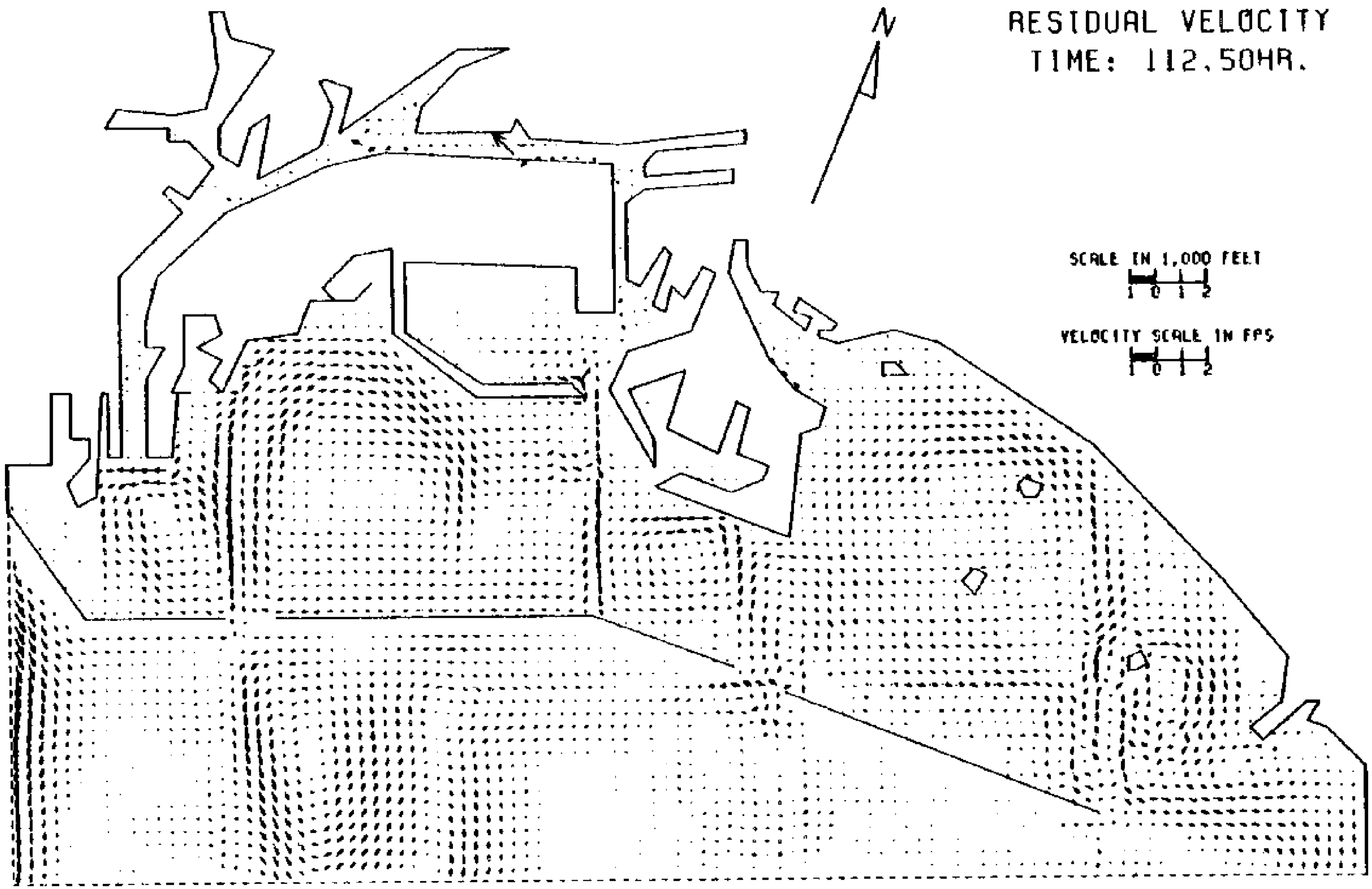

Figure 5.6 Fully Plotted Distribution of Residual Velocties for the Basic Test (Run #1).

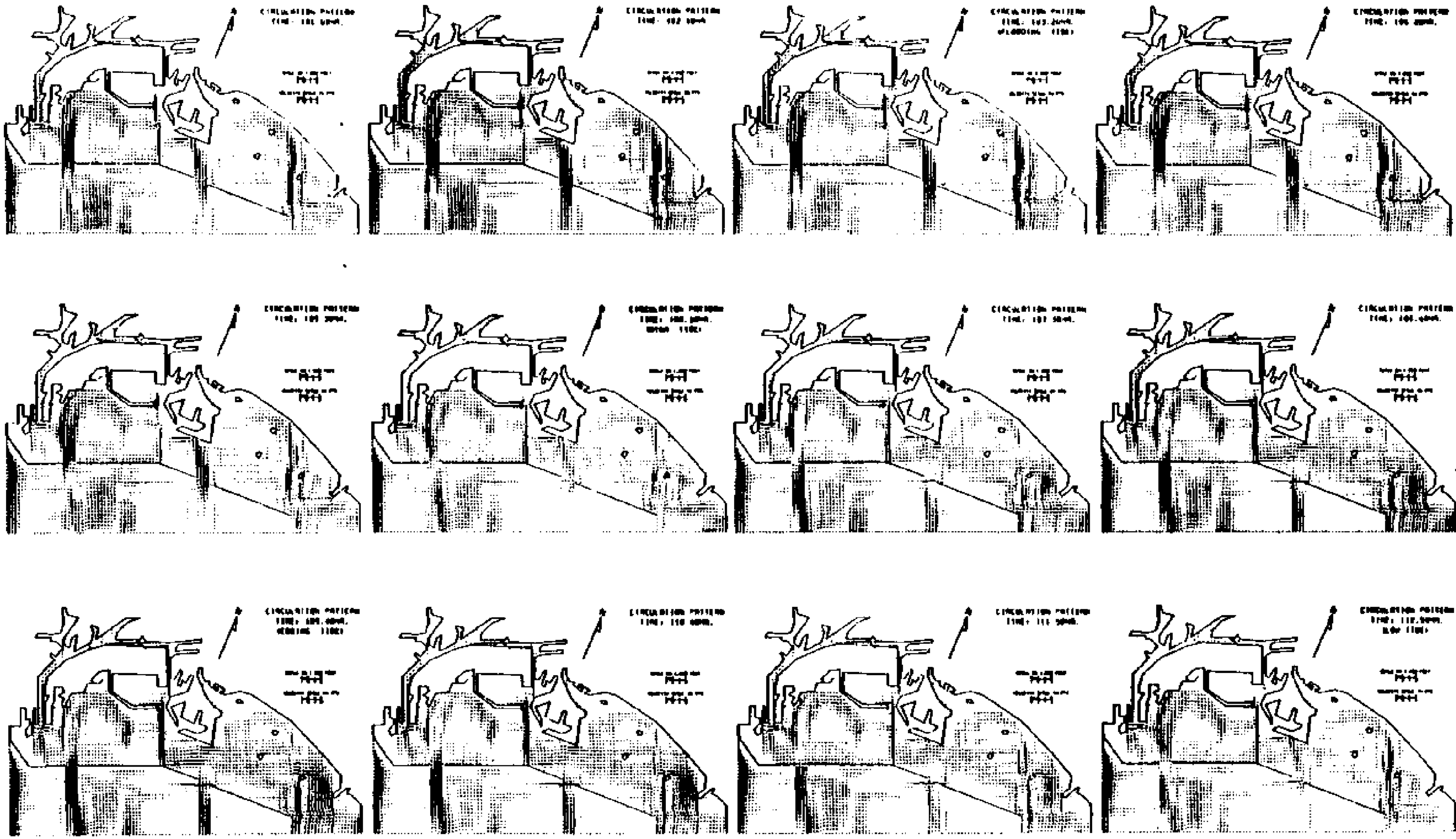

Figure 5.7 Circulation Patterns between t = 100.0 hr and t = 112.5 hr for the Basic Test (Run #1).

taken at approximately one-hour intervals for a tidal cycle. This figure is small and not clear but one may refer to Figures 5.1 to 5.4 which display clearly four of the twelve plots shown in Figure 5.7. Figure 5.7 shows that clockwise and counterclockwise gyres maintain their flow direction throughout the tidal cycle. The strengths are also almost constant during the cycle. Therefore, the pattern of residual velocity (which is the distribution of the velocity averaged over the tidal cycle) is a good indication of the gyre strength. The figure also shows the process of how the inflow currents mix with the large gyre during flood tide and how a part of the water inside the gyre escaped during ebb tide. This process improves the water quality by increasing the rates of mixing and reaeration.

Results after a 100-hour simulation time were presented for discussion because the results from the first few tidal cycles were believed to have large errors. The error is large before the simulation is "warmed up" from the initially motionless state. Whether the fluctuations of tidal motion have reached a dynamical stable state or not can be checked by comparing the computation results of repeated tidal cycles. Usually the data of surface elevations show repeated patterns within the first couple of tidal cycles. Therefore, the required warm-up period is short if the surface elevation is the only variable under consideration. However, if the current velocity is the important parameter for the study, the required warm-up period is usually longer. Velocity patterns at a certain stage of two repeated tidal cycles can be compared to see whether the patterns have attained a dynamical steady state. The simulation of a linear flow takes less warm-up time while simulating a circular motion (or gyre structure) takes longer time to set up the time-independent residual motion. Figure 5.8 shows the residual velocities from cycles 2, 4, 6, and 8 of the base run. Notice that the residual velocity is defined here as the mean velocity averaged over one tidal cycle. Before the "warm up" state is reached, the so-called residual velocity is still changing and is not the true residual velocity (the mean velocity over a large number of tidal cycles). From Figures 5.5 and 5.8, it is concluded that the warm-up time should be long enough (e.g., five to ten diurnal tidal cycles, depending on tidal elevations, geometry of the study area, etc.) in order to obtain true velocity distributions. If a smaller time steps is used in the simulation, the warm up time will be shorter but the number of time steps to reach a warmed up state may be of the same order of magnitude.

Summarized in Table 5.1 are the computer runs of which the results are discussed in this report. The

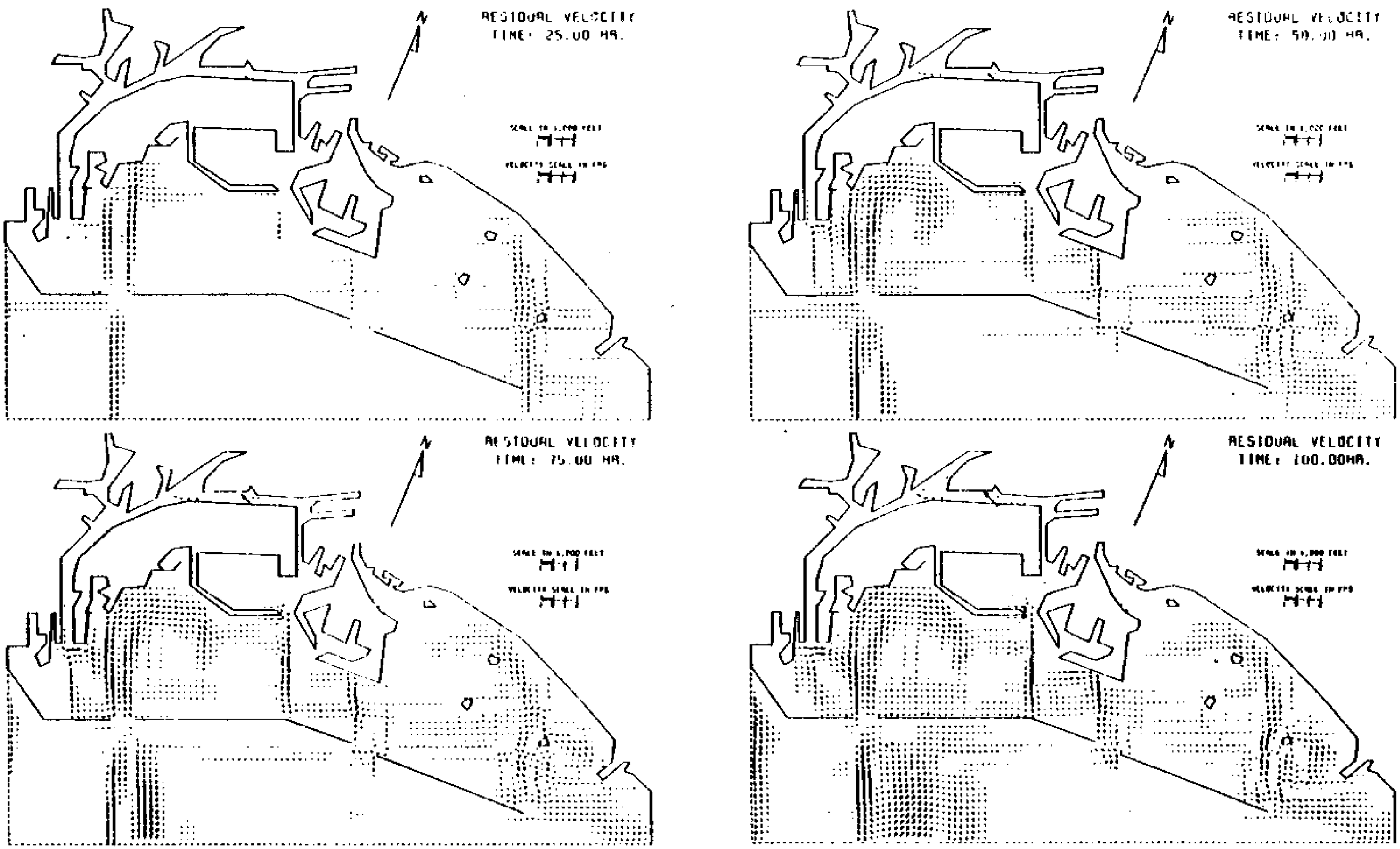

Figure 5.8 Distributions of Residual Velocities Obtained from the First Few Tidal Cycles of the Basic Test (Run #1).

Run #	Simulated period in no. of ΔT	Simulated period in hr. (real time)	Brief description of parameters which are different from what in the basic run
1	1327	132.7	--- (Basic run) (ΔT=360 sec; A=0)
2	2868	286.8	Used field data of spring tide
3	6129	612.9	Used field data of neap tide
4	1366	136.6	Modified harbor (tanker terminal)
5	2455	245.5	Spring tide; with tanker terminal
6	76	15.3	ΔT = 720 sec (Note, ΔT = 2Δt)
7	1062	212.5	ΔT = 720 sec; NI = 2
8	940	46.9	ΔT = 180 sec
9	1143	28.6	ΔT = 90 sec
10	1791	22.4	ΔT = 45 sec
11	1454	9.1	ΔT = 22.5 sec
12	1546	4.8	ΔT = 11.25 sec
13	2731	4.3	ΔT = 5.625 sec
14	> 6125	> 612.5	Without advective terms
15	1768	176.8	without Coriolis terms
16	1470	147.0	A = 10
17	3736	373.6	A = 100
18	2471	247.1	A = 173
19	2129	212.9	A = 200
20	1698	169.8	A = 300
21	1257	125.7	A = 400
22	86	8.6	A = 500
23	16	1.6	A = 1000
24	5	0.5	A = 10000
25	1145	114.5	n = 0
26	3366	336.6	n = 0.040
27	881	88.1	h(constant) = 30 ft
28	1021	102.1	h(constant) = 40 ft
29	1295	129.5	h(constant) = 45 ft
30	1815	181.5	Deepen channel (100 ft)
31	2636	263.6	Deepen channel (200 ft)
32	1331	133.1	Used double precision
33	1453	145.3	NI = 2
34	1144	57.2	NI = 2; ΔT = 180 sec
35	2315	57.9	ΔT = 90 sec; h(constnat) = 40 FT
36	2811	281.1	Spring tide starting from minimum
37	1435	143.5	Solid boundary on the west side
38	> 1000	> 100.0	60x34 grid points; h(constant) = 40 ft
39	> 1000	> 100.0	31x25 gird points; Δs = 1000 ft; h(constant) = 40 ft

Table 5.1 Summary of computer runs.

computer runs consist of the basic run, the runs using field tidal-data, and sensitivity test runs. Also shown in the table is the simulation time for each computer run. It was attempted to extend the simulation time for most of computer runs in order to reach a dynamical steady state as well as to test the stability of the numerical model. Many computer runs yielded satisfactory results before the end of simulation. However, the model is not absolutely stable although it may be more stable than any other similar model at the present time. It can not be run for an extremely long period, especially when the geometry of the study area is not simple. A few computer runs listed in Table 5.1 stopped when there appeared any overflow of variables, which indicated that the model is diverging. Some runs stopped when a designed format for a write statement could not handle the unexpectedly large value produced due to the numerical instability. Some runs were forced to stop by the instructions buried inside the computer program, when the model was considered of showing an unstable condition. In this study, unstable conditions were detected by comparing the difference of x-direction velocities of two successive time steps at an arbitrary chosen point (22,20) which is just inside the Angel's Gate. The simulation stopped whenever that difference is greater than 0.2 fps which was supposed to be a unreasonably large value. Therefore, the simulation ceased when the model showed either divergence or an indication of divergence. The numerical stability appeared in this study will be discussed later.

5.2 Numerical Tests with Field Data

In the basic run, the forcing function for the tide was sinusoidal. In addition, the numerical model was also tested with spring tide and neap tide (see Figure 4.4) as the inputted forcing functions. A spring tide occurs during new moon and full moon while a neap tide occurs at the first and the third of the moon. The data used in these tests were the same as in hydraulic model built in the U.S. Army Engineer Waterways Experiment Station (McAnally 1975; Outlaw 1979).

Figures 5.9 to 5.13 depict the circulation patterns and the distribution of residual velocities for Run #2 (see Table 5.1) which used the data of a spring tide (see Figure 4.4) as the boundary condition. The tidal range was 6.9 ft. During the simulation, the same tide was repeated with a period of 25 hr. Figures 5.9 to 5.13 were the results for the period between 100.0 hr and 125.0 hr, which was the fifth tidal cycle after the simulation started from a motionless state. Those figures show that the gyre strength is slightly smaller than that in the basic run but the general pattern of velocity distributions are the same.

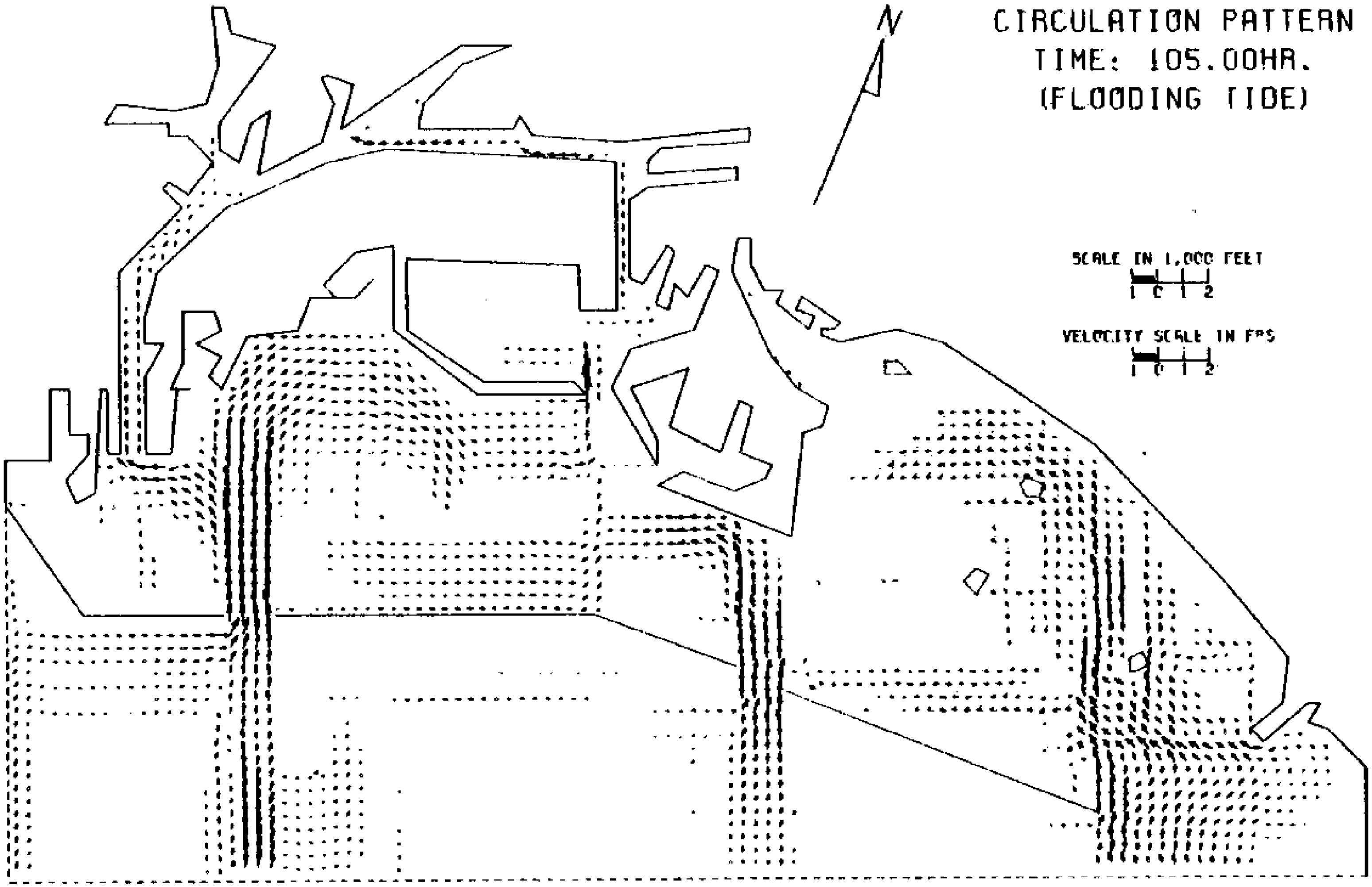

Figure 5.9 Circulation Pattern at t = 105.0 hr (Flooding Tide) for Spring Tide (Run #2).

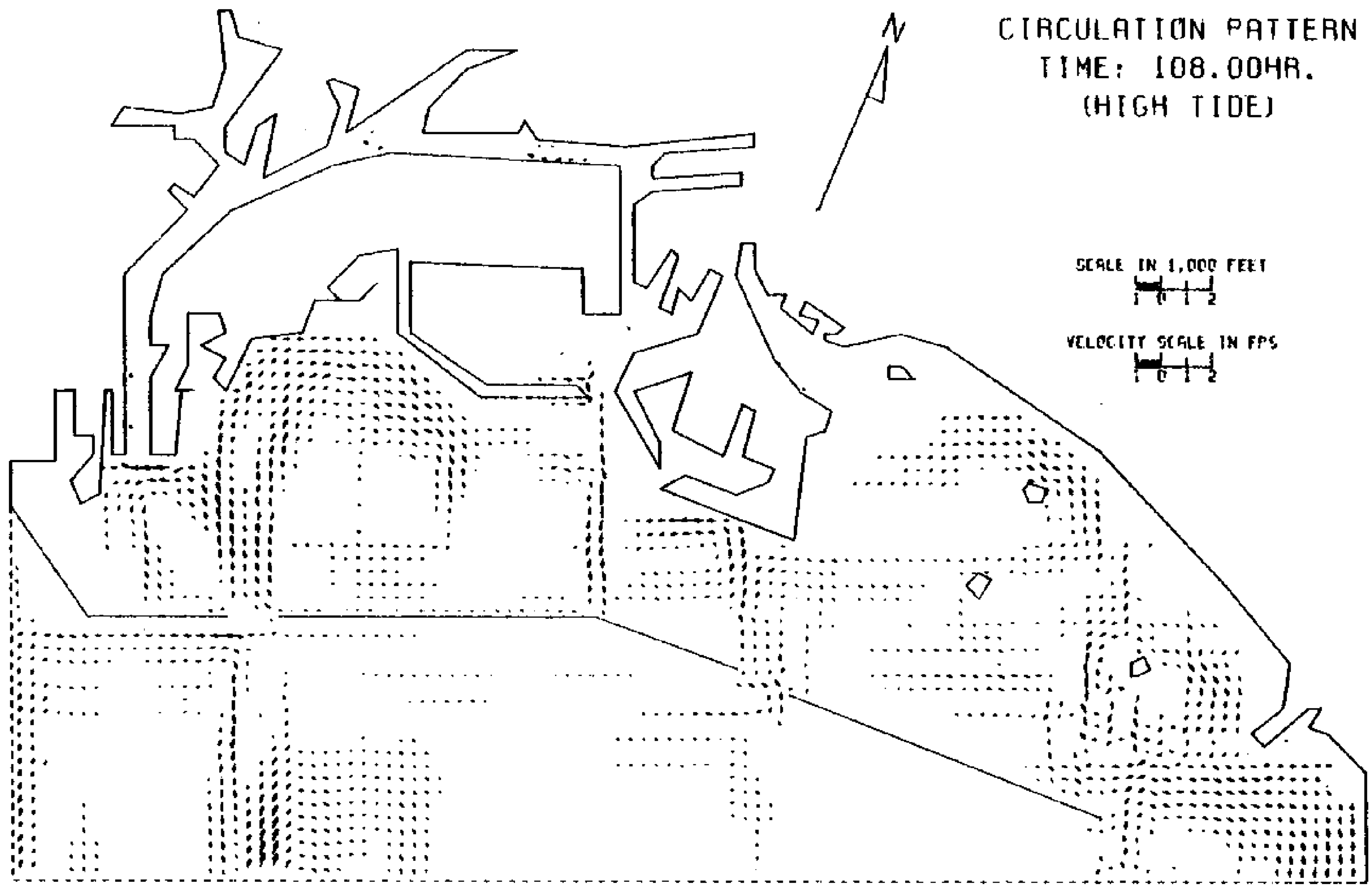

Figure 5.10 Circulation Pattern at t = 108.0 hr (High Tide) for Spring Tide (Run #2).

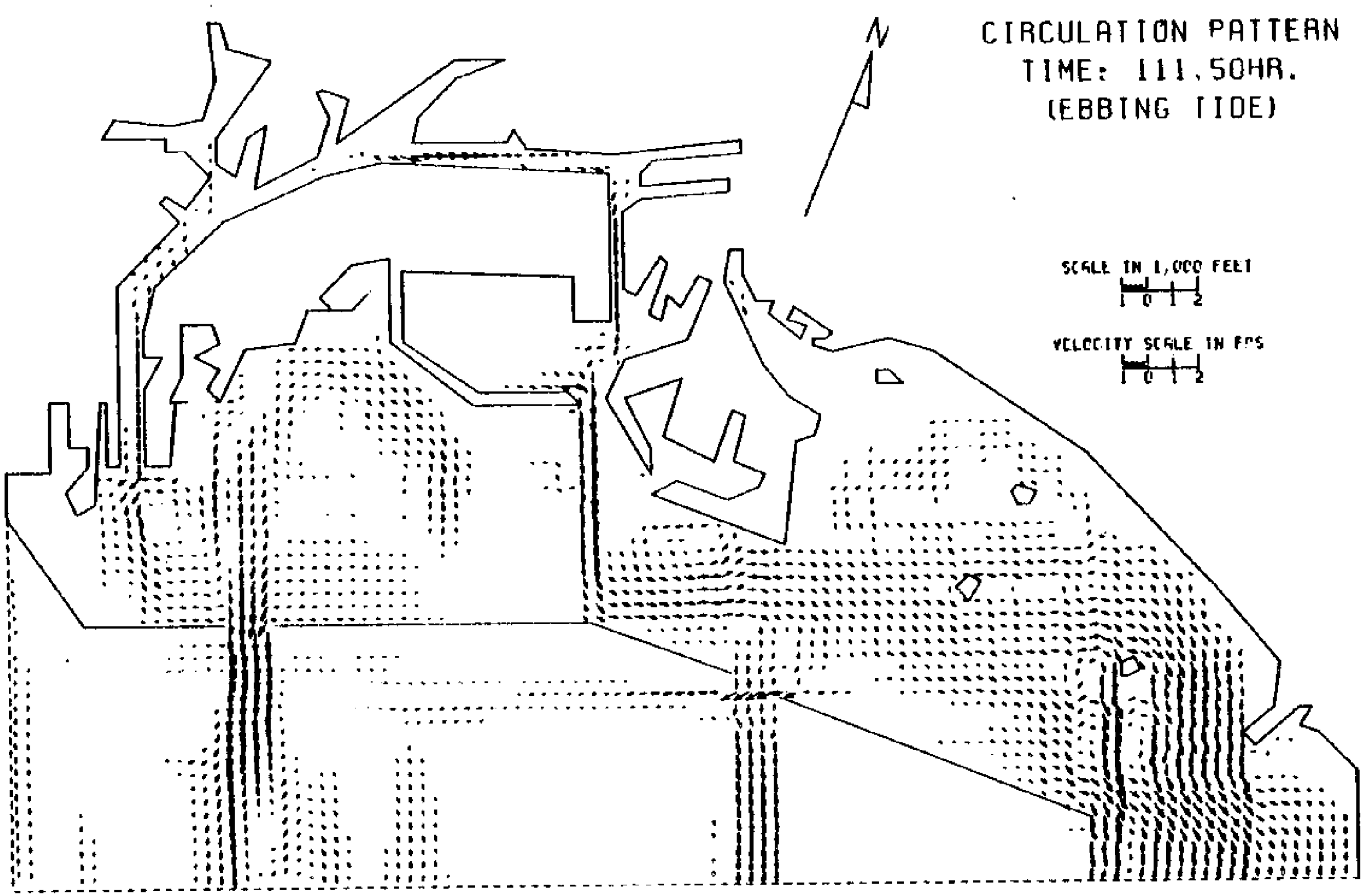

Figure 5.11 Circulation Pattern at t = 111.5 hr (Ebbing Tide) for Spring Tide (Run #2).

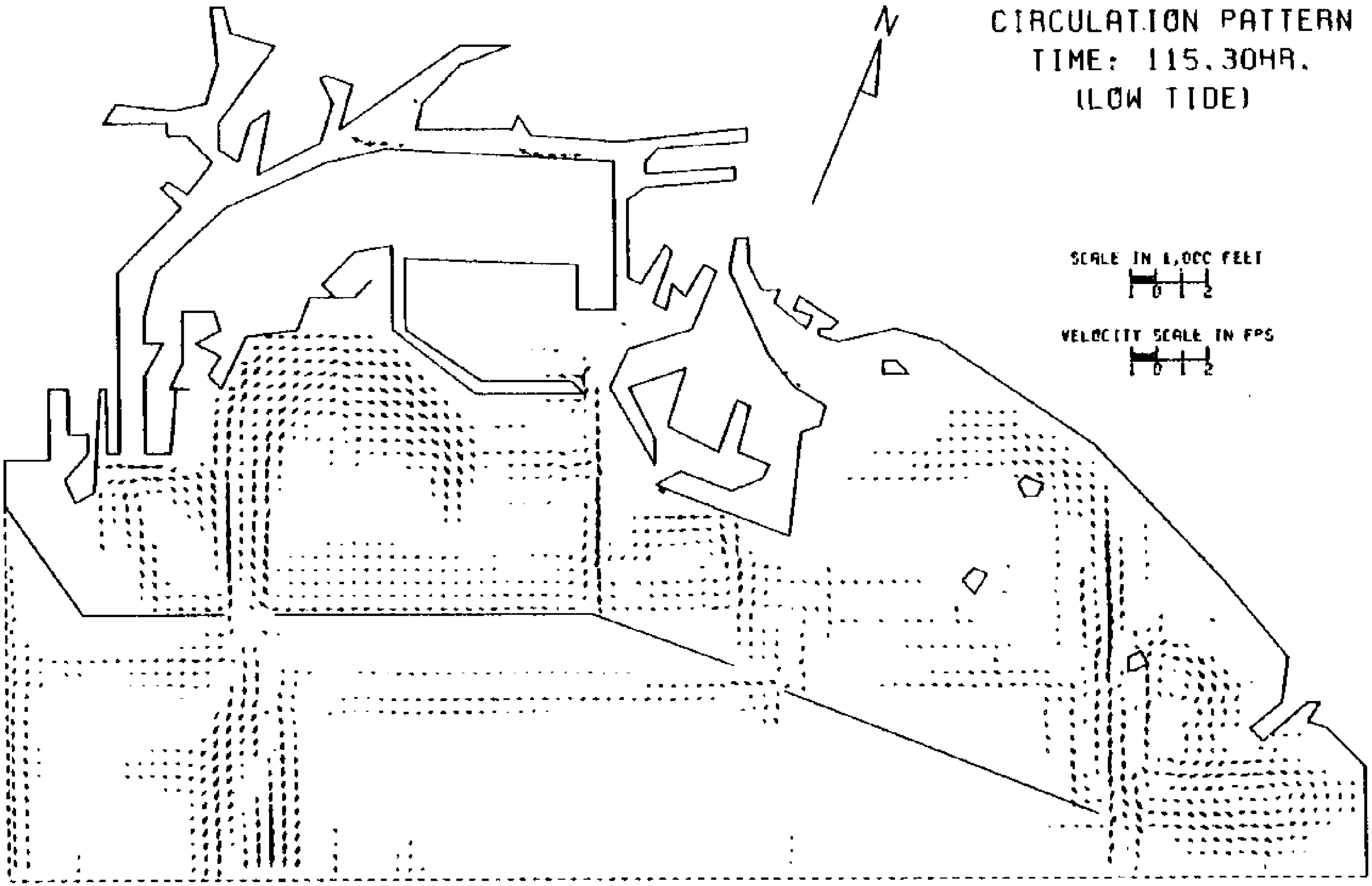

Figure 5.12 Circulation Pattern at t = 115.3 hr (Low Tide) for Spring Tide (Run #2).

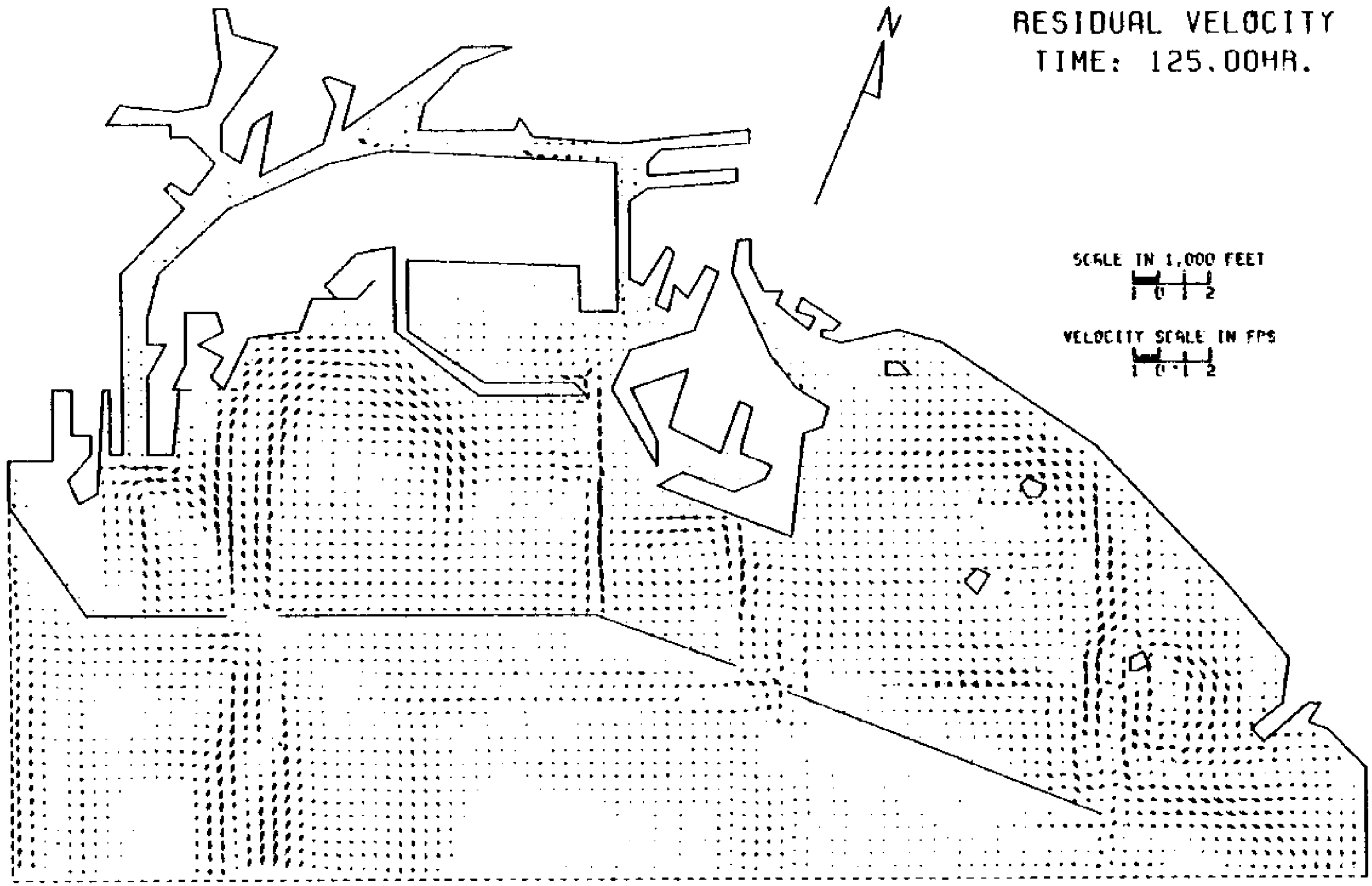

Figure 5.13 Distribution of Residual Velocities for Spring Tide (Run #2).

The number and locations of gyre structures are also unchanged. The current velocity of the large gyre can be higher than 0.2 fps. Throughout a tidal cycle, the large gyre maintains clockwise motion with slight velocity fluctuations. Fresh water joins the large gyre during flood tide (see Figure 5.9) and a portion of mixed water leaves during ebb tide (see Figure 5.11). Therefore, the gyre does not contain dead water but enhance the mixing of water in the harbor basin. The existence of the large gyre in Los Angeles-Long Beach Harbor is therefore helpful to the water quality there.

It appears in Figure 5.9 that the current passing through Angel's Gate (about 0.9 fps) is a little smaller than that in basic run. The reason is that the tidal range between higher low water at t = 102.0 hr and higher high water at t = 108.0 hr is only 4.7 ft compared to 5.6 ft in the basic run. Figure 5.13 is fully plotted in order to be compatible to Figure 5.6.

Figure 5.14 is a photograph of the circulation pattern, at t = 8.0 hr (high tide), obtained from a hydraulic model (McAnally 1975, Appendix B). The exposure time was 10 sec (400 sec prototype). The potential error sources include the usage of wide angle lens which introduce the photographic distortion, slight elevation difference between cameras which results in different length scale,

Figure 5.14 Surface Velocity at t = 108.0 hr (High Tide) for Spring Tide.

and deviation of film exposure time from the nominal duration (McAnally 1975).

Figure 5.15, which shows the circulation pattern at t = 108.0 hr or the eighth hour of the fifth diurnal cycle, obtained from Run #2, is comparable to Figure 5.14. The size, strength, and location of gyres in Figure 5.15 are close to those in Figure 5.14. One should note the fact that Figure 5.15 shows the depth-averaged velocity while Figure 5.14 shows the surface current pattern. From Figure 5.14 it is seen that the surface velocity on the southern side of the large gyre in outer Los Angeles Harbor is about the same as that on the northern side of the gyre. On the other hand, in Figure 5.15, the average velocity on the southern side is smaller than that on the northern side, because the water depth is larger on the southern side of the large gyre (see input data in Appendix B.1). Keeping in mind this kind of possible misleading and potential photographic error, one can reasonably conclude that the results simulated from the present numerical model are good when compared to those obtained from the hydraulic model.

Figure 5.16 to 5.18 depict the circulation pattern and the distribution of residual velocities for Run #3 (see Table 5.1) which used the data of a neap tide (see Figure 4.4) as the boundary condition. The tidal range is 3.5 ft. The circulation patterns of both high tide and low tide

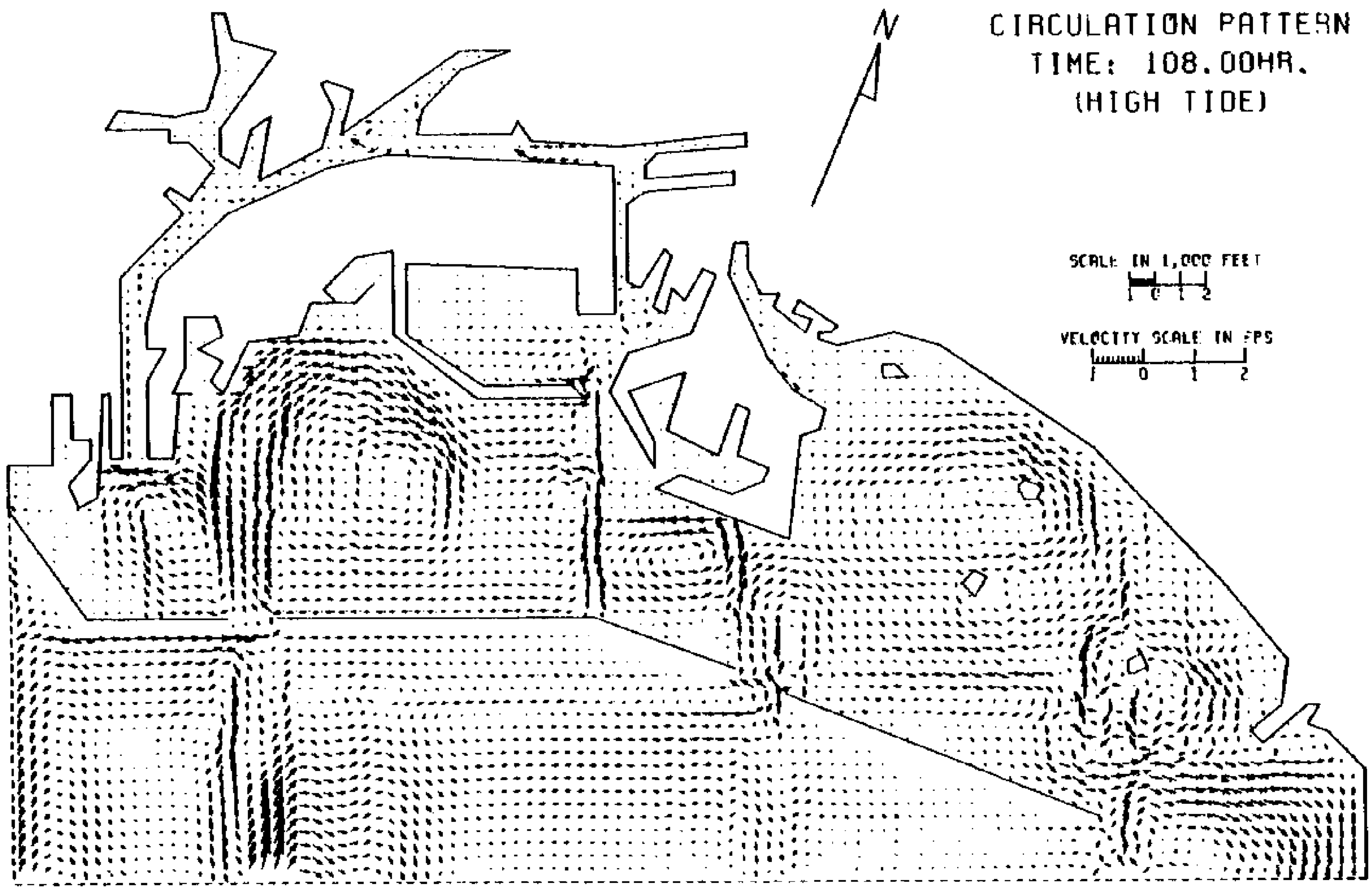

Figure 5.15 Averaged Velocity at t = 108.0 hr (High Tide) for Spring Tide (Run #2).

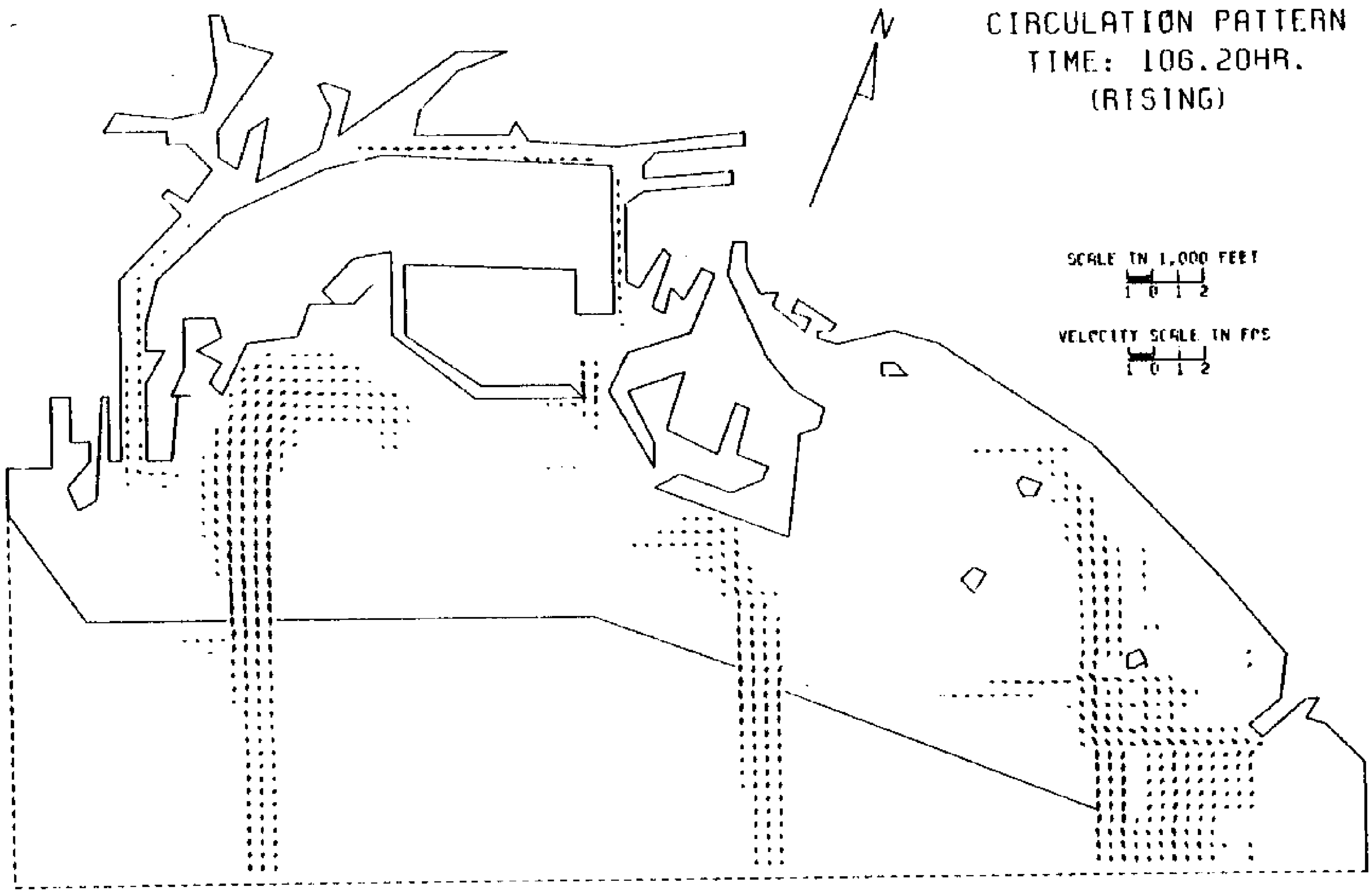

Figure 5.16 Circulation Pattern at t = 106.2 hr (Flooding Tide) for Neap Tide (Run #3).

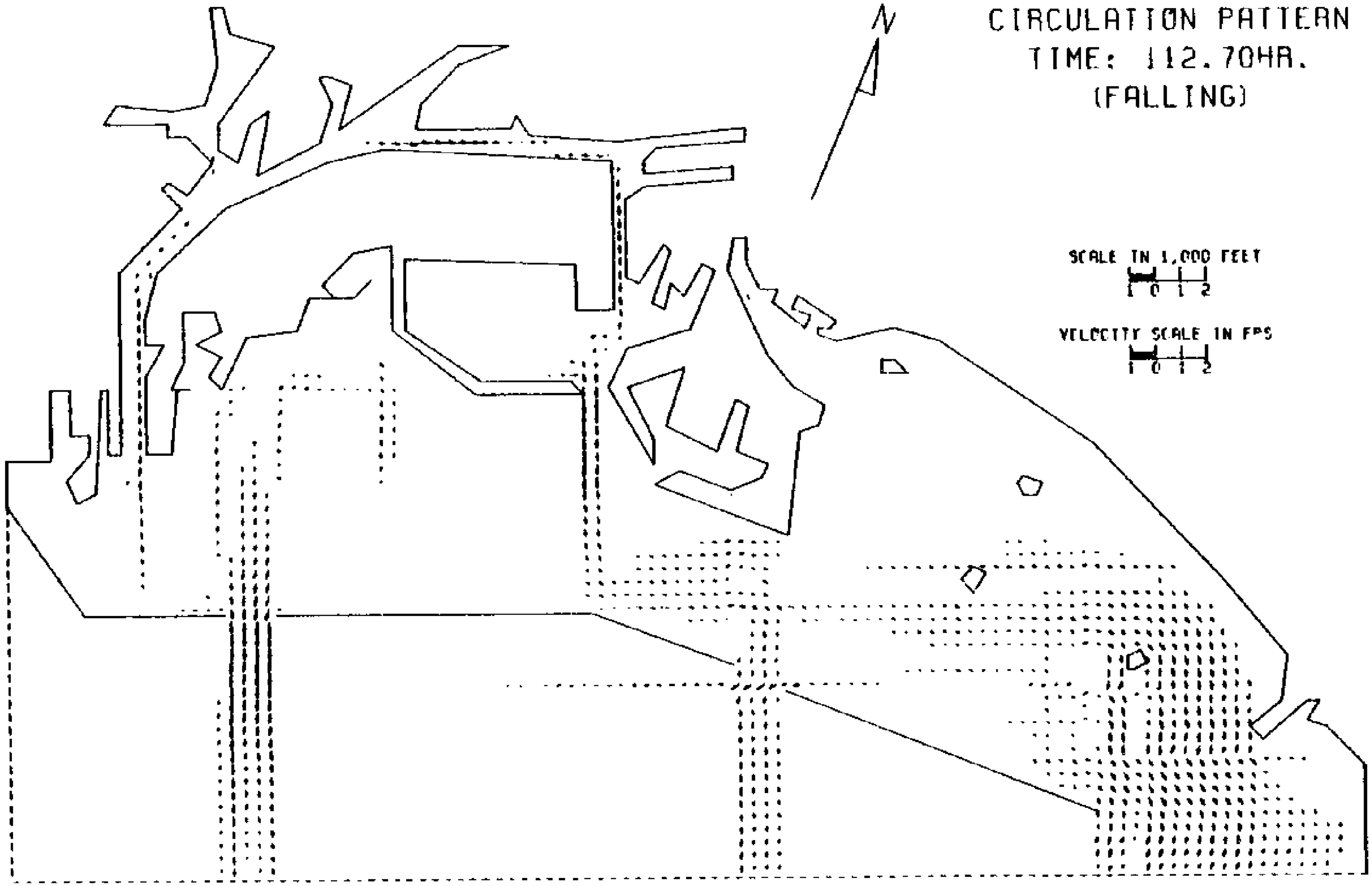

Figure 5.17 Circulation Pattern at t = 112.7 hr (Ebbing Tide) for Neap Tide (Run #3).

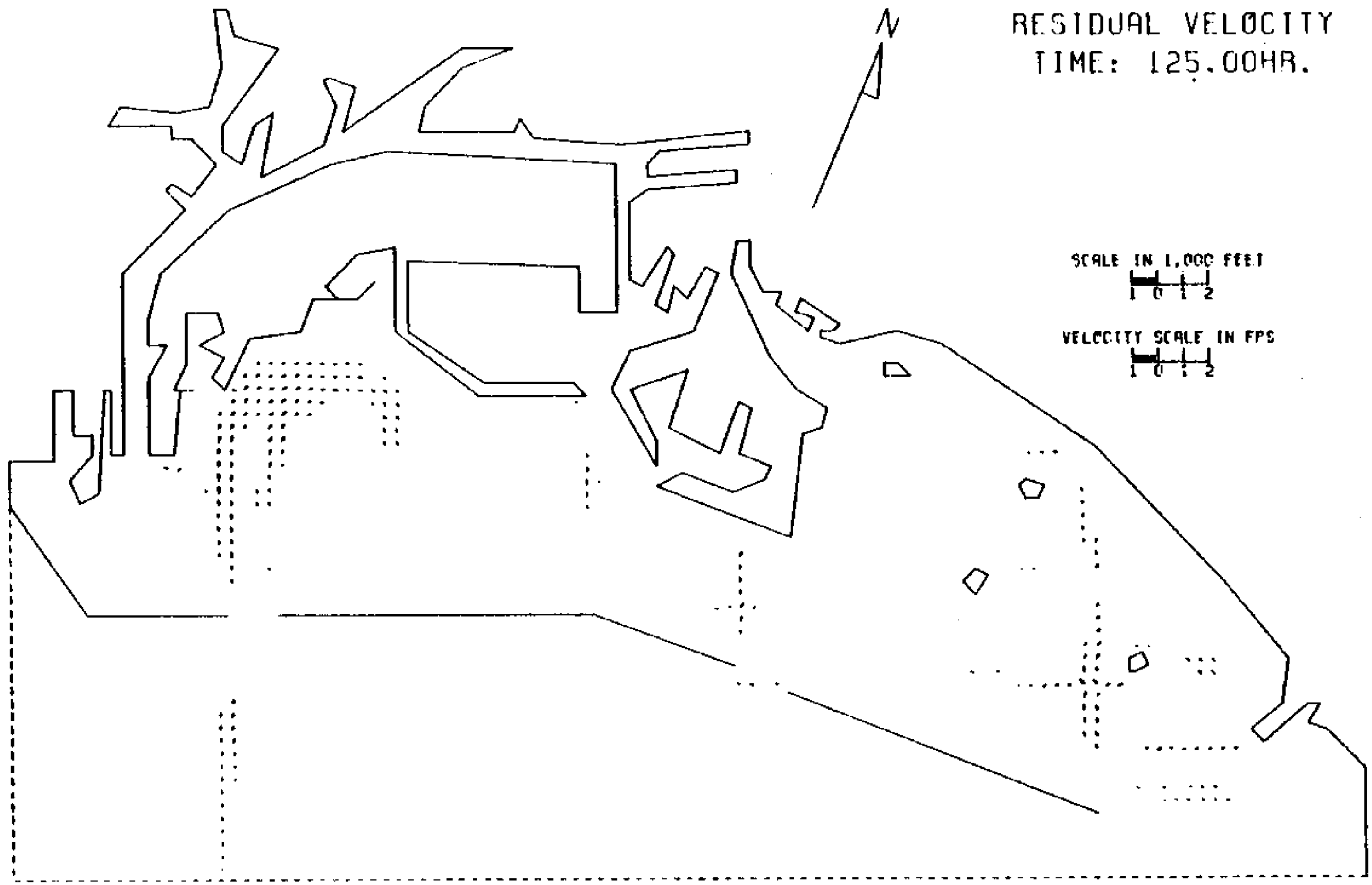

Figure 5.18 Distribution of Residual Velocities for Neap Tide (Run #3).

stages are almost identical to the pattern of residual velocity in Figure 5.18 and are not shown in this report. The current velocities are very small in this circulation which is induced by the neap tide. There is still a weak but large clockwise gyre appears between the breakwaters to the south and Terminal Island to the north. It seems that the simulation results are sensitive to the inputted tidal elevations.

Figure 5.19 shows the simulated circulation pattern at t = 606.2 hr. The velocity distribution is similar to that in Figure 5.16. Figure 5.19 indicates that the circulation pattern is close to a steady state condition at t = 106.2 hr. In the figure, velocity vectors plotted in Los Angeles East Basin show that the numerical results are diverging. This phenomenon will be discussed later in Section 5.13.

5.3 Effects of Harbor Modification

There have been many proposals of harbor modification for the Los Angeles-Long Beach Harbor. In order to see the ability of the present numerical model in predicting the effect on circulation patterns of harbor modification, the model was applied to the same study area with a major landfill in the harbor region (see the shaded area in Figure 5.20). This change in geometry is a part of the master

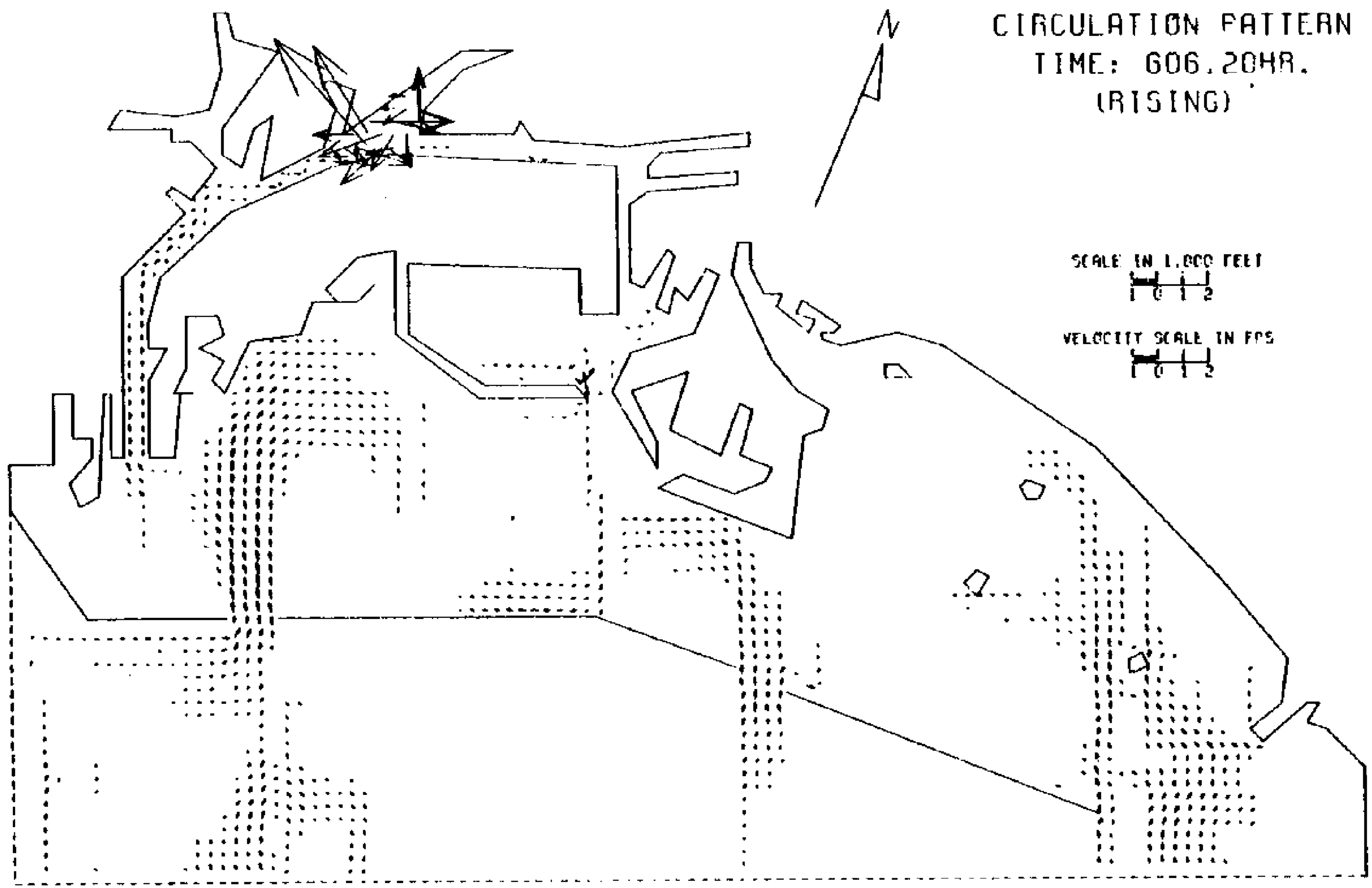

Figure 5.19 Circulation Pattern at t = 606.2 hr (Flooding Tide) for Neap Tide (Run #3).

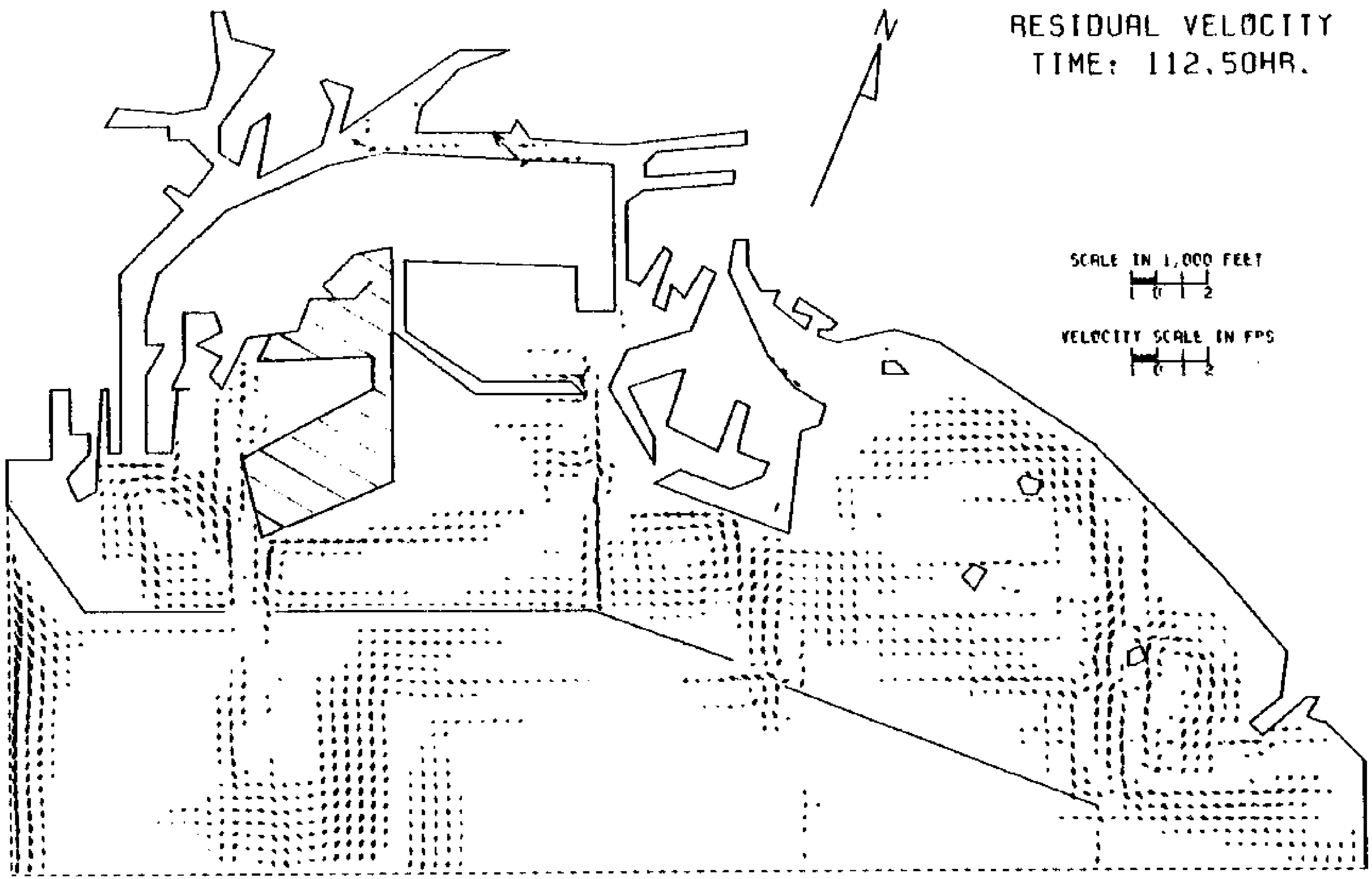

Figure 5.20 Distribution of Residual Velocities for Idealized SinusoidalTidal Input (Run #4).

plan 1A-2 of the Los Angeles-Long Beach Harbor (see Raney 1976).

Figure 5.20 depicts the distribution of residual velocities (induced by the same tide as that in the basic test) for the modified configuration. The only difference between the results in Figures 5.5 and 5.20 is in the velocity pattern near the proposed tanker terminal. The large gyre shown in Figure 5.5 was eliminated due to the existence of the new land. A smaller and less distinct circulation appeared to the southeast of the new terminal and a very small circular motion showed up to the west of the terminal. The effects of the newly created land on the flow conditions in other part of the harbor are negligible, if the tidal elevations at the entrance are the same.

If the spring tide shown in Figure 4.3 is used as the forcing function, the distribution of residual velocities for the study area with the same geometry modification is shown in Figure 5.21. Compared with Figure 5.13, it again shows that the main difference in the flow pattern is limited to the area nearby the tanker terminal. As was anticipated, the large gyre disappeared from the figure.

Figure 5.22 depicts the flow patterns in the ninth cycle of the same diurnal spring-tide. The difference of the distribution of residual velocities in Figures 5.21 and 5.22 indicates that the flow in the fifth cycle is not yet

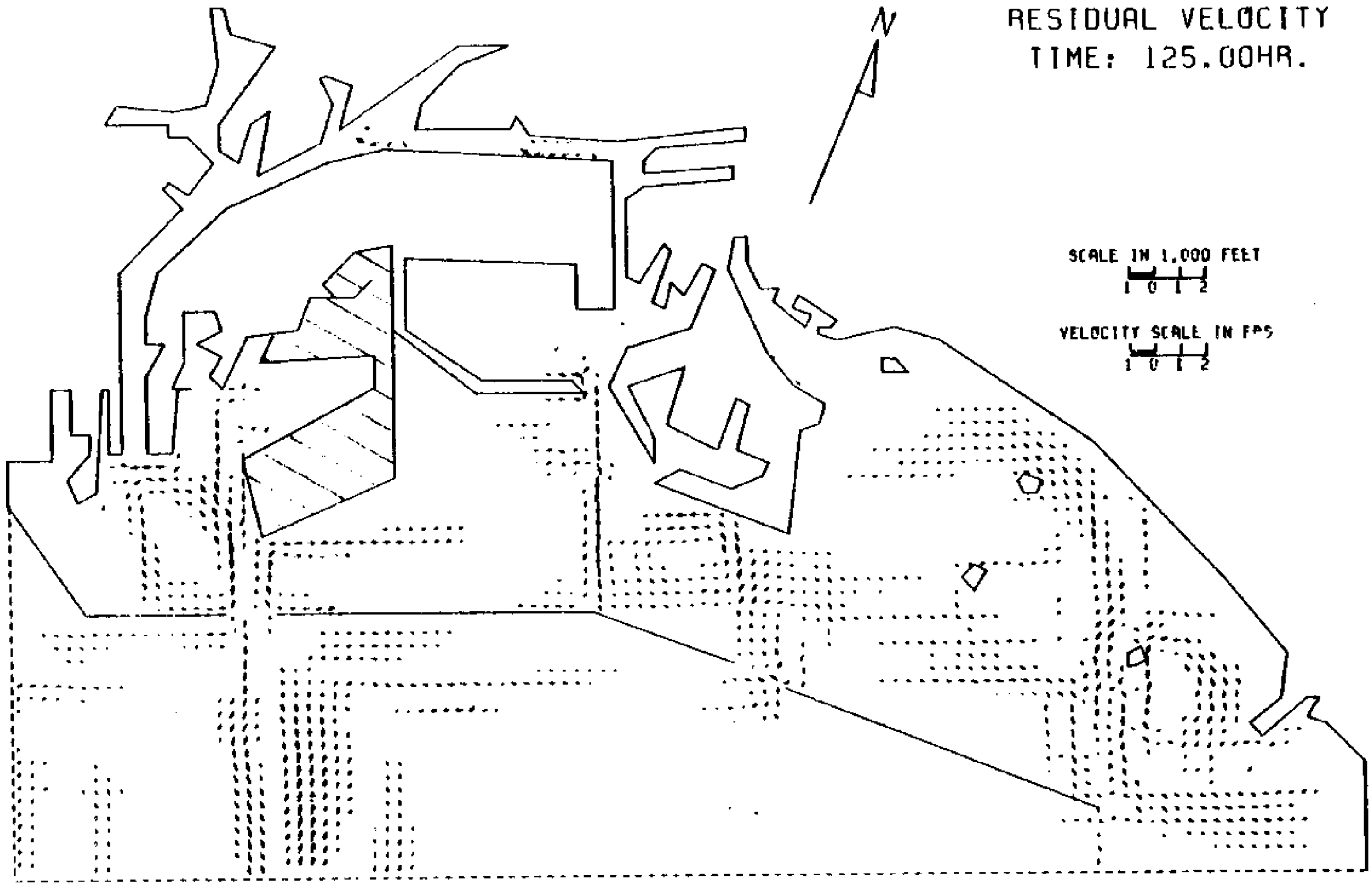

Figure 5.21 Distribution of Residual Velocities for Spring Tide Input (Run #5).

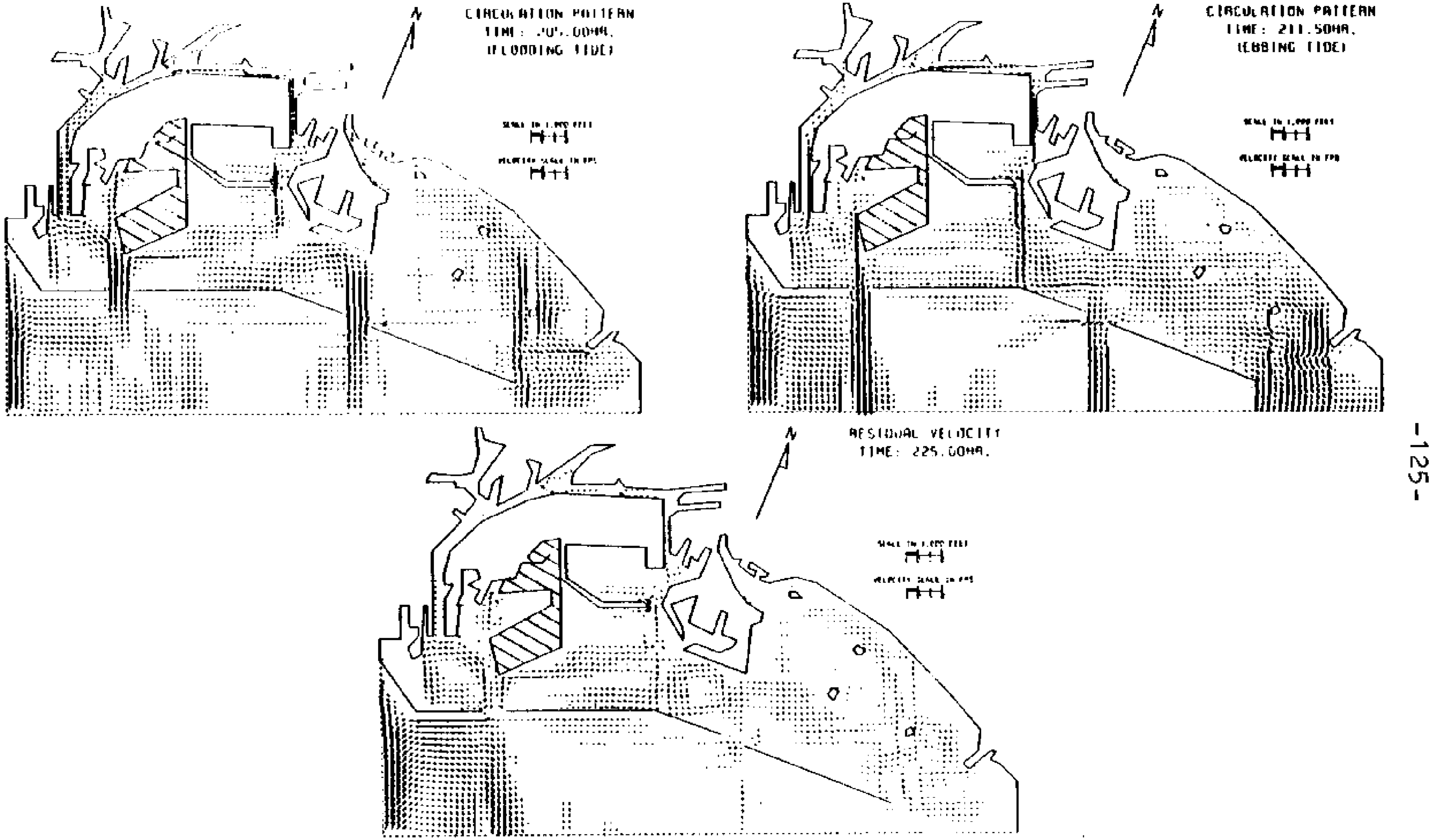

Figure 5.22 Flow Patterns between t = 200.0 hr and t = 225.0 hr for Spring Tide Input (Run #5).

steady. The large gyre to the southeast of the filled land was still developing in the fifth tidal cycle which ends at $t = 125$ hr.

It seems that the proposed numerical model is capable of being used as a predictive model to study the change of circulation patterns due to the harbor modification, if the simulation period is long enough.

5.4 Effects of Time Step

The first time-step value used to test this model was 180 sec. Later, it was found that 360 sec could not only save computer time but also yield satisfactory results. The basic test used 360 sec as the time step to calculate E and U in the first half-time-step and E and V in the second half-time-step. Run #6 (see Table 5.1) used 720 sec as the time step to test the performance of the numerical model. The simulation results from Run #6 diverged within a relatively short time, which was not good.

While most of the computer runs used NI = 1, where NI denotes the number of iterations, Run #7 used NI = 2 (see Table 5.1). NI equal to 1 means that the unknowns are computed only once in a half-time-step, and all terms of new time level on the right hand side of the finite difference equations (i.e., those terms marked with an asterisk in equations shown in Chapter 3) use the values calculated in the previous time level as predictive values. Extra iterations are performed to correct those predictive values n times when NI = n+1. With NI = 2, Run #7 performed a much longer real time simulation than Run #6 did. However, the time histories of the surface elevations averaged over one tidal cycle showed the values were oscillating from one cycle to the next one with an amplitude of approximately 0.04 ft. Therefore, the results of Run #7 were unsatisfactory.

For the computer simulation on Run #8 (see Table 5.1), time step of 180 sec was used. Figure 5.23 depicts the circulation pattern at the flood stage for the first four tidal cycles. Again it shows that the gyre structure in the first few tidal cycles is not correct. In general, longer simulations give better solutions. In the figure for t = 40.65 hr, a potential source of divergence around the west side of the open ocean appears. When this figure is compared to Figure 5.1, it can be found that the big gyre is not fully developed yet at t = 40.65 hr. Figure 5.24 shows how the circulation patterns for ebbing tide were improved through different tidal cycles. Figure 5.25 depicts the distributions of residual velocities for the first three tidal cycles of Run #8. Here, the gyres become larger when the simulation time is longer. By comparing figures 5.8 and 5.25, it is found that Run #8 warmed up faster (in terms of real time) than Run #1 did. The number

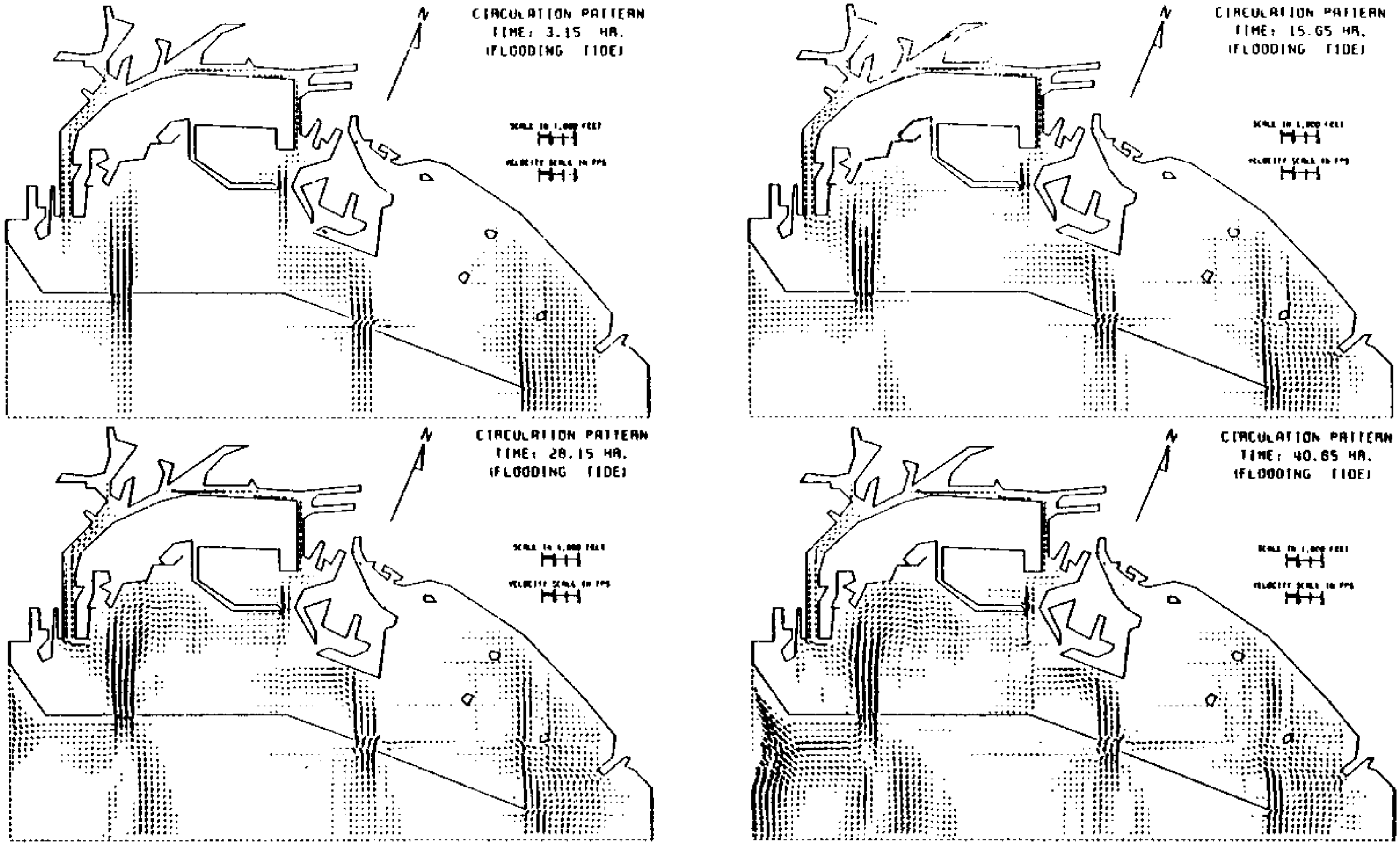

Figure 5.23 Circulation Patterns at Flooding Stages for Run #8 (ΔT = 180 sec).

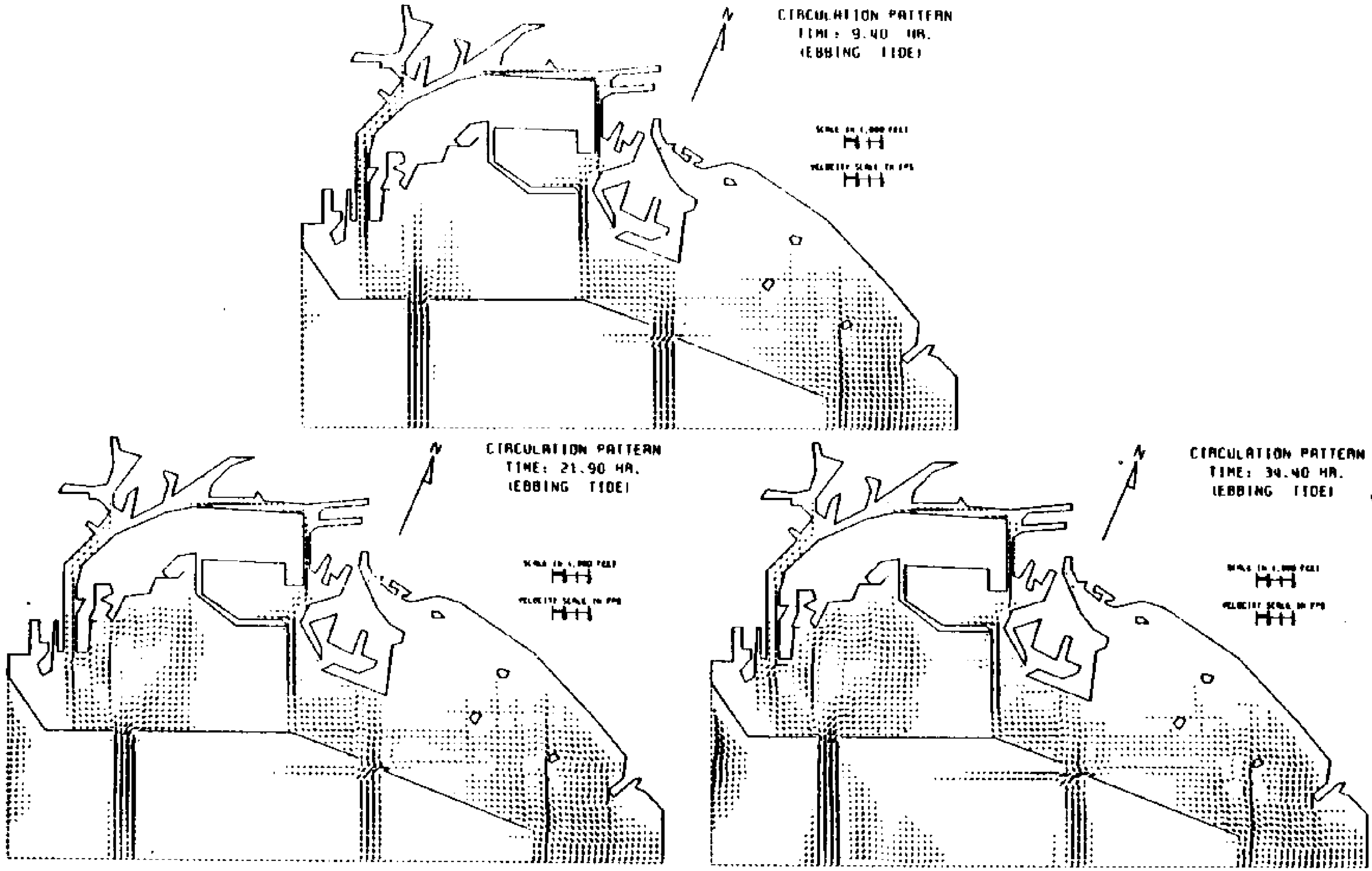

Figure 5.24 Circulation Patterns at Ebbing Stages for Run #8 (ΔT = 180 sec).

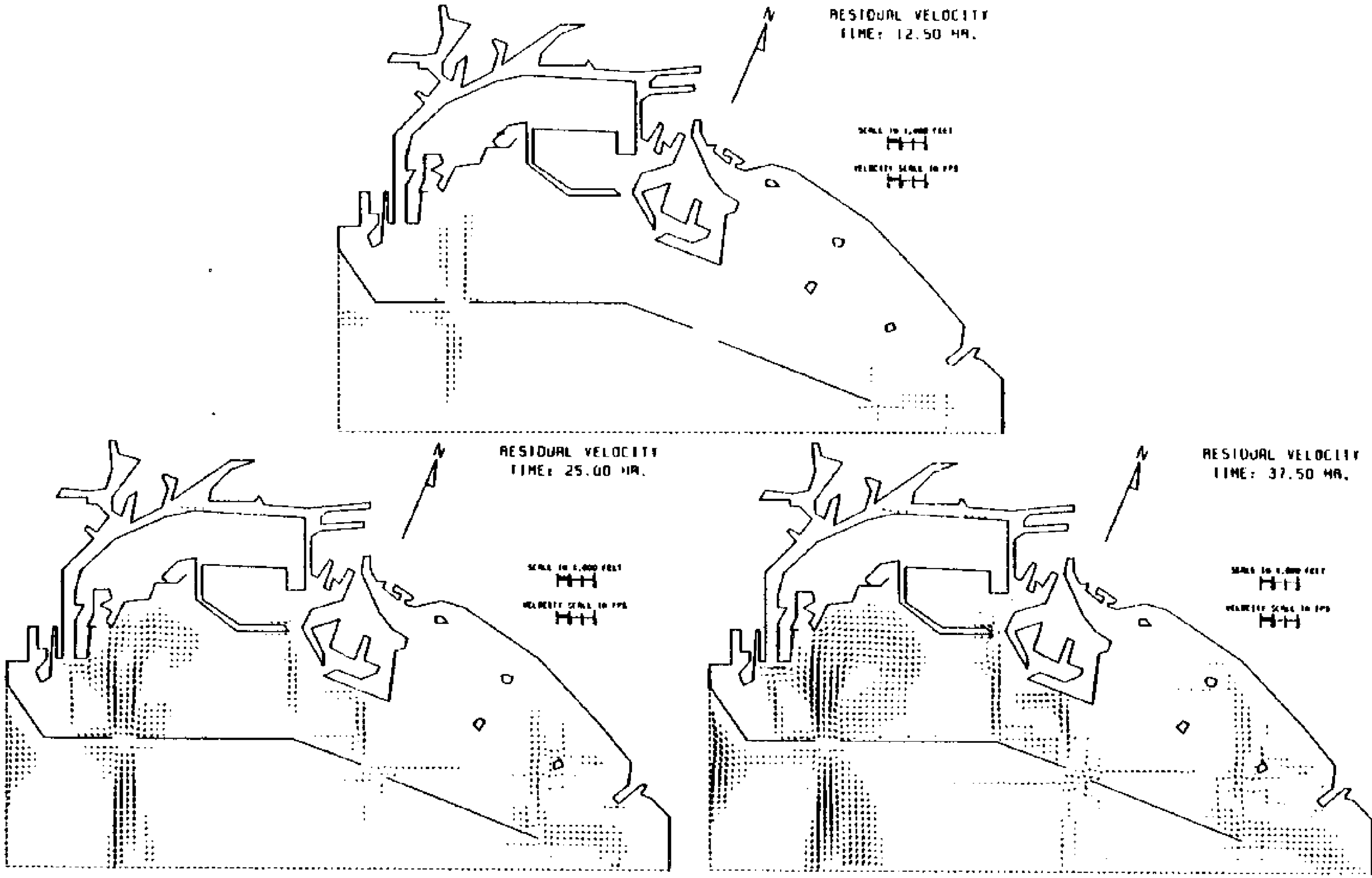

Figure 5.25 Distribution of Residual Velocities for the First Three Cycles of Run #8 (ΔT = 180 sec).

of time steps for these two runs to reach a certain degree of maturity are of the same order of magnitude. It seems that Run #8 gave finer resolutions, but for Run #1 the period for stable simulation is longer in real time or in terms of number of time steps.

Time step of 90 sec was used in Run #9 (see Table 5.1). For this computer run, Figure 5.26 depicts the circulation patterns at flooding stage and the distributions of residual velocities for the first two tidal cycles. The large gyre reached stable state at a faster pace than that in either Run #1 or Run #8. The center of the gyre moved slower toward the open area. The figure of residual velocity for the second tidal cycle indicates that there is source of instability appearing at the west boundary of the open ocean.

Figure 5.27 depicts the circulation patterns at about 3.125 hr intervals, from Run #10 (see Table 5.1) which had the time step set into 45 sec. The propagation of disturbances is slower than that in runs with a larger time step. Besides the abnormally strong current shown at the west side of the open boundary, a strange turbulence appears to the east of Queen's Gate. They were generated from numerical errors and may eventually induce numerical instability.

The time step was further reduced to 22.5 sec in Run #11 (see Table 5.1). Shown in Figure 5.28 are the

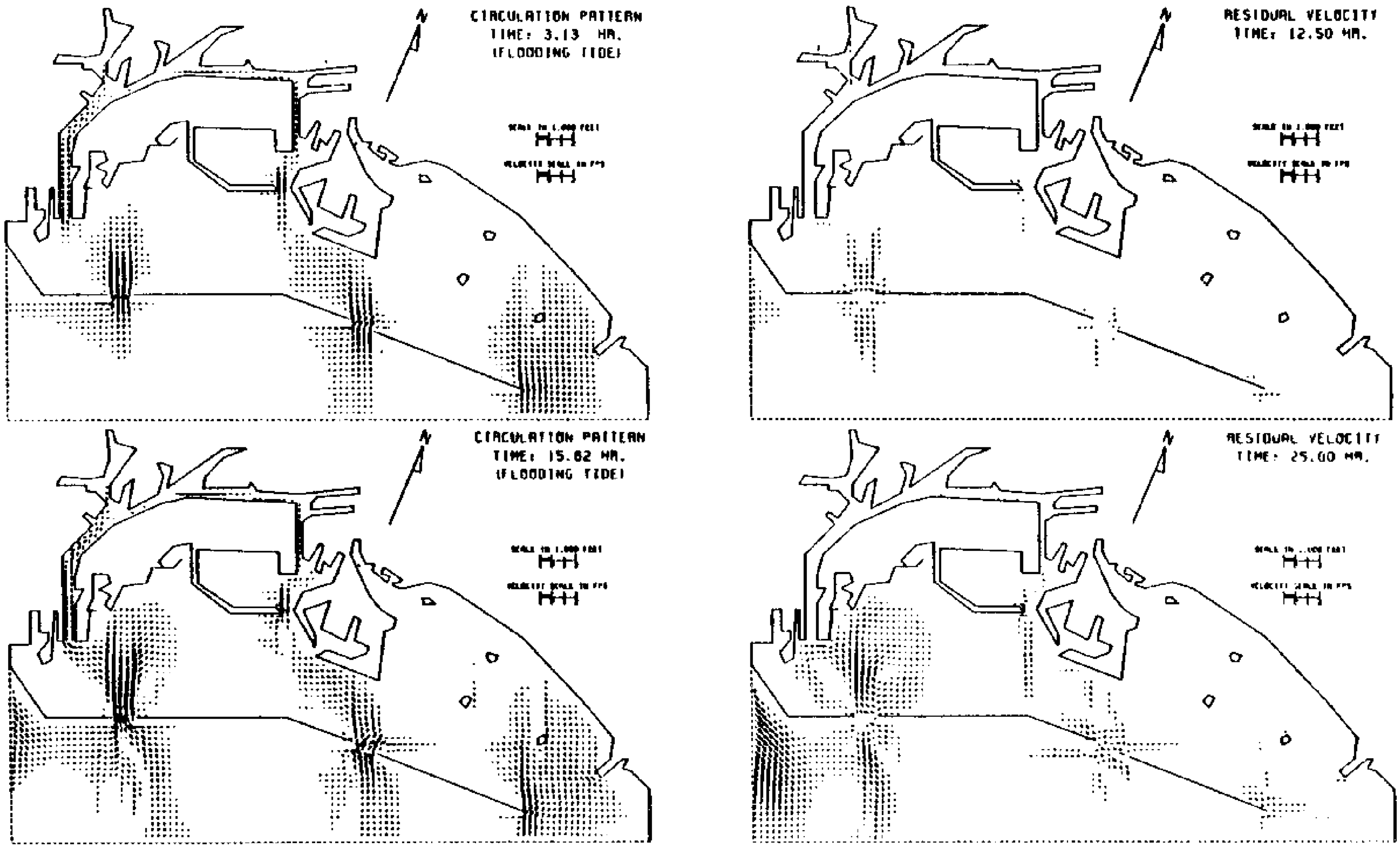

Figure 5.26 Flow Patterns for Run #9 (ΔT = 90 sec).

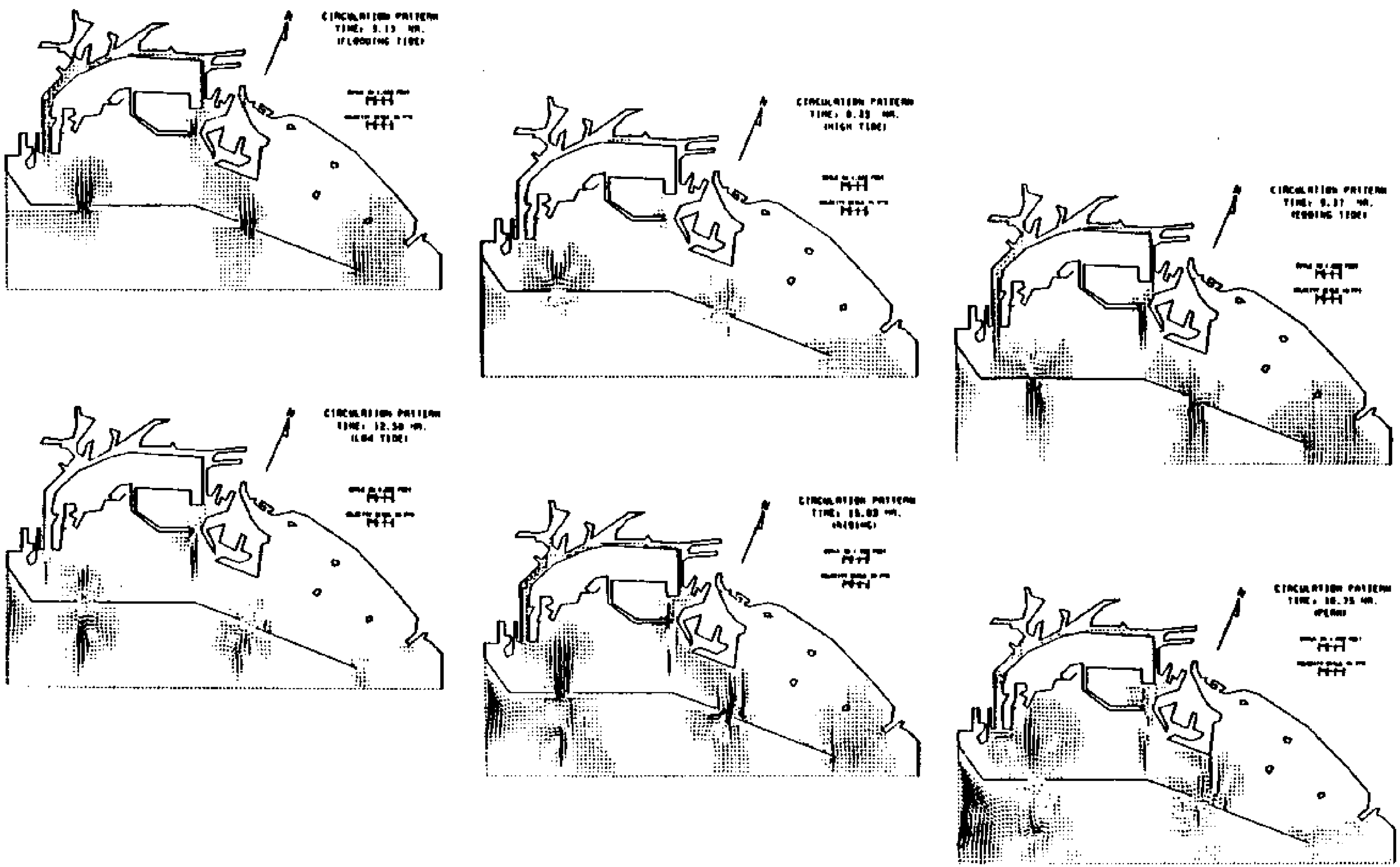

Figure 5.27 Circulation Patterns for Run #10 (ΔT = 45 sec).

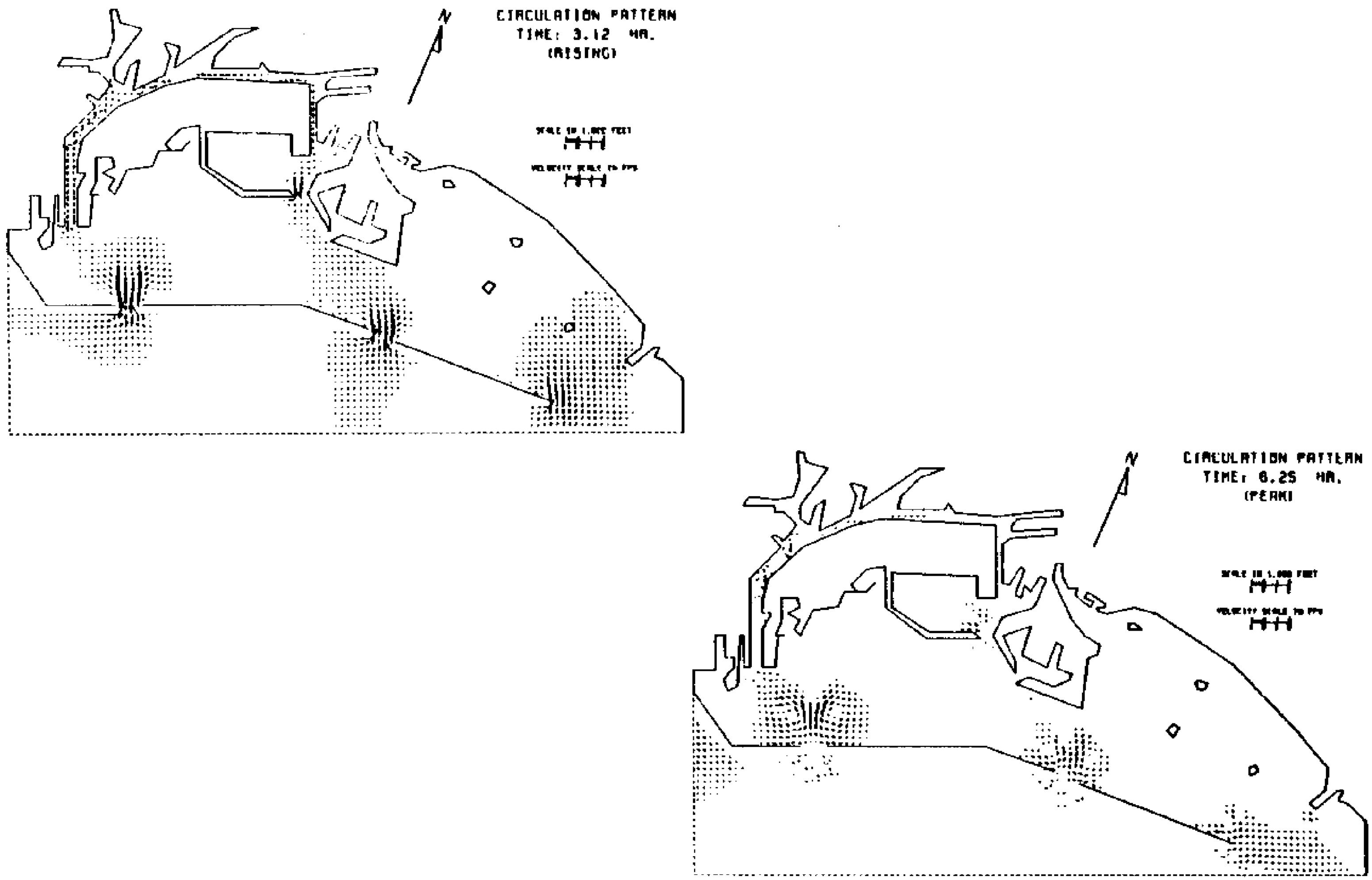

Figure 5.28 Circulation Patterns for Run #11 (ΔT = 22.5 sec).

circulation patterns for the first half cycle of this computer run. They are essentially the same as those in Figure 5.27. Within a certain time period, stronger vortices develop for the case of a smaller time step.

For Runs #12 and #13 (which used time steps of 11.25 sec and 5.625 sec, respectively, see Table 5.1), the plotted circulation patterns (not shown) at t = 3.125 hr are almost undistinguishable from that in Figure 5.28. It seems that up to a certain limit of time step, further reductions of time step would not produce any significant differences in the solutions.

5.5 Effects of Advective Terms

With the advective terms removed from the momentum equations, Run #14 (see Table 5.1) showed that the model can not reproduce any noticeable gyre structures. Figure 5.29 depicts the computed velocity patterns from Run #14. By comparing the distributions of residual velocities in Figure 5.5 and 5.29, one can conclude that the nonlinear advective term is the most important term in the governing equations that produces residual velocities. A model without nonlinear advective terms can not be used to study the vortex structure in two- or three-dimensional flows.

In order to be compatible to Figure 5.6, Figure 5.30 shows the fully plotted distribution of residual velocities which are based on the same velocity data as those in

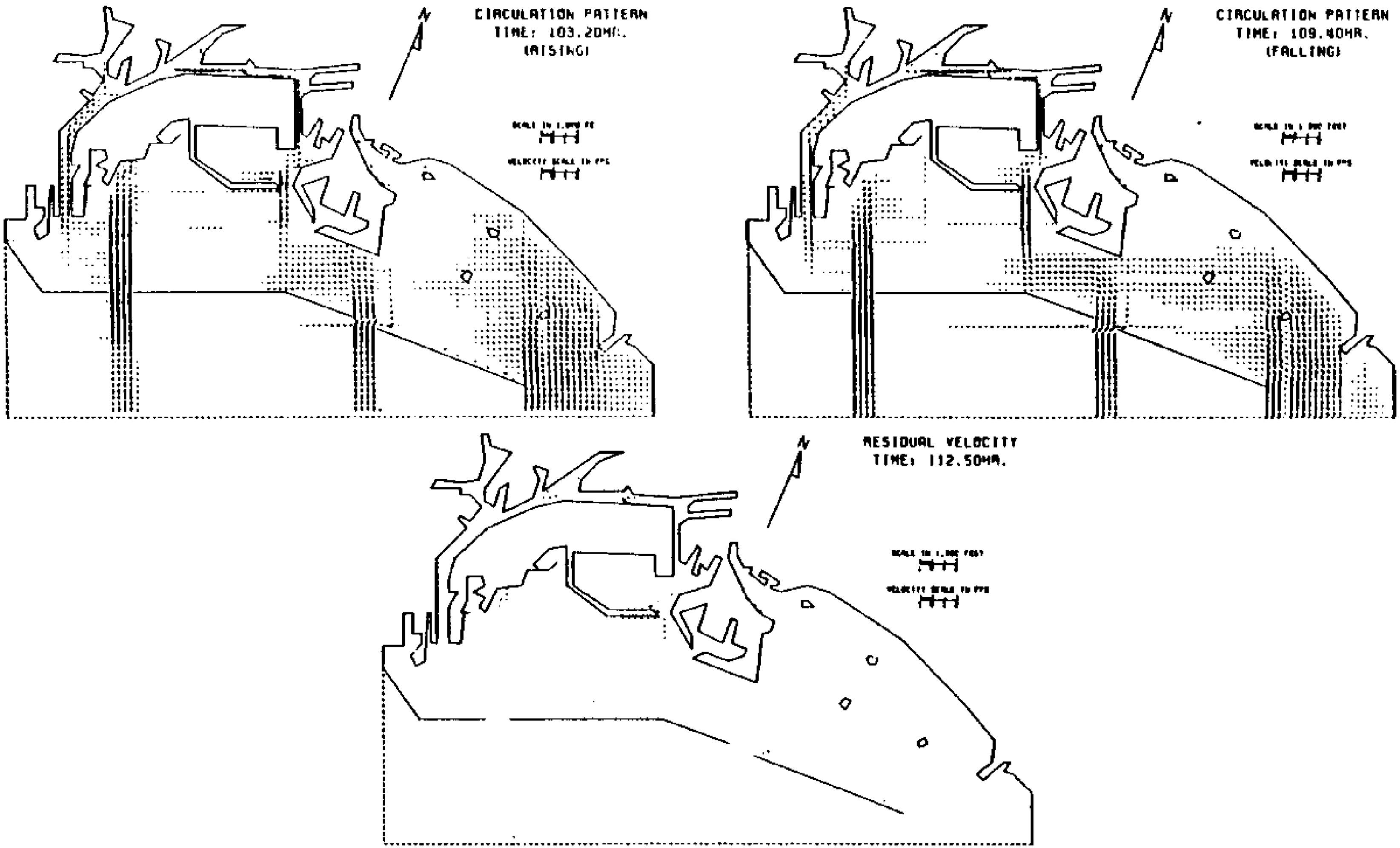

Figure 5.29 Flow Patterns for Run #14 (without Nonlinear Advective Terms).

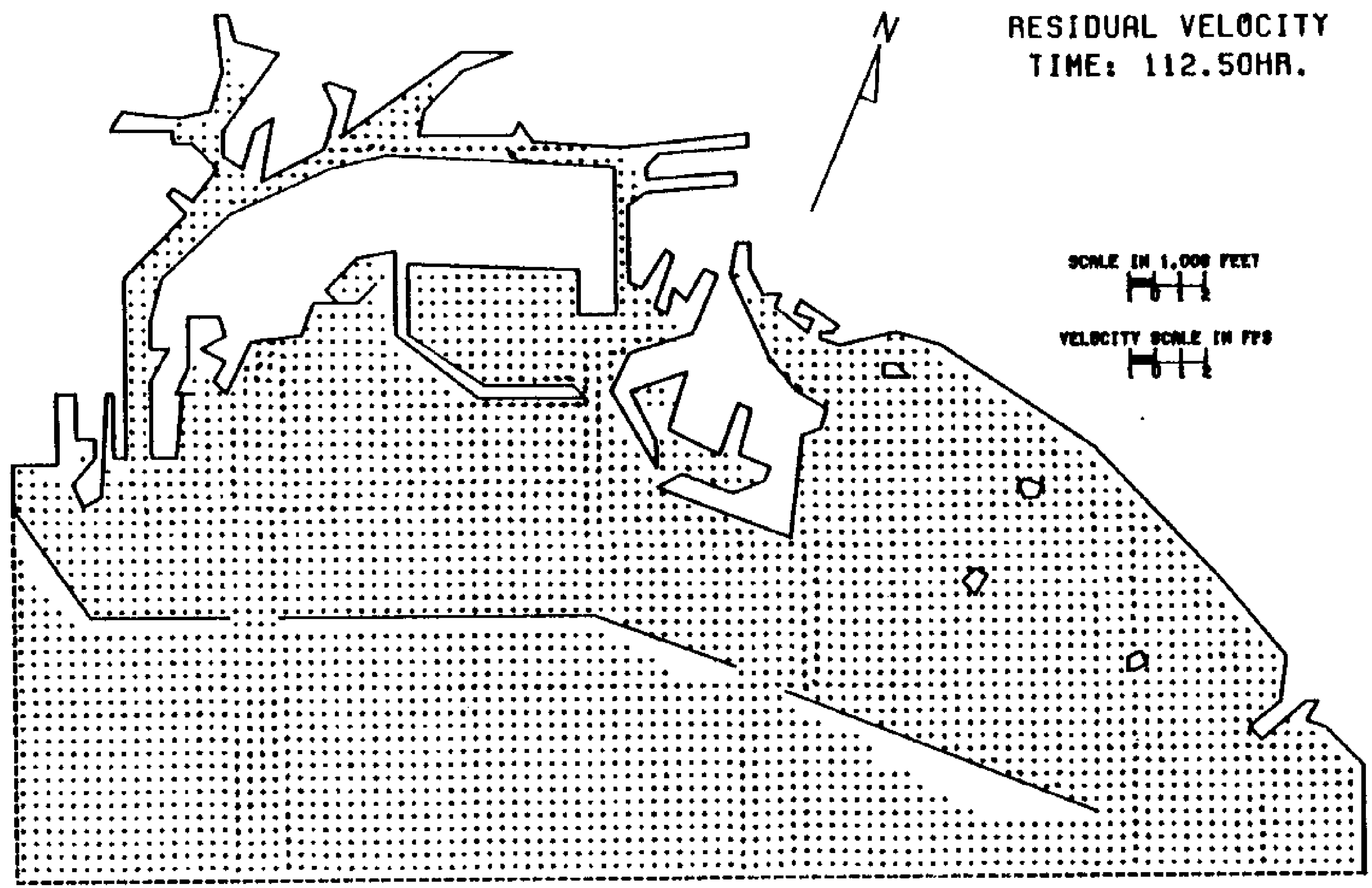

Figure 5.30 Distribution of Residual Velocities for Run #14 (without Nonlinear Advective Terms).

Figure 5.29.

In Run #14, the circulation was simulated for 6125 time steps (612.5 hr real time) without experiencing numerical instability. It indicates that the nonlinear advective term is an important factor of producing numerical instabilities.

5.6 Effects of Coriolis Force

When the Coriolis force terms were excluded from the model, Run #15 (see Table 5.1) showed little change of circulation pattern inside the harbor. Figure 5.31 depicts the distributions of residual velocities for this computer run. The clockwise gyres shown are a bit weaker than those in Figure 5.5. As a result, it seems that the Coriolis force can be neglected in studying gyres which are less than 10,000 ft in diameter.

5.7 Effects of Eddy Viscosity

The coefficient of eddy viscosity was set equal to zero in the basic run. When the coefficient was set to $A = 10\ ft^2/sec$ in Run #16 (see Table 5.1), the results in Figure 5.32 indicate that the strength of every gyre are somewhat smaller than that shown in Figure 5.5.

In Run #17 (see Table 5.1), the coefficient was set to 100 ft^2/sec. Here the smoothing effect is so large that all gyre structures become undetectable (see Figure 5.33),

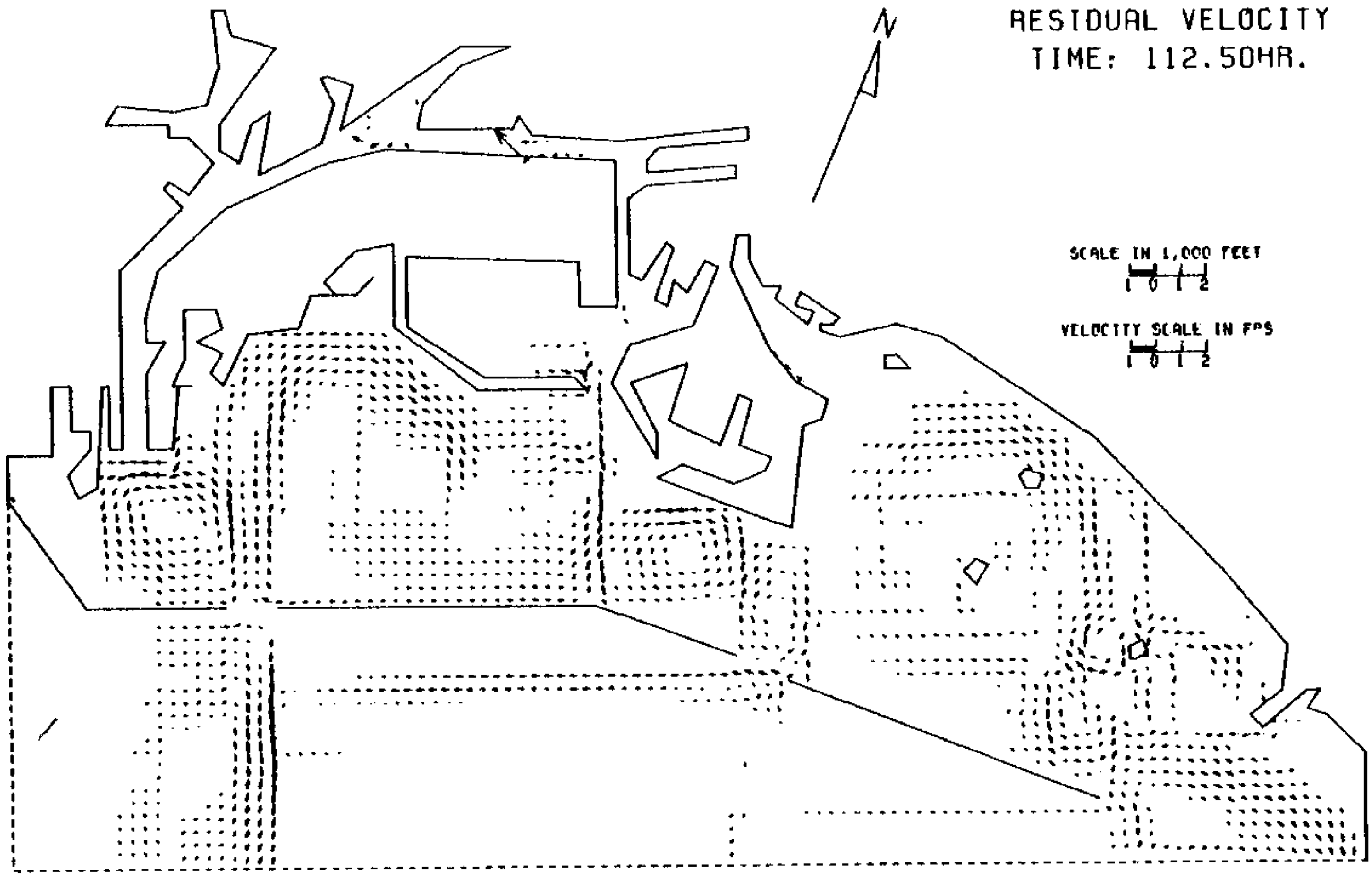

Figure 5.31 Distribution of Residual Velocities for Run #15 (without Coriolis Force).

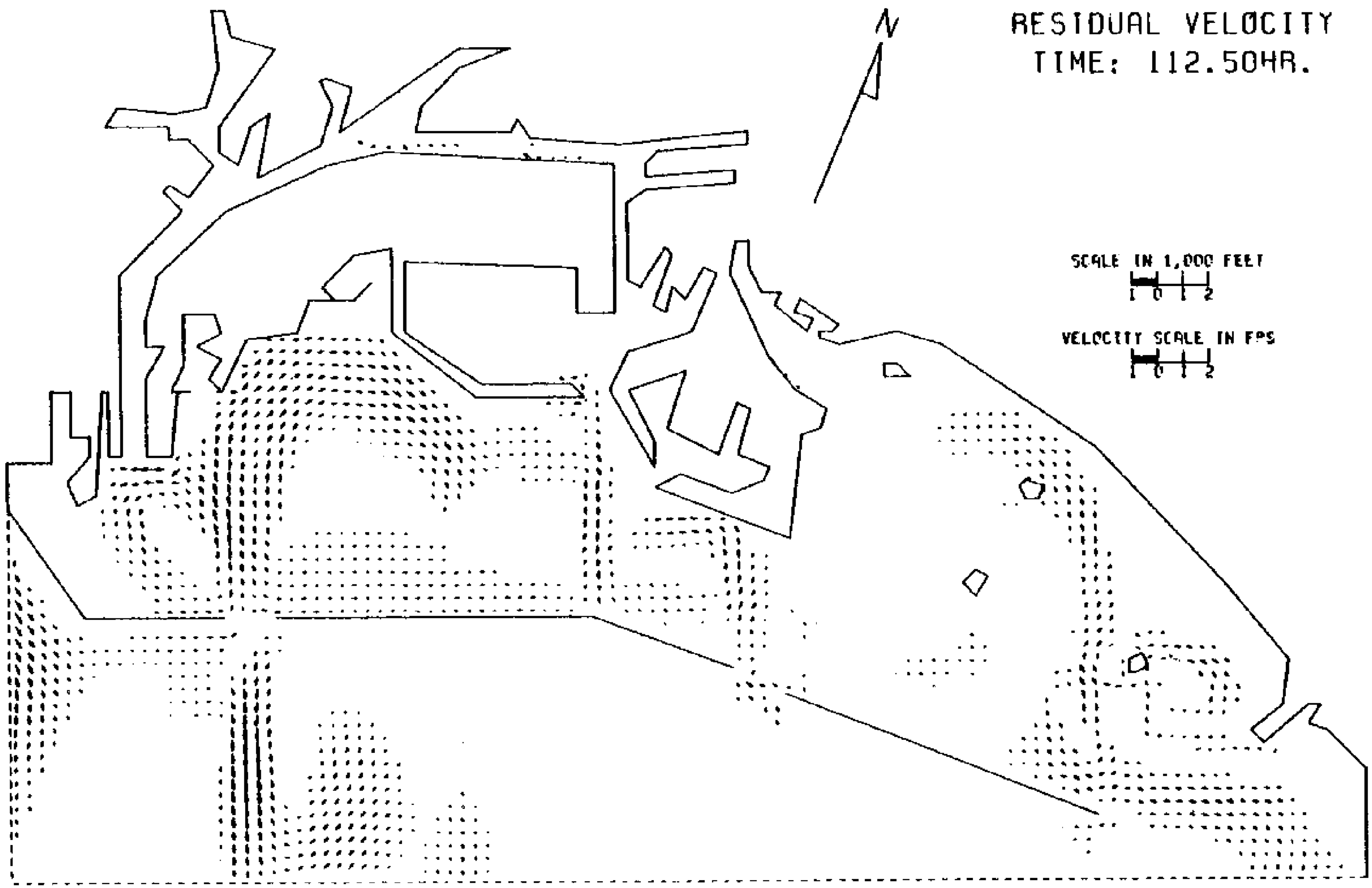

Figure 5.32 Distribution of Residual Velocities for Run #16 (Eddy Viscosity Coefficient = 10).

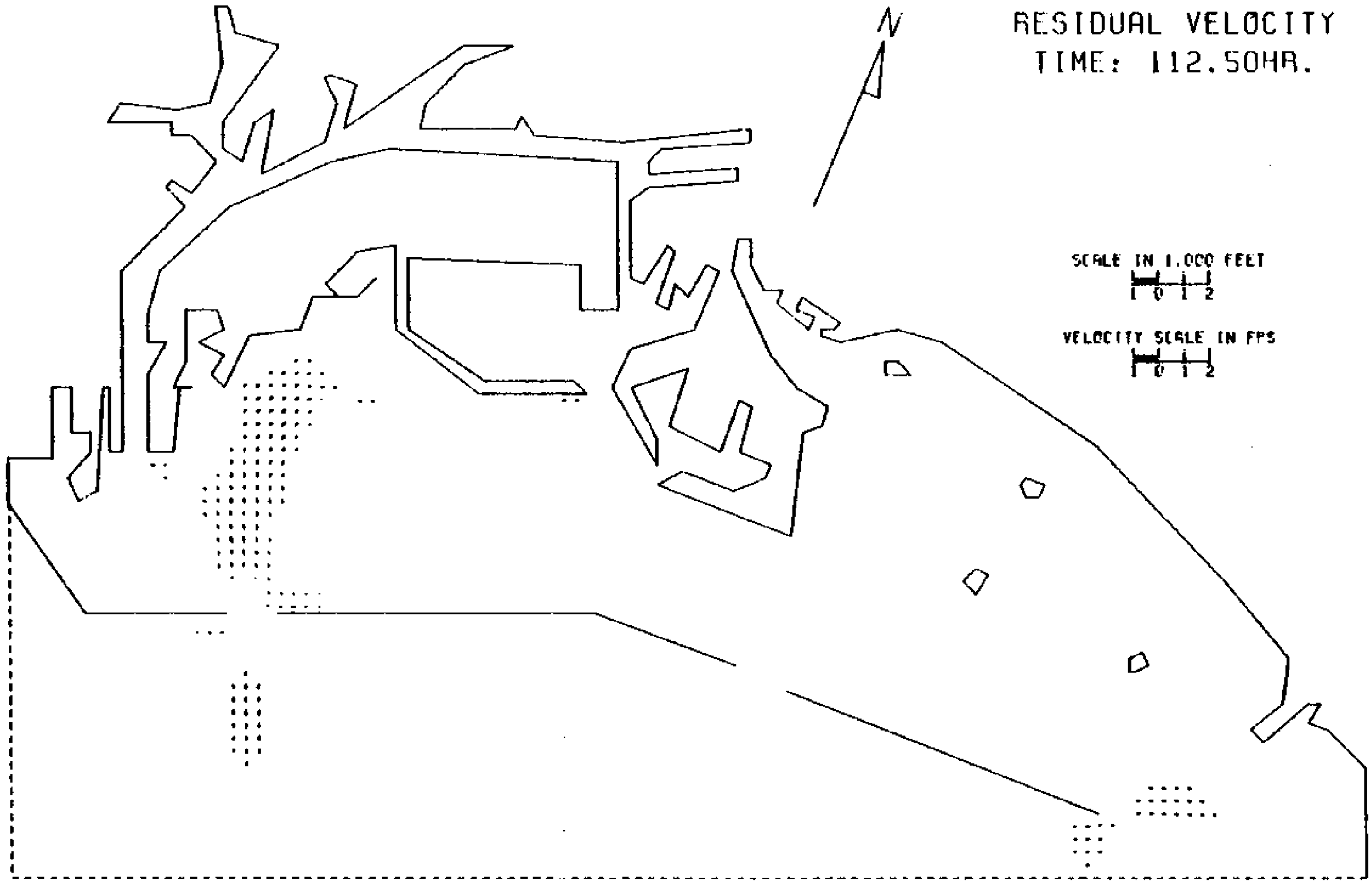

Figure 5.33 Distribution of Residual Velocities for Run #17 (Eddy Viscosity Coefficient = 100).

in contrast to what can be found in Figure 5.32. By comparing these results to those from the hydraulic model, one can conclude that $A = 100\ ft^2/sec$ is too large to be accepted.

Run #18 had $A = (\Delta s)^2/(8\Delta t) = 173\ ft^2/sec$ which followed equation (4.6) in Section 4.2. Part of the results were plotted in Figure 5.34. In this case, the tide moved forward and backward such that the residual currents were negligible all over the study area. Figure 5.35 shows the fully plotted distribution of residual velocities for this computer run and demonstrates the influence of eddy viscosity. The figures plotted for the results of the seventeenth tidal cycle are not distinguishable from those plotted for the ninth tidal cycle as shown in Figure 5.34.

Runs #19, #20, and #21 (see Table 5.1) used 200, 300, and 400 ft^2/sec, respectively, as the coefficient of eddy viscosity. The plotted results were almost identical to those from Run #18, therefore, those results are not shown here.

Runs #22, #23, and #24 (see Table 5.1) used 500, 1,000, and 10,000 ft^2/sec, respectively, as the coefficient of eddy viscosity. The results diverged within a very short time. This proved that an overestimated value of the coefficient, even if it has been used successfully in other models (as what has been discussed in Section 4.2), could

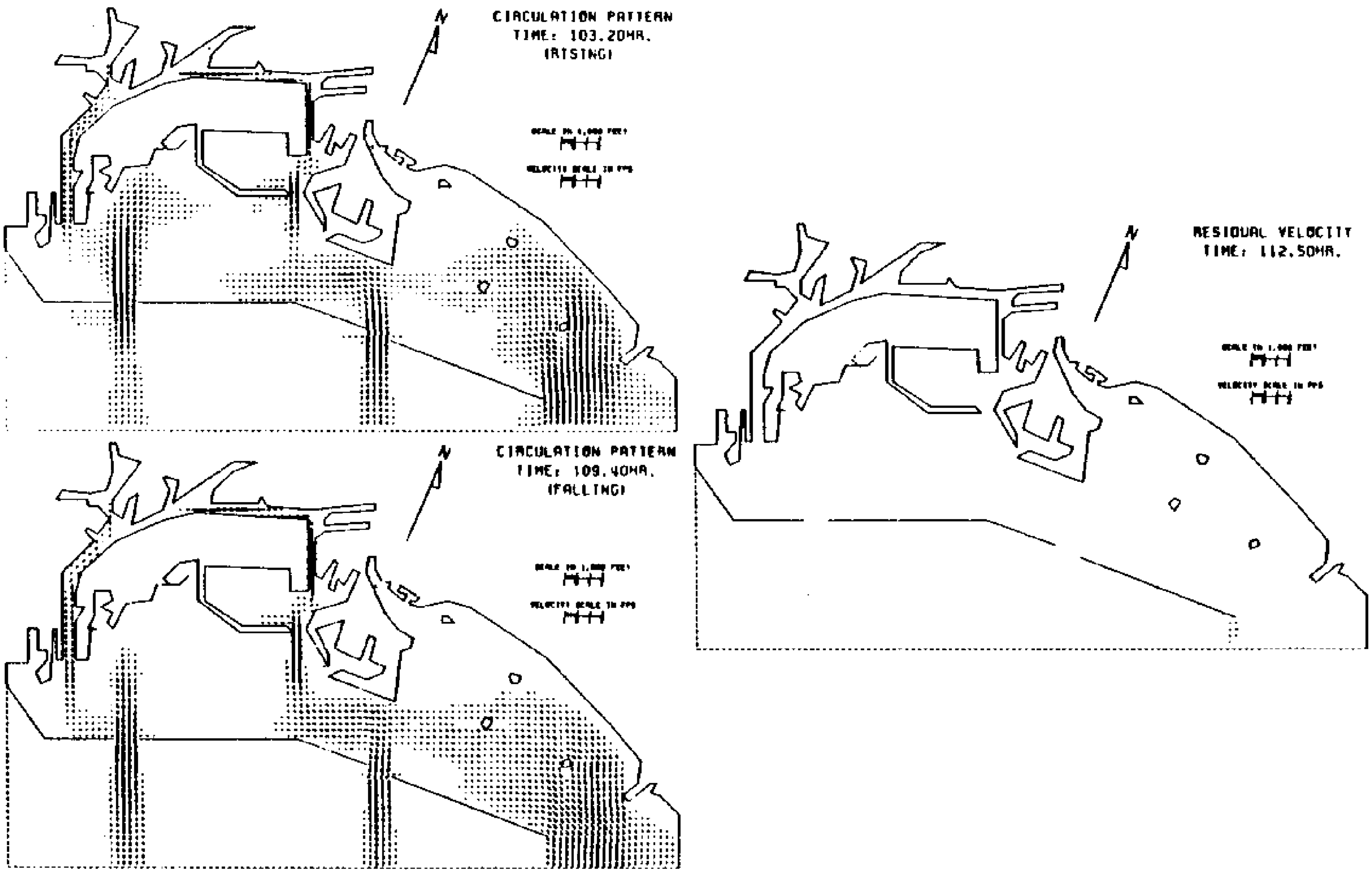

Figure 5.34 Flow Patterns for Run #18 (Eddy Viscosity Coefficient = 173).

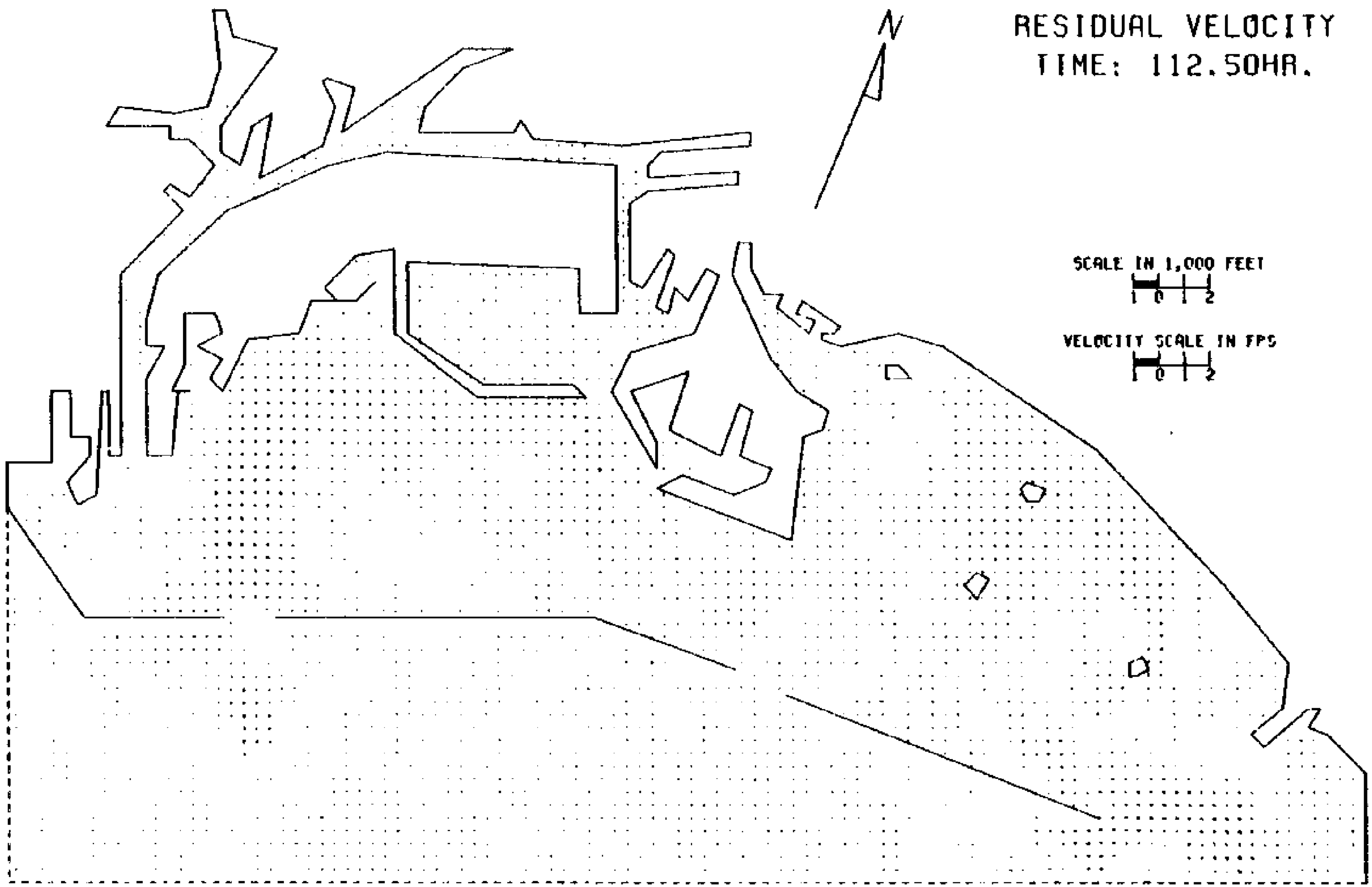

Figure 5.35 Distribution of Residual Velocities for Run #18
(Eddy Viscosity Coefficient = 173).

cause great difficulties during simulation.

When the coefficient of eddy viscosity is larger than 173 ft^2/sec, the results diverge more rapidly as the value of the coefficient is increased (as one can see from Table 5.1).

The indicator $A = (\Delta s)^2/(8\Delta t)$ given by equation (4.6) is not a criterion for stability. However, Runs #16 to #24 indicate that the effects of eddy viscosity are maximized by using the value given by this indicator and that a larger value could increase the instability of the model.

The above tests indicate that the simulated results are sensitive to the changes of eddy viscosity. However, in studying the residual current in the Minas Channel and Minas Basin, Tee (1976) concluded that there was no significant difference of residual currents between the case of $A = 0$ and the case of $A = 10^6$ $cm^2/sec = 1.1\times10^3$ ft^2/sec. This is reasonable, since with $\Delta s = 2830$ m and $\Delta T = 31.04$ sec in his model of Minas Channel and Minas Basin, $A = 10^6$ cm^2/sec is only a very small fraction of the indicator $(\Delta s)^2/(4\Delta T) = 6.46\times10^8$ cm^2/sec.

In conclusion, the effect of eddy viscosity is negligible when the coefficient is small and becomes obvious when the coefficient reaches a certain level. After this level, the model is sensitive to the change of eddy viscosity. The effects reaches maximum when the value of linear eddy viscosity is about $(\Delta s)^2/(4\Delta T)$. This value should be the higher limit of the possible value for the linear coefficient.

5.8 Effects of Bottom Friction

Figure 5.35 depicts the distribution of residual velocities for Run #25 (see Table 5.1) in which the bottom friction was neglected. In this case, strong currents appeared everywhere and there was no momentum dissipation. The results became unstable by the ninth tidal cycle in which the velocity vectors in Figure 5.36 were calculated.

The basic run used 0.020 as the Manning's roughness coefficient while Run #26 (see Table 5.1) used 0.040 instead. The corresponding Chezy coefficient and the non-dimensional roughness coefficient are shown in Figure 4.3. The distribution of residual velocities is shown in Figure 5.37. Weak currents and gyres, comparing to those in Figure 5.5, indicate that the model is sensitive to the change of bottom friction. If this is true, the results from a hydraulic model may be questionable because it is difficult to physically model the bottom roughness. A suitable calibrated numerical model may be able to yield better resolutions.

This test of sensitivity of model with respect to the bottom friction gave different conclusions from those given by Tee (1976) in which it was concluded that there was no

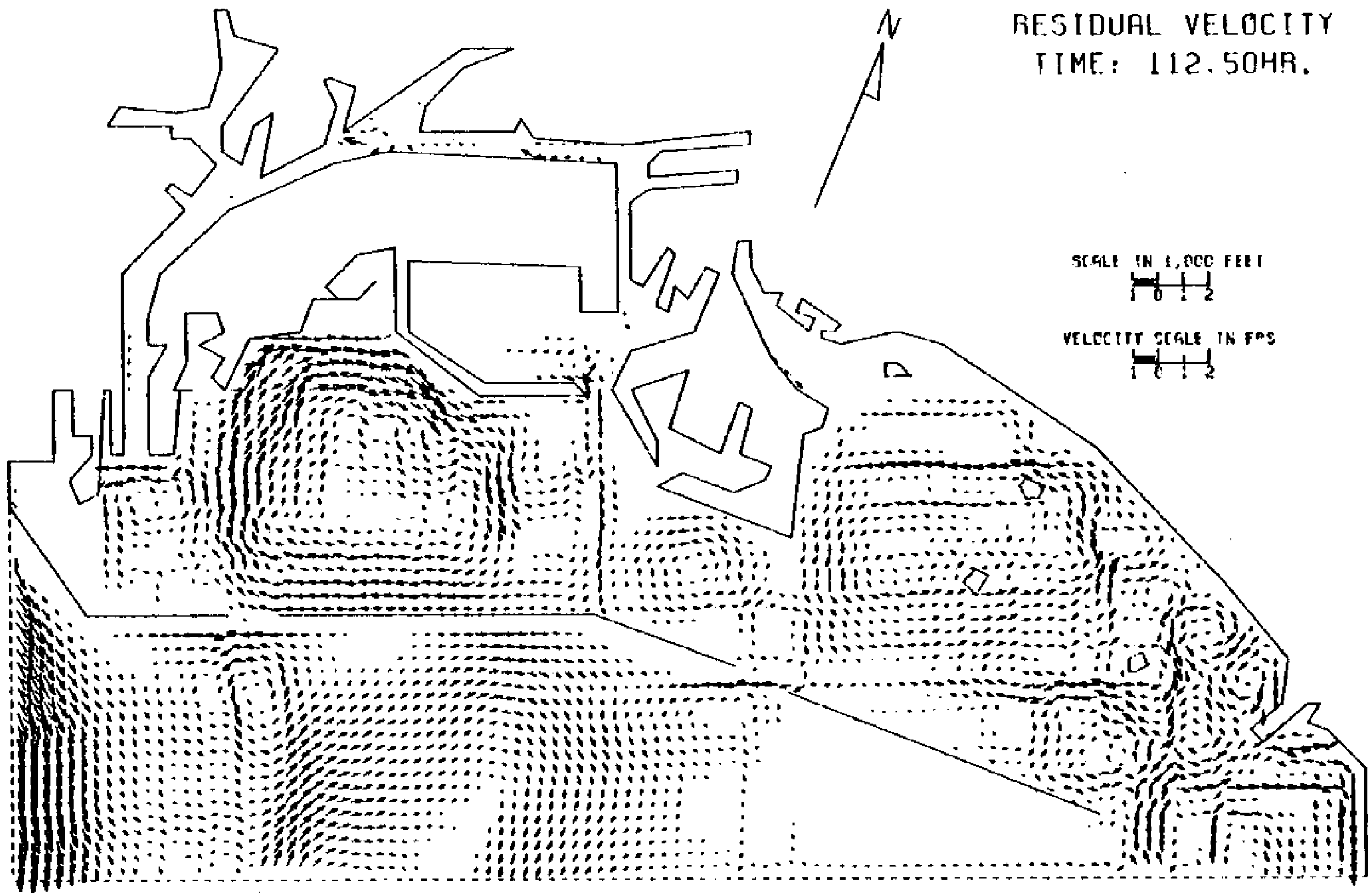

Figure 5.36 Distribution of Residual Velocities for Run #25 (Manning's Coefficient = 0).

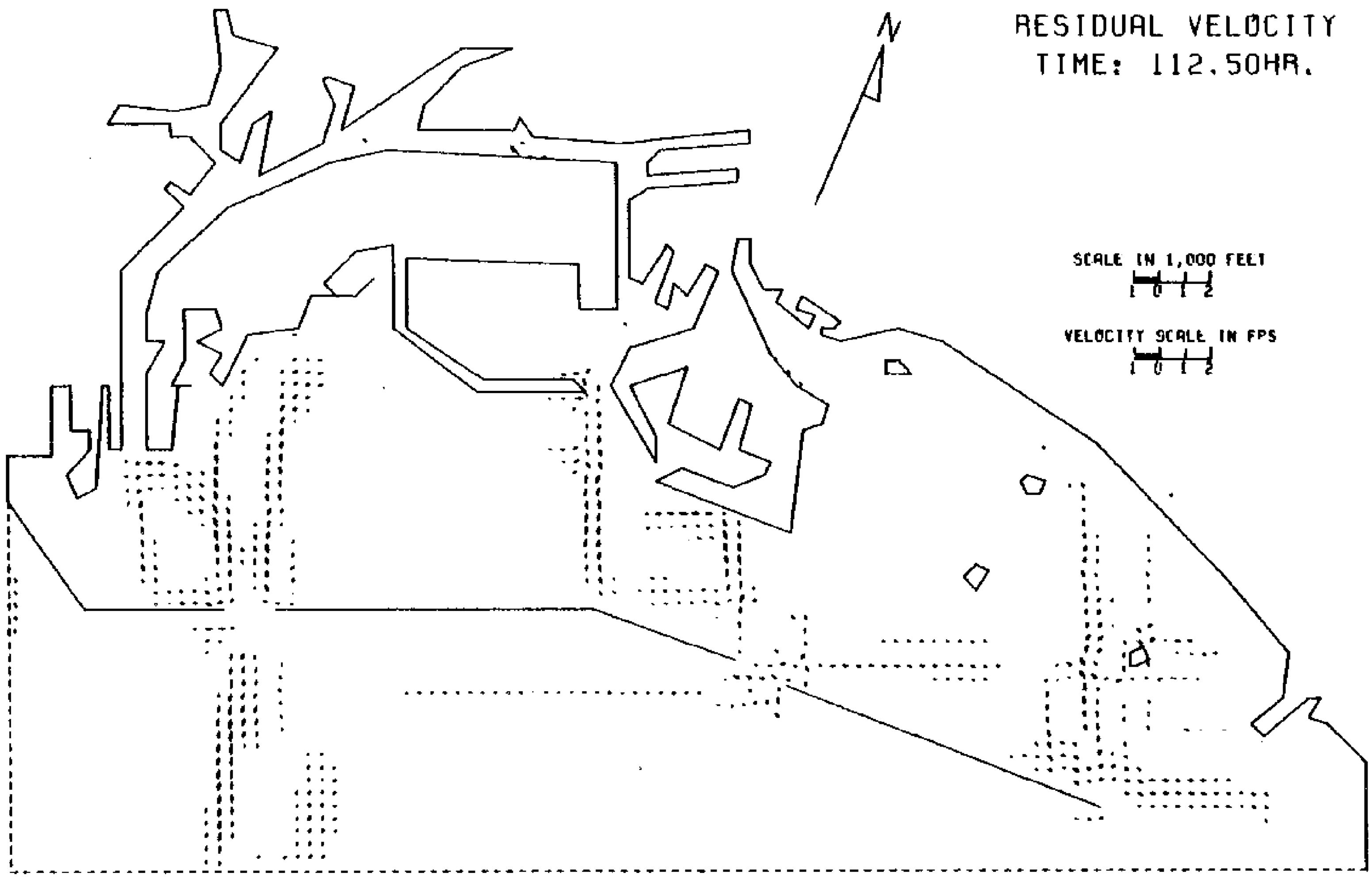

Figure 5.37 Distribution of Residual Velocities for Run #26 (Manning's Coefficient = 0.040).

significant difference of the residual current in the Minas Basin, between the case of C' = 0.001 and the case of C' = 0.003, where C' is the nondimensional roughness coefficient defined in equation (3.9). Allender (1975) also stated that there is not remarkable change in the flow patterns for different friction coefficients. The difference may be insignificant for flows in approximately linear motions and for the results obtained during the warm-up period.

In this numerical model, there are two experimental coefficients, i.e., the coefficient of eddy viscosity and coefficient of bottom roughness, to be calibrated. Increasing either of these two values will decrease the strengths of both currents and vortices. It requires personal expertise in order for one to adjust these two coefficients in an optimal way.

For the preliminary estimation, there are more guidances available in the literature for the roughness coefficient than for the eddy viscosity coefficient. The latter is very difficult to be chosen through the literature survey (see Section 4.2). If there is no data available for a study area, one may start with A = 0 (i.e., no eddy viscosity) and calibrate the roughness coefficient. The present study started with A = 0 and n = 0.020 and then conducted the sensitivity tests for both two coefficients. There is no conclusion on what the value of the eddy viscosity should be. By comparing to the results from the hydraulic model, it seems that the combination of A = 0 and n = 0.020 is a good choice for the simulation. May be the case with n = 0.025 (not tested in this study) can also give satisfactory results.

5.9 Effects of Bathymetry

The basic run utilized field data for determining the water depth. In order to test the behavior of the model when using a constant depth, Run #27 (see Table 5.1) chose 30 ft as the lower low water for the whole study area. The results diverged faster than those for the basic run. Runs #28 and #29 (see Table 5.1) increased the constant value to 40 and 45 ft respectively.

Figure 5.38 depicts the velocity patterns obtained from Run #29. The circulation patterns are similar to those in the figures obtained from basic run. The results should be closer to each other if the unit width discharge is used (instead of averaged velocity) to plot the figures. Comparing the residual velocity in Figures 5.38 and 5.5, it can be found that the large eddy is a little bit stronger in Run #29 than in the basic run. This might be caused by the increased jet velocity through Angel's Gate when the water depth there was assumed 45 ft in Run #29 rather than 49 ft in the basic run.

It was suspected that one of the factors causing

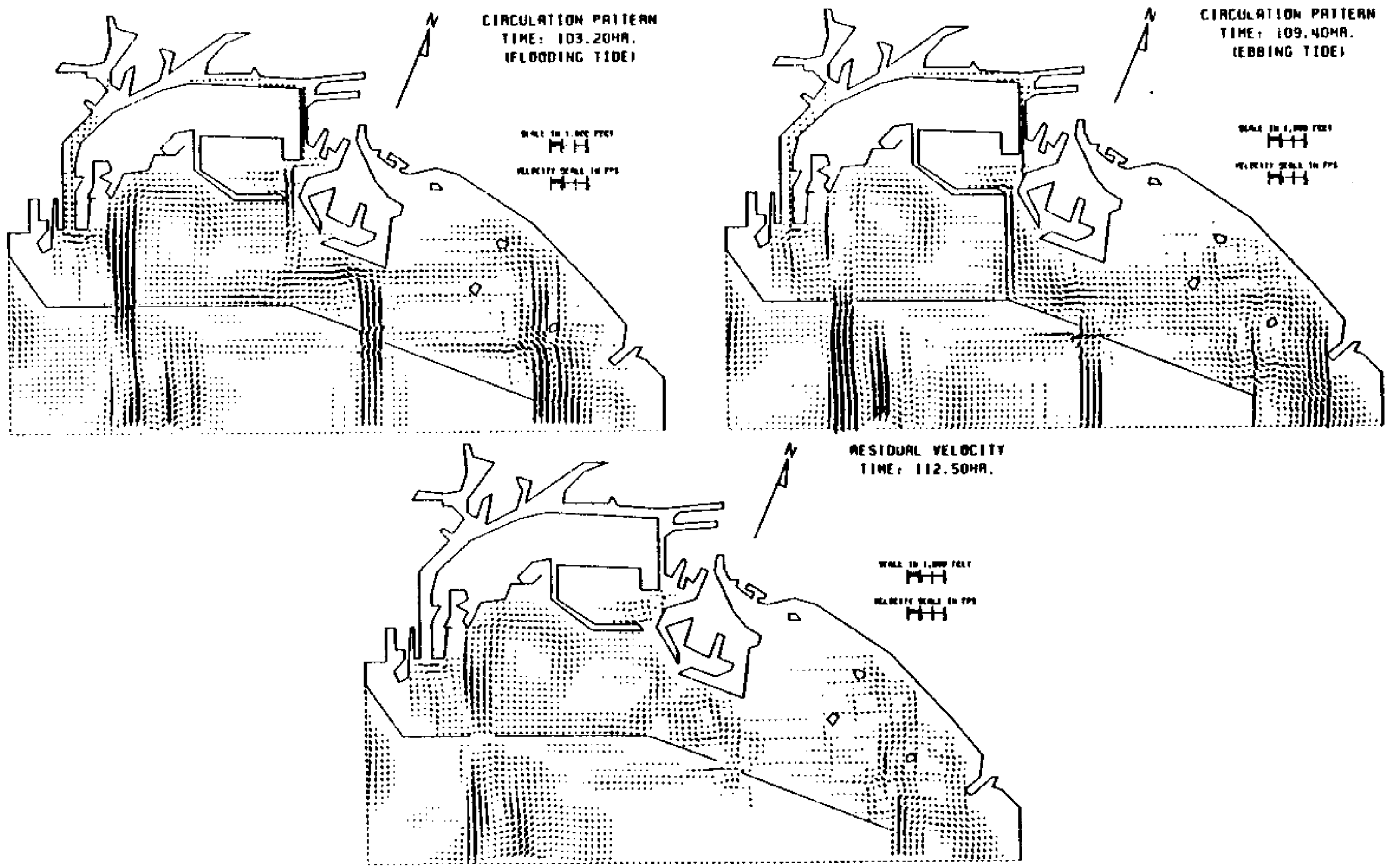

Figure 5.38 Flow Patterns for Run #29 (Constant Depth = 45 ft).

numerical instability was the high gradient of velocity at the boundary of the jet passing through Angel's Gate. Run #30 (see Table 5.1) had the depth values of grid points for columns 18 to 23 modified. These columns pass through Angel'S Gate and are perpendicular to the breakwaters. Those grid points outside the harbor were assigned a constant depth of 100 ft while those inside the harbor had values decreased gradually, (with 2% slope) from 100 ft to their field values. In other words, the channel passing through Angel's Gate was artificially deepened, in order to have smaller velocity and smaller lateral velocity-gradient around the opening of harbor. Run #31 (see Table 5.1) had the depth of this artificial channel increased from 100 ft to 200 ft. The simulations were more stable in these two cases, as can be seen from Table 5.1.

The distributions of residual velocities for Runs #30 and #31 are shown in Figures 5.39 and 5.40, respectively. When the intruding velocity is reduced due to the deeper channel, the amount of vortices produced at the harbor entrance is smaller, and so the size of gyres is decreased. The weak gyre in Figure 5.40 is also possible due to its requirement of longer simulation time before it would reach steady results, since the velocity at entrance has been small.

Hence Runs #27 to #31 showed that the velocity

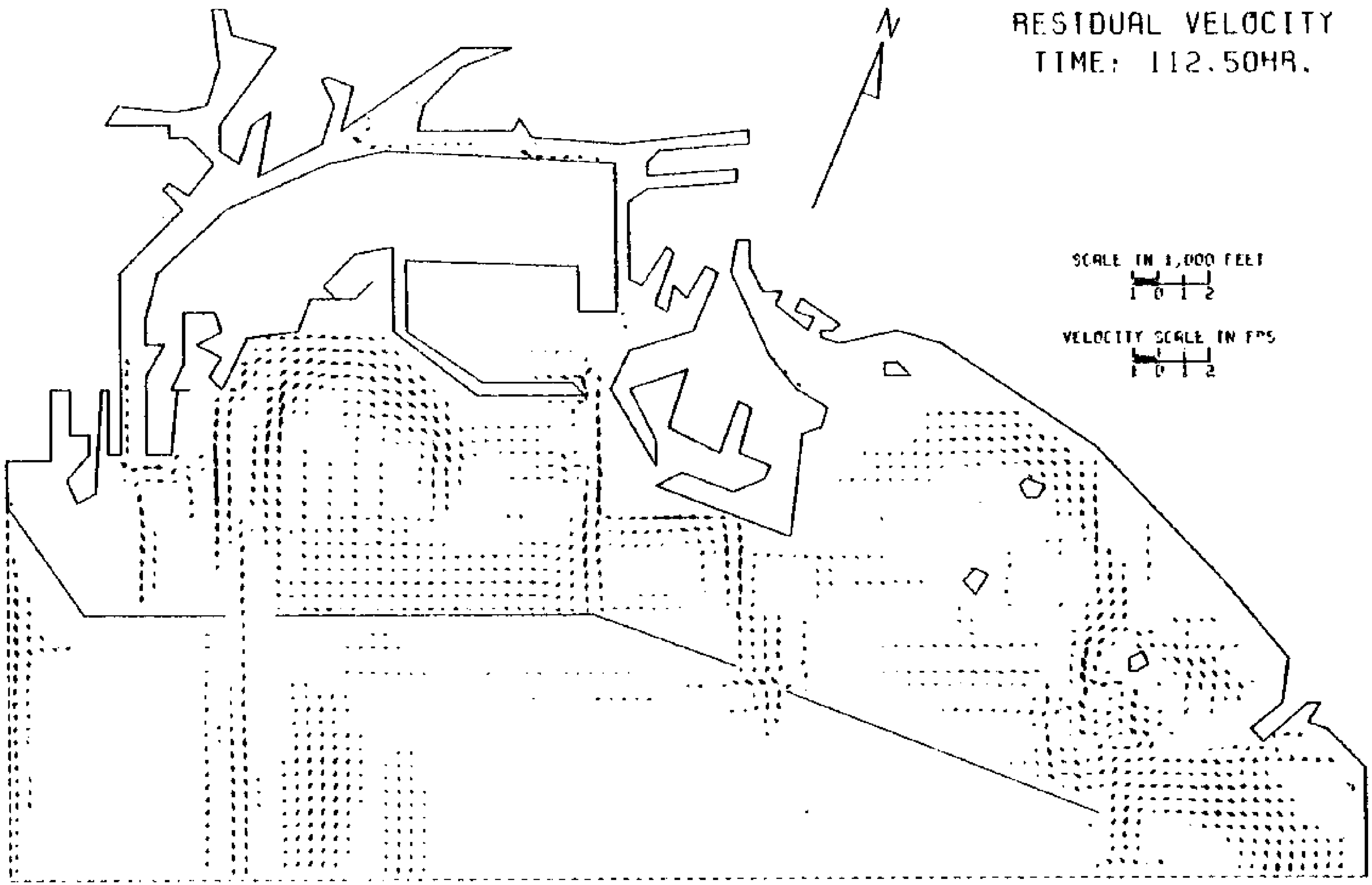

Figure 5.39 Distribution of Residual Velocities for Run #30 (with the Channel near Angel's Gate Deepen to 100 ft).

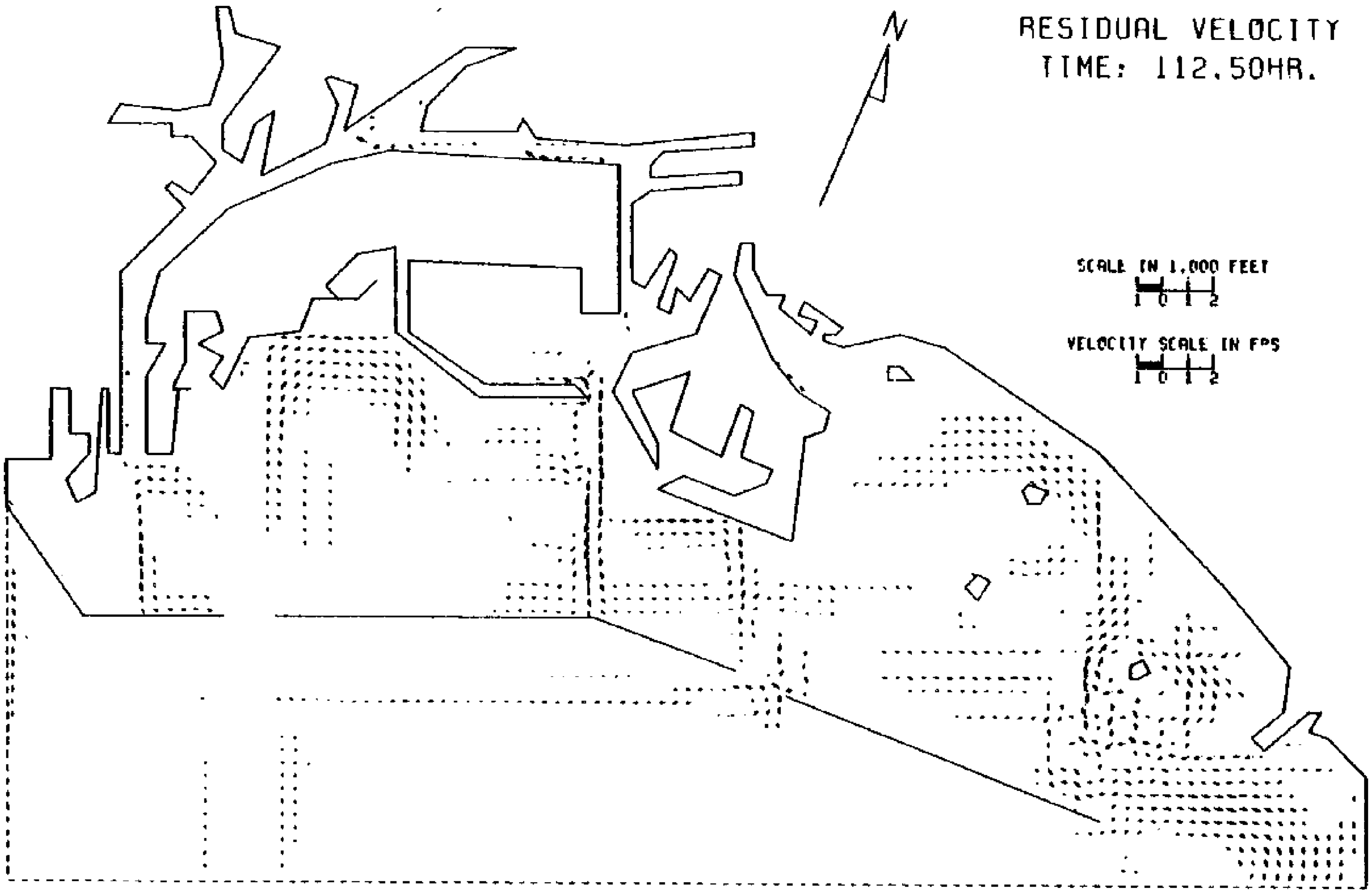

Figure 5.40 Distribution of Residual Velocities for Run #31 (with the Channel neal Angel's Gate Deepen to 200 ft).

patterns were affected by changes of bathymetry. When a constant depth model is used, the depths at harbor entrances should be close to those of the field data in order to have correct jet velocities. Incorrect jet velocities may yield erroneous vortex strengths.

5.10 Effects of Network Orientation

The simulation results can be affected by the orientation of computational network used in the ADI (alternating-direction-iteration) method, especially if the Courant number is greater than unity.

During ebb tide, the direction of the current coming out of a small harbor opening is supposed to be more or less normal to the cross section of the opening. Yet Figure 5.3 shows that the current discharges through Queen's Gate are separated into two jets, one in the x-direction and the other in the y-direction. This is an error due to using a large time step in ADI method. When the Courant number is large, a signal propagates several grid spacings within a single time step. With a high elevation gradient, the x-direction computation will produce an x-direction jet, and the y-direction computation a y-direction jet. The computed results for a flux at an angle of about 45 degrees will appear as two separated jets along x- and y-directions.

Another error could appear in and beyond a narrow channel which is directed between x- and y-directions such that it becomes a zigzag path when the ADI method is applied. It takes at least N time-steps for a signal to make N turns in this zigzag path, while a signal in an x- or y-direction channel can travel several grid spacings within a time step if the Courant number is high. The delay of signal in the zigzag path introduces errors. A different orientation of the network may give different results in those areas beyond the long narrow channels. Therefore, in this study of Los Angeles-Long Beach model, there might be relatively large errors associated with the computed surface elevations in the inner channels. This kind of error will not appear in an open area beside an open boundary where the tidal elevations are specified. Unfortunately, there is no data available in the present study to check the error of surface elevations.

Even if the Courant number is not greater than one, the duration for a signal to turn around a certain obstruction may still be different for the cases of different orientation and the simulated results may be different.

5.11 Effects of Numerical Precision

All computer runs in this study used single precision except Run #32 (see Table 5.1) in which velocities and surface elevations were expressed in double precision. The plotted velocity patterns for the ninth tidal cycle of Run #32 show no detectable differences from those shown in Figures 5.1 to 5.5.

In the basic run, NI = 1, the predicted values for the terms marked with an asterisk in the finite difference equations were not corrected. In Run #33 (see Table 5.1), NI = 2, the predicted values were corrected once in every time step. The pattern of residual velocity in Run #33 (as shown in Figure 5.41) is very close to that in the basic run (Figure 5.5). The correction of the predicted values improved local numerical stability somewhat. The same conclusion can be achieved by comparing the simulated periods for Run #34 and Run #8 (see Table 5.1). However, Run #7 kept the computation from divergence for a much longer time than that in Run #6 by having the predicted values corrected once. This might due to the fact that Run #6 yielded very poor results.

Figure 5.42 depicts the distribution of residual velocities based on the same data in plotting Figure 5.41, but with a different velocity scale. For the same data, the arrow size in Figure 5.42 is twice that shown in Figure 5.41. Hence one may have a different interpretation of the result depending on how the result is presented.

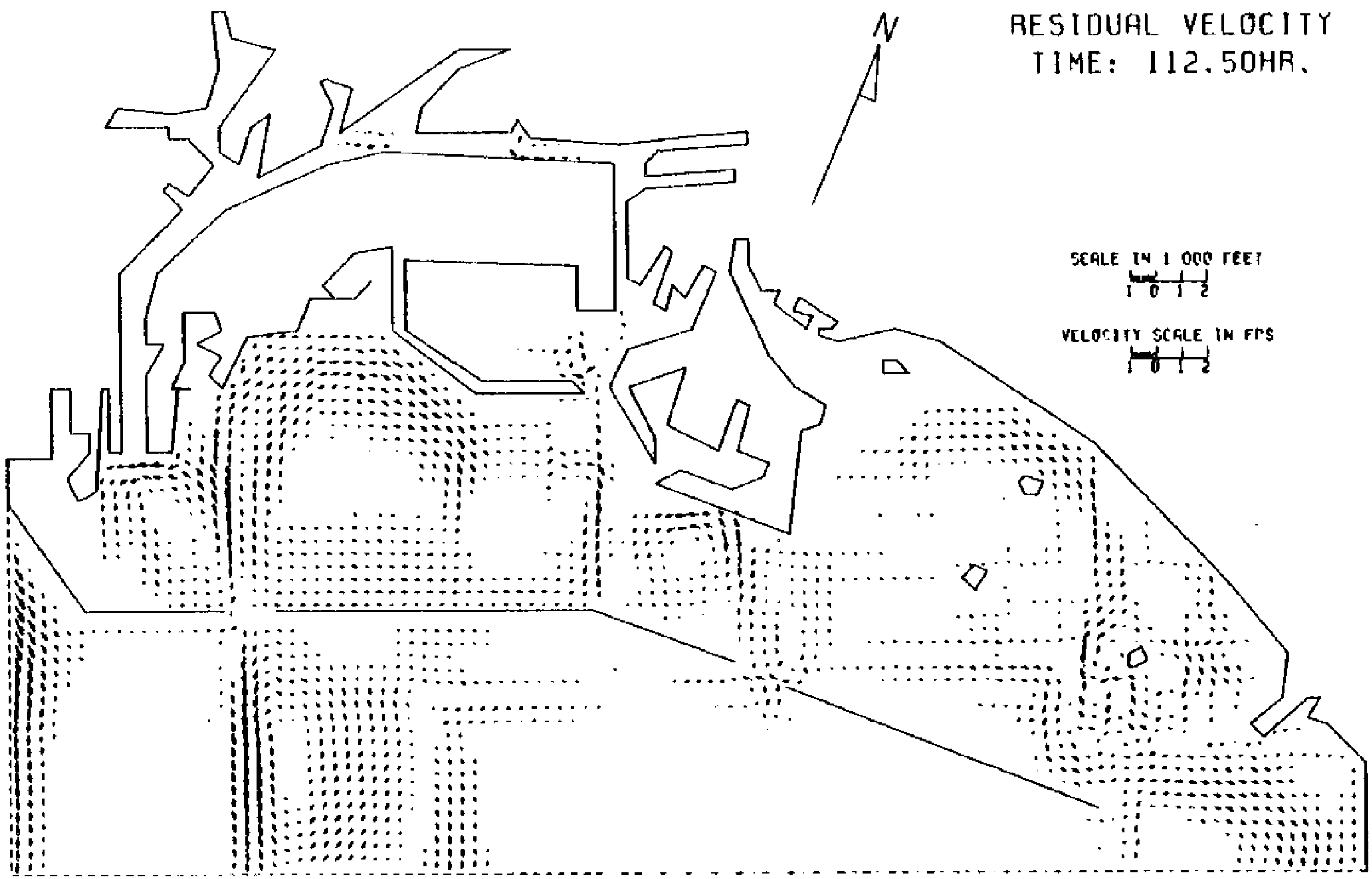

Figure 5.41 Distribution of Residual Velocities for Run #33
(Iteration Number = 2).

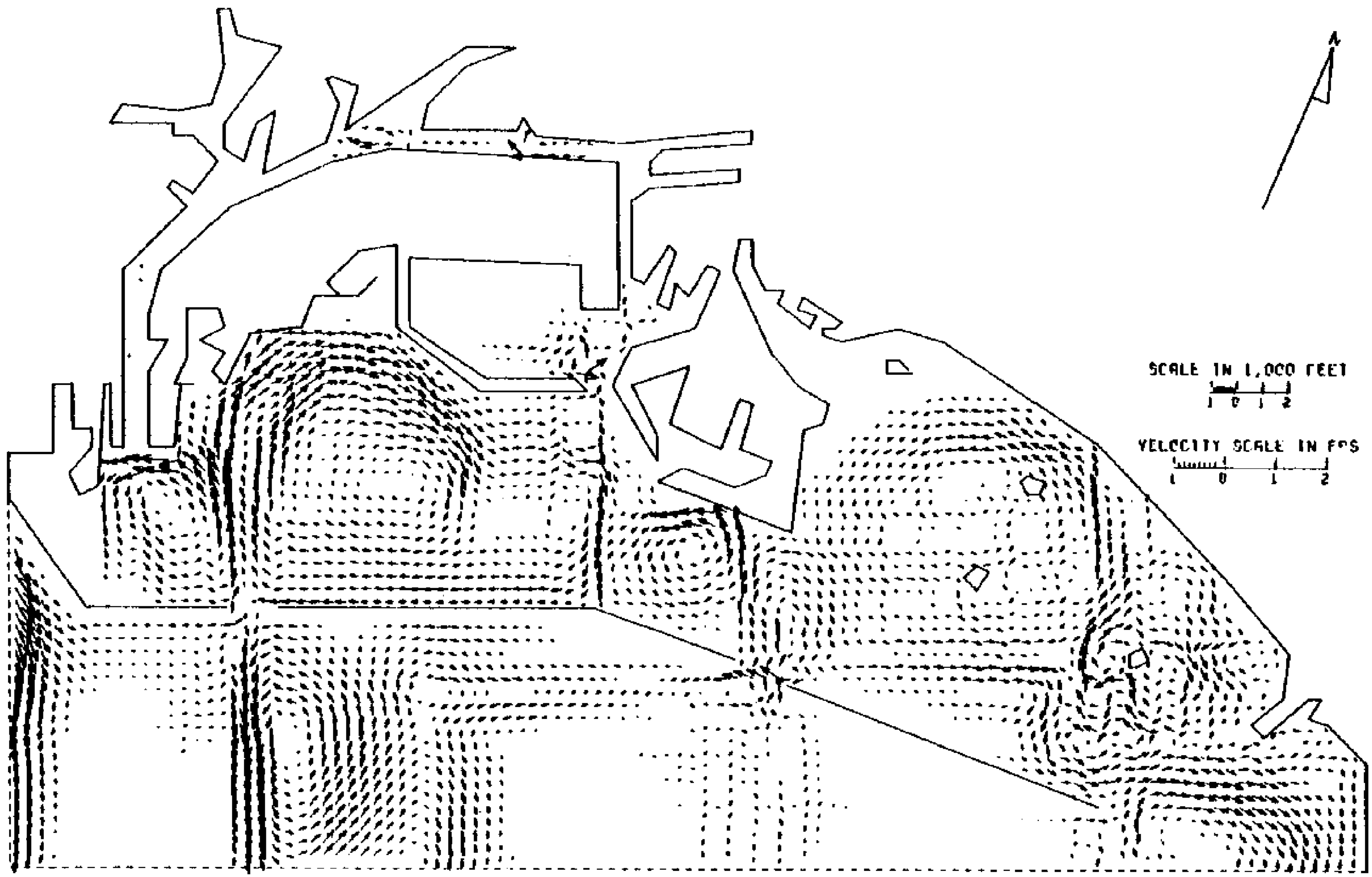

Figure 5.42 Distribution of Residual Velocities, Plotted with a Different Scale, for Run #33 (Iteration Number = 2).

5.12 Other Numerical Tests

Other minor tests were performed by the numerical model developed in the present study. Run #35 (see Table 5.1) used 45 sec for the time step and 40 ft as the constant value of mean water depth. The stability condition was improved when compared to Run #9 in which the water depths were varied as what was shown in the field data. The comparison gives different conclusions from the comparison of Run #28 and #1, in which the result diverges a bit faster when the depth is set at the constant value of 40 ft.

Both Run #28 and Run #35 used a constant depth of 40 ft, while Run #28 used 180 sec for the time step and Run #35 used 45 sec. Table 5.1 shows that Run #35 has kept stable for more than twice the number of time steps used in Run #28 but, because it used a quarter of the time step used in Run #28, the real simulation time before divergence was shorter in Run #35.

Since a simulation usually starts from a motionless state, it is reasonable to start from either a high tide or low tide of a tidal cycle. In this study, all runs using a sinusoidal-type tide as the forcing function had the starting time set at the time of minimum tidal elevation. All runs using the tidal data supplied by U.S. Army Engineer Waterways Experiment Station, except Run #36 (see Table

5.1), used as starting times the same as those in the original spring-tide and neap-tide data sheets, which were also the same as those used by McAnally (1975). Those starting times were a few hours prior to the time of higher low water. Run #36 was tested to see if there would be any difference if the simulation started from the time of higher low water of the spring tide used in Run #2. The plotted results show little difference between Run #36 and #2. From Table 5.1, it is difficult to say which run has given the more stable simulation.

The basic run gave an abnormal current near the west boundary (see Figures 5.1 to 5.7). Run #37 (see Table 5.1) had the open boundary on the west side of the study area replaced by a reflective boundary. The circulation patterns inside the harbor basin are the same as those obtained from the basic run. Figure 5.43 depicts the distribution of residual velocities comparable to that in Figure 5.5.

Since this study put the focus on the gyre which appeared to the north-northeast of Angel's Gate, the large 108x69 network used in Run #1 to Run #37 may be replaced by a simpler network to obtain approximate figures with a lower cost. Run #38 (see Table 5.1) used a 60x34 network with a constant mean water depth of 40 ft. The flows in the inner channels were neglected. Figure 5.44 depicts the

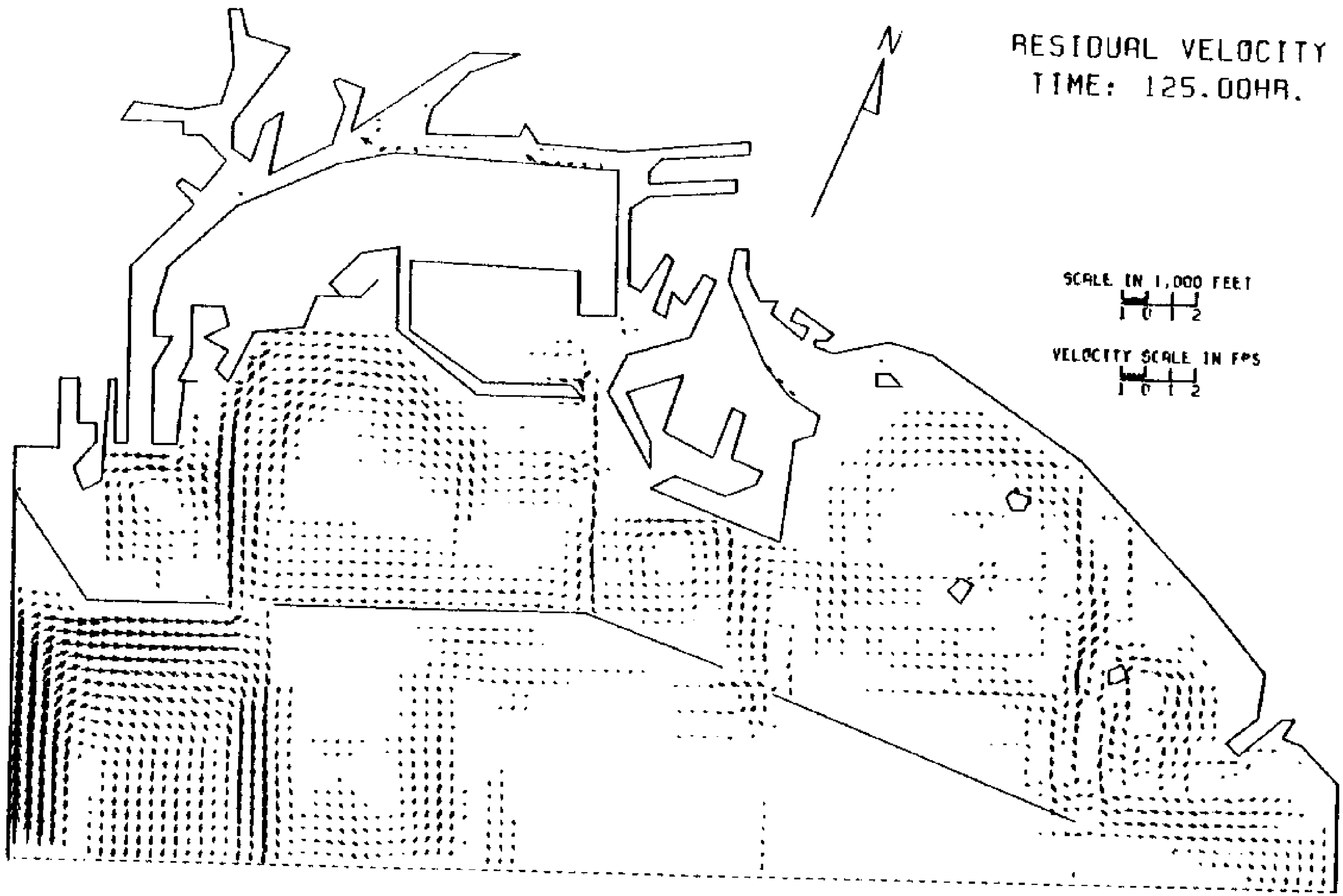

Figure 5.43 Distribution of Residual Velocities for Run #37
(with a Solid Boundary on the West Side).

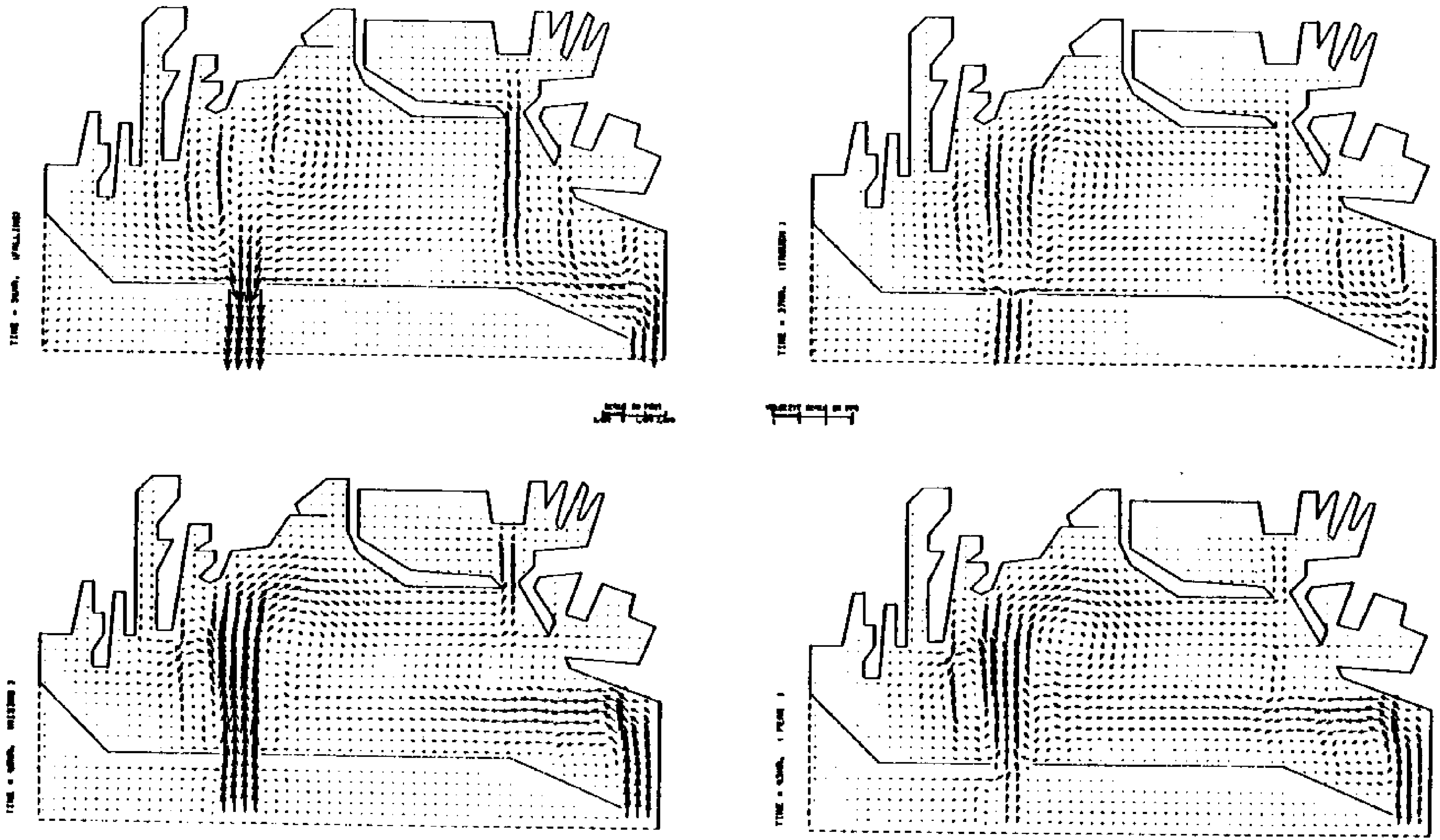

Figure 5.44 Circulation Patterns for Run #38 (with 60x34 Grid Points).

circulation patterns at four different tidal stages in the third semi-diurnal tidal cycle.

The results of basic run for four tidal stages corresponding to those in Figure 5.44 are shown in Figure 5.45 for comparison. In Figure 5.45, the ratio of the velocity scale to the length scale is 20% higher than those in Figures 5.1 to 5.41. By comparing Figures 5.44 and 5.45, it is found that the error of results obtained from a reasonably simplified geometry is insignificant. It is acceptable to use the simplified geometry of Run #38 to study the large gyre in outer Los Angeles Harbor.

Run #39 (see Table 5.1) was another test with simplified geometry. The grid spacing was 1,000 ft instead of 500 ft in other computer runs. The network consisted of 31x25 grid points. The study area was the same as that in Run #38 except that the inner channels were included. The mean water depth was assumed to be 40 ft for the whole study area. Figure 5.46 depicts the circulation patterns of Run #39. The general patterns are similar to those shown in Figures 5.44 and 5.45. Again it shows that a reasonably simplified geometry can be used to study the general trend of flow patterns. However, the detailed flows near boundaries are not expected to be correct in this case.

Besides all those tests, a computer run has been

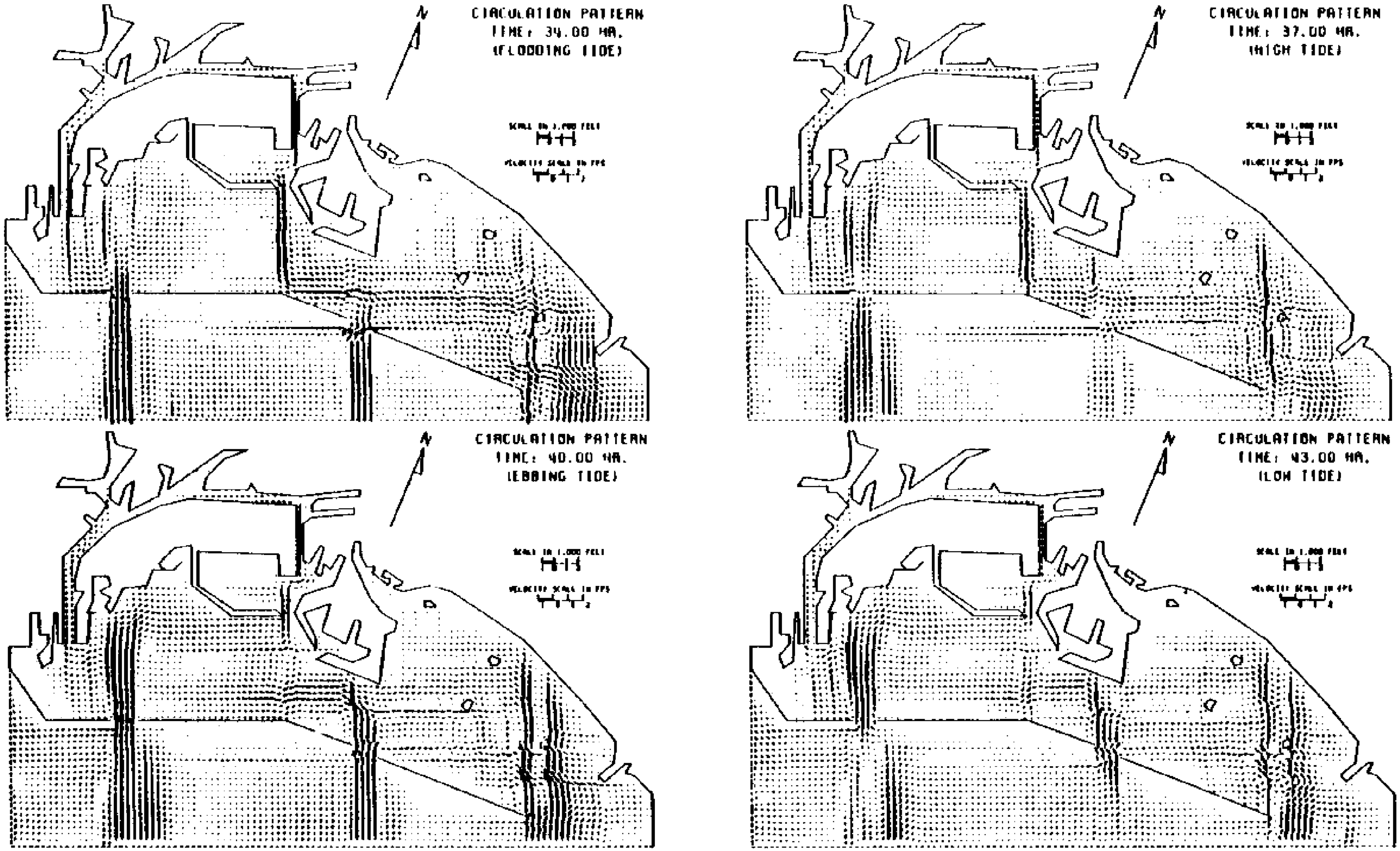

Figure 5.45 Comparative Circulation Patterns from Run #1 (Basic Test).

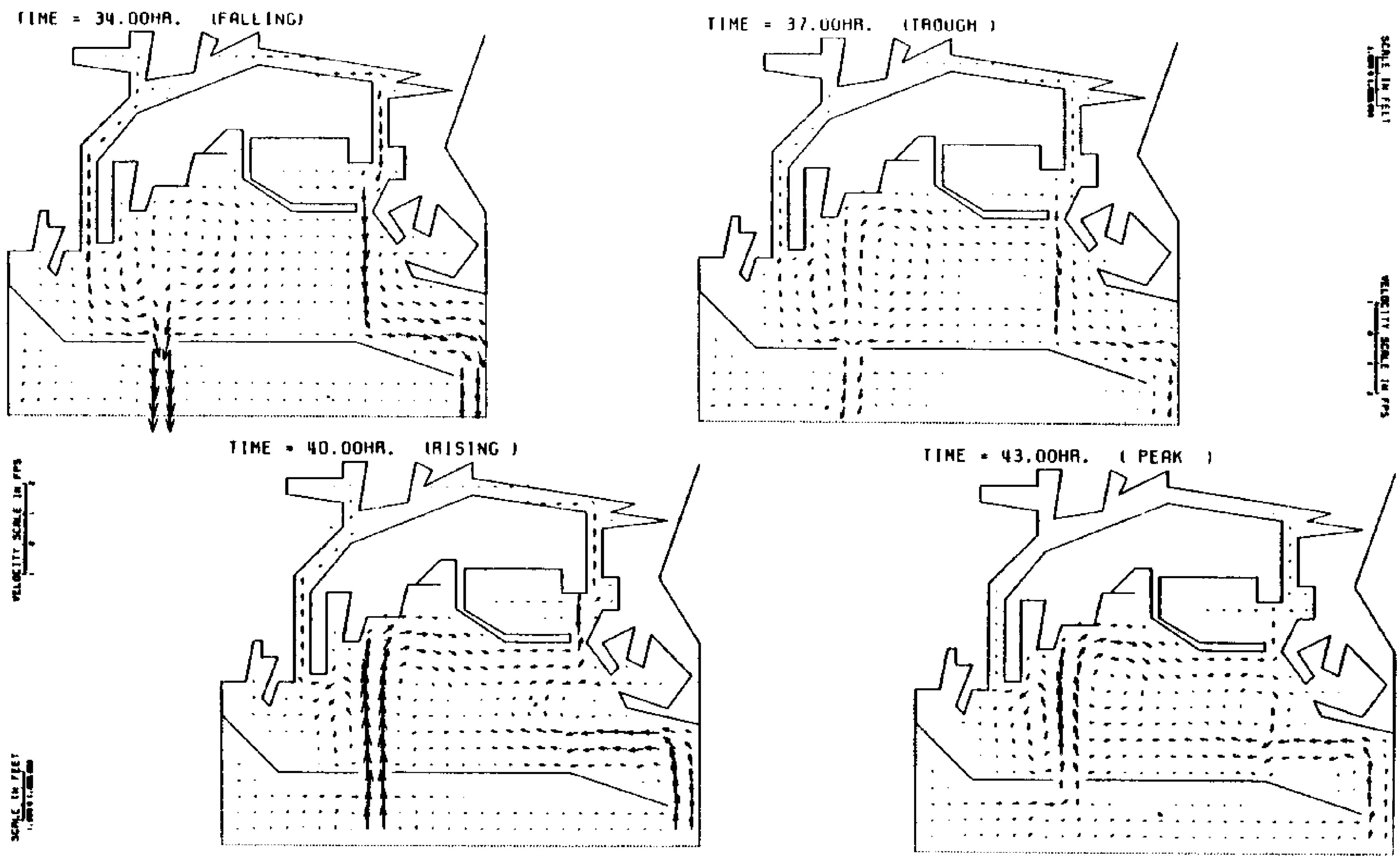

Figure 5.46 Circulation Patterns for Run #39 (Grid Spacing = 1000 ft).

performed to supply the hydrodynamic data for an ecological simulation model with which Kremer & Kremer (1979) have evaluated the potential impact of the Terminal Island Treatment Plant secondary waste effluent on the Los Angeles Harbor ecosystem. The computer run used a 31x17 network with 650-m grid-spacing to cover the whole outer Los Angeles-Long Beach Harbor. It took only 24-min computer time with 25-K memory to simulate 3000-hr real time (300 time-steps) flows, and yielded results which were good and stable.

5.13 Numerical Instability

For the nonlinear model described in Chapter 3, an implicit method utilizing the ADI technique was used. Care has been taken to use the central difference to a large extent in order to improve the numerical stability. The stability state has been improved during the numerical experiments. Through the present study, satisfactory results can be obtained before computations diverge, although the problem is not yet completely solved.

In this study, it was found that the divergence could start from the area near the open boundary (see Figures 5.23 and 5.47), from inside the open boundary (see Figure 5.48), and from inside the inner channels (see Figures 5.19 and 5.49). Figures 5.47, 5.48, and 5.49 were obtained from Runs #10, #28, and #11, respectively. The unstable area in

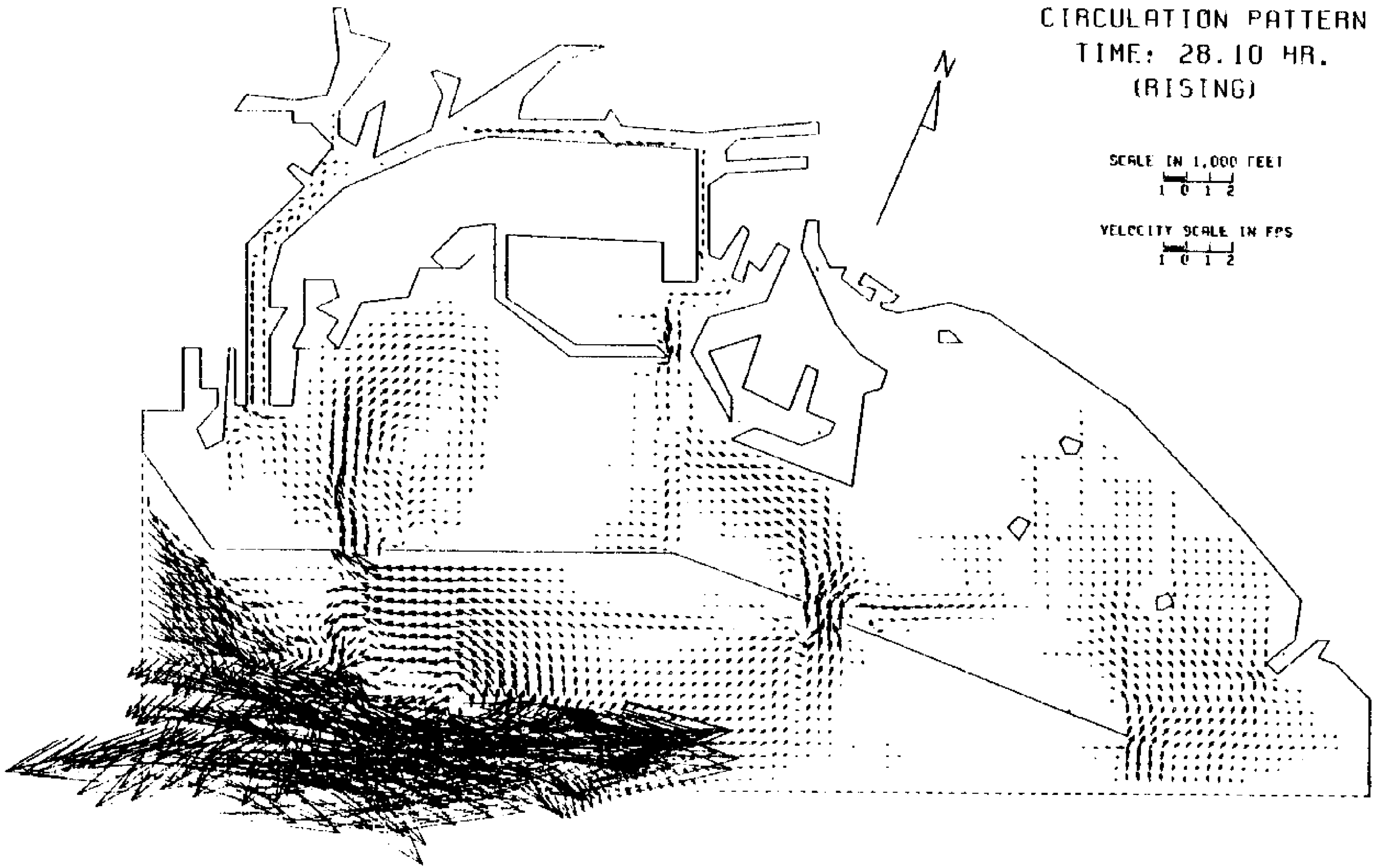

Figure 5.47 Circulation Pattern Obtained from Run #9 (ΔT = 90 sec), Showing the Area of Instability.

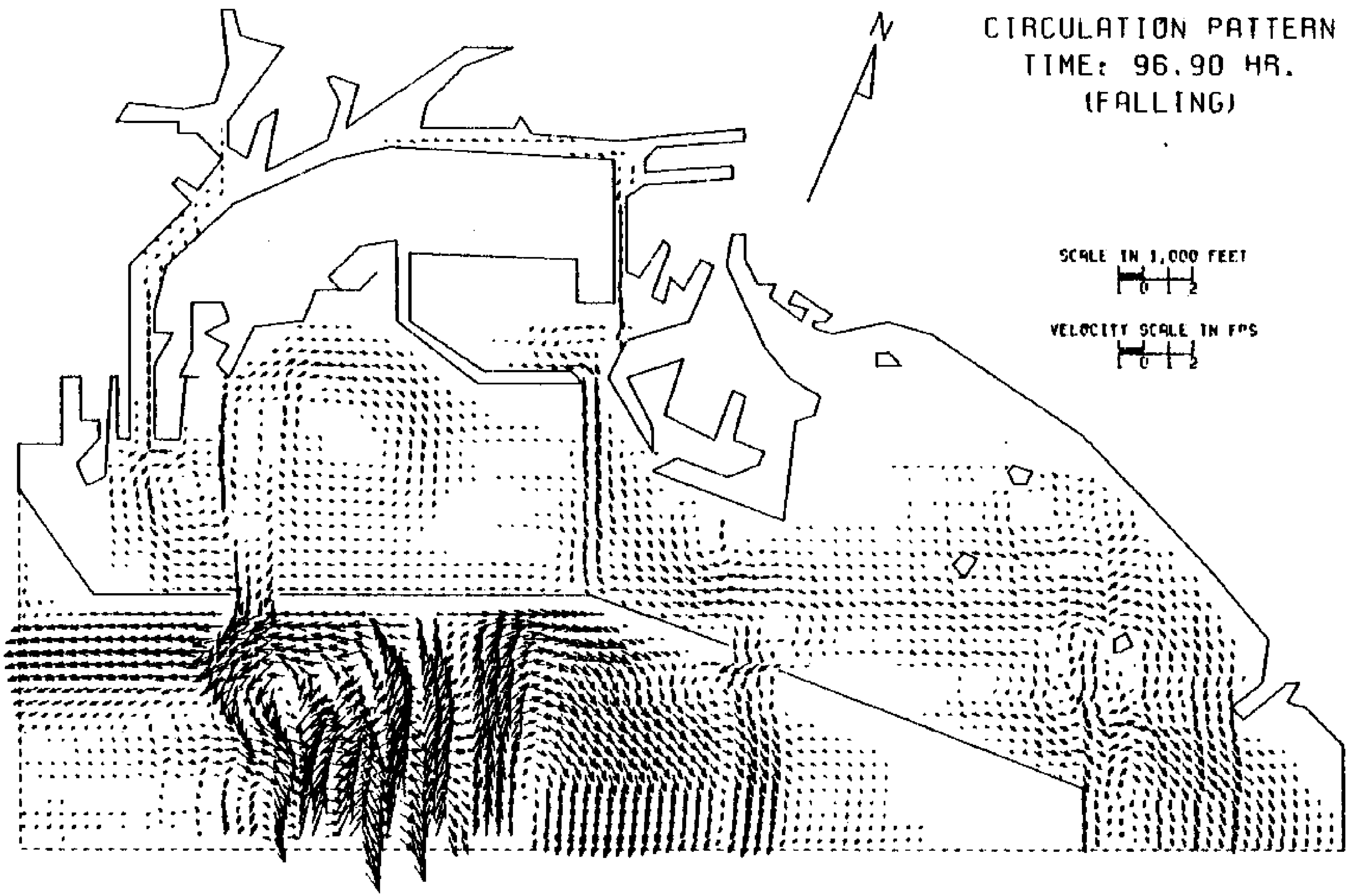

Figure 5.48 Circulation Pattern Obtained from Run #28 (with a Constant Depth = 40 ft), Showing the Area of Instability.

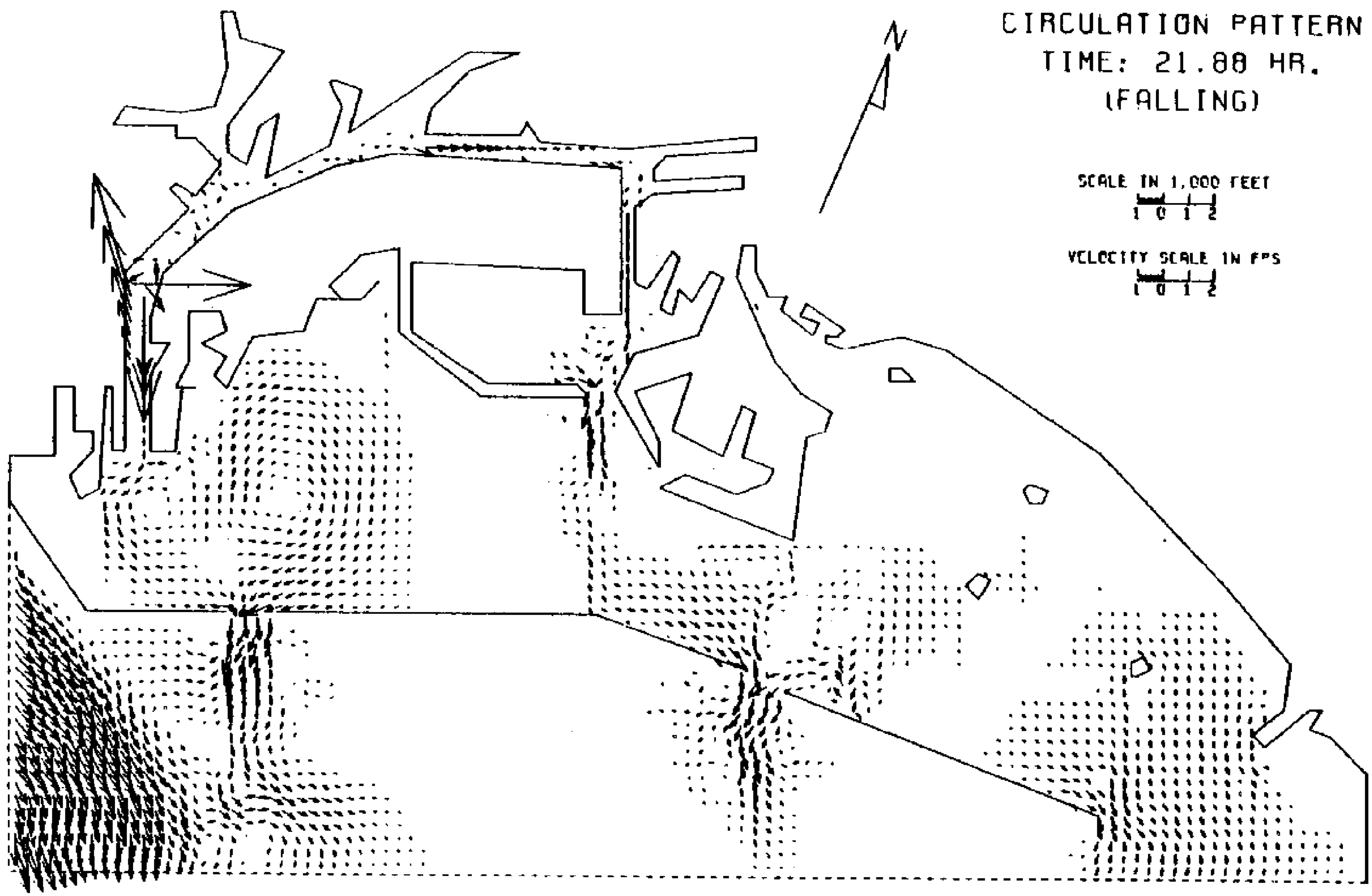

Figure 5.49 Circulation Pattern Obtained from Run 10 (ΔT = 45 sec), Showing Areas of Instability.

Figure 5.48 shows what Crean (1978) and Liu & Leendertse (1978) called "noodling."

The appearance of a strange current near the west side boundary (see Figures 5.1 to 5.7) is probably due to the simultaneous tidal motions assumed along both west and south boundaries. As a matter of fact,the tidal functions are different everywhere. Because the difference of tidal elevations is the main forcing function in this model, a small error of the difference could have large effects. This small error could accumulate to the extent as what was shown in the last plot of Figure 5.23, and finally to what was shown in Figure 5.47 before the computation blew up.

The mechanism of numerical instability is still under investigation. The smoothing effect due to eddy viscosity could help the stability. But the problem exists in finding an appropriate coefficient of eddy viscosity. Simulation results are sensitive to the coefficient which is high enough to affect the flow, as what has been discussed previously. A nonlinear eddy viscosity might be able to yield better resolutions.

Based on Test #14, it is concluded that the instability problem will not show up if the nonlinear advective terms are removed from the model.

In Runs #1 to #5, the time step was set to be 360 sec and the grid spacing was 500 ft. Based on the maximum depth of 109 ft at the southwest corner of the study area, and based on equation (2.1), the Courant number reached 60. It is unusual to have a numerical model run for long simulation with such a high Courant number and still produced satisfactory results. In studying a small scale motion like that in a harbor or a smaller area, a model which can be run with high Courant number is valuable as far as the computation time is concerned.

5.14 Volumetric Flow Rates

Presented in Table 5.2 are the net tidal flows during the fifth cycle of a diurnal tide for three cases: Run #2 (existing condition with spring tide), Run #3 (existing condition with neap tide), and Run #5 (harbor modification with spring tide). In the case of Run #5, the only harbor modification in this study was the addition of a tanker terminal which is shown as the shaded area in Figure 5.21. In the physical model as well as the numerical model of Raney (1976), the modification included both the landfill of the tanker terminal and the extension of Pier J (see Raney 1976, Figure 8).

Flow rates were measured at Ranges 1, 2, 3, 5, and 8. As defined by McAnally (1975, Figure 3), Range 1 covers the whole width of Angel's Gate; Range 2 covers Queen's Gate from breakwater to breakwater; Range 3 covers the whole opening east of the Long Beach breakwater; Range 5 covers

Case	Range	Prototype: Adjusted Net flow 10^6 ft	Prototype: Apparent Net flow 10^6 ft	Physical model: Apparent Net flow 10^6 ft	Numerical model (Raney 1976): Adjusted Net flow 10^6 ft	Numerical model (this study): Adjusted Net flow 10^6 ft
Run #2	1	+310	+990	+1230	+ 446	+ 296
	2	-	-	+ 520	+ 641	+ 980
	3	-	-	-1700	- 146	-1279
	1+2+3	-	-	+ 50	+ 941	- 3
	5	- 60	- 30	- 40	+ 53	- 68.2
	8	-160	-170	- 50	- 64	+ 61.1
	5+8	-220	-200	- 90	- 9	- 7.1
Run #3	1	-	-	- 180	-	+ 76.7
	2	-	-	+ 1	-	+ 356
	3	-	-	+ 690	-	- 432
	1+2+3	-	-	+ 511	-	+ 1
	5	-	-	+ 90	-	- 23.4
	8	-	-	+ 30	-	+ 22.7
	5+8	-	-	+ 120	-	- 0.7
Run #5	1	-	-	+1090	+ 218	+ 494
	2	-	-	+ 80	+ 698	+ 935
	3	-	-	+ 480	+ 223	-1507
	1+2+3	-	-	+1650	+1139	- 78
	5	-	-	- 160	+ 13.2	- 76.7
	8	-	-	+ 80	+ 31.1	+ 58.1
	5+8	-	-	- 80	+ 44.3	- 18.6

Table 5.2. Net flows per tidal cycle.

the entrance to Long Beach Harbor (Middle Harbor) between Pier F and the Navy Mole; and Range 8 was placed at the entrance to the inner Los Angeles Main Channel. Ranges 5 and 8 control a closed system which includes the inner Main Channel and Cerritos Channel. If all breakwaters are impervious, Ranges 1, 2, and 3 control a closed system covering the whole harbor areas inside the breakwaters. In Table 5.2, 1+2+3 denoted the sum of data from Ranges 1, 2, and 3; 5+8, the sum from Ranges 5 and 8.

The prototype readings were obtained from McAnally (1975, Table 3). The data were not available at Ranges 2 and 3. Readings from the physical model were obtained from McAnally (1975) for the cases of Run #2 and Run #3, and from Raney (1976) for the case of Run #5. Calculated results from numerical models of Raney (1976) and this study were also included in Table 5.2.

The apparent net flow was calculated using the magnitude of current velocity regardless of its orientation relative to the velocity range, except that the magnitude was given a positive value for a flood flow and a negative value for an ebb flow. By using the term "apparent net flow," one assumes the velocity vector to be normal to the velocity range. The adjusted net flow was calculated using the velocity component normal to the range. The details of calculating net flows can be found in the program listed in Appendix B.1.

Both McAnally (1975) and Raney (1976) stated that their values of net flow could have large errors and should be used only to indicate flow trends. However, the results from this study appeared to be quiet reasonable. The data in the last column of Table 5.2 indicate that there is a net flood flow through Ranges 1 and 2 and a large net ebb flow through Range 3. There is slight eastward net flow through Cerritos Channel. The algebraic sum of net flows passing through Ranges 1, 2, and 3 and that passing through Ranges 5 and 8 are supposed to be zero in a steady tidal cycle when the breakwaters are impervious. In this respect, the errors are very small in this study. The errors in the case of Run #5 are a bit larger than those in other two cases because the fifth tidal cycle in Run #5 has not been completely "warmed up" (as discussed in Section 5.3).

CHAPTER 6

CONCLUSIONS AND RECOMMENDATIONS

A finite-difference model for two-dimensional shallow water flows has been developed, with special emphasis on treating the nonlinear advective terms, to simulate tide-induced circulations in harbors of arbitrary shape. The model has been applied to Los Angeles-Long Beach Harbor, wherein various sensitivity tests have been conducted.

From this study the following major conclusions can be drawn:

1. The results of the model test indicate that the model has performed adequately in simulating tidal circulations in Los Angeles-Long Beach Harbor. With proper coefficients of bottom friction and eddy viscosity, the model can be used as a predictive model to study the change of circulation due to modification of harbor shape. The model is efficient and economical. It takes less than 50-minute computer time to simulate 1,000 time steps (or eight semi-diurnal tidal cycles when the time step is 360 sec) of tidal

circulation in a 108x69 network. The required computer core is 251K.

2. Owing to the tidal forces, a large clockwise gyre appears in outer Los Angeles Harbor, of which the center is north-northeast of Angel's Gate and the current velocity can be higher than 0.2 fps. Throughout tidal cycles, this tide-induced gyre maintains a clockwise motion with slight velocity fluctuations. The gyre is an open system such that flush water joins in during flood tide and a portion of mixed water leaves during ebb tide. This exchanges of water would enhance the mixing of water in the harbor basin. When wind stress does not exist, there are net inflows through both Angel's Gate and Queen's Gate and the sum of these two inflows becomes the net outflow through the opening to the east of the Long Beach breakwater. Without the wind effect, there is a small net eastward flow through the Cerritos Channel. During the spring tide, which appear around the times of new and full moon, the maximum current is about 0.9 fps near Angel's Gate. The large gyre becomes very weak during the period of neap tide, which occurs at the first and the third quarters of the moon.

3. If the original data for the diurnal tidal elevation is not smooth, an oscillation with the period the same as the time interval of the tidal data may appear on the time history of velocity. In order to have a set of smooth input data, the tidal data can be fitted into a function which consists of four cosine functions. The "four-cosine" function developed in the present study fit quite well to the original data and is able to produce good results without oscillations.
4. The time from a initially motionless state to a dynamical steady state is much longer when there is large circular motion (or gyre structure) in the study area. Vorticities obtained in the first few tidal cycles are usually underestimated. A numerical model which can stay stable for long simulation time is needed to study the gyre structures of the dimension larger than ten grid spacings, especially in a semi-closed area where the progress of a signal will be delayed due to the existence of obstructions.
5. A relatively large time step may be used for a long wave problem in a small grid-size model. Usually a fine-grid model needs very small time step and therefore, requires long computation

time. The present study shows that the simulation results are satisfactory even when the Courant number reaches 60 (based on the maximum water depth at a corner of the study area). However, using a smaller time step will obtain a finer resolution and reach a dynamical steady state in a shorter real simulation time, although the number of time steps required to reach the steady state are of the same order of magnitude.

6. The nonlinear advective terms in the momentum equation have been found to be the most important factor in producing circulating motions (or gyre structures) in a semi-enclosed basin. Therefore, any model designed to study such gyre structures must include the nonlinear advective terms.
7. As opposed to some other studies, it has been found that the eddy viscosity has a noticeable effect on velocity pattern once a threshold value in eddy viscosity is reached. Furthermore, when this linear coefficient reaches $A = (\Delta s)^2/(4\Delta T)$, the residual currents vanish almost everywhere. A further increase in the coefficient results in faster computational divergence.
8. The model is sensitive to the change of roughness coefficient. In the present Los Angeles-Long

Beach Harbor model, the case of Manning's coefficient n = 0.040 gave totally different flow patterns than the case of n = 0.020.

9. For a model with constant depth, the results may be acceptable if the depth at a harbor entrance is close to the field data.
10. The simulation results may be affected by the orientation of computational network when the algorithm applies the alternating-direction-iteration technique. Thus, it may be necessary to test the study area with different orientations.
11. Satisfactory results may be obtained through a reasonably simplified network thereby significantly reducing the computational effort.
12. Numerical instability can originate either from the region near the open boundary or from the interior grid points. The model stays stable when the nonlinear advective terms are excluded.

Recommendations for future research on the numerical model of harbor circulation are:

1. To study further the problem of numerical instability.
2. To study the case with pervious breakwaters.
3. To use a nonlinear eddy viscosity.

4. To include the effect of wind stresses into the tested model.
5. To use two- or three-layer models if the wind stress is considered.
6. To verify the model with other field data.

LIST OF REFERENCES

Abbott, M. B.; Damsgaard, A. & Rodenhuis, G. S. 1973 System 21, "Jupiter" (a design system for two-dimensional nearly horizontal flows.) Journal of Hydraulic Research, 11(1), 1-28.

Allender, J. H. 1975 Numerical simulation of circulation and advection diffusion processes in Saginaw Bay, Michigan. Ph.D. thesis, University of Michigan, Ann Arbor, Michigan.

Amein, M. & Fang, C. S. 1969 Stream routing (with applications to North Carolina rivers). Report No. 17, Water Resources Research Institute of the University of North Carolina. Chapel Hill, North Carolina.

Baltzer, R. A. Schaffransk, R. W. 1978 Simulation modeling in coastal waters: A case study. In: Summaries of Papers to be Presented at the 16th International Conference on Coastal Engineering, Paper No. 121. The German Organizing Committee.

Batchelor, G. K. 1967 An Introduction to Fluid Dynamics. Cambridge University Press, Cambridge, U.K.

Beyer, W. H., ed. 1976 Standard Mathematical Table. 24th ed. CRS Press, Cleveland, Ohio.

Blumberg, A. F. 1977a Numerical tidal model of Chesapeake Bay. Journal of the Hydraulic Division, ASCE, 103(HY1), Proc. Paper 12661, 1-10.

Blumberg, A. F. 1977b Numerical model of estuarine circulation. Journal of the Hydraulic Division, ASCE, 103(HY3), Proc. Paper 12815, 295-310.

Boericke, R. R. & Hall, D. W. 1974 Hydraulics and thermal dispersion in an irregular estuary. Journal of the Hydraulics Division, ASCE, 100(HY1), Proc. Paper 10282, 85-102.

Bowden, K. F. 1953 Note on wind drift in a channel in the presence of tidal currents. Proceedings of the Royal Society of London, A219, 426-446.

Bowden, K. F. 1956 The flow of water through the Strait of Dover related to wind and differences in sea level. Philosophical Transactions of the Royal Society of London, A248, 517-551.

Bowden, K. F. 1962 Turbulence. In: Hill, M. N. (ed.), The Sea, Volume 1, Physical Oceanography, 802-825. Interscience Publishers, New York, New York.

Bowman, M. J. 1978 Spreading and mixing of the Hudson River effluent into the New York Bight. In: Nihoul, J. C. J. (ed.), Hydrodynamics of Esturies and Fjod, 373-386. Elsevier Scientific Publishing Company, Amsterdam, The Netherlands.

Bryan, K. 1966 A scheme for numerical integration of the equations of motion on an irregular grid free of nonlinear instability. Monthly Weather Review, 94(1), 39-40.

Butler, H. L. 1978a Numerical simulation of tidal hydrodynamics, Great Egg Harbor and Corson Inlet, New Jersey. Technical Report H-78-11, U.S. Army Waterways Experiment Station, Vicksburg, Mississippi.

Butler, H. L. 1978b Numerical simulation of the Coos Bay-South Slough Complex. Technical Report H-78-22, U.S. Army Waterways Experiment Station, Vicksburg, Mississippi.

Butler, H. L. 1978c Coastal flood simulation in stretched coordinates. Paper presented at the 16th International conference on Coastal Engineering, 19pp.

Bye, J. A. T. 1970 Eddy friction in the ocean. Journal of Marine Research, 28(2), 124-134.

Cheng, R. T.; Powell, T. M. & Dillon, T. M. 1976 Numerical models of wind-driven circulation in lakes. Applied Mathematical Modeling, 1, 141-159.

Chiang, W.-L. 1977 Further development and testing of a stream-aquifer system model. Master's thesis, University of Kansas, Lawrence, Kansas.

Chorin, A. J. 1973 Numerical study of slightly viscous flow. Journal of Fluid Mechanics, 57, pt. 3, 785-796.

Chow, V. T. 1959 Open-Channel Hydraulics. McGraw-Hill Book Company, Inc., New York, New York.

Cooper, C.; Nelson, S. & Pearce, B. R. 1978 3-D current model with depth varying eddy viscosity. In: Summaries of Papers to be Presented at the 16th International Conference on Coastal Engineering, Paper No. 152. The German Organizing Committee.

Crean, P. B. 1978 A numerical model of baratropic mixed tides between Vancouver Island and the mainland and its relation to studies of the esturine circulation. In: Nihoul, J. C. J. (ed.), Hydrodynamics of Esturies and Fjords, 283-313. Elsevier Scientific Publishing Company, Amsterdam, The Netherlands.

Crowley, W. P. 1968 A global numerical ocean model: Part I. Journal of Computational Physics, 3(1), 111-147.

Crowley, W. P. 1970 A numerical model for viscous, free-surface, barotropic wind driven ocean circulations. Journal of Computational Physics, 5, 139-168.

Damsguaard, A. & Dinsmore, A. F. 1975 Numerical simulation of storm surge in bays. Symposium of Modeling Techniques, Second Annual Symposium of the Waterways, Harbors, and Coastal Engineering, San Francisco, California, September 3-5, 1975, Vol. II, 1535-1551.

Deacon, E. L. & Webb, E. K. 1962 Interchange of properties between sea and air. In: Hill, M. N. (ed.), The Sea, Volume 1, Physical Oceanography, Chapter 3, Section 2, 43-87. Interscience Publishers, New York, New York.

Dean, R. G. 1966 Tides and harmonic analysis. In: Ippen, A. T. (ed.), Estuary and Coastline Hydrodynamics, 197-230. McGraw-Hill Book Company, Inc., New York, New York.

Deardorff, J. W. 1971 On the magnitude of the subgrid scale eddy coefficient. Journal of Computational Physics, 7(1), 120-133.

Denman, K. L. & Miyake, M. 1973 Behavior of the mean wind, the drag coefficient, and the wave field in the open ocean. Journal of Geophysical Research, 78(12), 1917-1931.

DiPrima, R. C. & Rogers, E. H. 1969 Computing problems in nonlinear hydrodynamic stability. Physics of Fluids, 12(12), II155-II165.

Dorn, W. C., van 1953 Wind stress on an artificial pond. Journal of Marine Research, 12, 249-276.

Douglas, J., Jr. 1955 On the numerical iteration of $\partial^2 u/\partial x^2 + \partial^2 u/\partial y^2 = \partial u/\partial t$ by implicit methods. Journal of the Society for Industrial and Applied Mathematics, 3, 42-65.

Dronkers, J. J. 1964 Tidal Computations in Rivers and Coastal Waters. North-Holland Publishing Company, Amsterdam, The Netherlands.

Dronkers, J. J. 1975 Tidal theory and computations. In: Chow, V. T. (ed.), Advances in Hydroscience, Volume 10-1975, 145-230. Academic Press, New York, New York.

Durst, C. S. 1924 The relationship between current and wind. Quarterly Journal of the Royal Meteorology Society, 50, 113.

Fischer, G. 1965 A survey of finite difference approximatins to the primitive equations. Monthly Weather Review, 93, 1-46.

Fischer, H. B. 1973 Longitudinal dispersion and turbulent mixing in open-channel flow. Annual Review of Fluid Mechanics, 5, 59-78. Annual Reviews Inc., Palo Alto, California.

Fischer, H. B. 1976a Mixing and dispersion in estuaries. Annual Review of Fluid Mechanics, 8, 107-133. Annual Reviews Inc., Palo Alto, California.

Fischer, H. B. 1976b Some remarks on computer modeling of coastal flows. Journal of the Waterways, Harbors and Coastal Engineering Division, ASCE, 102(WW4), Proc. Paper 12520, 395-406.

Fofonoff, N. P. 1962 Dynamics of ocean currents. In: Hill, N. M. (ed.), The Sea, Volume 1, Physical Oceanography, Section III, 323-395. Interscience Publishers, New York, New York.

Forristall, G. Z. 1974 Three-dimensional structure of storm-generated currents. Journal of Geophysics Research, 79(18), 2721-2729.

Gates, W. L. 1966 A numerical study of the wind-driven transient circulation in a homogeneous ocean. Rand Corporation, Santa Monica, California.

Giles, R. V. 1962 Theory and Problems of Fluid Mechanics and Hydraulics. 2nd ed. Schaum Publishing Company, New York, New York.

Groen, P. & Groves, G. W. 1962 Surges. In: Hill, M. N. (ed.), The Sea, Volume 1, Physical Oceanography, Chapter 17, 611-646. Interscience Publishers, New York, New York.

Grotkop, G. 1973 Finite element analysis of long-period water waves. Computer Methods in Applied Mechanics and Engineering, 2(2), 147.

Gustafsson, B. 1971 An alternating direction implicit method for solving the shallow water equations. Journal of Computational Physics, 7, 239-254.

Haney, R. l. & Wright, J. M., Jr. 1975 The relationship between the grid size and the coefficient of nonlinear lateral eddy viscosity in numerical ocean circulation models. Journal of Computational Physics, 19(3), 257-266.

Hansen, W. 1962 Tides. In: Hill, M. N. (ed.), The Sea, Volume 1, Physical Oceanography, 764-801.

Heaps, N. S. 1969 A two-dimensional numerical sea model. Philosophical Transactions of the Royal Society of London, A265(1160), 93-137.

Heaps, N. S. 1973 Three-dimensional numerical model for the Irish Sea. Geophysical Journal of Research for Astronomical society, 35, 99-120.

Heaps, N. S. 1976 On formulating a non-linear numerical model in three dimensions for tides and storm surges. In: Glowinski, P. & Lions, J. L. (eds.), Computing Methods in Applied Sciences, (Lecture Notes in Physics, 58), 368-387. Springer-Verlag, Berlin, West Germany.

Henderson, F. M. 1966 Open Channel Flow. The Macmillan Company, New York, New York.

Hess, K. W. & White, F. W. 1974 A numerical tidal model of Narragansett Bay. Marine Technical Report No. 20, University of Rhode Island, Kingston, Rhode Island.

Hidaka, K. & Tsuchiya, M. 1953 On the Antarctic circumpolar current. Journal of Marine Research, 12, 214-222.

Hinwood, J. B. & Wallis, I. G. 1975 Classification of models of tidal waters. Journal of the Hydraulic Division, ASCE, 101(HY10), Proc. Paper 11643, 1315-1331.

Holland, W. R. 1977 Oceanic general circulation models. In: Goldberg, E. D.; McCave, I. N.; O'Brien, J. J. & Steele, J. H. (eds.), The Sea, Volume 6, Marine Modeling, Part I, Chapter 1, 3-45. John Wiley & Sons, New York, New York.

Hseuh, Y. & Peng, C.-Y. 1973 A numerical study of the steady circulation in an open bay. Journal of Physical Oceanography, 3(2), 220-225.

Kremer, J. N. & Kremer, P. 1979 Ecological simulation model of Los Angeles Harbor receiving Waters. Addendum to: Soule, D. F. & Oguri, M. (eds.), Marine Studies of San Pedro Bay, California, Part 16, Ecological Changes in Outer Los Angeles-Long Beach Harbors Following Initiation of Secondary Waste Treatment and Cessation of Fish Cannery Waste Effluent, 66pp. Allen Hancock Foundation and The Office of Sea Grant Programs, Institute for Marine and Coastal Studies, University of Southern California, Los Angeles, California.

Lamb, H. 1924 Hydrodynamics. Cambridge university Press, Cambridge, U.K.

Lax, P. & Wendroff, B. 1960 Systems of conservation laws. Communications on Pure and Applied Mathematics, 13(2), 217-237.

Lee, J. J. & Walther, J. A. 1974 Wave energy permeation of San Pedro Breakwater. Offshore Technology Conference Proceedings, Paper No. OTC 2124, 951-958.

Leendertse, J. J. 1967 Aspects of a computational model for long-period water-wave propagation. Memorandum RM-5294-PR, The Rand Corporation, Santa Monica, California.

Leendertse, J. J. 1970 A water-quality simulation model for well mixed estuaries and coastal seas: Vol. I, Principles of computation. RM-6230-RC, The Rand Corporation, New York, New York.

Leendertse, J. J. 1972 A water-quality simulation model for well mixed estuaries and coastal seas: Vol. IV, Jamaica Bay tidal flows. R-1009-NYC, The Rand Corporation, Santa Monica, California.

Leendertse, J. J.; Alexander, R. C. & Liu, S. K. 1973 A three-dimensional model for estuaries and coastal seas: Volume I, Principles of computation. R-1417-OWRR, The Rand Corporation, Santa Monica, California.

Leendertse, J. J. & Liu, S.-K. 1977 A three-dimensional model for esturies and coastal seas: Volume IV, Turbulent energy computation. R-2187-OWRT, The Rand Corporation, Santa Monica, California.

Leith, C. E. 1968 Diffusion approximation for two-dimensional turbulence. The Physics of Fluids, 11(3), 671-673.

Leith, C. E. 1969 Numerical simulation of turbulent flow. In: Mark, H. & Fernbach, S. (eds.), Properties of Matter Under Unusual Conditions, 267-271. Interscience Publishers, New York, New York.

Li, H.-W. 1977 A barotropic multi-layered model of the Kiel Bay. ACTA Oceanographica Taiwanica, Science Reports of the National Taiwan University, No. 7, 79-92.

Li, Y.-Y. 1968 University Physics, 2nd ed. Tung-Hwa Book Company, Ltd., Taipei, Republic of China.

Liggett, J. A. 1969 Unsteady circulation in shallow, homogeneous lakes. Journal of the Hydraulic Division, ASCE, 95(Hy4), Proc. Paper 6686, 1273-1288.

Liggett, J. A. 1970 Cell method for computing lake circulation. Journal of the Hydraulic Division, ASCE, 96(HY3), Proc. Paper 7152, 725-743.

Liggett, J. A. & Hadjtheodorou, C. 1969 Circulation in a shallow homogeneous lake. Journal of the Hydraulic Division, ASCE, 95(HY2), Proc. Paper 6454. 609-620.

Liu, S.-K. & Leendertse, J. J. 1978 Multidimensional numerical modeling of estuaries and coastal seas. In: Chow, V. T. (ed.), Advances in Hydroscience, 11, 95-164. Academic Press, New York, New York.

McAnally, W. H., Jr. 1975 Los Angeles and Long Beach Harbors model study, Report 5, Tidal verification and basin circulation tests. Technical Report H-75-4, Report 5, U.S. Army Engineer Waterways Experiment Station, Vicksburg, Mississippi.

Madsen, O. S. 1977 A realistic model of the wind-induced Ekman boundary layer. Journal of Physical Oceanography, 7(2), 248-255.

Matthews, J. B. & Mungall, J. C. H. 1970 Variable boundary, two dimensional tidal model. Nature, 226, 835-836.

Matthews, J. B. & Mungall, J. C. H. 1972 A numerical tide model and its application to Cook Inlet, Akaska. Journal of Marine Research, 30(1), 27-38.

Moe, J.; Mathisen, J. P. & Hodgins, S. 1978 An improved method for the computation of shallow water waves. In: Taylor, C.; Morgan, K. & Brebbia, C. A. (eds.), Numerical Methods in Laminar and Tubulent Flow, 609-618. Pentech Press, London, U. K.

Montgomery, R. B. & Palmén, E. 1940 Contribution to the question of the equational counter current. Journal of Marine Research, 3, 112-133.

Munk, W. H. 1950 On the wind-driven ocean circulation. Journal of Meteorology, 7(2), 79-93.

Neumann, G. 1954 Notes on the wind-driven ocean circulation. Technical Report, Research Division, College of Engineering, New York University, New York, New York.

Neumann, G. 1968 Ocean Currents. Elsevier Scientific Publishing company, Amsterdam, The Netherlands.

Nihoul, J. C. J. 1975a Marine systems analysis. In: Nihoul, J. C. J. (ed.), Modelling of Marine Systems, Part I, chapter 1, 3-39. Elsevier Publishing company, Amsterdam, The Netherlands.

Nihoul, J. C. J. 1975b Hydrodynamic models. In: Nihoul, J. C. J. (ed.), Modelling of Marine Systems, Part I, chapter 2, 41-67. Elsevier Publishing company, Amsterdam, The Netherlands.

Nihoul, J. C. J. 1976 Mathematical hydrodynamic models for the study of marine circulation and dispersion of pollutants in a shallow sea. In: Glowinski, R. & Lions, J. L. (eds.), Computing Methods in Applied Sciences, (Lecture Notes in Physics, 58), 447-472. Springer-Verlag, Berlin, West Germany.

Nihoul, J. C. J.; Ronday, F. C.; Peters, J. J. & Sterling, A. 1978 Hydrodynamics of the Scheldt Estuary. In: Nihoul, J. C. J. (ed.), Hydrodynamics of Estuaries and Fjords, 27-53, Elsevier Scientific Publishing Company, Amsterdam, The Netherland.

Outlaw, D. 1979 Personal letter.

Patridge, P. W. & Brebbia, C. A. 1976 Quardratic finite elements in shallow water problems. Journal of the Hydraulic Division, ASCE, 102(HY9), Proc. Paper 12418, 1299-1313.

Peaceman, D. W. & Rachford, H. H. 1955 The numerical solution of parabolic and elliptic differential equations. Journal of the Society for Industrial and Applied Mathematics, 3(1), 28-41.

Pearson, W. J. 1964 The interpretation of wave spectrums in terms of the wind profile instead of the wind measured at a constant height. Journal of Geophysical Research, 69, 5191-5203.

Pinder, G. F. & Gray, W. G. 1977 Finite Element Simulation in Surface and Subsurface Hydrology. Academic Press, Inc., New YOrk, New York.

Prandle, D. 1972 A numerical model of the St. Lawrence River. Proceedings of the 13th Conference on Coastal Engineering, Vancouver, Britich Columbia Canada, 3, 2291-2306.

Proudman, J. 1953 Dynamical Oceanography. Methuen, London, U.K.

Raney, D. C. 1976 Numerical analysis of tidal circulation for Long Beach Harbor, Report 1, Existing conditions and alternate plans for Pier J completion and tanker terminal study. Miscellaneous Paper H-76-4, Report 1, U.S. Army Engineer Waterways Experiment Station, vicksburg, mississippi.

Reichard, R. P. & Celikkol, B. 1978 Application of a finite element hydrodynamic model to the Great Bay Estuary system, New Hampshire, U.S.A. In: Nihoul, J. C. J. (ed.), Hydrodynamics of Estuaries and Fjords, 349-372. Elsevier Scientific Publishing Company, Amsterdam, The Netherlands.

Reid, R. O. 1956 Approximate response of water level on a sloping shelf to a wind fetch which moves towards shore. Technical Memorandum No. 83, U.S. Army Beach Erosion Board.

Reid, R. O. & Bodine, B. R. 1968 Numerical model for storm surges in Galveston Bay. Journal of Waterways and Harbors Division, ASCE, 94(WW1), Proc. Paper 5805, 33-57.

Reynolds, W. C. 1976 Computation of turbulent flows. Annual Review of Fluid Mechanics, 8, 183-208. Annual reviews Inc., Palo Alto, california.

Robinson, K. S. & Porath, H. 1974 Current measurements in the outer Los Angeles Harbor. In: Soule, D. F. & Oguri, M. (eds.), Marine Studies of San Pedro, California, Part VI, Circulation Investigations, (USC-SG-7-74), 1-91. The Allen Hancock Foundation and The Office of Sea Grant Programs, University of Southern California, Los Angeles, California.

Sheppard, P. A. 1958 Transfer across the earth's surface and through the air above. Quartery Journal of the Royal Meteorological Society, 84, 205-224.

Sheppard, P. A.; Tribble, D. T. & Garratt, J. R. 1972 Studies of turbulence in the surface layer over water, Part I, Instrumentation, programme, profiles. Quarterly Journal of the Royal Meteorological Society, 98, 627-641.

Sielecki, A. & Wurtele, M. G. 1970 The numerical integration of the nonlinear shallow-water equations with sloping boundaries. Journal of Computational Physics, 6, 219-236.

Silvester, R. 1974a Coastal Engineering, I. Elsevier Scientific Publishing Company, Amsterdam, The Netherlands.

Silvester, R. 1974b Coastal Engineering, II. Elsevier Scientific Publishing Company, Amsterdam, The Netherlands.

Smagorinsky, J. 1963 General circulation experiments with the primitive equation, I. The basic experiment. Monthly weather review, 91(3), 99-165.

Soule, D. F. & Oguri, M. 1972 Marine studies of San Pedro, California, Part one, Circulation patterns in Los Angeles-Long Beach Harbor, Drogue study atlas and data report. USC-SG-6-72, The Allen Hancock Foundation and The Office of Sea Grant, University of Southern California, Los Angeles, California.

Soule, D. F. & Oguri, M. 1976 Bioenhancement studies of the receiving waters in outer Los Angeles Harbor. In: Soule, D. F. & Oguri, M. (eds.), Marine Studies of San Pedro, California, Part 12, Bioenhancement Studies of the Receiving Waters in Outer Los Angeles Harbor, (USC-SG-5-76), 3-58. Harbors Environmental Projects, Allen Hancock Foundation, and The Office of Sea Grant Programs, Institute of Marine and Coastal Studies, University of Southern California, Los Angeles, California.

Southern California Coastal Water Research Project. 1973 The ecology of the Southern California bight: Implications for water quality management. SCCWRP TR104, Southern California Coastal Water Research Project, El Segundo, California.

Stolzenbach, K. D.; Madsen, O. S.; Adams, E. E.; Pollack, A. M. & Cooper, C. K. 1977 A review and evaluation of basic techniques for predicting the behavior of surface oil slicks. Report No. MITSG 77-8, M.I.T. Sea Grant Program, Massachusetts Institute of Technology, Cambridge, Massachusetts.

Stommel, H. 1955 Lateral eddy diffusivity in the Gulf Stream system. Deep-Sea Research, 3, 88-90.

Sverdrup, H. U. 1942 Oceanography for Meteorologists, Prentice-Hall, Inc., New York, New York.

Sverdrup, H. U.; Johnson, M. W. & Fleming, R. H. 1942 The Oceans--Their Physics, Chemistry, and General Biology. Prentice-Hall, Inc., New York, New York.

Taylor, C. & Davis, J. 1975 Tidal and long wave propagation--a finite element approach. Computers & Fluids, 3(2/3), 125-148.

Tee, K. T. 1976 Tide-induced residual current, a 2-D nonlinear numerical tidal model. Journal of Marine Research, 34(4), 603-628.

Tee, K. T. 1977 Tide-induced residual current-- verification of a numerical model. Journal of Physical Oceanography, 7, 396-402.

Thomson, J. A. L. & Meng, J. C. S. 1975 Studies of free buoyant and sheer flows by the vortex-in-cell method. In: Richtmyer, R. D. (ed.), Proceedings of the Fourth International Conference on Numerical Methods in Fluid Dynamics, June 24-28, 1974, University of Colorado, (Lecture Notes in Physics, 35), 403-416. Springer-Verlag, Berlin, West Germany.

Tsai, Y. J. & Chang, Y. C. 1974 Prediction and verification of storm surges in Lake Ontario and Lake Erie. The 17th Conference on Great Lakes Research, McMaster University, Hamilton, Ontario, Canada, August 12-14, 1974.

U.S. Department of Commerce. National Oceanic and Atmospheric Administration. National Ocean Survey. 1977a San Pedro Bay. 21st ed. Chart 18749. U.S. Department of Commerce, Washington, D.C.

U.S. Department of Commerce. National Oceanic and Atmospheric Administration. National Ocean Survey. 1977b Los Angeles and Long Beach Harbors. 23rd ed. Chart 18751. U.S. Department of Commerce, Washington, D.C.

U.S. Department of Commerce. National Oceanic and Atmospheric Administration. National Ocean Survey. 1977c Tide table 1978, High and Low Water Predictions, West Coast of North and South America, Including the Hawaiian Islands. Washington, D.C.

U.S. Department of the Army. Office of the Chief of Engineers. 1974 Los Angeles-Long Beach Harbors (Final Environmental Statement). Washington, D.C.

Von Arx, W. S. 1962 An Introduction to Physical Oceanography. Addison-Wisley Publishing Company, Inc., Reading, Massachusetts.

Von Neumann, J. & Richtmyer, R. D. 1950 A method for the numerical calculations of hydrodynamic shocks. Journal of Applied Physics, 21(3), 232-237.

Wang, J. D. & Connor, J. J. 1975 Mathematical modeling of near coastal circulation. Report No. MITSG 75-13, M.I.T. Sea grant Program, Massachusetts Institute of Technology, Cambridge, Massachusetts.

Weare, T. J. 1976 Instability in tidal flow computational scheme. Journal of the Hydraulic Division, ASCE, 102(HY5), Proc. Paper 12100, 569-580.

Welander, P. 1966 A two-layer frictional model of wind-driven motion in a rectangular basin. Tellus, 18, 54-62.

Wilson, B. W. 1960 Note on surface wind stress over water at low and high wind speeds. Journal of Geophysical Research, 65, 3337-3382.

Wu, J. 1969 Wind stress and surface roughness at air-sea interface. Journal of Geophysical Research, 74(2), 444-455.

Wu, J. C.; Spring, A. H. & Sanker, N. L. 1975 A flowfield segmentation method for the numerical solution of viscous flow problem. In: Richtmyer, R. D. (ed.), Proceedings of the Fourth International Conference on Numerical Methods in Fluid Dynamics, June 24-28, 1974, University of Colorado, (Lecture Notes in Physics, 35), 453-457. Springer-Verlag, Berlin, West Germany.

Yeh, G. T. & Chou, F. K. 1979 Moving boundary numerical surge model. Journal of the Waterway, Port, Coastal and Ocean Division, ASCE, 115(WW3), Proc. paper 14758, 247-263.

Yeh, G. T. & Yeh, F. F. 1976 A generalized model for storm surges. Proceedings of the Fifteenth International Conference on Coastal Engineering, Honolulu, Hawaii, July 7-11, 1976, Vol. I, Chapter 54, 921-933.

APPENDIX A

DERIVATION OF EQUATIONS

A.1 Continuity Equation

Based on the conservation of mass and momentum, partial differential equations are derived in an Eulerian framework using an Cartesian coordinate system. Consider a infinitesimal control volume represented by a rectangular parallelepiped Δx-Δy-Δz which has its center at (x,y,z). Conservation of mass requires that the local rate of change of mass in the control volume, added to the net flux out, be equal to the rate of adding mass, or

$$\begin{aligned}
\Delta t(\rho\Delta x\Delta y\Delta z)_{,t} &+ [\rho u + 0.5\Delta x(\rho u)_{,x}]\Delta y\Delta z\Delta t \\
&- [\rho u - 0.5\Delta x(\rho u)_{,x}]\Delta y\Delta z\Delta t \\
&+ [\rho v + 0.5\Delta y(\rho v)_{,y}]\Delta x\Delta z\Delta t \\
&- [\rho v - 0.5\Delta y(\rho v)_{,y}]\Delta x\Delta z\Delta t \\
&+ [\rho w + 0.5\Delta z(\rho w)_{,z}]\Delta x\Delta y\Delta t \\
&- [\rho w - 0.5\Delta z(\rho w)_{,z}]\Delta x\Delta y\Delta t = S\Delta x\Delta y\Delta z\Delta t \qquad (A.1)
\end{aligned}$$

where u, v, and w are components of fluid velocity at the point (x,y,z), ρ denotes the density of the fluid, S denotes the internal source of mass per unit volume per unit time (henceforth a sink is defined as a negative source), and F denotes the partial differentiation of any function F with respect to i while i can be any of x, y, z, or t. Rearranging equation (A.1) and dividing by the product of the fixed dimensions Δx, Δy, Δz, and Δt, the result becomes

$$\rho_{,t} + (\rho u)_{,x} + (\rho v)_{,y} + (\rho w)_{,z} = S \tag{A.2}$$

In the case of an incompressible fluid, the equation becomes

$$u_{,x} + v_{,y} + w_{,z} = S \tag{A.3}$$

When there is no internal source or sink,

$$u_{,x} + v_{,y} + w_{,z} = 0 \tag{A.4}$$

which is the common expression of the continuity equation for an incompressible fluid.

A.2 Navier-Stokes Equation

Consider the same control colume as mentioned in Section A.1, acted upon by forces in the x-direction. According to Newton's second law, with the frame of reference fixed at a position in the space,

$$D(Mu)/Dt = [D(\rho u)/Dt]\ \Delta x \Delta y \Delta z$$

$$= (uD\rho/Dt + \rho Du/Dt) \Delta x \Delta y \Delta z$$

$$= [uD\rho/Dt + \rho(u_{,t} + uu_{,x} + vu_{,y} + wu_{,z})] \Delta x \Delta y \Delta z$$

$$= [(s_{xx}+0.5\Delta x s_{xx,x}) - (s_{xx}-0.5\Delta x s_{xx,x})] \Delta y \Delta z$$

$$+ [(s_{xx}+0.5\Delta y s_{yx,y}) - (s_{yx}-0.5\Delta y s_{yx,y})] \Delta z \Delta x$$

$$+ [(s_{zx}+0.5\Delta z s_{zx,z}) - (s_{zx}-0.5\Delta z s_{zx,z})] \Delta x \Delta y$$

$$+ \rho X \Delta x \Delta y \Delta z$$

$$= (s_{xx,x} + s_{yx,y} + s_{zx,z} + \rho X) \Delta x \Delta y \Delta z \qquad (A.5)$$

where X represents the external forces per unit mass and s the stress acting on the mass M. For a Newtonian fluid, shear stress is linearly proportional to the rate of angular deformation:

$$s_{yx} = 2\mu e_{yx} = \mu(u_{,y} + v_{,x}) \qquad (A.6)$$

$$s_{zx} = 2\mu e_{zx} = \mu(u_{,z} + w_{,x}) \qquad (A.7)$$

where e represents the rate of strain and μ, the proportional constant, is the viscosity of fluid. From a hypothesis of Stokes, the normal stresses on an isotropic Newtonian fluid depend not only on μ and e but also on the pressure p and the divergence of the velocity

$$\theta = u_{,x} + v_{,y} + w_{,z} \qquad (A.8)$$

The relationship is

$$s_{xx} = -p + [\ \mu' - (2/3)\mu\ ]\theta + 2\mu e_{xx}$$

$$= -p + [\ \mu' - (2/3)\mu\ ]\theta + 2\mu u_{,x} \qquad (A.9)$$

where u' is termed the second coefficient of viscosity. For an invicid fluid,

$$s_{xx} = -p \qquad (A.10)$$

Derivatives of equation (A.6), (A.7), and (A.9) gives

$$s_{xx,x} = -p_{,x} + \{\ [\ \mu'-(2/3)\mu\ ]\theta\ \}_{,x} + 2(\mu u_{,x})_{,x} \qquad (A.11)$$

$$s_{yx,x} = [\mu\ (\ u_{,y}+v_{,x}\ )\ ]_{,y} \qquad (A.12)$$

and $$s_{zx,x} = [\mu\ (\ u_{,z}+w_{,x}\ )\ ]_{,z} \qquad (A.13)$$

Using these three expressions, equation (A.5) becomes

$$uD\rho/Dt + \rho(\ u_{,t} + uu_{,x} + vu_{,y} + wu_{,z}\ )$$

$$= -p_{,x} + \{\ [\ \mu'-(2/3)\mu\ ]\theta\ \}_{,x} + 2(\mu u_{,x})_{,x}$$

$$+ [\mu(\ u_{,y}+v_{,x}\ )]_{,y} + [\mu(\ u_{,z}+w_{,x}\ )]_{,z} + \rho X \qquad (A.14)$$

When both u and u' are assumed uniform through out the fluid, the above equation becomes

$$uD\rho/Dt + \rho(\ u_{,t} + uu_{,x} + vu_{,y} + wu_{,z}\ )$$

$$= -p_{,x} + [\ \mu' - (2/3)\mu\ ]\theta_{,x} + \mu(\ u_{,xx} + u_{,yy} + u_{,zz} + \theta_{,x}\ ) + \rho X$$

$$= -p_{,x} + (\ \mu' - \ /3\ )\theta_{,x} + \mu(\ u_{,xx} + u_{,yy} + u_{,zz}\ ) + \rho X \qquad \text{(A.15)}$$

For an incompressible fluid, ρ is unaffected by changes of pressure. If ρ is considered invariant, θ vanishes as shown in equation (A.4), and so equation (A.15) becomes

$$u_{,t} + uu_{,x} + vu_{,y} + wu_{,z} = -p_{,x}/\rho + \nu(u_{,xx} + u_{,yy} + u_{,zz}) + X \qquad \text{(A.16)}$$

where μ/ρ is replaced by ν, the kinematic viscosity. Similarly, for the y- and z-directions,

$$v_{,t} + uv_{,x} + vv_{,y} + wv_{,z} = -p_{,y}/\rho + \nu(v_{,xx} + v_{,yy} + v_{,zz}) + Y \qquad \text{(A.17)}$$

and

$$w_{,t} + uw_{,x} + vw_{,y} + ww_{,z} = -p_{,z}/\rho + \nu(w_{,xx} + w_{,yy} + w_{,zz}) + Z \qquad \text{(A.18)}$$

where Y and Z represent the external forces per unit mass in y and z directions, respectively. The above three equations are known as the Navier-Stokes equations of motion relative to a rigid frame fixed at a position in the primary inertial space. For a frictionless flow, the viscous terms drop out and the Navier-Stokes equations reduce to Euler's equations:

$$u_{,t} + uu_{,x} + vu_{,y} + wu_{,z} = -p_{,x}/\rho - X \qquad \text{(A.19)}$$

$$v_{,t} + uv_{,x} + vv_{,y} + wv_{,z} = -p_{,x}/\rho - Y \qquad \text{(A.20)}$$

and $$w_{,t} + uw_{,x} + vw_{,z} + ww_{,z} = -p_{,z}/\rho - Z \qquad \text{(A.21)}$$

When the local derivatives vanish,

$$u_{,t} = v_{,t} = w_{,z} = 0 \tag{A.22}$$

the motion is said to be stationary. When the sum of all forces is zero,

$$Du/Dt = Dv/Dt = Dw/Dt = 0 \tag{A.23}$$

an equilibrium state exists. Both stationary and equilibrium state are steady states. The condition of equilibrium flow without friction is called geostrophic flow.

A.3 Two-Dimensional Flow

For shallow-water problems, the vertical acceleration of water particles is very small compared to the gravitational acceleration. The vertical acceleration can therefore be neglected, especially when the fluid is assumed to be homogeneous. Under this assumption, equations (A.16) to (A.18) becomes

$$u_{,t}+uu_{,x}+vu_{,y}+wu_{,z} = -p_{,x}/\rho + \nu(u_{,xx}+u_{,yy}+u_{,zz}) + X \tag{A.24}$$

$$v_{,t}+uv_{,x}+vv_{,y}+wv_{,z} = -p_{,y}/\rho + \nu(v_{,xx}+v_{,yy}+v_{,zz}) + Y \tag{A.25}$$

and

$$p_{,z} = \rho Z \tag{A.26}$$

The external force Z consists of the gravity force, the z-component of the forces induced by earth rotation, and the z-component of tide-generating forces. The latter two components are very small compared to the first force and are neglected in shallow-water problems. Hence, equation (A.26) becomes

$$p_{,z} = -\rho g \tag{A.27}$$

which states that the pressure distribution is hydrostatic.

Let the Cartesian coordinate framework fixed on the rotating earth be such that the origin is on the still water level and the z-axis vertically upward. Let h denote the mean water depth, E denote the fluctuation of the water surface relative to the mean water surface, and

$$H = h+E \tag{A.28}$$

denotes the total water depth at a particular time. For a homogeneous fluid, integration of equation (A.27) gives

$$p(z) = \rho g(E-z) + p_a \tag{A.29}$$

where p_a denotes the atmospheric pressure. Therefore,

$$p_{,x} = \rho g E_{,x} + p_{a,x} \tag{A.30}$$

$$p_{,y} = \rho g E_{,y} + p_{a,y} \tag{A.31}$$

and equations (A.24) and (A.25) can be expressed as

$$u_{,t}+uu_{,x}+vu_{,y}+wu_{,z}+gE_{,x} = -p_{a,x}/\rho+\nu(u_{,xx}+u_{,yy}+u_{,zz})+X \tag{A.32}$$

and

$$v_{,t}+uv_{,x}+vv_{,y}+wv_{,z}+gE_{,y} = -p_{a,y}/\rho+ (v_{,xx}+v_{,yy}+v_{,zz})+Y \tag{A.33}$$

The term by term integration of the last two equations requires the usage of the Leibniz' rule

$$\left(\int_{-h}^{E} f dz\right)_{,\eta} = \int_{-h}^{E} f_{,\eta} dz+E_{,\eta}f(E)+h_{,\eta}f(-h) \tag{A.34}$$

Repeating the same rule gives

$$\left(\int_{-h}^{E} f dz\right)_{,\eta\eta} = \int_{-h}^{E} f_{,\eta\eta} dz+2E_{,\eta}f_{,\eta}(E)+2h_{,\eta}f_{,\eta}(-h)$$

$$+E_{,\eta\eta}f(E)+h_{,\eta\eta}f(-h) \tag{A.35}$$

Define the vertically averaged velocity components as

$$U = \left(\int_{-h}^{E} u dz\right) / H \tag{A.36}$$

and

$$V = \left(\int_{-h}^{E} v dz\right) / H \tag{A.37}$$

Define the measures of difference between the true velocity and the averaged velocity as

$$u'(z) = [u(z)-U] / U \tag{A.38}$$

and

$$v'(z) = [v(z)-V] / V \tag{A.39}$$

Then $$u(z) = U[\ 1+u'(z)\ ] \tag{A.40}$$

and so $$\int_{-h}^{E} u\,dz = U[\ H+\int_{-h}^{E} u'\,dz\ ] \tag{A.41}$$

Substituting equation (A.36) into equation (A.41) gives

$$\int_{-h}^{E} u'\,dz = 0 \tag{A.42}$$

and consequently

$$\left(\int_{-h}^{E} u'\,dz\right)_{,x} = \int_{-h}^{E} u'_{,x}\,dz + E_{,x}u'(E) + h_{,x}u'(-h)$$

$$= 0 \tag{A.43}$$

with the aid of equation (A.34).

If the velocity distributions over the depth were constant, the fluctuation term $u'(z)$ would be zero. Here it is assumed that the velocity distribution over the vertical lines is fairly constant such that $u'(z)$ is very small, so that the product $u'u'$ is negligible, and

$$\int_{-h}^{E} u'u'\,dz = 0 \tag{A.44}$$

Since $u'_{,x}(z)$ is of the order no higher than that of $u'(z)$, it follows that

$$\int_{-h}^{E} u'u'_{,x}dz = 0 \tag{A.45}$$

The spatial variation of the surface elevation is very small in a tidal flow. Therefore, the product $u'E_{,x}$ is negligible and equation (A.43) gives

$$\int_{-h}^{E} u'_{,x}dz = 0 \tag{A.46}$$

The differentiation of equation (A.40) gives

$$u_{,x} = Uu'_{,x} + U_{,x}(1+u') \tag{A.47}$$

Integrating the product of equation (A.40) and (A.47), it follows that

$$\int_{-h}^{E} uu_{,x}dz = \int_{-h}^{E}[\ U^2(u'_{,x}+u'u'_{,x}) + UU_{,x}(1+u')^2\ ]dz$$

$$= U \int_{-h}^{E}(u'_{,x}+u'u'_{,x})dz + UU_{,x}\int_{-h}^{E}(1+u')^2\ dz$$

$$= HUU_{,x} \tag{A.48}$$

with the aid from equations (A.42) and (A.44) to (A.46). Similarly,

$$\int_{-h}^{E} vu_{,y}dz = HVU_{,y} \tag{A.49}$$

and $$\int_{-h}^{E} wu_{,z}dz = 0 \tag{A.50}$$

because $$U_{,z} = 0 \tag{A.51}$$

From equation (A.34) to (A.36),

$$\int_{-h}^{E} u_{,t}dz = HU_{,t} - E_{,t}u(E)$$

$$\cong HU_{,t} \tag{A.52}$$

and $$\int_{-h}^{E} u_{,xx}dz \cong HU_{,xx} - 2E_{,x}u_{,x}(E) - 2h_{,x}u_{,x}(-h)$$

$$- E_{,xx}u(E) - h_{,xx}u(-h)$$

$$\cong HU_{,xx} \tag{A.53}$$

Similarly, $$\int_{-h}^{E} u_{,yy}dz \cong HU_{,yy} \tag{A.54}$$

Finally, $$\nu \int_{-h}^{E} u_{,zz}dz = [\ u_{,z}(E)-u_{,z}(-h)\ ]$$

$$= s_{ax}/\rho - s_{bx}/\rho \tag{A.55}$$

where $$s_{ax} = \mu u_{,z}(E) \tag{A.56}$$

and $$s_{bx} = \mu u_{,z}(-h) \tag{A.57}$$

denote the x-direction surface stress and bottom stress, respectively. The first stress is that exerted by the atmosphere on the sea; the second is that exerted by the sea on the bottom.

Integrating equation (A.32) over z=-h to z=E with the aid of equations (A.48) to (A.55) yields

$$U_{,t} + UU_{,x} + VU_{,y} + gE_{,x} = \nu(U_{,xx}+U_{,yy}) - F_x + W_x \qquad (A.58)$$

where
$$W_x = s_{ax}/(\rho H) \qquad (A.59)$$

and
$$F_x = s_{bx}/(\rho H) \qquad (A.60)$$

denote the x-direction wind force and bottom friction per unit mass, respectively. Other external forces such as barometric pressure gradients and tide-generating forces are all neglected.

Similarly, from equation (A.33),

$$V_{,t} + UV_{,x} + VV_{,y} + gE_{,y} = \nu(V_{,xx}+V_{,yy}) - F_y + W_y \qquad (A.61)$$

Integration of the continuity equation (A.4) over z=-h to z=E results in

$$(HU)_{,x} - E_{,x}u(E) - h_{,x}u(-h)$$
$$+ (HV)_{,y} - E_{,y}v(E) - h_{,y}v(-h) + w(E) - w(-h) = 0 \qquad (A.62)$$

with the aid of equations (A.34), (A.36), and (A.37). The vertical velocity of a fluid particle at (x,y,z) is the derivative of z with respect to time and so

$$w(z) = Dz/Dt = z_{,t} + uz_{,x} + vz_{,y} \tag{A.63}$$

On the free surface, one has the kinematic free surface condition

$$w(E) = E_{,t} + E_{,x}u(E) + E_{,y}v(E) \tag{A.64}$$

At the bottom, the boundary condition is

$$w(-h) = - h_{,x}u(-h) - h_{,y}v(-h) \tag{A.65}$$

Substitute with these two boundary conditions, equation (A.62) becomes

$$E_{,t} + (HU)_{,x} + (HV)_{,y} = 0 \tag{A.66}$$

or

$$H_{,t} + (HU)_{,x} + (HV)_{,y} = 0 \tag{A.67}$$

which is the continuity equation for the depth averaged two-dimensional, incompressible flow.

Another way of deriving this continuity equation is to consider directly a two-dimensional, incompressible flow with a free surface. Consider a water column of height H with small rectangular cross-section Δx-Δy. In an infinitesimal time-interval, the rate of volume increment should equal the rate of flux into the control volume, i.e., similar to equation (A.1),

$$\begin{aligned}\Delta t(H\Delta x\Delta y)_{,t} &+ [\ HU+0.5(\Delta x)(HU)_{,x}\ ]\Delta y\Delta t \\ &- [\ HU-0.5(\Delta x)(HU)_{,x}\ ]\Delta y\Delta t \\ &+ [\ HV+0.5(\Delta y)(HV)_{,y}\ ]\Delta x\Delta t \\ &- [\ HV-0.5(\Delta y)(HV)_{,y}\ ]\Delta x\Delta t = S'\Delta x\Delta y\Delta t \qquad (A.68)\end{aligned}$$

where S' denotes the volume recharge per unit area per unit time. Rearrangng this equation and dividing it by the product of the fixed dimensions x, y, and t, it yields

$$H_{,t} + (HU)_{,x} + (HV)_{,y} = S' \qquad (A.69)$$

When there is no internal source or sink, this equation reduces to equation (A.67).

A.4 The Coriolis Force

Equations (A.14) to (A.21) and (A.52) to (A.55) are the equations of motion with reference to a coordinate system fixed in the primary inertial space. The motion of fluid of interest is actually the motion with reference to a frame which is rotating along with the earth. This can be found by using the transformation of frame of reference. Referring to Bachelor (1967), the equations for the fluid motions on the rotating earth is derived as follows.

Consider a frame S' rotating with a constant angular velocity $\underline{\Omega}$ about a point O. (Throughout this section, an underline denotes a vector.) If a set of orthogonal unit vectors ($\underline{i}$,$\underline{j}$,$\underline{k}$) is fixed in S', a position vector x can be expressed as

$$\underline{x} = x_1\underline{i} + x_2\underline{j} + x_3\underline{k} \tag{A.70}$$

The velocity relative to the point O is

$$\underline{v} = D\underline{x}/Dt = \sum_i [\ (dx_i/dt)\underline{i} + x_i(d\underline{i}/dt)\ ]$$

$$= \sum_i [\ (dx_i/dt)\underline{i} + x_i\ \underline{\Omega}\ X\ \underline{i}\ ]$$

$$= (d\underline{x}/dt)_{S'} + \underline{\Omega}\ X\ \underline{x} \tag{A.71}$$

where the first term on the right hand side of the equation is the apparent velocity for an observer in S'. Similarly, the acceleration of a fluid particle relative to the point O is

$$\underline{a} = D\underline{v}/Dt = (d\underline{v}/dt)_{S'} + \underline{\Omega}\ X\ \underline{v} \tag{A.72}$$

Substituting equation (A.71) into equation (A.72) yields

$$\underline{a} = (d^2\underline{x}/dt^2) \quad + 2\ \underline{\Omega}\ X\ (d\underline{x}/dt)_{S'} + \underline{\Omega}\ X\ (\underline{\Omega}X\underline{x})$$

$$= \underline{a}_{S'} + 2\ \underline{\Omega}\ X\ \underline{v}_{S'} + \underline{\Omega}\ X\ (\ \underline{\Omega}\ X\ \underline{x}\ ) \tag{A.73}$$

where $\underline{a}_{S'}$ and $\underline{v}_{S'}$ are the apparent acceleration and apparent velocity, respectively, for an observer in S'.

Based on equation (A.73), the equation of motion with reference to a coordinate system fixed at the center of the earth can be used as those with reference to a rotating frame fixed on the earth surface, provided a fictitious force of unit mass

$$\underline{f}' = -2\,\underline{\Omega} \times \underline{v}_{S'} - \underline{\Omega} \times (\,\underline{\Omega} \times \underline{x}\,) \qquad (A.74)$$

is supposed to act upon the fluid in addition to the real forces.

To transform the equation with reference to a fixed star, or the center of the galaxy, to the equation with reference to a frame fixed on the earth surface, there are at least two more transformations. The first of them considers the rotation of the earth about the sun, with an angular velocity of $2\pi/3.2\times10^{7}\ \text{sec}^{-1}$; the second considers the rotation of the sun about the galaxy center, with an angular velocity of $2\pi/7.9\times10^{15}\ \text{sec}^{-1}$ (Li 1968). Both these two transformations require fictitious forces of the same form as that in equation (A.74). Since these two angular velocities are much smaller than that of revolution of the earth, their effects can be neglected.

All these rotations are not a true circulation motion. There are some other relative motions between the frams of reference. However, these relative motions are too small to be considered in a coastal flow problem.

The first term on the right hand side of equation (A.74) is the Coriolis force per unit mass. The second term is the centrifugal force per unit mass, which is a vector perpendicular to the axis of revolution of the earth with a magnitude of

$$C = \Omega^2 R\cos\phi \tag{A.75}$$

where R is the radius of the earth, ϕ is the latitude of the fluid particle, and

$$\Omega = 2\pi / 86400 \text{ sec}^{-1} \tag{A.76}$$

is the angular velocity of rotation of the earth.

The vertical component of this centrifugal force per unit mass is

$$C_v = C\cos\phi = \Omega^2 R\cos^2\phi \tag{A.77}$$

The effect of this component is included in the gravity force which is acted on the opposite direction of the same line. The maximum value of the centrifugal force is

$$C_{max} = \Omega^2 R = 0.111 \text{ ft/sec}^2 \tag{A.78}$$

whcih occurs at the equator where the radius of the earth is 6,378.388 Km (Beyer 1976). This value is about 1/290 of the gravitational acceleration (32.088 ft/sec^2 at the equator) and can be neglected. At ϕ=33.72^o for the Los Angeles Harbor, the vertical component of the centrifugal acceleration, 0.077 ft/sec^2, is even smaller.

The horizontal component of the centrifugal force per unit mass is

$$C_h = C\sin\phi = \Omega^2 R\sin\phi\cos\phi \tag{A.79}$$

which is pointed toward the equator.

Since a fluid particle at rest on the earth remains in place, the centrifugal force must be balanced out by other forces. The vertical component of the centrifugal force results in the negative weight of the particle. The horizontal component is balanced by a poleward component of gravitational force due to the earth's ellipticity (see Von Arx 1962).

The remaining fictitious force in equation (A.74) is the Coriolis force

$$\underline{f}' = -2\ \underline{\Omega} \times \underline{v}_S, \tag{A.80}$$

In the case of flow relative to a coordinate system rotating with angular velocity Ω about the z-axis, this unit Coriolis force lies in the (x,y)-plane and is

$$\underline{f}' = -2\Omega V\underline{i} + 2\Omega U\underline{j} \tag{A.81}$$

where U and V denote the velocities along the x- and y-directions, respectively. At a location of latitude ϕ on the Northern Hemisphere, the angle between the z-axis and the axis of rotation of the earth is $(\pi/2-\phi)$, the angular velocity of the (x,y)-plane about the z-axis is $\Omega\sin\phi$, and the Coriolis force is, neglecting the effect of vertical velocity,

$$\underline{f}' = -2\Omega(\sin\phi)V\underline{i} + 2\Omega(\sin\phi)U\underline{j}$$

$$= -fV\underline{i} + fU\underline{j} \tag{A.82}$$

where $$f = 2\Omega\sin\phi \tag{A.83}$$

is the Coriolis parameter. The sign of f should be reversed to be applied to the Southern Hemisphere.

With the Coriolis force included, the two-dimensional Navier-Stokes equations (A.58) and (A.61) become

$$U_{,t} + UU_{,x} + VU_{,y} - fV + gE_{,x} = \nu(U_{,xx}+U_{,yy}) - F_x + W_x \tag{A.84}$$

and

$$V_{,t} + UV_{,x} + VV_{,y} + fU + gE_{,y} = \nu(V_{,xx}+V_{,yy}) - F_y + W_y \tag{A.85}$$

which are two of the governing equations used in Chapter 3.

APPENDIX B

LISTING of COMPUTER PROGRAMS

B.1 Program and Sample Input for the Basic Run

```
!!!!!!!!!!!!!!!!!!!!!!!!!!!!!!!!!!!!!!!!!!!!!!!!!!!!!!!!!!!!!!
      PROGRAM   MAIN
!
!                                          Revised May 25, 1979
!                                              by W.-L. Chiang
!
!       This program was written in VAX/11 FORTRAN IV-PLUS.
!
!       Subprograms referenced by MAIN:  DATAOB, DSINOB,
! FIND, and SIMULA.
!       Other subprograms to be linked:  OBRY and PRT.
!
!       To change B.C., change:  A) name of program; B) in
! data statement, IFPLT, MMAX, MINDO, MOBD, NINDO, NMAX,
! NOBD, NSMAX; C) check dimension; D) in SUBROUTINE OBRY,
! XI's; E) in the section of print instructions; and
! F) in data file.
!       To change to double precision, be aware of 1 SIN
! function in MAIN, 1 COS in DSINOB, and 1 ABS & 6 SQRT in
! SIMULA.
!
! CAH1  dominate AH if CAH1.NE.0
! E0    =Initial elev.
! IECHK =0, if no check on the last elevation map is req'd.
!       <>0, otherwise
! IFPLT =Frequency of plotting data, i.e., the no. of "NS"
!        at which a set of data for plotter is to be written
! ICON  =-2, when the run is continued from another run & is
!        to be continued
!       =-1, when the run is continued from another run & is
!        not going to be continued
!       = 1, when normal
!       = 2, when it starts from steady state & it is to be
!        continued
! IMAP  =0, if no map of no. of computational pts. is req'd
!       <>0, otherwise
```

```
! MIND  =No. of compu.-pts. segments along y (N) dir.
! MINDO =No. of open-bdry. segments along y (N) dir.
! NHIST =0, if no histographs of velocity are req'd
! IDATA =0, if no tidal data are supplied, a cosine function
!        of AMP=TIDAMMP and PERIOD=12.5-hr will be used as
!        the open-boundary condition
!
      IMPLICIT  INTEGER*2 (I,J,K,L,M,N)
      CHARACTER*10  ATEN(7)
      CHARACTER*35  ATEN70(2)
      CHARACTER*72  TITL
C
      COMMON/ALL/  MAP(69,108)
      COMMON/MD/   NEOMAX,      TIDAMP
      COMMON/MDO/  EOB(500),      NEOB
      COMMON/MDOS/ EP(4696)
      COMMON/MDP/  EO
      COMMON/MDS/  DT
      COMMON/MF/   MINDO, MMAXM1, NINDO, NMAXM1, NSECT
      COMMON/MFO/  MOBM(1), MOBNA(1), MOBNZ(1),
     *             NOBN(1), NOBMA(1), NOBMZ(1)
      COMMON/MFP/  IHTEM(69),      MMAX, NMAX
      COMMON/MFS/  NCP
      COMMON/MO/   IEOB
      COMMON/MS/   C(4696), H(4696),
     *        ICHK(16), IPLT(16), IRPLT(8),
     *        U(4696), UP(4696), VP(4696),
     *        AG, CAH1, DELTA, DL, FF,
     *        ICON, ICON1, ICON2, ICONAB, IECHK, IFPLT,
     *        NERROR, NHIST, NI,
     *        NS, NSMAX, NSPRTB, NSPRTI,      TIME, WMDEL
C
C  Constants which are invariable for most cases
C
      DATA  AG/32.17/, ANGLAT/33.72/,
     *  ATEN/7*'1234567890'/,
     *  ATEN70/'         1111111112222222222333333',
     *  '3333444444444455555555556666666666667'/,
     *  DELTA/.5/, DL/500./,
     *  MINDO/1/, MMAX/108/,
     *  MOBM/1/, MOBNA/2/, MOBNZ/27/,
     *  NCPMAX/4696/, NEOMAX/500/, NINDO/1/, NMAX/69/,
     *  NOBN/1/, NOBMA/2/, NOBMZ/107/,
     *  NSECT/323/,
     *  PI/3.14159265359/
C
C  Case dependent constants
C
```

```
      DATA  AH/0./, CAH1/.0/, CN/.020/, DT/180./,
     *  ICHK/125, 250, 375, 500, 625, 750, 875, 1000,
     *  1125, 1250, 1375, 1500, 1625, 1750, 1875, 2000/,
     *  ICON/2/, ICON1/1000/, ICON2/2000/, IDATA/0/,
     *  IECHK/1/, IFPLT/1/, IMAP/0/,
     *  IPLT/1032, 1063, 1094, 1125, 12*0/,
     *  IRPLT/1125, 7*0/, NHIST/1/, NI/1/, NSMAX/2000/,
     *  NSPRTB/14400/, NSPRTI/20/,
     *  TIDAMP/2.8/
C
C  OPEN units used 1, 5, 6, 7, 20, 21, 22, 23, 24, 25, 63
C
      OPEN(UNIT=5,NAME='LAD',TYPE='OLD')
      OPEN(UNIT=6,NAME='LAO')
      OPEN(UNIT=7,NAME='CHK')
        IF (NSPRTB.GT.NSMAX) GO TO 1
      OPEN(UNIT=20,NAME='PRT.DAT')
1       IF (NHIST.EQ.0) GO TO 3
      OPEN(UNIT=22,NAME='U.DAT')
      OPEN(UNIT=23,NAME='V.DAT')
      OPEN(UNIT=24,NAME='E.DAT')
C
C
C
3     READ(5,5002)  TITL
      WRITE(7,5002) TITL
        IF (IPLT(1).GT.NSMAX.AND.IRPLT(1).GT.NSMAX) GOTO 4
      OPEN(UNIT=25,NAME='PLT')
      WRITE(25,5002) TITL
      WRITE(25,5004) DL, DT
4     WRITE(7,5004) DL, DT
C
C  Constants
C
        IF (CAH1.EQ.0.)      CAH1=AH*DT*2./DL/DL
      FF       = PI * SIN(ANGLAT*PI/180.) / 21600.
      ICONAB  =ABS(ICON)
      MMAXM1  =MMAX-1
      NMAXM1  =NMAX-1
      WMDEL   =1.-DELTA
C
C  Map
C
      WRITE(6,5012)
5012    FORMAT(1H1,10X,21HWATER LEVELS IN FIELD)
      WRITE(6,5021) ATEN70, ATEN
5021    FORMAT('0  M '2A/5X,7A)
      DO 30 M =1,MMAX
        READ(5,5023) (MAP(N,M), N=1,NMAX)
```

```
30          IF (    MAP(1,M).NE.0 .OR.
    1           MAP(NMAX,M).NE.0      ) GO TO 1023
        DO 31 N=2,NMAXM1
31        IF (    MAP(N,1).EQ.1 .OR.
    1           MAP(N,MMAX).EQ.1      ) GO TO 1023
        DO 32 N=MOBNA(1),MOBNZ(1)
32        MAP(N,MOBM(1))          =2
        DO 34 M=NOBMA(1),NOBMZ(1)
34        MAP(NOBN(1),M)          =2
        DO 36 M=1,MMAX
36        WRITE(6,5024) M, (MAP(N,M), N=1,NMAX)
C
        CALL    FIND
C
        TYPE *, NCPMAX
        WRITE(7,5040) NCP
          IF (NCP.GT.NCPMAX)      STOP
          IF (IMAP.EQ.0) GO TO 48
        OPEN (UNIT=63, NAME='MAP.DAT')
        WRITE(63,5040) NCP, MMAX, NMAX
        WRITE(63,5041) ((MAP(N,M), N=1,NMAX), M=1,MMAX)
        CLOSE (UNIT=63)
C
C  Read depth & determine Chezy coefficients
C
48      OSIXTH  =1./6.
        RCN     =1.486/CN
        SHFT    =0.
          IF (IDATA.EQ.0)       SHFT=TIDAMP
        N1      =1
        N2      =23
50        IF (N2.GT.NMAX)       N2=NMAX
        READ (5,5002) TITL
        WRITE(6,5002) TITL
        DO  60 M=1,MMAX
          READ (5,5060) (IHTEM(N), N=N1,N2)
          WRITE(6,5060) (IHTEM(N), N=N1,N2)
          DO 60 N=N1,N2
              IF (MAP(N,M) .EQ. 0) GO TO 60
C  Adjust to mean water depth from LLW
            TEM =IHTEM(N)+SHFT
            H(MAP(N,M)) =TEM
            C(MAP(N,M)) =TEM**OSIXTH*RCN
60          CONTINUE
          IF (N2.EQ.NMAX) GO TO 70
        N1      =N1+23
        N2      =N2+23
        GO TO 50
```

```
C
C  Read boundary condition
C
70          IF (IDATA.EQ.O) GO TO 72
C
        CALL    DATAOB
C
        GO TO 80
C
72      CALL    DSINOB
C
80      CLOSE(UNIT=5)
        CLOSE(UNIT=6)
          IF (ICON.GT.O) GO TO 110
C
C  Read data to continue computation
C
        OPEN(UNIT=1,NAME='CONIN',TYPE='OLD')
        READ  (1,*) NS,TIME
        READ  (1,*) (EP(J), J=1,NCP)
        READ  (1,*) (UP(J), J=1,NCP)
        READ  (1,*) (VP(J), J=1,NCP)
        CLOSE(UNIT=1)
        DO 105 J=1,NCP
105       U(J)  =UP(J)
        IEOB    =NS+NS
108       IF (IEOB.LE.NEOB) GO TO 200
        IEOB    =IEOB-NEOB
        GO TO 108
C
110     NS      =0
        TIME    =0.
        DO 120 J=1,NCP
          EP(J) =EO
          U(J)  =0.
          UP(J) =0.
120       VP(J) =0.
C
200     CALL SIMULA
C
CCC       IF (NERROR.NE.O) GO TO 999
C
999   STOP
C
C  Error
C
1023    TYPE 6023
6023      FORMAT(' CHECK DATA.  BDRY. OF FIELD MAP = 1?')
        GO TO 999
```

```
C
C  Format
C
5002     FORMAT(A72)
5004     FORMAT(7F10.2)
5023     FORMAT(69I1)
5024     FORMAT(1H ,I3,1X,69I1)
5060     FORMAT(1X23I3)
5040     FORMAT(3I5)
5041     FORMAT(1X17I4)
       END
C
C        *       *       *       *       *       *       *
C
       SUBROUTINE  DATAOB
C                                              Coded by W.-L. Chiang
C                                               Revised June 7, 1979
C
C        This subprogram representing the input data of open
C   bdry. elev. for a diurnal tidal cycle by 4 cosine func-
C   tions such that bdry. data behave like a smooth curve.
C
C        Called by MAIN.
C        Input data are elevs. & time for 4 extreme pts.
C   (higher low, higher high, lower low, lower high)
C        Extreme pt. 5 yields the same data as those of pt. 1
C
C   DT     - Half-time-step used in simulation
C   EXTM   - Elev. of extreme pts.
C   NEOB   - No. of elev. data along open bdry. for a tidal
C              cycle, with DT as the time interval
C   TPRD   - Period of the whole cycle, in hr. when inputed
C   TXTM   - time for the extreme pts. corresponding to EXTM,
C              in hr. when inputed
C
        IMPLICIT INTEGER*2  (I,J,K,L,M,N)
        CHARACTER*50 TITL
        DIMENSION    EXTM(5), TXTM(5)
        COMMON/MD/   NEOMAX
        COMMON/MDO/  EOB(500),      NEOB
        COMMON/MDOS/ EP(4696)
        COMMON/MDP/  EO
        COMMON/MDS/  DT
C
        READ (5,5002) TITL
        WRITE(6,5002) TITL
        READ (5,5004) TPRD, (EXTM(N),N=1,4), (TXTM(N),N=1,4)
        WRITE(6,5004) TPRD, (EXTM(N),N=1,4), (TXTM(N),N=1,4)
        TPRD    =TPRD*3600.
```

```
          DO  10 N=1,4
10          TXTM(N)=TXTM(N)*3600.
C
          NEOB     =TPRD/DT+.001
          TYPE *, NEOB, NEOMAX
            IF (NEOB.GT.NEOMAX)       STOP
          EXTMNP   =EXTM(1)
          EXTM(5)  =EXTMNP
          NP1      =1
          T        =TXTM(1)
          TXTMNP   =T
          TXTM(5)  =T+TPRD
          DO  20 J=1,NEOB
            T      =T+DT
              IF (T.LE.TXTMNP) GO TO 20
            NP1    =NP1+1
            EXTMN  =EXTMNP
            EXTMNP=EXTM(NP1)
            EMEAN =(EXTMN+EXTMNP)*.5
            AMP    =(EXTMN-EXTMNP)*.5
            TXTMN  =TXTMNP
            TXTMNP=TXTM(NP1)
            HPRD   =TXTMNP-TXTMN
            WRITE(6,*) NP1, EMEAN, AMP, TXTMN, HPRD
20          EP(J) =  COS( (T-TXTMN)*3.14159265359/HPRD ) * AMP
     1                 + EMEAN
          TYPE *, NP1
            IF (NP1.NE.5)       STOP
C
          JJ       =NEOB-TXTM(1)/DT
          DO  30 J=1,NEOB
            JJ     =JJ+1
              IF (JJ.GT.NEOB)       JJ=1
30          EOB(J)=EP(JJ)
          EO       =EOB(NEOB)
          WRITE(6,5060) EO, EOB
C
5002      FORMAT(A45)
5004      FORMAT(7F10.2)
5060      FORMAT(20F6.2)
C
      RETURN
      END
C
C         *       *       *       *       *       *       *
C
      SUBROUTINE DSINOB
C                                                Coded May 25, 1979
C                                                  by W.-L. Chiang
```

```
C
C        This subprogram defines open-bdry. elevs. as a
C   sinusoidal fctn.
C        Called by MAIN.
C
         IMPLICIT INTEGER*2  (I,J,K,L,M,N)
         COMMON/MD/   NEOMAX,      TIDAMP
         COMMON/MDO/  EOB(500),      NEOB
         COMMON/MDOS/ EP(4696)
         COMMON/MDP/  EO
         COMMON/MDS/  DT
C
         DATA  PI/3.14159265359/
         DATA  PHASE/0./
C
         EO       =-TIDAMP
C
         PERIOD  =12.5*3600.
         TPIDT   =2.*PI*DT/PERIOD
         NEOB    =PERIOD/DT+.001
         TYPE *, NEOB, NEOMAX
           IF (NEOB.GT.NEOMAX)       STOP
         DO 100 I=1,NEOB
           PHASE =PHASE+TPIDT
100        EOB(I)=-COS(PHASE)*TIDAMP
C
      RETURN
      END
C
C        *       *       *       *       *       *       *
C
      SUBROUTINE FIND
C
C                                Modified from Leendertse (1967)
C                                               by W.-L. Chiang
C                                      Revised February 4, 1979
C
C        Called by MAIN.
C
         IMPLICIT INTEGER*2 (I,J,K,L,M,N)
         LOGICAL START
C
         COMMON/ALL/  MAP(69,108)
         COMMON/FS/   MKV(323), MLV(323), MBRY(323), MV(323),
     *                NKV(323), NLV(323), NBRY(323), NV(323),
     *                MIND, NIND
         COMMON/MF/   MINDO, MMAXM1, NINDO, NMAXM1, NSECT
         COMMON/MFO/  MOBM(1), MOBNA(1), MOBNZ(1),
     *                NOBN(1), NOBMA(1), NOBMZ(1)
```

```
      COMMON/MFP/  MAPS(69),      MMAX, NMAX
      COMMON/MFS/  NCP
C
      DO  10 J=1,NSECT
        MBRY(J)       =0
10      NBRY(J)       =0
C
      NIN      =0
      DO  50 N=2,NMAXM1
        START =.TRUE.
        DO 50 M=2,MMAX
            IF (.NOT.START)  GO TO 20
            IF (MAP(N,M) .NE. 1)  GO TO 50
          NIN =NIN+1
          MKV(NIN)     =M
          START        =.FALSE.
          GO TO 50
20          IF (  MAP(N,M).EQ.1 )  GO TO 50
          MLV(NIN)     =M-1
          NV (NIN)     =N
          START        =.TRUE.
50        CONTINUE
C
      MIN      =0
      DO 150 M=2,MMAXM1
        START =.TRUE.
        DO 150 N=2,NMAX
            IF (.NOT.START) GO TO 120
            IF (MAP(N,M) .NE. 1) GO TO 150
          MIN =MIN+1
          NKV(MIN)     =N
          START        =.FALSE.
          GO TO 150
120         IF (  MAP(N,M).EQ.1 )  GO TO 150
          NLV(MIN)     =N-1
          MV (MIN)     =M
          START =.TRUE.
150       CONTINUE
C
        IF (MIN.GT.NSECT .OR. NIN.GT.NSECT .OR.
     1      MIN.LE.0     .OR. NIN.LE.0    ) GO TO 1200
C
        IF (MINDO.EQ.0) GO TO 240
      DO 240 I=1,NIN
        N      = NV(I)
        KLEF  =MKV(I)-1
        LRIG  =MLV(I)+1
        DO 240 NO=1,MINDO
          IF (N.LT.MOBNA(NO) .OR. N.GT.MOBNZ(NO)) GOTO 240
```

```
           IF (KLEF .EQ. MOBM(NO))      NBRY(I)=NBRY(I)+10
           IF (LRIG .EQ. MOBM(NO))      NBRY(I)=NBRY(I)+ 1
240        CONTINUE
C
         IF (NINDO.EQ.0) GO TO 340
       DO 340 I=1,MIN
         M     = MV(I)
         KBOT  =NKV(I)-1
         LTOP  =NLV(I)+1
         DO 340 NO=1,NINDO
           IF (M.LT.NOBMA(NO) .OR. M.GT.NOBMZ(NO)) GOTO 340
           IF (KBOT .EQ. NOBN(NO))      MBRY(I)=MBRY(I)+10
           IF (LTOP .EQ. NOBN(NO))      MBRY(I)=MBRY(I)+ 1
340        CONTINUE
C
       MIND    =MIN
       NIND    =NIN
       TYPE 401, MIND, NIND
401      FORMAT(' MIND, NIND = '2I5)
C
C  Construct mapping function
C  (4 statements which followed by a line starting with 'CM'
c  individually, can be omitted for most of cases)
C
       NCP     =0
       DO 510 N=1,NMAXM1
510      MAPS(N)        =0
       DO 560 M=1,MMAXM1
         MAPSV =0
         MP1   =M+1
         DO 540 N=1,NMAXM1
           MAPNM          =MAP(N,M)
             IF (MAPNM          .NE. 0) GO TO 520
             IF (MAPSV          .NE. 0) GO TO 520
             IF (MAPS(N)        .NE. 0) GO TO 520
             IF (MAPS(N+1)      .EQ. 1) GO TO 520
CM           IF (MAPS(N+1)      .EQ. 1) GO TO 520
             IF (MAP(N,MP1)     .NE. 0) GO TO 520
             IF (MAP(N+1,M)     .NE. 0) GO TO 520
             IF (MAP(N+1,MP1)   .EQ. 1) GO TO 520
CM           IF (MAP(N+1,MP1)   .EQ. 1) GO TO 520
           GO TO 530
520        NCP =NCP+1
           MAP(N,M)     =NCP
530        MAPSV        =MAPNM
540        MAPS(N)      =MAPNM
           IF (MAP(NMAX,M) .NE. 0) GO TO 550
           IF (MAPSV       .NE. 0) GO TO 550
CM         IF (MAPSV       .NE. 0) GO TO 550
```

```
          GO TO 560
550       NCP   =NCP+1
          MAP(NMAX,M)   =NCP
560       continue
        DO 580 N=1,NMAXM1
            IF (MAP(N,MMAX) .NE. 0) GO TO 570
            IF (MAPS(N)     .NE. 0) GO TO 570
CM          IF (MAPS(N)     .NE. 0) GO TO 570
          GO TO 580
570       NCP   =NCP+1
          MAP(N,MMAX)   =NCP
580       CONTINUE
        TYPE 601, NCP
601       FORMAT(' No. of computational pts. = 'I5)
C
      RETURN
C
1200    TYPE 6200, MIN, NIN, NSECT
6200        FORMAT(' Check MIN, NIN, & NSECT.  They =', 3I5)
      STOP
      END
C
C       *       *       *       *       *       *       *
C
      SUBROUTINE OBRY
C                                              Coded by W.-L. Chiang
C                                               Revised May 25, 1979
C       Called by SIMULA
C       Set open bounds at every half-time-step, based on
C  the functions calculated in either DATAOB or DSINOB.
        IMPLICIT INTEGER*2 (I,J,K,L,M,N)
C
        COMMON/ALL/  MAP(69,108)
        COMMON/MFO/  MOBM(1), MOBNA(1), MOBNZ(1),
     *               NOBN(1), NOBMA(1), NOBMZ(1)
        COMMON/MDO/  EOB(500),      NEOB
        COMMON/MDOS/ EP(4696)
        COMMON/MO/   IEOB
C
        IEOB    =IEOB+1
          IF (IEOB.GT.NEOB)      IEOB=1
        XI      =EOB(IEOB)
CCC     DO  10 N=MOBNA(1),MOBNZ(1)
CCC10     EP(MAP(N,MOBM(1)))    =XI
CCC     DO 110 M=NOBMA(1),NOBMZ(1)
CCC110    EP(MAP(NOBN(1),M))    =XI
        DO  10 N=2,27
10        EP(MAP(N,1))  =XI
```

```
          DO 110 M=2,107
110         EP(MAP(1,M))   =XI
        RETURN
        END
C
C         *       *       *       *       *       *       *
C
        SUBROUTINE  PRT(EUVP, FAC, IUNIT)
C
C                                           Coded by W.-L. Chiang
C                                            Revised June 8, 1979
C
C         Called by MAIN
C
          IMPLICIT INTEGER*2 (I,J,K,L,M,N)
C
          DIMENSION  EUVP(4696)
          COMMON/ALL/  MAP(69,108)
          COMMON/MFP/  JACK(69),      MMAX, NMAX
          COMMON/MDP/   EO
C
          NA       =1
          NB       =32
50        WRITE (IUNIT,5050)
            IF (NB.GT.NMAX)       NB=NMAX
C
          WRITE (IUNIT,5055) (N, N=NA,NB)
          DO  61 M=1,MMAX
            DO 60 N=NA,NB
                IF (MAP(N,M) .EQ. 0) GO TO 59
              TEM =EUVP(MAP(N,M))
                IF (ABS(TEM-EO) .LE. 1.E-6) GO TO 59
              JACK(N)      =TEM*FAC
              GO TO 60
59            JACK(N)      =0
60            CONTINUE
61          WRITE (IUNIT,5061) M, (JACK(N), N=NA,NB)
            IF (NB.EQ.NMAX)       RETURN
          NA       =NA+32
          NB       =NB+32
          GO TO 50
5050      FORMAT()
5055      FORMAT(4X,32I4)
5061      FORMAT(33I4)
        END
C
C         *       *       *       *       *       *       *
C
```

```
      SUBROUTINE SIMULA
C
C
C                                                  Revised June 23, 1979
C                                                        by W.-L. Chiang
C
C       Subprogram referenced:  OBRY and PRT
C       Called by MAIN
C
C       If IT.GT.1, Kick out 38 "CIT's" at the beginning of
C   statements
C
        IMPLICIT INTEGER*2 (I,J,K,L,M,N)
        REAL*8  TTGDL
        DOUBLE PRECISION  DIS1, DIS2, DIS3, DIS4, DIS5,
     *          E1, E2, E3, E4, E5, SUMRU, SUMRV,SURU,SURV
C
        DIMENSION  E(4696), P(108), Q(108), R(108),
     *          RU(4696), RV(4696), S(108),
     *          UPLT(5), V(4696), VPLT(5)
        COMMON/ALL/  MAP(69,108)
        COMMON/FS/   MKV(323), MLV(323), MBRY(323), MV(323),
     *               NKV(323), NLV(323), NBRY(323), NV(323),
     *               MIND, NIND
        COMMON/MDOS/ EP(4696)
        COMMON/MDS/  DT
        COMMON/MFS/  NCP
        COMMON/MS/   C(4696), H(4696),
     *          ICHK(16), IPLT(16), IRPLT(8),
     *          U(4696), UP(4696), VP(4696),
     *          AG, CAH1, DELTA, DL, FF,
     *          ICON, ICON1, ICON2, ICONAB, IECHK, IFPLT,
     *          NERROR, NHIST, NI,
     *          NS, NSMAX, NSPRTB, NSPRTI,      TIME, WMDEL
C
        EQUIVALENCE  (ALPHAO, BETAO), (ALPHA5, BETA5),
     *               (DELTA, GAMMA), (WMDEL, WMGAM)
C
        DATA  ALPHAO/O./, ALPHA5/.5/, DIS1/O./, DIS2/O./,
     *          DIS3/O./, DIS4/O./, DIS5/O./,
     *          E1/O./, E2/O./, E3/O./, E4/O./, E5/O./,
     *          ICH/1/, IP/1/, IRP/1/, NERROR/O/, NSR/O/,
     *          SUMRU/O./, SUMRV/O./,SURU/O./,SURV/O./
C
C   Constant
C
        AG4     =AG*4.
        DT2     =DT+DT
```

```
C  Remove the next 100 statements in general case
       M0687   =MAP(6,87)
       M0688   =MAP(6,88)
       M0689   =MAP(6,89)
       M0690   =MAP(6,90)
       M0691   =MAP(6,91)
       M0692   =MAP(6,92)
       M0693   =MAP(6,93)
       M0694   =MAP(6,94)
       M0695   =MAP(6,95)
       M0696   =MAP(6,96)
       M0697   =MAP(6,97)
       M0698   =MAP(6,98)
       M0699   =MAP(6,99)
       M0700   =MAP(7,100)
       M0787   =MAP(7,87)
       M0788   =MAP(7,88)
       M0789   =MAP(7,89)
       M0790   =MAP(7,90)
       M0791   =MAP(7,91)
       M0792   =MAP(7,92)
       M0793   =MAP(7,93)
       M0794   =MAP(7,94)
       M0795   =MAP(7,95)
       M0796   =MAP(7,96)
       M0797   =MAP(7,97)
       M0798   =MAP(7,98)
       M0799   =MAP(7,99)
       M0800   =MAP(8,100)
       M0899   =MAP(8,99)
       M0900   =MAP(9,100)
       M0999   =MAP(9,99)
       M1000   =MAP(10,100)
       M1099   =MAP(10,99)
       M1100   =MAP(11,100)
       M1199   =MAP(11,99)
       M1659   =MAP(16,59)
       M1660   =MAP(16,60)
       M1661   =MAP(16,61)
       M1662   =MAP(16,62)
       M1663   =MAP(16,63)
       M1759   =MAP(17,59)
       M1760   =MAP(17,60)
       M1761   =MAP(17,61)
       M1762   =MAP(17,62)
       M2119   =MAP(21,19)
       M2120   =MAP(21,20)
       M2121   =MAP(21,21)
       M2122   =MAP(21,22)
```

```
M2219    =MAP(22,19)
M2220    =MAP(22,20)
M2221    =MAP(22,21)
M2222    =MAP(22,22)
M2260    =MAP(22,60)
M3411    =MAP(34,11)
M3412    =MAP(34,12)
M3511    =MAP(35,11)
M3512    =MAP(35,12)
M3947    =MAP(39,47)
M3948    =MAP(39,48)
M4047    =MAP(40,47)
M4048    =MAP(40,48)
H0686    =H(MAP(6,86))
H0687    =H(M0687)
H0688    =H(M0688)
H0689    =H(M0689)
H0690    =H(M0690)
H0691    =H(M0691)
H0692    =H(M0692)
H0693    =H(M0693)
H0694    =H(M0694)
H0695    =H(M0695)
H0696    =H(M0696)
H0697    =H(M0697)
H0698    =H(M0698)
H0699    =H(M0699)
H0799    =H(M0799)
H0899    =H(M0899)
H0999    =H(M0999)
H1099    =H(M1099)
H1199    =H(M1199)
H1562    =H(MAP(15,62))
H1658    =H(MAP(16,58))
H1659    =H(M1659)
H1660    =H(M1660)
H1661    =H(M1661)
H1662    =H(M1662)
H2118    =H(MAP(21,18))
H2119    =H(M2119)
H2120    =H(M2120)
H2121    =H(M2121)
H2122    =H(M2122)
H3410    =H(MAP(34,10))
H3411    =H(M3411)
H3412    =H(M3412)
H3946    =H(MAP(39,46))
H3947    =H(M3947)
H3948    =H(M3948)
```

```
C
        TDL      =DT/DL
        TG16     =DT*AG*16.
        TTGDL    =TDL*AG*2.
C
        CAH1B    =CAH1
        CAH2     =1.-CAH1*4.
        CAH2B    =1.-CAH1*2.
        DLDT2    =DL*DT2
        DHR2     =DT2/3600.
        DT2FF    =DT2*FF
        HTDL     =TDL*.5
C
C  Initial values
C
        HR       =TIME/3600.
C  Remove the next statemenT in general case
        USAVE    =UP(M2220)
        DO 10 J=1,NCP
          RU(J) =0.
10        RV(J) =0.
C
C  Output instructions
C
100     CONTINUE
CCC100    IF (NS.LT.NSPRTB) GO TO 110
CCC       IF ( MOD(NS-NSPRTB,NSPRTI) .NE. 0) GO TO 110
CCCC
CCC     WRITE (20,5101) HR
5101      FORMAT(/////' EP*100 AT TIME(HR) ='F7.3)
CCC     CALL PRT(EP, 100., 20)
CCC     WRITE (20,5102) HR
CCC5102   FORMAT(/////' UP*1000 AT TIME(HR) ='F7.3)
CCC     CALL PRT(UP, 1000., 20)
CCC     WRITE (20,5103) HR
CCC5103   FORMAT(/////' VP*1000 AT TIME(HR) ='F7.3)
CCC     CALL PRT(VP, 1000., 20)
C
C  Remove the next 8 statements in general case
110     UU1      =UP(M2220)
          IF (ABS(UU1-USAVE) .GT. .2) GO TO 1117
        USAVE    =UU1
C
CCC       IF (NHIST .EQ. 0) GO TO 120
CCC       IF ( MOD(NS,IFPLT) .NE. 0) GO TO 120
        WRITE(22,5112) UU1, UP(M2260)
        WRITE(23,5112) VP(M2220), VP(M2260)
        WRITE(24,5112) EP(M2220), EP(M2260)
C
```

```
120       IF (NS .NE. IPLT(IP)) GO TO 150
        IP       =IP+1
        WRITE (25,5124)
5124      FORMAT(' CIRCULATION PATTERN')
        WRITE (25,5125) HR
        JJ       =1
        DO 140 J=1,NCP
        UPLT(JJ)=( U(J)+UP(J) )*.5
        VPLT(JJ)=VP(J)
          IF (JJ.LT.5) GO TO 140
        WRITE(25,5130) (UPLT(JJ), VPLT(JJ), JJ=1,5)
        JJ       =0
140     JJ       =JJ+1
          IF (JJ.EQ.1) GO TO 150
        WRITE(25,5130) (UPLT(J), VPLT(J), J=1,JJ-1)
C
150       IF (NS.NE.IRPLT(IRP)) GO TO 175
        IRP      =IRP+1
        DO 160 J=1,NCP
          RU(J) =RU(J)/NSR
160       RV(J) =RV(J)/NSR
        WRITE (25,5154)
5154      FORMAT('  RESIDUAL VELOCITY')
        WRITE(25,5125) HR
        WRITE(25,5130) (RU(J), RV(J), J=1,NCP)
C
C  Remove the next 41 statements in general case
175       IF (NS.NE.ICHK(ICH)) GO TO 230
        ICH      =ICH+1
        WRITE(7,5125) HR
        DIS1     =DIS1*.5*DLDT2
        DIS2     =DIS2*.5*DLDT2
        DIS3     =DIS3*.5*DLDT2
        DIS4     =DIS4*.5*DLDT2
        DIS5     =DIS5*.5*DLDT2
        DISO     =DIS1+DIS2+DIS3
        E1       =E1/NSR
        E2       =E2/NSR
        E3       =E3/NSR
        E4       =E4/NSR
        E5       =E5/NSR
        SUMRU    =0.
        SUMRV    =0.
        DO 180 J=1,NCP
          SUMRU =RU(J)+SUMRU
          SUMRV =RV(J)+SUMRV
          RU(J) =0.
180       RV(J) =0.
        SURU     =SURU/NSR
```

```
      SURV     =SURV/NSR
      SUMRU    =SUMRU/NSR
      SUMRV    =SUMRV/NSR
      WRITE(7,5183) DIS0, DIS1, DIS2, DIS3, DIS4, DIS5,
     1         E1, E2, E3, E4, E5, SUMRU, SUMRV, SURU, SURV
5183    FORMAT(' DIS0 TO DIS5 (CU. FT.) ='6E10.3//
     1         ' E1 TO E5 (FT.) ='5F10.5//
     4         ' SUMRU & SUMRV (FPS) ='4F10.0////)
      DIS1     =0.
      DIS2     =0.
      DIS3     =0.
      DIS4     =0.
      DIS5     =0.
      E1       =0.
      E2       =0.
      E3       =0.
      E4       =0.
      E5       =0.
      NSR      =0
      SURU=0.
      SURV=0.
C
230     IF (ICONAB.NE.2) GO TO 250
        IF (NS.LT.ICON1) GO TO 250
        IF (NS.GT.ICON1) GO TO 240
      OPEN (UNIT=21, NAME='CONou1')
      WRITE(21,*) NS, TIME
      WRITE(21,*) (EP(J), J=1,NCP)
      WRITE(21,*) (UP(J), J=1,NCP)
      WRITE(21,*) (VP(J), J=1,NCP)
      CLOSE(UNIT=21)
      GO TO 245
240     IF (NS.NE.ICON2) GO TO 250
      OPEN (UNIT=31, NAME='CONou2')
      WRITE(31,*) NS, TIME
      WRITE(31,*) (EP(J), J=1,NCP)
      WRITE(31,*) (UP(J), J=1,NCP)
      WRITE(31,*) (VP(J), J=1,NCP)
      CLOSE(UNIT=31)
245     IF (NS.EQ.NSMAX) GO TO 900
      WRITE(7,5101) HR
      CALL     PRT( EP, 100., 7)
250     IF (NS.GE.NSMAX) GO TO 900
260   NS       =NS+1
CCC     IF (MOD(NS,50) .EQ. 0)      TYPE *, NS
      HR       =HR+DHR2
      TIME     =TIME+DT2
      DO 270 J=1,NCP
      E(J)     =EP(J)
```

```
270     V(J)    =VP(J)
C   Set open bound
        CALL    OBRY
C
C   Compute UP & EP on row N ( 1st half timestep )
C
CIT     IT      =1
300     DO 360 I=1,NIND
          IBRY  =NBRY(I)
          N     = NV(I)
          K     =MKV(I)
          L     =MLV(I)
          KM1   =K-1
          NM1   =N-1
          NP1   =N+1
          R(KM1)=0.
          S(KM1)=0.
            IF (IBRY.LT.10)  GO TO 310
CS          IF (IBRY.LT.10 .OR. IBRY.GT.11)  GO TO 310
          NK    =MAP(N,K)
          NKM1  =MAP(N,KM1)
          NKP1  =MAP(N,K+1)
          NM1KM1=MAP(NM1,KM1)
          NP1KM1=MAP(NP1,KM1)
          UNKM1 =U(NKM1)
          UNMKM =U(NM1KM1)
            IF (UNMKM.EQ.O.) GO TO 306
CIT         IF (IT.GT.1) GO TO 303
          U2NMKM=UNMKM+UNMKM
          GO TO 307
CIT303    U2NMKM=UP(NM1KM1)+UNMKM
CIT       GO TO 307
306       UNMKM =UNKM1
          U2NMKM=UP(NKM1)+UNKM1
307       UNPKM =U(NP1KM1)
            IF (UNPKM.EQ.O.) GO TO 308
          U2NPKM=UP(NP1KM1)+UNPKM
          GO TO 309
308       UNPKM =UNKM1
          U2NPKM=UP(NKM1)+UNKM1
309       VAV   =( V(NK)+V(MAP(NM1,K)) )/2.
CS        TEM1  =1. + TTDL*( U(NK)-UNKM1 )*ALPHAO
          R(KM1)=TTGDL
CS    1            /TEM1
          S(KM1)=TTGDL*EP(NKM1)
      1          + UNKM1*(   CAH2B
      2                    - SQRT(UNKM1*UNKM1+VAV*VAV)*TG16
      3                    /((H(NM1KM1)+H(NKM1)+E(NKM1)+E(NK))
      4                             *( C(NM1KM1)+C(NKM1))**2)  )
```

```
     5          + VAV*( DT2FF-HTDL*(U2NPKM-U2NMKM) )
     6          + CAH1B*(UNMKM+UNPKM)
CS   5          + VAV*( DT2FF - TDL*( WMGAM*(UNPKM-UNKM1)
CS   6                                +GAMMA*(UNKM1-UNMKM) )
CS   7          + CAH1B*(UNMKM+UNPKM)
CS        S(KM1)=S(KM1)/TEM1
          DU    =U(NKP1)-UNKM1
          DUP   =DU
CIT         IF (IT.GT.1)       DUP=UP(NKP1)-UP(NKM1)
          GO TO 320
310       NK    =MAP(N,K)
          NKP1  =MAP(N,K+1)
          DU    =( U(NKP1)-U(NK) )*2.
          DUP   =DU
CIT         IF (IT.GT.1)       DUP=( UP(NKP1)-UP(NK) )*2.
320       DO 330 M=K,L
            MM1  =M-1
            MP1  =M+1
            NM   =MAP(N,M)
            NM1M=MAP(NM1,M)
            NMM1=MAP(N,MM1)
            NMP1=MAP(N,MP1)
            NP1M=MAP(NP1,M)
            ENM  =E(NM)
            EPNM=EP(NM)
            HNM  =H(NM)
            HNM1M        =H(NM1M)
            HNMM1        =H(NMM1)
            HNMMM        =H(MAP(NM1,MM1))
            H2   =HNM1M+HNM
            UNM1M        =U(NM1M)
            UNMM1        =U(NMM1)
            UNMP1        =U(NMP1)
            VNM  =V(NM)
            VNM1M        =V(NM1M)
CIT           IF (IT.GT.1) GO TO 324
            EPNMM1       =E(NMM1)
            EPNMP1       =E(NMP1)
            U2NM1M       =UNM1M+UNM1M
              IF (M.EQ.K) GO TO 325
            DU   =UNMP1-UNMM1
            DUP  =DU
CIT         GO TO 325
CIT324      EPNMM1       =EP(NMM1)
CIT         EPNMP1       =EP(NMP1)
CIT         U2NM1M       =UP(NM1M)+UNM1M
CIT           IF (M.EQ.K) GO TO 325
CIT         DU   =UNMP1-UNMM1
CIT         DUP  =UP(NMP1)-UP(NMM1)
```

```
325         TEMH=( HNMMM+HNMM1+EPNMM1+EPNM )*HTDL
            TEMR=TEMH*R(MM1)+1.
            P(M)=HTDL*(H2+EPNM+EPNMP1)/TEMR
            Q(M)=( ENM - HTDL*( (HNMM1+HNM+ENM+E(NP1M))*VNM
     1                        -(HNMMM+HNM1M+ENM+E(NM1M))*VNM1M )
     2                     + TEMH*S(MM1) )/TEMR
              IF (M.EQ.L) GO TO 330
            UNM =U(NM)
              IF (UNM1M.NE.0.) GO TO 327
            UNM1M        =UNM
            U2NM1M       =UP(NM)+UNM
327         UNP1M        =U(NP1M)
              IF (UNP1M.EQ.0.) GO TO 328
            U2NP1M       =UP(NP1M)+UNP1M
            GO TO 329
328         UNP1M        =UNM
            U2NP1M       =UP(NM)+UNM
329         VAV =( VNM+V(NMP1)+VNM1M+V(MAP(NM1,MP1)) )/4.
            TEM1=( AG4*P(M)+DUP )*HTDL+1.
CS          TEM1=1.+TTDL*( AG*P(M)+ALPHA5*DUP )
            R(M)=TTGDL/TEM1
            S(M)=( UNM*( CAH2-DU*HTDL
     1                 -SQRT(UNM*UNM+VAV*VAV)*TG16
     2           /( (H2+ENM+E(NMP1))*(C(NM1M)+C(NM))**2 ) )
     3          + VAV*( DT2FF-HTDL*(U2NP1M-U2NM1M) )
     4          + CAH1*(UNMM1+UNMP1+UNM1M+UNP1M)
     5          + TTGDL*Q(M) )/TEM1
CS   3          + ( DT2FF - TDL*( WMGAM*(UNP1M-UNM)
CS   3                          +GAMMA*(UNM-UNM1M) ) )*VAV
CS   4          + CAH1*(UNMM1+UNMP1+UNM1M+UNP1M)
CS   5          + TTGDL*Q(M) )/TEM1
330         CONTINUE
            IF (IBRY.NE.1 .AND .IBRY.NE.11) GO TO 350
          LP1   =L+1
          NL    =MAP(N,L)
          NLP1  =MAP(N,LP1)
          NM1L  =MAP(NM1,L)
          NP1L  =MAP(NP1,L)
          UNL   =U(NL)
          UNM1L =U(NM1L)
            IF (UNM1L.EQ.0.) GO TO 336
CIT         IF (IT.GT.1) GO TO 333
          U2NM1L=UNM1L+UNM1L
          GO TO 337
CIT333    U2NM1L=UP(NM1L)+UNM1L
CIT       GO TO 337
336       UNM1L =UNL
           U2NM1L=UP(N)+UNL
337       UNP1L =U(NP1L)
```

```
              IF (UNP1L.EQ.O.) GO TO 338
            U2NP1L=UP(NP1L)+UNP1L
            GO TO 339
338         UNP1L =UNL
            U2NP1L=UP(NL)+UNL
339         VAV   =( V(NL)+V(NM1L) )/2.
            UP(NL)=( TTGDL*( Q(L)-EP(NLP1) )
     1            + UNL*( CAH2B - SQRT(UNL*UNL+VAV*VAV)*TG16
     2                    /( ( H(NM1L)+H(NL)+E(NL)+E(NLP1) )
     3                    *( C(NM1L)+C(NL))**2 ) )
     4            + ( DT2FF-HTDL*(U2NP1L-U2NM1L) )*VAV
     5            + CAH1B*(UNM1L+UNP1L) )
     6            / ( 1.+TTGDL*P(L) )
CS   4            + ( DT2FF - TDL*( GAMMA*(UNL-UNM1L)
CS   5                             +WMGAM*(UNP1L-UNL) ) )*VAV
CS   6            + CAH1B*(UNM1L+UNP1L) )
CS   7            /(1. + TTDL*( AG*P(L)
CS   8                          +(UNL-U(MAP(N,L-1)))*ALPHAO) )
350         CONTINUE
            M     =L
            DO 360 J=K,L
              MM1  =M-1
              NM   =MAP(N,M)
              EP(NM)        =-P(M)*UP(NM)+Q(M)
              UP(MAP(N,MM1))        =-R(MM1)*EP(NM)+S(MM1)
360           M    =MM1
C
CIT       IT       =IT+1
CIT         IF (IT.LE.NI) GO TO 300
C
          DO 560 J=1,NCP
            U(J)   =UP(J)
560         E(J)   =EP(J)
C   Set open bounds
          CALL     OBRY
C
C   Compute VP & EP on col. M ( 2nd half timestep )
C
CIT       IT       =1
600       DO 660 I=1,MIND
            IBRY   =MBRY(I)
            M      =MV(I)
            K      =NKV(I)
            L      =NLV(I)
            MM1    =M-1
            MP1    =M+1
            KM1    =K-1
            R(KM1)=O.
            S(KM1)=O.
```

```
              IF (IBRY.LT.10) GO TO 610
CS            IF (IBRY.LT.10 .OR. IBRY.GT.11) GO TO 610
            KM     =MAP(K,M)
            KM1M   =MAP(KM1,M)
            KM1MM1=MAP(KM1,MM1)
            KM1MP1=MAP(KM1,MP1)
            KP1M   =MAP(K+1,M)
            VKM1M  =V(KM1M)
            VKMMM  =V(KM1MM1)
              IF (VKMMM.EQ.0.) GO TO 606
CIT           IF (IT.GT.1) GO TO 603
            V2KMMM=VKMMM+VKMMM
            GO TO 607
CIT603      V2KMMM=VP(KM1MM1)+VKMMM
CIT         GO TO 607
606         VKMMM  =VKM1M
            V2KMMM=VP(KM1M)+VKM1M
607         VKMMP  =V(KM1MP1)
              IF (VKMMP.EQ.0.) GO TO 608
            V2KMMP=VP(KM1MP1)+VKMMP
            GO TO 609
608         VKMMP  =VKM1M
            V2KMMP=VP(KM1M)+VKM1M
609         UAV    =( U(KM)+U(MAP(K,MM1)) )/2.
CS          TEM1   =1. + TTDL*( V(KM)-VKM1M )*BETAO
            R(KM1)=TTGDL
CS     1                /TEM1
            S(KM1)= EP(KM1M)*TTGDL
       1           + VKM1M*(   CAH2B
       2                    - SQRT(VKM1M*VKM1M+UAV*UAV)*TG16
       3                 /(( H(KM1MM1)+H(KM1M)+E(KM1M)+E(KM)  )
       4                          *( C(KM1MM1)+C(KM1M))**2)  )
       5           - ( DT2FF+HTDL*(V2KMMP-V2KMMM)  )*UAV
       6           + CAH1B*(VKMMM+VKMMP)
CS     5           - (DT2FF + (  (VKMMP-VKM1M)*WMDEL
CS     6                      +(VKM1M-VKMMM)*DELTA  )*TDL)*UAV
CS     7           + CAH1B*(VKMMM+VKMMP)
CS          S(KM1)=S(KM1)/TEM1
            DV     =V(KP1M)-VKM1M
            DVP    =DV
CIT           IF (IT.GT.1)   DVP=VP(KP1M)-VP(KM1M)
            GO TO 620
610         KM     =MAP(K,M)
            KP1M   =MAP(K+1,M)
            DV     =( V(KP1M)-V(KM)  )*2.
            DVP    =DV
CIT           IF (IT.GT.1)   DVP=( VP(KP1M)-VP(KM)   )*2.
620         DO 630 N=K,L
              NM1  =N-1
```

```
              NP1  =N+1
              NM   =MAP(N,M)
              NM1M=MAP(NM1,M)
              NMM1=MAP(N,MM1)
              NMP1=MAP(N,MP1)
              NP1M=MAP(NP1,M)
              ENM  =E(NM)
              EPNM=EP(NM)
              HNM  =H(NM)
              HNM1M          =H(NM1M)
              HNMM1          =H(NMM1)
              HNMMM          =H(MAP(NM1,MM1))
              H2   =HNMM1+HNM
              VNMM1          =V(NMM1)
              VNM1M          =V(NM1M)
              VNP1M          =V(NP1M)
              UNM  =U(NM)
              UNMM1          =U(NMM1)
CIT             IF (IT.GT.1) GO TO 624
              EPNM1M         =E(NM1M)
              EPNP1M         =E(NP1M)
              V2NMM1         =VNMM1+VNMM1
                IF (N.EQ.K) GO TO 625
              DV   =VNP1M-VNM1M
              DVP  =DV
CIT           GO TO 625
CIT624        EPNM1M         =EP(NM1M)
CIT           EPNP1M         =EP(NP1M)
CIT           V2NMM1         =VP(NMM1)+VNMM1
CIT             IF (N.EQ.K) GO TO 625
CIT           DV   =VNP1M-VNM1M
CIT           DVP  =VP(NP1M)-VP(NM1M)
625           TEMH=( HNMMM+HNM1M+EPNM1M+EPNM  )*HTDL
              TEMR=TEMH*R(NM1)+1.
              P(N)=HTDL*(H2+EPNM+EPNP1M)/TEMR
              Q(N)=( ENM
     1              - HTDL*( (HNM1M+HNM   +ENM+E(NMP1))*UNM
     2                      -(HNMMM+HNMM1+ENM+E(NMM1))*UNMM1  )
     3              + TEMH*S(NM1) )/TEMR
                IF (N.EQ.L) GO TO 630
              VNM  =V(NM)
                IF (VNMM1.NE.0.) GO TO 627
              VNMM1          =VNM
              V2NMM1         =VP(NM)+VNM
627           VNMP1          =V(NMP1)
                IF (VNMP1.EQ.0.) GO TO 628
              V2NMP1         =VP(NMP1)+VNMP1
              GO TO 629
628           VNMP1          =VNM
```

```
               V2NMP1       =VP(NM)+VNM
 629           UAV  =( UNM+U(NP1M)+UNMM1+U(MAP(NP1,MM1)) )*.25
               TEM1=(AG4*P(N)+DVP)*HTDL+1.
 CS            TEM1=1.+TTDL*(AG*P(N)+BETA5*DVP)
               R(N)=TTGDL/TEM1
               S(N)=( VNM*( CAH2-DV*HTDL
      1             -SQRT(VNM*VNM+UAV*UAV)*TG16
      2              /( (H2+ENM+E(NP1M))*( C(NMM1)+C(NM))**2 ) )
      3             - ( DT2FF+HTDL*(V2NMP1-V2NMM1) )*UAV
      4             + CAH1*(VNMM1+VNMP1+VNM1M+VNP1M)
      5             + TTGDL*Q(N) )/TEM1
 CS   3             -( ( WMDEL*(VNMP1-VNM)
 CS   3                 +DELTA*(VNM-VNMM1) )*TDL + DT2FF )*UAV
 CS   4             + CAH1*(VNMM1+VNMP1+VNM1M+VNP1M)
 CS   5             + TTGDL*Q(N) )/TEM1
 630           CONTINUE
               IF (IBRY.NE.1 .AND. IBRY.NE.11) GO TO 650
             LM     =MAP(L,M)
             LMM1   =MAP(L,MM1)
             LMP1   =MAP(L,MP1)
             LP1    =L+1
             LP1M   =MAP(LP1,M)
             VLM    =V(LM)
             VLMM1  =V(LMM1)
               IF (VLMM1.EQ.O.) GO TO 636
 CIT           IF (IT.GT.1) GO TO 633
             V2LMM1=VLMM1+VLMM1
             GO TO 637
 CIT633      V2LMM1=VP(LMM1)+VLMM1
 CIT         GO TO 637
 636         VLMM1 =VLM
             V2LMM1=VP(LM)+VLM
 637         VLMP1 =V(LMP1)
               IF (VLMP1.EQ.O.) GO TO 638
             V2LMP1=VP(LMP1)+VLMP1
             GO TO 639
 638         VLMP1 =VLM
             V2LMP1=VP(LM)+VLM
 639         UAV   =( U(LM)+U(LMM1) )/2.
             VP(LM)=( ( Q(L)-EP(LP1M) )*TTGDL
      1             + VLM*( CAH2B - SQRT(VLM*VLM+UAV*UAV)*TG16
      2                   /( ( H(LMM1)+H(LM)+E(LM)+E(LP1M) )
      3                           *( C(LMM1)+C(LM))**2 )      )
      4             - ( DT2FF+HTDL*(V2LMP1-V2LMM1) )*UAV
      5             + CAH1B*(VLMM1+VLMP1) )
      6   / ( 1.+TTGDL*P(L) )
 CS   4             - ( ( (VLMP1-VLM)*WMDEL
 CS   5                  +(VLM-VLMM1)*DELTA )*TDL + DT2FF )*UAV
 CS   6             + CAH1B*(VLMM1+VLMP1) )
```

```
CS   7  / (1.+TTDL*(AG*P(L)+BETAO*(VLM-V(MAP(MAP(L-1,M))))))
650       N      =L
          DO 660 J=K,L
            NM   =MAP(N,M)
            NM1  =N-1
            EP(NM)        =-P(N)*VP(NM)+Q(N)
            VP(MAP(NM1,M))        =-R(NM1)*EP(NM)+S(NM1)
660         N    =NM1
C
CIT     IT       =IT+1
CIT       IF (IT.LE.NI) GO TO 600
C
C   Data summation & residual currents
C
C   Remove the next 42 statements in general case
        NSR      =NSR+1
C
        E1       =EP(M2121)+E1
        DIS1     =DIS1
     1  +(  VP(M2119)*( EP(M2119)+EP(M2219)+H2118+H2119 )
     2    + VP(M2120)*( EP(M2120)+EP(M2220)+H2119+H2120 )
     3    + VP(M2121)*( EP(M2121)+EP(M2221)+H2120+H2121 )
     4    + VP(M2122)*( EP(M2122)+EP(M2222)+H2121+H2122 ) )
        E2       =EP(M1661)+E2
        DIS2     =DIS2
     1  +(  VP(M1659)*( EP(M1659)+EP(M1759)+H1658+H1659 )
     2    + VP(M1660)*( EP(M1660)+EP(M1760)+H1659+H1660 )
     3    + VP(M1661)*( EP(M1661)+EP(M1761)+H1660+H1661 )
     4    + VP(M1662)*( EP(M1662)+EP(M1762)+H1661+H1662 )
     5    + UP(M1662)*( EP(M1662)+EP(M1663)+H1562+H1662 ) )
        E3       =EP(M0689)+E3
        DIS3     =DIS3
     1  +(  VP(M0687)*( EP(M0687)+EP(M0787)+H0686+H0687 )
     2    + VP(M0688)*( EP(M0688)+EP(M0788)+H0687+H0688 )
     3    + VP(M0689)*( EP(M0689)+EP(M0789)+H0688+H0689 )
     4    + VP(M0690)*( EP(M0690)+EP(M0790)+H0689+H0690 )
     5    + VP(M0691)*( EP(M0691)+EP(M0791)+H0690+H0691 )
     6    + VP(M0692)*( EP(M0692)+EP(M0792)+H0691+H0692 )
     7    + VP(M0693)*( EP(M0693)+EP(M0793)+H0692+H0693 )
     8    + VP(M0694)*( EP(M0694)+EP(M0794)+H0693+H0694 )
     9    + VP(M0695)*( EP(M0695)+EP(M0795)+H0694+H0695 )
     *    + VP(M0696)*( EP(M0696)+EP(M0796)+H0695+H0696 )
     1    + VP(M0697)*( EP(M0697)+EP(M0797)+H0696+H0697 )
     2    + VP(M0698)*( EP(M0698)+EP(M0798)+H0697+H0698 )
     3    + VP(M0699)*( EP(M0699)+EP(M0799)+H0698+H0699 ) )
        DIS3     =DIS3
     1  -(  UP(M0799)*( EP(M0799)+EP(M0700)+H0699+H0799 )
     2    + UP(M0899)*( EP(M0899)+EP(M0800)+H0799+H0899 )
     3    + UP(M0999)*( EP(M0999)+EP(M0900)+H0899+H0999 )
```

```
      4    + UP(M1099)*( EP(M1099)+EP(M1000)+H0999+H1099 )
      5    + UP(M1199)*( EP(M1199)+EP(M1100)+H1099+H1199 ) )
        E4      =EP(M3412)+E4
        DIS4    =DIS4
      1 +(  VP(M3411)*( EP(M3411)+EP(M3511)+H3410+H3411 )
      2    + VP(M3412)*( EP(M3412)+EP(M3512)+H3411+H3412 ) )
        E5      =EP(M3948)+E5
        DIS5    =DIS5
      1 +(  VP(M3947)*( EP(M3947)+EP(M4047)+H3946+H3947 )
      2    + VP(M3948)*( EP(M3948)+EP(M4048)+H3947+H3948 ) )
C
        DO 810 J=1,NCP
          RU(J)  =RU(J)+UP(J)
          SURU   =UP(J)+SURU
          SURV   =VP(J)+SURV
810       RV(J)  =RV(J)+VP(J)
      GO TO 100
C
900       IF (IECHK.EQ.0) GO TO 999
        WRITE(7,5101) HR
        CALL     PRT( EP, 100., 7)
999   RETURN
1117    TYPE 6117, HR, UU1, USAVE
6117      FORMAT(/' OSCILLATION???   HR, UU1, USAVE ='
     1              F10.5,2E15.7)
        NERROR  =1
        GO TO 900
C
C
5112    FORMAT(1X6E11.3)
5125    FORMAT(1XF10.2)
5130    FORMAT(1X10F6.3)
C
      END
```

```
Column   111111111122222222223333333333444444444455555555556666666666777
!23456789012345678901234567890123456789012345678901234567890123456789012
!
!       Following is the list of the sample input data for
! Run #1 to #37 except Runs #4, #5, and #36:
 108X69H
 0
 11111111111111111111111111  1111
 111111111111111111111111   11111
 11111111111111111111111  1111111
 1111111111111111111111 11111111
 111111111111111111111 111111111111111
 11111111111111111111 11111111   11
 1111111111111111111 111111111
 1111111111111111111 11111111111111111
 1111111111111111111 111111111111                          1
 1111111111111111111 11111111111111111111111111            1
 1111111111111111111 1111111111111111111111111111          1
 1111111111111111111 111111111111       11    1111         1
 1111111111111111111 111111111111               111        1
 1111111111111111111 11111111111111111           111 1    11
 1111111111111111111 11111111111111111 11111      1111    11
 1111111111111111111 11111111111111111111 11       1111  111
 1111111111111111111 111111111111111111 1  1        1111111111
 11111111111111111111111111111111111111              1111   11111111
 1111111111111111111111111111111111111111            111     11111
 111111111111111111111111111111111111111111          111111   111
 111111111111111111111111111111111111111111           1  111    1
 1111111111111111111 1111111111111111111111           11
 1111111111111111111 1111111111111111111111            1
 1111111111111111111 11111111111111111111111           11
 1111111111111111111 111111111111111111111111           1
 1111111111111111111 111111111111111111111111 1         111  11
 1111111111111111111 111111111111111111111111 11        111111
 1111111111111111111 111111111111111111111111 111       111
 1111111111111111111 1111111111111111111111111 11        111
 1111111111111111111 1111111111111111111111111111        111
 1111111111111111111 1111111111111111111111              1111
 1111111111111111111 111111111111111111111 11111         11111
 1111111111111111111 11111111111111111111 111111         1 111
 1111111111111111111 1111111111111111111  111111         1   11
 1111111111111111111 1111111111111111111 1111111         1    11
 1111111111111111111 111111111111111111 11111111         1     11
 1111111111111111111 11111111111111111  11111111         1      1
 1111111111111111111 11111111111111111 111111111         1      1
 1111111111111111111 11111111111111111 111111111         1      1
 1111111111111111111 11111111111111111 111111111         1
 1111111111111111111 11111111111111111 111111111         11
 1111111111111111111 11111111111111111 111111111        11
```

```
111111111111111111111111111
11111111111111111111111111
1111111111111111111111111
111111111111111111111111
1111111111111111111111
111111111111111111111
11111111111111111111
1111111111  1111111
11111111111  11111
111111111111
1111111111111
11111111111 1
11111111111
1111111111
111111111
0
DEPTH MAP, PAGE 1:
110109108108106105103101103105106100 96 93 90 81 81 81 77 71 62 50 44
107108107106105101 98 94 96 98 98 97 90 85 83 81 80 77 73 68 60 50 45
103102102103104 98 94 93 92 90 89 88 88 86 83 81 79 75 69 64 56 51 44
 99 98 97 95103 98 91 90 90 90 89 87 86 84 82 75 73 73 69 60 56 52 45
 97 97 94 93 96 96 92 90 90 89 88 87 84 82 80 74 72 70 65 59 57 52 46
 96 96 95 97 96 94 93 91 90 89 89 87 82 82 80 73 72 66 63 62 56 52 40
 93 94 90 94 94 91 90 90 90 89 89 87 83 82 80 78 75 68 66 61 55 41 42
 90 92 92 92 88 88 89 90 90 91 89 87 83 82 80 77 73 71 66 60 57 44 44
 91 92 92 92 90 89 90 90 90 91 88 86 83 80 80 75 71 70 64 59 56 43 44
 90 91 92 92 91 91 90 90 89 89 87 86 81 77 76 73 70 71 64 58 56 42 44
 89 90 90 84 84 87 88 88 88 88 86 84 80 78 75 72 70 67 62 57 55 41 42
 88 86 87 86 84 86 87 86 86 86 84 82 78 75 73 70 70 66 62 58 55 41 43
 87 85 87 88 88 87 86 86 86 85 82 80 76 72 70 70 69 62 60 58 55 41 42
 84 84 85 85 72 70 84 84 85 85 78 75 73 68 65 63 65 63 60 58 55 40 43
 83 84 83 82 82 74 82 84 84 82 78 70 70 68 64 62 63 62 62 57 55 44 44
 83 83 83 83 84 76 80 84 82 79 78 71 68 64 59 62 60 59 57 53 53 44 42
 83 82 83 84 83 76 81 83 82 80 78 73 65 60 59 57 59 57 53 50 50 45 42
 84 84 84 85 83 80 83 82 80 82 78 68 64 58 57 57 56 54 51 49 48 46 45
 85 85 85 84 83 84 83 81 80 81 78 70 68 59 58 58 57 53 51 49 49 48 47
 83 83 83 83 82 80 79 79 80 79 78 71 68 62 60 58 57 53 52 50 48 47 44
 80 78 77 77 77 77 78 78 78 76 74 72 68 62 58 58 56 55 52 54 48 44 43
 79 78 77 77 77 78 77 76 72 70 72 70 68 62 60 59 56 54 52 49 48 44 43
 79 79 78 77 77 77 75 72 67 67 68 68 67 64 60 61 56 54 53 50 47 45 44
 74 74 73 72 71 72 71 69 68 67 68 66 64 62 61 60 58 56 54 53 49 45 46
 74 70 70 70 70 69 66 65 64 65 65 63 63 62 60 61 58 57 55 53 50 46 46
 72 69 69 68 67 66 66 63 65 64 62 62 63 62 61 60 59 58 55 53 51 40 46
 72 69 68 68 67 68 68 65 65 65 62 60 65 64 62 60 59 61 56 53 52 46 46
 73 72 70 68 70 70 69 67 72 66 66 67 67 65 63 60 60 62 59 56 52 47 47
 72 72 71 68 73 72 71 72 73 70 67 65 67 66 64 60 61 60 58 55 52 47 47
 72 72 73 73 74 73 72 76 74 72 73 68 68 65 64 60 61 62 58 55 52 48 48
 76 76 75 75 76 76 77 77 74 73 73 72 69 67 65 61 60 60 58 55 53 49 49
 78 78 77 77 77 77 78 77 75 75 73 72 68 66 64 61 61 59 57 55 54 49 48
```

78	78	77	77	76	78	78	76	76	76	72	72	68	65	64	60	60	60	55	55	53	49	48
78	78	77	77	77	78	77	77	77	75	72	71	67	65	63	60	59	57	54	52	52	48	48
78	78	78	78	79	79	78	78	77	74	73	71	66	65	63	60	59	55	54	53	52	48	48
78	77	78	78	79	78	78	78	75	74	73	71	66	65	60	59	59	57	54	54	52	48	48
78	78	79	79	79	78	77	77	76	74	73	69	67	64	60	59	59	59	55	52	52	48	48
78	78	79	79	79	78	77	76	72	73	72	69	66	63	60	58	57	57	55	51	51	49	48
77	78	78	79	78	78	77	74	73	73	71	68	65	62	60	58	56	55	54	52	52	49	48
77	78	79	79	78	78	76	74	73	73	70	67	64	61	60	58	56	55	54	52	51	49	49
78	79	79	78	78	77	76	75	73	72	69	66	63	61	59	57	55	55	53	52	51	49	48
79	79	79	78	78	77	75	74	72	69	67	66	63	61	59	57	55	55	53	52	51	48	49
79	78	78	78	77	77	75	72	69	68	67	65	63	62	58	57	55	55	53	53	52	49	49
79	77	77	78	76	75	73	70	66	64	65	64	62	60	57	56	55	55	53	53	52	49	49
78	76	76	78	76	74	71	69	67	65	66	64	62	60	57	56	54	56	54	53	52	50	48
77	76	75	78	74	73	69	68	67	64	64	63	62	60	57	56	55	55	54	53	52	50	48
75	75	74	73	72	71	70	69	67	64	61	61	60	60	58	57	56	55	54	53	52	50	48
75	74	72	72	71	71	69	68	68	64	61	60	60	59	58	57	56	54	54	53	53	50	48
75	74	72	72	71	70	68	67	66	64	61	61	59	58	57	56	55	54	54	53	50	50	55
74	73	72	73	73	68	67	66	64	64	62	61	59	58	57	56	55	54	53	53	50	50	60
73	73	73	74	72	67	67	67	65	64	62	61	59	58	57	56	55	54	52	52	50	50	67
72	74	74	72	69	68	68	67	65	64	63	60	59	58	57	55	55	55	53	52	52	57	68
73	74	72	71	69	67	67	67	66	63	62	60	58	57	57	55	55	54	52	52	52	60	68
74	72	70	70	70	66	66	66	64	63	62	60	59	57	57	55	55	53	52	52	56	68	71
72	70	70	69	69	67	67	66	65	63	62	60	60	58	57	56	56	53	52	52	60	68	65
70	70	70	69	68	68	67	66	65	63	62	60	60	58	58	57	56	52	52	52	57	64	60
71	70	69	69	68	68	66	66	65	64	62	60	59	59	58	58	57	53	53	56	60	58	56
71	69	69	68	68	67	66	65	64	64	62	60	60	59	58	58	53	54	58	60	57	53	52
73	69	69	68	67	66	65	64	63	62	61	60	60	59	59	59	59	60	59	55	54	52	51
71	68	69	68	66	65	64	63	62	61	61	59	59	58	60	59	60	58	55	54	54	52	51
70	69	69	66	65	64	63	63	63	61	61	59	59	58	58	58	58	55	55	55	54	53	52
69	69	68	66	65	64	63	63	63	61	61	60	50	58	58	47	57	55	55	55	52	52	52
69	69	68	66	65	64	63	62	61	60	60	59	59	57	50	57	57	57	56	55	53	52	52
68	67	66	64	64	63	61	61	60	59	60	59	59	57		58	57	57	54	54	54	53	52
68	66	65	64	64	63	62	61	60	59	60	59	58	58	58	58	58	57	52	53	55	53	52
67	67	66	64	64	63	62	61	58	59	60	59	58		57	57	57	56	52	53	55	52	51
66	66	66	64	64	63	62	61	59	58	58	58	58	57	57	57	57	55	54	54	53	51	50
66	65	64	64	64	61	61	61	60	60	61	58	58	55	55	55	55	54	55	53	51	50	49
66	65	64	64	64	61	61	60	60	60	60	59		54	54	54	55	53	52	51	49	49	48
65	65	64	64	64	61	61	61	60	60	60	59	54	54	54	53	52	52	52	50	49	48	48
64	64	64	63	62	61	61	60	60	60	59		54	54	54	53	52	51	51	49	49	48	47
64	64	63	62	61	61	61	60	59	59	58	53	53	54	54	53	52	51	50	49	48	47	46
64	63	62	62	63	62	60	60	59	58	58	54	52	53	54	53	52	51	49	48	48	45	43
63	63	63	63	62	60	60	58	58	58		55	53	54	53	52	51	50	49	48	46	46	43
63	63	63	62	60	59	58	58	58	58	55	55	52	53	52	51	50	49	48	47	44	43	43
64	63	62	61	60	58	57	57	57		55	54	52	52	52	51	49	47	46	45	43	43	43
63	62	61	59	59	58	55	55	54	53	54	53	52	52	52	50	48	47	45	44	43	43	41
61	60	58	58	58	57	55	54	54	52	52	52	51	51	50	49	48	46	45	44	43	43	40
60	59	58	57	57	56	55	54		52	52	51	51	51	51	46	45	45	45	44	43	40	39
59	58	57	56	55	54	54	53	52	52	51	50	49	48	46	44	43	43	43	43	42	40	39
58	58	56	55	54	52	52		51	51	50	49	48	47	45	43	43	43	42	41	40	39	39

57	57	56	55	54	52	49	51	51	50	49	48	47	46	45	44	43	42	40	39	39	39	38
55	55	55	55	53	51	45	50	50	49	47	45	44	44	44	43	43	40	40	38	38	36	35
55	55	54	53	52	51		48	49	48	47	45	43	43	43	42	40	39	38	37	36	35	34
55	55	53	51	51	50	44	45	45	45	45	44	42	42	41	39	38	37	37	35	35	34	33
54	52	50	49	50	48	43	43	43	43	43	43	42	42	39	38	37	36	34	33	33	32	30
53	51	50	49	46	43	43	43	41	42	42	41	38	38	38	37	36	34	33	32	30	29	29
51	50	49	49	46	43	43	42	40	42	40	38	38	37	37	36	35	33	32	30	29	28	28
49	49	47	46	44	42	42	41	39	39	38	36	36	35	35	33	34	32	30	28	28	27	27
49	47	43	43	42	42	42	40	38	37	36	35	34	33	33	31	30	24	24	22	26	25	23
45	45	43	42	40	39	39	38	37	37	35	34	34	32	30	29	28	26	24	20	24	23	23
43	42	42	41	39	37	36	37	35	34	32	31	32	29	27	27	27	23	24	23	23	23	23
42	42	40	39	38	37	36	36	35	31	30	30	29	27	25	24	23	23	23	22	21	19	19
41	40	38	37	36	35	34	32	30	30	27	26	26	25	22	22	22	22	21	21	20	19	18
39	38	37	36	35	34	33	31	30	28	26	25	25	24	22	21	22	18	18	17	17	16	17
38	37	36	35	33	32	31	29	28	27	26	25	24	23	21	20	18	13	16	16	16	15	14
36	35	34	34	31	30	29	28	27	26	25	21	20	20	18	17	14	13	13	15	14	14	13
35	34	33	31	30	28	28	27	24	20	22	21	19	17	16	15	14	13	13	13	13	12	
33	31	30	29	29	27	27	23	20	19	18	18	18	15	14	13	13	13	12	10	10		
30	29	28	25	25	25	25	22	19	17	12	8			12	11	10	11	10	11			
29	28	26	24	23	23	23	21	18	15	12	9	6			8	9	10	9				
28	26	24	23	23	22	19	17	16	14	12	7	6	5									
26	24	23	23	20	20	18	16	15	12	11	9	6	5	5								
25	20	23	22	19	18	17	16	13	11	10	8	7										
26	24	21	19	18	16	15	13	12	10	9	7											
22	22	21	18	16	15	14	11	11	8	7												
21	20	17	16	15	12	12	9	8	6													

0

DEPTH MAP, PAGE 2:

38	31	25	18	8		3	3	3	4	3												
38	28	19	22	3	8	9	11	7	3	3												
39	26	18	30	25	12	10	12	9	3	3												
35	20	30	37	34	25	18	20	12	8	15												
15	35	41	41	40	30	24	41	40	25	31	34	33	32	33	34							
40	42	42	42	43	46	45	47	41	25	20	25	36	36	34	34							
43	43	42	42	47	47	47	47			5	10	20										
41	42	41	42	47	47	47	49	51	51	38	39	36	35	35	36							
42	43	42	41	45	47	47	47	30	25	27	37	35	35	34	32							
42	42	41	41	44	47	47	40	25	25	25	33	33	34	34	32	26	29	30	30	30	32	32
39	41	42	42	43	47	47	38	34	34	35	35	35	35	35	34	33	33	33	34	34	34	34
43	42	43	43	44	47	44	38	36	34	25	34	40	33	33	34	34	35	35	34	34	34	34
42	42	43	40	44	47	40	38	30	22	21								31	28			
44	41	40	41	45	45	33	28	28	21	19	16	15	16	12	8							
45	42	40	43	47	35	33	30	30	26	21	21	20	18	16	15	13	15	15	15	18	18	
43	39	45	46	35	33	31	27	28	30	21	20	20	19	18	18	16	23	18	18	18	18	
40	46	44	41	38	34	30	27	27	25	22	21	19	19	17	17	22	24	23	18	18	18	
47	43	40	41	40	35	31	30	26	23	22	21	21	20	18	15	15		24		17		
45	41	41	41	39	32	31	27	26	25	24	21	20	19	18	16	14	13	10				
42	40	40	41	42	42	29	29	28	28	24	22	21	20	19	17	10	11	10	6	5		
42	41	42	42	42	38	31	29	28	28	25	23	22	20	19	19	13	10	9	7	5		

43	41	40	42	43	40	32	30	29	27	25	24	23	20	20	20	17	12	11	8	8		
45	40	41	42	42	43	33	32	29	28	26	25	25	23	23	21	20	17	15	13	13		
41	41	41	42	42	40	34	33	30	30	28	27	27	24	23	21	19	18	17	14	13	15	
42	43	40	40	42	41	35	34	31	30	29	28	26	25	24	22	21	20	19	17	16	16	15
44	43	41	40	40	40	35	34	33	31	29	28	28	27	25	22	22	21	20	18	17	16	16
45	42	40	40	40	40	35	34	33	32	29	28	28	27	26	25	23	21	21	19	18	17	16
46	44	41	39	40	40	38	33	33	32	30	29	27	27	26	25	24	23	22	20	19	18	16
46	46	41	40	40	40	36	33	33	33	30	29	28	26	25	25	24	23	22	21	19	18	17
47	44	42	41	41	41	36	35	34	33	31	30	28	27	26	26	25	23	22	20	20	19	18
47	43	42	41	40	41	35	35	34	33	31	30	29	28	27	26	25	23	22	21	20	19	18
47	44	43	42	39	41	37	35	34	33	31	31	30	29	28	27	24	22	21	20	36	30	26
46	44	44	44	40	42	37	36	35	34	33	32	30	29	28	27	23	21	16	25	35	36	36
47	45	44	43	41	41	38	37	36	35	35	32	30	29	28	28	25	21		30	36	37	36
47	46	44	43	42	41	38	36	36	36	35	31	35	39	40	50	39	23	35	37	36	37	39
46	44	44	42	42	41	39	36	36	36	35	33	48	52	48	50	25	18	40	46	40	38	38
47	47	46	50	43	43	65	58	37	36	35	33	46	48	48	37	15	44	44	45	47	48	47
47	47	53	64	60	44	68	67	37	37	35	33	46	47	46	20	30	46	47	47	47	49	48
47	46	57	65	61	41	68	63	38	36	35	33	45	44	40	29	30	47	48	47	47	48	48
47	46	53	69	61	44	71	66	45	37	36	35	34	49	45	28	30	46	47	47	48	48	48
47	58	62	69	60	42	65	68	45	39	36	35	34	40	45	25	30	42	47	47	48	48	50
59	70	66	65	60	45	68	66	45	38	37	36	34	48	45	18	30	46	46	47	48	49	48
59	70	66	68	66	68	69	66	45	38	37	36	45	48	36	24	40	42	45	47	48	49	49
59	69	67	68	71	69	64	67	45	38	37	46	47	48	35	19	35	45	46	47	48	48	49
58	68	68	69	69	69	65	67	45	39	37	40	47	44	37	18	30	44	48	54	46	45	48
60	70	70	72	71	70	67	67	45	39	38	46	52	40	30	16	30	49	59	60	49	44	47
60	68	71	71	71	71	68	67	45	48	57	56	56	55	31	55	60	60	60	60	58	44	
64	69	70	71	71	71	73	66	50	57	57	59	59	60	60	56	50	61	60	60	60	40	
64	70	68	67	71	69	70	60	57	60	60	60	58	60	36	35	24	19	35	59	60	50	38
67	67	65	73	72	72	68	61	60	61	56	56	47	40	38	50	38		36	47	58	60	60
68	67	66	66	68	64	60	59	57	61	48	40	34	39	38	60	65			44	45	55	52
69	66	68	63	62	59	52	55	48	61	33	35	50	54	64	65	63			43	45	47	44
70	65	63	60	58	51	53	40	40	61	62	62	60	45	64	65	64	40		41	49	44	45
65	62	60	57	51	46	42	38	34	62	62	63	37		47	46	62	38		44	50	51	48
60	59	51	48	43	43	42	39	39	45	52	50	30								46	50	49
56	52	44	45	43	42	40	39	42	60	62	30										48	44
52	49	43	43	41	41	35		47	50	53	45											
51	46	42	39	32	35	35		47	48	48	54	59	58	56								
50	44	38	38	29	25	34		48	49	44	44	49	53	53								
48	39	37	35	29	31			40	45	49											20	4
49	38	38	31	33														15	18	20	27	8
49	47	40	36	38													12	19	29	28	27	15
47	45	43	41	49	47	45	44	43	42	40	40					18	22	23	24	25		
49	47	46	46	49	46	45	45	43	42	40	40	40			16	31	31	29	31	27	8	7
49	48	47	48	48	45	45	44	43	41	40	39	35			30	35	35	31	30	19	12	
50	49	48	49	47	46	45	44	42	41	41	38	31	37	30	35	35	35	31	28			
49	49	49	49	45	46	45	43	41	41	40	37	37	50	57	62	38	37	36	25			
48	48	48	48	46	44	43	42	41	42	38	37	42	60	62	45	39	29	30	28			
48	49	46	46	46	44	42	41	41	38	35	30	35	51	58	40	31	37	27	25			
48	47	46	45	43	43	40	40	40	36	27	27	30	40	40	30	31	33	28	24			

```
45 46 46 45 42 42 40 40 38 35 30 31 31 30 29 29 29    26 19  3
45 45 45 42 41 40 40 40 36 34 33 33 33 33 29 29 28 24 22 15  3
44 45 43 42 39 39 40 36 35 34 33 33 32 31 29 29 27 25 19 12
45 45 42 41 39 38 38 35 35 33 33 33 32 30 30 29 26 22 12  3
44 42 41 39 38 37 36 35 34 33 33 32 30 29 28 26 23 18 10
42 40 40 39 38 36 35 34 33 32 32 31 29 29 27 25 20 16
41 39 40 38 37 35 34 33 32 32 31 29 28 27 26 24 15  8
40 39 38 37 36 35 34 33 31 31 30 28 27 26 24 20 10
38 37 37 35 34 33 33 32 30 29 27 28 26 25 23 18
38 37 35 35 34 32 31 30 30 29 28 28 25 23 17
38 35 32 33 32 31 30 28 28 28 27 25 24 20 12
37 31 33 32 30 29 30 28 26 26 25 24 21 15  5
34 34 33 30 30 29 29 27 26 25 24 23 15 10
33 33 30 29 29 29 28 27 25 24 23 18 10
31 29 29 29 29 29 27 24 24 23 20 12
29 27 28 28 29 25 24 24 23 21 14  6
20 20 20 26 24 24 24 23 20 15 13
26 24 20 24 24 23 24 22 17 12
25 24 24 23 23 23 23 19 13
23 23 23 22 22 22 19 15
23 22 22 21 21 17 12
22 21 21 19 16 12
20 19 18 15 11
17 17 15 10
18 13 11
14
 0
 0
 0
 0
 0
 0
 0
 0
 0
 0
 0
 0
DEPTH MAP, PAGE 3:
 0
 0
 0
 0
 0
 0
 0
 0

                                                25 25
 30 28                                          27 25
```

33	33	27	25										25	28								
34	35	34	34	34									30	32								
33	34	35	35	34	34								30	37								
		36	35	35	34	34	38	33				27	35	37								
			35	35	35	35	35	30				24	35	35								
				35	35	35	32	31	32		37	36	36	34								
					36	35	35	35	34	35	37	36	37	36	36							
						35	35	35	35	37	37	35	37	36	36	36	35	33	37	35	34	34
							34	34	35	33				36	36	35	36	37	38	34	32	
							34	34	34	37	36	34	34		36	35	35	36	36	39		
							34	34	34	35	35	34	36	35		35	33	37	37			
								35	35	35	33	34	35	36				33	35			
								35	35	35												
									35	35	35											
									35	35	35											
5	5									35	35	35	36		33	25						
14	10	3								30	35	36	37	36	36	34	31					
17	16	10								25	25	35	30	38	37	33						
15	14	10	3							25	25	35	36	25								
15	12	9	6								25	39	36	35								
16	13	9	7								20	36	35	36	33							
28	9	9									20	36	30	35	35	33						
35	18	17									20	35	13	10	30	37						
36	19	18									20	35	10	10	18	30	35					
36	19	18									20	35			12	20	25	35				
39	20	20									20	35				20	20	25	25			
45	31	27									20	35					20	25	23			
48	40	38									25	35						23	22			
49	48	40									41	41						20	24			
40	40	35									51	45						20	27			
47	40	38									54	45	20									
47	39	41								20	54	35	20									
47	41	37								25	57	40										
51	47	23								35	58	33										
49	50	45								45	58	36										
47	38	30								44	58	30										
										40	55	40										
										50	45	10										
40	35	54	54	40	45	45	45	29	50	57	58											
58	57	60	54	49	45	45	60	58	61	59	54											
45	47							54	52	52	54											
46	47	49	47				36	35	51	53	54	53										
45	49	48	48				38	40	52		50	41										
45								44	47		41	41										
38	43							40	45		42	45										
48	48	49						38	35		45	43										
39	40	37						34	38		36	38										
		7	4					35	35		30	40										
4	4	8	5								30	35										

```
 4  3
10
 0
 0
 0
 0
 0
 0
 0
 0
 0
 0
 0
 0
 0
 0
 0
 0
 0
 0
 0
 0
 0
 0
 0
 0
 0
 0
 0
 0
 0
 0
 0
 0
 0
 0
 0
 0
 0
 0
 0
 0
 0
 0
 0
 0
 0
 0
 0
```

```
DATA FOR OPEN BDRY. ELEVS. (1 25-HR. TIDAL CYCLE), SPRING TIDE
  25.        1.3       6.0        -.91       4.61       2.0        8.0
  15.25     21.25
DATA FOR OPEN BDRY. ELEVS. (1 25-HR. TIDAL CYCLE), NEAP TIDE
  25.        2.55      4.95       1.40       3.79       3.2        9.2
  16.2      21.75
COLUMN  111111111122222222223333333333444444444455555555556666666666677
2345678901234567890123456789012345678901234567890123456789012345678901 2
END OF INPUT DATA
```

B.2 Program to Plot Curves with a Line Printer

```
!!!!!!!!!!!!!!!!!!!!!!!!!!!!!!!!!!!!!!!!!!!!!!!!!!!!!!!!!!!!!
      PROGRAM   PLOT
!
!                                               Coded by W.-L. Chiang
!                                               Revised June 24, 1979
!       This program was written in VAX/11 FORTRAN IV-PLUS.
!       This program calls the subroutine PLOTS which plots
! the input data on x- and y-axes.  The length of y-axis has
! to be either 6 or 12 inches.
!       The x-data have to be a data string of equal incre-
! ment or decrement.
!       The input data are supplied by file "PLOTI.DAT."  To
! produce the input file "PLOTI.DAT," each x and its corres-
! ponding (up tp 10) y-values should be put into one single
! line in any kind of format with data separated by either
! space(s) or comma (with or without extra spaces).  Notice
! that there should be N+1 columns of input data if you have
! N sets of y-data.  However, x-data may be omitted such
! that there are only N columns in the input file which is
! still to be read by the free format.
!       The output will be stored in the file "PLOTO.DAT."
!       In response to the first question which asks for the
! title of graph, you may type in up to 120 characters in
! one line or you may just type a <CR> if no title is
! needed.
!       In response to an yes-or-no question, any word
! starting with capital Y will be interprete to be "Yes,"
! otherwise, "No."
!       Scaling (user y-data units per inch of paper) can
! either be automatic or be manually specified.  When speci-
! fying the scale, only one scale can be specified and that
! one will be applied to all y-data.  If not specified, the
! scaling is determined by the program on the basis of all
! y-data to be plotted.  In this case, the scaling will be
! round-up to a simple number related to one of the "RHO"
! data defined in the subroutine PLOTS.
!       The subroutine PLOTS, together with the subroutine
! ONED, can be separated from this main program and be
! called by other program in which all variables in the
! "CALL PLOTS" statement, except X and Y, should have been
! defined.  In this case, all "CCC's" in the subroutine
! PLOTS should be removed.
!       Suggestions and bugs to Wen-Li Chiang.
!
```

```
! Subprograms referenced:  ONED, PLOTS
! CHARACTER*1   ANS, BOTTOM, CENTER, PDATA, YSYMBL(*)
! CHARACTER*4   TITLE(*), XNAME(*), YNAME(*,*)
! REAL  SCALE, VLARGE, X(*), Y(*,*), YSIZE
! INTEGER(dummy)        I, L, N
! INTEGER          MAXNC, MXNPLTS, NC, NPTS
!
        CHARACTER*1   ANS, BOTTOM, CENTER, PDATA, YSYMBL(10)
        DIMENSION  Y(3001,10),
     1          TITLE(30), X(3001), XNAME(8), YNAME(8,10)
C
        DATA  VLARGE/1.E38/, MAXNC/10/, MXNPTS/3001/,
     1    YSYMBL/'+', '*', 'O', 'X', ':', '$', 'H', '8',
     2          '#', 'O'/
C
        OPEN (UNIT=1, NAME='PLOTI', TYPE='OLD')
        OPEN (UNIT=63, NAME='PLOTO')
C
        TYPE 1
1         FORMAT(6X'WHAT''S THE TITLE OF THIS GRAPH?')
        ACCEPT 6001, TITLE
C
10      TYPE 11
11        FORMAT(6X'HOW MANY CURVES IN A GRAPH?')
        ACCEPT *, NC
          IF (NC .GT. MAXNC  .OR.  NC .LT. 1) GO TO 4013
C
20      TYPE 21
21        FORMAT(6X'HOW MANY DATA SETS?')
        ACCEPT *, NPTS
          IF (NPTS .GT. MXNPTS) GO TO 4023
          IF (NPTS .LT. 2     ) GO TO 4024
C
        TYPE 26
26        FORMAT(6X'ARE X-DATA IN THE INPUT FILE?')
        ACCEPT 6053, ANS
          IF (ANS .NE. 'Y') GO TO 1028
C
        DO  30 I=1,NPTS
30        READ (1,*,END=4030) X(I), (Y(I,N), N=1,NC)
C
C
31      TYPE 35
35        FORMAT(6X'TYPE THE LENGTH OF Y-AXIS IN INCHES.')
36      ACCEPT *, YSIZE
          IF (YSIZE .EQ.  6.) GO TO 39
          IF (YSIZE .EQ. 12.) GO TO 39
        TYPE 37
```

```
37        FORMAT(6X    ,'SORRY.  I AM STILL TOO YOUNG TO ',
     1          'HANDLE SUCH A COMPLEX CASE.'/
     2    6X'IT MUST BE EITHER 6 OR 12.  PLEASE RETYPE.')
        GO TO 36
C
39      TYPE 40
40        FORMAT(6X'TYPE THE TITLE FOR X-AXIS.')
        ACCEPT 6001, (XNAME(L), L=1,8)
          IF (NC .GT. 1) GO TO 149
        TYPE 50
50        FORMAT(6X'TYPE THE TITLE FOR Y-AXIS.')
        ACCEPT 6001, (YNAME(L,1), L=1,8)
C
        TYPE 6052
        ACCEPT 6053, ANS
          IF (ANS .NE. 'Y') GO TO 200
        TYPE 60
60        FORMAT(6X'NAME IT!')
        ACCEPT 6053, YSYMBL(1)
        GO TO 200
C
C
C
149     CALL     ONED(MXNPTS,NPTS,NC,Y)
C
        TYPE 150
150       FORMAT(6X'TYPE THE TITLES OF Y-CURVES.'/
     1    6X'(TYPE <CR> AFTER THE TITLE OF EACH CURVE)')
        DO  151 N=1,NC
151       ACCEPT 6001, (YNAME(L,N), L=1,8)
C
        TYPE 6052
        ACCEPT 6053, ANS
          IF (ANS .NE. 'Y') GO TO 200
        TYPE 160
160       FORMAT(6X'NAME THE SYMBOLS FOR ALL CURVES!'/
     1           6X'(PUNCH <CR> AFTER EACH SYMBOL)')
        DO 162 N=1,NC
162       ACCEPT 6053, YSYMBL(N)
C
C
C
200     TYPE 201
201       FORMAT(6X'DO YOU LIKE TO FIX THE X-AXIS ALONG '
     1             'THE CENTER LINE OF GRAPH?')
        ACCEPT 6053, CENTER
          IF (CENTER .EQ. 'Y') GO TO 205
        TYPE 203
203       FORMAT(6X'BOTTOM LINE?')
```

```
        ACCEPT 6053, BOTTOM
C
205     TYPE 210
210       FORMAT(6X
     1  'DO YOU LIKE TO SPECIFY THE SCALE FACTOR YOURSELF?')
        ACCEPT 6053, ANS
          IF (ANS .NE. 'Y') GO TO 1212
        TYPE 221
221       FORMAT(6X
     1    'TYPE IT IN UNITS OF Y-VALUES PER INCH OF PAPER.')
        ACCEPT *,SCALE
C
230     TYPE 231
231       FORMAT(6X,'DO YOU LIKE TO HAVE THE DATA PRINTED?')
        ACCEPT 6053, PDATA
C
        CALL     PLOTS(BOTTOM,CENTER,NC,NPTS,PDATA,SCALE,
     1          TITLE,VLARGE,X,XNAME,Y,YSIZE,YNAME,YSYMBL)
999     STOP
C
C Branches
C
1028    TYPE 1029
1029      FORMAT(6X'WHAT''S THE INITIAL X-VALUES?')
        ACCEPT *, X(1)
        TYPE 1031
1031      FORMAT(6X'WHAT''S THE INCREMENT FOR X-DATA?')
        ACCEPT *,XINC
        IM1     =1
        DO 1034 I=2,NPTS
          X(I)  =X(IM1)+XINC
1034      IM1   =I
        DO 1036 I=1,NPTS
1036      READ (1,*,END=4030) (Y(I,N),N=1,NC)
        GO TO 31
C
1212    SCALE   =VLARGE
        GO TO 230
C
C Error
C
4013    TYPE 6013, MAXNC
        GO TO 10
4023    TYPE 6013, MXNPTS
        GO TO 20
4024    TYPE 6024
        GO TO 20
4030    I        =I-1
        TYPE 4031, NPTS
```

```
4031      FORMAT(/6X'DID YOU SAY THAT THERE ARE'I5
    1      ' SETS DATA IN THE INPUT FILE?'
    2            6X'I DO''NT THINK SO.  PLEASE CHECK IT.  '
    3            'SEE YOU AGAIN.')
        GO TO 999
C
C Format
C
6001    FORMAT(30A4)
6013    FORMAT(6X
    1   'IT HAS TO BE A POSITIVE INTEGER NO GREATER THAN'
    2   I5/)
6024    FORMAT(6X'IT MUST BE GREATER THAN 1.')
6052    FORMAT(6X
    1   'DO YOU LIKE TO ASSIGN THE SYMBOL(S) YOURSELF?')
6053    FORMAT(A1)
      END
C
C       *       *       *       *       *       *       *
C
      SUBROUTINE ONED(MXNPTS,NPTS,NC,Y)
C
C                                          Coded October 13, 1977
C                                                by W.-L. Chiang
C       This subroutine rearrange the data in the
C (MXNPTSxMAXNC) matrix Y into a 1-D array so that, after
C returning to the main program, the data will be stored in
C an (NPTSxNC) matrix.
C
C       Called by MAIN
C REAL  Y(*,*)
C INTEGER(dummy)         I, N
C INTEGER        I1, I2, MXNPTS, NC, NPTS
C
        DIMENSION Y(1)
        I1      =NPTS
        DO  10 N=2,NC
          I2    =MXNPTS*(N-1)
          DO 10 I=1,NPTS
            I1  =I1+1
            I2  =I2+1
10          Y(I1)       =Y(I2)
        RETURN
      END
C
C       *       *       *       *       *       *       *
C
      SUBROUTINE PLOTS(BOTTOM,CENTER,NC,NPTS,PDATA,SCALE,
    1          TITLE,VLARGE,X,XNAME,Y,YSIZE,YNAME,YSYMBL)
```

```
C
C                                          Coded by W.-L. Chiang
C                                          Revised June 24, 1979
C
C Definition of Symbols:
C
C ALINE = A line to be printed
C BOTTOM= A logic variable.  The x-axis will be fixed along
C         the bottom line of graph if this variable = 'Y.'
C CENTER= A logic variable.  The x-axis will be fixed along
C         the center line of the graph if this variable =
C         'Y.'  If neither BOTTOM nor CENTER = 'Y,' the axis
C         will be set at an optimum position such that the
C         maximum and minimum of data stand symetric to the
C         center line.
C DRHO  = Dimension of RHO
C NC    = No. of Y-curves
C NPTS  = Nummber of data points in each array
C PDATA = A logic variable.  Print data if PDATA = 'Y.'
C RHO   = Vector of available round-uped numbers
C SCALE = Scale factor, units of Y-values per inch of print-
C         out
C TITLE = Title of the graph
C         (up to 120 characters, including spaces)
C X     = Vector of length NPTS to be plotted on x-axis
C         (in equal increments)
C XNAME = Name of X-curve (no more than 30 characters,
C         including spaces)
C Y     = A NPTSxNC matrix (YN,N) where YN is vector of the
C         nth curve
C YSIZE = Length of y-axis, in inches
C YNAME = Names of Y-curves
C         (no more than 30 characters each)
C YSYMBL= Symbols to be plotted for Y-curves, in FORMAT (A1)
C         (vector of length NC)
C VLARGE= A very large constnat set in a data statement of
C         the main program
C
C Subprograms referenced:  ABS, ALG10, EXIT, FLOAT, INT, MOD
C Called by MAIN
C CHARACTER*1   ALINE(*), AMINUS, AXIS, BLANK, BOTTOM,
C       CENTER, EQUAL, PDATA, QUES, YSYMBL(*)
C CHARACTER*4   TITLE(*), XNAME(*), YNAME(*,*)
C REAL  FACTOR, R, RANGE, RHO(*), RLOG, SCAL, SCALE,
C       TOP, TS, VLARGE, X(*), XMAX,
C       Y(*,*), YO, YLOG, YMAX, YMIN, YSIZE
C INTEGER(dummy)          I, J, K, L, N
C INTEGER       IJ(*), JI, JYO, KTOP, NAXIS, NC, NLINE,
C               NLINEP, NLNHP1, NPTS, NQUES, NRHO
```

```
      CHARACTER*1     ALINE(122), AMINUS, AXIS, BLANK,
     1          BOTTOM, CENTER, EQUAL, PDATA, QUES,
     2          YSYMBL(NC)
      DIMENSION  RHO(6), TITLE(24), X(NPTS),
     1  XNAME(8), Y(NPTS,NC), YNAME(8,NC)
      DIMENSION  IJ(10)
C
      DATA  AMINUS/'-'/, AXIS/'I'/, BLANK/' '/,
     1          EQUAL/'='/, NRHO/6/, QUES/'?'/,
     2          RHO/1., 2., 2.5, 4., 5., 8./
C
C       All "CCC's" must be removed if this subroutine is to
C be called by any program other than the conversational
C main program "PLOT."
C
CCC     DATA  MAXPTS/3001/
CCC     OPEN (UNIT=63, NAME='PLOTO')
CCC       IF (NC .EQ. 1) GO TO 40
CCC     CALL    ONED(MXNPTS,NPTS,NC,Y)
CCC40   CONTINUE
C
C NLINE = Total number of the spaces along a Y-line
C NLINEP= NLINE plus 1
C NLNHP1= Half of 'NLINE' plus 1
C The const. 10 here is the number of spaces per inch for
C the output
C
      NLINE   =YSIZE*10+1.5
      NLINEP  =NLINE+1
      NLNHP1  =NLINE/2+1
C
C Factorize X-data
C FACTOR=Factor to be multiplied to the printed X-values
C XMAX  =Max. of the abs. values of X-data
C
      XMAX    =ABS( X(NPTS) )
        IF ( XMAX .LT. ABS( X(1) ) )      XMAX=ABS( X(1) )
      FACTOR  =10.**INT(ALOG10(XMAX))
        IF (FACTOR .LT. 1.)       FACTOR=FACTOR/10.
      DO  70 I=1,NPTS
70      X(I)  =X(I)/FACTOR
C
C Find range of data to be plotted
C YMAX  = Max. of all Y-values, if CENTER.NE.'Y'
C       = Max. of abs. values of all Y-data, if CENTER='Y'
C YMIN  = Min. of all y-values
C
      YMAX    =Y(1,1)
      YMIN    =1.E37
```

```
        DO 100 N=1,NC
          IJ(N) =1
          DO 100 I=1,NPTS
              IF (Y(I,N) .LT. YMIN) GO TO 95
              IF (Y(I,N) .GT. YMAX) YMAX=Y(I,N)
            GO TO 100
95          YMIN        =Y(I,N)
100         CONTINUE
          IF (YMAX .EQ. YMIN) GO TO 1101
          IF (CENTER .EQ. 'Y') GO TO 104
          IF (BOTTOM .EQ. 'Y') GO TO 106
        RANGE   =YMAX-YMIN
        GO TO 200
104       IF (SCALE.LT.VLARGE) GO TO 211
          IF (-YMIN .GT. YMAX)      YMAX=-YMIN
        RANGE   =YMAX+YMAX
        GO TO 200
106       IF (SCALE.LT.VLARGE) GO TO 211
        RANGE   =YMAX
C
C Calculate optimal scale factor
C
C If opt. scale without rounding up is preferred, replace
C this section by
C       SCALE   =RANGE/NLINE
C and   SCAL    =SCALE/10.
C
C KTOP  = A ceiling value
C RANGE = Range of all Y-values
C SCAL  = Scale factor per character width
C TS    = Trial value of scale
C
200     YLOG    =ALOG10(RANGE/YSIZE)
        DO 210 K=1,NRHO
          RLOG  =ALOG10(RHO(K))
          TOP   =YLOG-RLOG
          KTOP  =TOP
            IF (TOP .GE. 0.  .AND.  FLOAT(KTOP) .NE. TOP)
     1                                                 KTOP=KTOP+1
          TS    =RHO(K)*10.**KTOP
            IF (SCALE .GT. TS)      SCALE=TS
210       CONTINUE
211     SCAL    =SCALE/10
C
C Find position of x-axis
C
C NAXIS = No. of x-axis.  In other words, print x-axis if
C           NAXIS=1.
```

```
C JYO    = Positin of the x-axis, in number of characters,
C          counted from the bottom (includes)
C YO     = Positin of the x-axis, in number of characters
C          (in this section only), counted from the center
C
           IF (CENTER .NE. 'Y') GO TO 300
         JYO      =NLNHP1
         GO TO 330
300        IF (BOTTOM .NE. 'Y') GO TO 310
         JYO      =1
         GO TO 330
310      YO       =(RANGE*.5-YMAX)/SCAL
           IF (YO .GE. 0.) GO TO 320
         YO       =YO-.5
         GO TO 321
320      YO       =YO+.5
321      JYO      =NLNHP1+YO
         NAXIS    =0
           IF (JYO .GE. 1  .AND.  JYO .LE. NLINE)    NAXIS=1
         GO TO 600
330      NAXIS    =1
C
C Write heading and top of plot
C
C YO     = Position of the x-axis, in inches (in this section
C          only), counted from the center
C
600      WRITE(63,5600) TITLE
         WRITE(63,611) XNAME
611        FORMAT(15X'CURVE - (I.E., X-AXIS) = '8A4)
         DO 620 N=1,NC
620        WRITE(63,621) YSYMBL(N), (YNAME(L,N), L=1,8)
621          FORMAT(30X'CURVE 'A1' = '8A4)
           IF (JYO .EQ. NLNHP1) GO TO 632
           IF (JYO .EQ. 1) GO TO 634
         YO       =YO/10
         WRITE(63,631) YO
631        FORMAT(22X'ORIGIN FOR PLOT ='F5.1
     1           ' INCHES FROM THE CENTER OF Y-AXIS')
         GO TO 640
632      WRITE(63,633)
633        FORMAT(22X'ORIGIN FOR PLOT = CENTER OF Y-AXIS')
         GO TO 640
634      WRITE(63,635)
635        FORMAT(22X'ORIGIN FOR PLOT = BOTTOM OF Y-AXIS')
640      WRITE(63,641) SCALE, XNAME
641        FORMAT(14X'SCALE FACTOR FOR Y-DATA = 'G10.2
     1           ' DATA UNITS PER INCH'//1X,8A4)
         WRITE(63,5643) FACTOR
```

```
          IF (YSIZE .GT. 6.) GO TO 668
          IF (BOTTOM .EQ. 'Y') GO TO 650
        WRITE(63,649)
649       FORMAT(7X, 2H-3, 8X, 2H-2, 8X, 2H-1, 9X, 1HO, 9X,
     1           1H1, 9X, 1H2, 9X, 1H3)
        GO TO 655
650     WRITE(63,651)
651       FORMAT(8X'0'9X'1'9X'2'9X'3'9X'4'9X'5'9X'6')
655     WRITE(63,5650)
        GO TO 749
668       IF (BOTTOM .EQ. 'Y') GO TO 670
        WRITE(63,669)
669       FORMAT(7X'-6'8X'-5'8X'-4'8X'-3'8X'-2'8X,2H-1,9X,
     1           1HO,9X,1H1,9X,1H2,9X,1H39X'4'9X'5'9X'6')
        GO TO 675
670     WRITE(63,671)
671       FORMAT(8X'0'9X'1'9X'2'9X'3'9X'4'9X'5'9X'6'9X'7'9X
     1           '8'9X'9'8X'10'8X'11'8X'12')
675     WRITE(63,5670)
C
749     DO 750 J=1,NLINE
750       ALINE(J) =BLANK
        ALINE(NLINEP)   =AMINUS
          IF (NAXIS .EQ. 1)      ALINE(JYO)=AXIS
C
C Loop through for each pt.
C
        NQUES   =0
        DO 850 I=1,NPTS
          DO 800 N=1,NC
            JI   =(Y(I,N)/SCAL+.5)+JYO
              IF (JI .GE. 1) GO TO 770
            NQUES         =1
            ALINE(1)=QUES
            IJ(N)         =1
            GO TO 800
770           IF (JI .LE. NLINE) GO TO 780
            NQUES         =1
            ALINE(NLINE)          =QUES
            IJ(N)         =NLINE
            GO TO 800
780           IF (ALINE(JI).EQ.BLANK .OR. ALINE(JI).EQ.AXIS)
     1                                                 GO TO 790
            ALINE(JI)     =EQUAL
            GO TO 800
790         ALINE(JI)     =YSYMBL(N)
            IJ(N)         =JI
800         CONTINUE
            IF (MOD(I-1,5) .EQ. 0) GO TO 820
```

```
            WRITE(63,815) (ALINE(J), J=1,NLINEP)
 815          FORMAT(7X'-'122A1)
            GO TO 830
 820        WRITE(63,821) X(I), (ALINE(J), J=1,NLINEP), AMINUS
 821          FORMAT(1XF6.3'-'123A1)
 830        DO 840 N=1,NC
              JI   =IJ(N)
 840          ALINE(JI)   =BLANK
              IF (NAXIS .EQ. 1)      ALINE(JYO)=AXIS
 850        CONTINUE
 C
            IF (YSIZE .GT. 6.) GO TO 860
          WRITE(63,5650)
          GO TO 870
 860      WRITE(63,5670)
 870      WRITE(63,5643) FACTOR
            IF (NQUES .EQ. 0) GO TO 950
          WRITE(63,900)
 900        FORMAT(//10X'NOTE:  THE QUESTION MARK, ?,'
     1      ' INDICATES THAT THE DATA POINT IS OUT OF RANGE.')
 950        IF (PDATA .NE. 'Y')      RETURN
          WRITE(63,5951) XNAME(1), XNAME(2), XNAME(3),
     1                     (YNAME(1,N), YNAME(2,N),N=1,NC)
          WRITE(63,5643) FACTOR
          DO 960 I=1,NPTS
 960        WRITE(63,5960) X(I), (Y(I,N), N=1,NC)
        RETURN
 C
 C Error
 C
 1101     TYPE 1102, YMAX, YMIN
 1102       FORMAT(///' ARE YOU SERIOUS?'
     1      ' ALL Y-VALUES YOU GAVE ME ARE EQUAL TO 'E10.3'.'/
     2      ' IT IS NO FUN TO PLOT A STRAIGHT LINE Y ='E10.3
     3      '.'/' I QUIT!')
          CALL EXIT
 C
 C Format
 C
 5600     FORMAT(8X30A4//)
 5643     FORMAT(' (X '1PE6.0')')
 5650     FORMAT(8X6('I'9('.'))'I')
 5670     FORMAT(8X12('I'9('.'))'I')
 5951     FORMAT(1H1,13(1X2A4,A1))
 5960     FORMAT(1X1P13E10.3)
 C
        END
```

B.3 Program To Plot Flow Patterns with a CalComp Plotter

```
//* UCC SERVICE=DELAYED
// EXEC FORTGCG,RG=160K,TIME=2
C
C                                                  CODED BY W.-L. CHIANG
C                                                REVISED APRIL 20, 1979
C
C        THIS PROGRAM WAS WRITTEN IN FORTRAN IV TO BE RUN BY
C  IBM 370/158 MVS IN UNIVERSITY COMPUTING CENTER, UNIVER-
C  SITY OF SOUTHERN CALIFORNIA.
C
C  I   FOR NO. OF CLOSED-BOUNDARY LINES
C  J   FOR MISCELLANEOUS
C  K   FOR NO. OF FIGS.
C  L   FOR NO. OF COMPUTATIONAL PTS.
C  M   FOR X-DIRECTION GRID PTS.
C  N   FOR Y-DIRECTION GRID PTS.
C
C  AFSIZ   ACTUAL FIG. SIZE(Y-DIRECTION), IN IN.
C  APSIZ   ACTUAL PLOT SIZE(Y-DIRECTION), OR,
C          WIDTH OF PAPER, IN IN.
C  ASBF    ACTUAL SPACING BETWEEN FIGS.(Y-DIRECTION), IN IN.
C  ASBP    ACTUAL SPACING BETWEEN PAGES(X-DIRECTION), IN IN.
C  AXMAX   ACTUAL MAX. FOR X-AXIX, OR, LIMIT SIZE IN X-DIR.,
C          IN IN.
C  AYMAX   ACTUAL MAX. FOR Y-AXIX, OR, LIMIT SIZE IN Y-DIR.,
C          IN IN.
C  DX      GRID SPACING, IN FIG. UNITS,
C          DX=1 IN THIS PROGRAM
C  DYSS    DIFF. OF Y-COORDINATES BN. 2 SCALES, IN FIG. UNIT
C  FALNTH  FIGURE LENGTH OF NORTH ARROW IN FIGURE UNITS
C  FCTR    SIZE PER FIG. UNIT, IN IN.
C  FHSL    FIG. HT. OF SCALE LETTERS
C  FHSN    FIG. HT. OF SCALE NUMBERS
C  FHSTTL  FIG. HT. OF SUBTITLE, TIME LEBEL, AND STATE
C  HLSTTL  HALF THE LENGTH OF SUBTITEL, IN FIG. UNIT
C  VGRIDR  RATIO OF VEL., IN ITS UNIT, TO GRID SPACING, IN
C          ITS UNIT
C  VRATIO  RATIO OF VEL. VECTORS IN FIG. UNIT TO VEL. VALUES
C          IN THEIR UNIT
C  XNORTH  X-COOR. FOR THE SOUTH END OF N-ARROW
C  XLC     X-COOR. OF THE CENTER OF LEGEND
C  XSL     X-COOR. OF 1ST (LENGTH) SCALE LETTER
C  XSS     STARTING X-COOR. OF (LENGTH) SCALE LINE
C  XST     X-COOR. OF STATE LEBEL
C  XSVL    X-COOR. OF 1ST VEL. SCALE LETTER
C  XSVS    X-COOR. OF VEL. SCALE LINE
```

```
C   XTL      X-COOR. OF TIME LETTERS
C   XTN      X-COOR. OF TIME NUMBER
C   YNORTH   Y-COORDINATE FOR THE SOUTH END OF N-ARROW
C   YSL      Y-COOR. OF (LENGTH) SCALE LETTERS
C
C        SUBPROGRAMS REFERENCED:  BRY, SCAL, BLOCK DATA, AND
C   CALCOMP SUBROUTINES.
C
      REAL*8  STATE1(20), STATE2(20), TITLE(9)
      DIMENSION  CBX(113,9), CBY(113,9), MAP(69,108),
     *  OBX(5,1), OBY(5,1),
     *  BXP(113), BYP(113),
     *  KPLOT(20), NPCB(9), NPOB(1),
     *  SUBTTL(5), U(4696), V(4696)
      COMMON/MB/  MAXNP, MAXNP2
      COMMON/BMS/  VSCLU(4),      FHSN
      COMMON/MS/  QFHSN, XSS
C
C   DATA
C
      MAXNP   =111
      MAXNP2  =MAXNP+2
C
      DATA  KPLOT/1, 2, 3, 4, 5, 6, 7, 8, 9, 10,
     *  0, 12, 13, 14, 15, 16, 17, 18, 19, 20/
      DATA  AFSIZ/11./, AHMIN/.007/, ANGNTH/66.5/,
     *  APSIZ/11./, ASBF/1./, ASBP/2./, AXMAX/9./,
     *  AYMAX/5./, DYS1/.5/, DYS2/1./, DYS3/1.5/, DYS4/2.6/,
     *  DYSS/6./, FALNTH/14./, FHSL/.8/, FHSTTL/1.5/,
     *  MAXK/20/, MAXM/108/, MAXN/69/, MAXNCB/9/,
     *  MAXNCP/4696/,
     *  STATE1/' (FLOODI', '   (HIGH', '  (EBBIN',
     *         '    (LOW ', ' ',
     *         ' (FLOODI', '   (HIGH', '  (EBBIN',
     *         '    (LOW ', ' ',
     *         ' (FLOODI', '   (HIGH', '  (EBBIN',
     *         '    (LOW ', ' ',
     *         ' (FLOODI', '   (HIGH', '  (EBBIN',
     *         '    (LOW ', ' '/,
     *  STATE2/'NG TIDE)', ' TIDE)', 'G TIDE)','TIDE)',' ',
     *         'NG TIDE)', ' TIDE)', 'G TIDE)','TIDE)',' ',
     *         'NG TIDE)', ' TIDE)', 'G TIDE)','TIDE)',' ',
     *         'NG TIDE)', ' TIDE)', 'G TIDE)','TIDE)',' '/,
     *  VRATIO/2./, XNORTH/65./, YNORTH/53./
C
C   BOUNDARY CONDITIONS
C
      READ (1,6002) NCB
      WRITE(6,6002) NCB
```

```
      IF (NCB .EQ. 0) GO TO 20
      IF (NCB .GT. MAXNCB) GO TO 3001
      J1        =1-MAXNP2
      JA        =J1
      DO  10 I=1,NCB
10    CALL      BRY(CBX, CBY, I, J1, NPCB)
      CALL      BRY(OBX, OBY, 1, JA, NPOB)
      READ (2,6002) NCP, MMAX, NMAX
      WRITE(6,6002) NCP, MMAX, NMAX
      IF (NCP .GT. MAXNCP) GO TO 3002
      IF (MMAX .GT. MAXM  .OR.  NMAX .GT. MAXN) GO TO 3003
      IF (MMAX.LT.10) GO TO 3004
      READ (2,6025) ((MAP(N,M), N=1,NMAX), M=1,MMAX)
C
C  READ DATA
C
20    READ (5,6000) TITLE
      WRITE(6,6000) TITLE
      READ (5,6001) DL, DT
      WRITE(6,6001) DL, DT
C
C  CONSTANTS
C
      FCTR     =AMIN1( AFSIZ/NMAX, AXMAX/MMAX, AYMAX/NMAX )
C
      AHMIN    =AHMIN/FCTR
      ANGN     =ANGNTH-90.
      ANGNTH   =ANGNTH*3.14159265329/180.
      FHSTL2   =FHSTTL+FHSTTL
      FSBP     =ASBP/FCTR
      FSBF     =ASBF/FCTR
      HLSTTL   =FHSTTL*20.*.5
      MMAXM1   =MMAX-1
      NMAXM1   =NMAX-1
      QFHSN    =FHSN*.25
      SCLNG    =3000./DL
      SCLNG3   =SCLNG/3.
      VSCLNG   =VRATIO*3.
      XLC      =MMAX-HLSTTL
      XNTIP    =FALNTH * COS(ANGNTH) + XNORTH
      XSL      =XLC-FHSL*9.5
      XSS      =XLC-SCLNG*.5
      XST      =XLC-FHSTTL*8.
      XSTTL    =XLC-HLSTTL
      XSVL     =XLC-FHSL*10.5
      XSVS     =XLC-VSCLNG*.5
      XTL      =XLC-FHSTTL*7.
      XTN      =XTL+FHSTTL*6.
      Y0       =APSIZ/FCTR+FSBF
```

```
      YNTIP    =FALNTH * SIN(ANGNTH) + YNORTH
      YNMAX    =NMAX
      YSTTL    =YNMAX-FHSTTL-1.
      YTL      =YSTTL-FHSTL2
C
      AHLNTH   =FALNTH*.3
      FSIZP    =FSBF+YNMAX
      YOO      =YO-FSIZP
      YST      =YTL-FHSTL2
      YSL      =YST-DYSS-DYSS
      YS1      =YSL-DYS1
      YS2      =YSL-DYS2
      YS3      =YSL-DYS3
      YS4      =YSL-DYS4
      YSV1     =YS1-DYSS
      YSV2     =YS2-DYSS
      YSV3     =YS3-DYSS
      YSV4     =YS4-DYSS
      YSVL     =YSL-DYSS
C
C   PLOT TITLES AND CONSTANTS
C
      CALL     PINIT(21)
      CALL     SYMBOL(0., 0., .14, TITLE, 90., 72)
      CALL     SYMBOL(.21, 0., .14,
     1                        'VRATIO =                FCTR =
     2DL =      FT           DT =      SEC', 90., 74)
      CALL     NUMBER(.21, .14*9., .14, VRATIO, 90., 5)
      CALL     NUMBER(.21, .14*31., .14, FCTR, 90., 3)
      CALL     NUMBER(.21, .14*46., .14, DL, 90., -1)
      CALL     NUMBER(.21, .14*67., .14, DT, 90., -1)
      CALL     PLOT(ASBP, APSIZ, -3)
      CALL     FACTOR(FCTR)
C
C   READ CIRCULATION DATA
C
      IK       =1
      K        =0
30    READ (5,6030,END=990) SUBTTL, TIME
      WRITE(6,6030) SUBTTL, TIME
      IF (K.GE.MAXK) GO TO 3032
      IF (TIME.LT..9) GO TO 3040
      READ (5,6040) (U(L), V(L), L=1,NCP)
      K        =K+1
      IF ( K.NE.KPLOT(IK) ) GO TO 30
      WRITE(6,40) IK
40    FORMAT(20X,'PLOT',I3)
```

```
C
C  NEW ORIGIN
C
      IK       =IK+1
      IF (YO .LT. YNMAX) GO TO 140
      CALL     PLOT(O., -YNMAX, -3)
      YO       =YO-FSIZP
      GO TO 150
140   CALL     PLOT(FSBP+MMAX, YOO-YO, -3)
      YO       =YOO
C
C  OPEN BOUNDARY
C
150   IF (NCB .EQ. O) GO TO 200
      CALL     PLOT(OBX(1,1), OBY(1,1), 3)
      NPI      =NPOB(1)
      DO 160 J=2,NPI
160   CALL     DASHP(OBX(J,1), OBY(J,1), .5)
C
C  SOLID BOUNDARIES
C
      DO 190 I=1,NCB
      NPI      =NPCB(I)
      NPP2     =NPI+2
      DO 180 J=1,NPP2
      BXP(J)   =CBX(J,I)
180   BYP(J)   =CBY(J,I)
190   CALL     LINE(BXP, BYP, NPI, 1, O, O)
C
C  PLOT VELOCITY VECTORS
C
200   DO 210 M=2,MMAXM1
      DO 210 N=2,NMAXM1
      NM       =MAP(N,M)
      IF (NM.EQ.O) GO TO 210
      NM1M     =MAP(N-1,M)
      IF (NM1M.EQ.O) GO TO 210
      NMM1     =MAP(N,M-1)
      IF (NMM1.EQ.O) GO TO 210
      UF       =U(NM)*VRATIO
      VF       =V(NM)*VRATIO
      AHLEN    =SQRT(UF*UF+VF*VF)*.4
      IF (AHLEN .LE. AHMIN) GO TO 210
      X        =M
      Y        =N
      CALL     AROHD(X, Y, X+UF, Y+VF, AHLEN, O., 14)
210   CONTINUE
```

```
C
C  PLOT NORTH ARROW, SUBTITLE, TIME, AND STATE
C
      CALL    AROHD(XNORTH, YNORTH, XNTIP, YNTIP, AHLNTH,
     *              0., 13)
      CALL    SYMBOL(XNTIP-.4, YNTIP+.8, 2., 'N', ANGN, 1)
      CALL    SYMBOL(XSTTL, YSTTL, FHSTTL, SUBTTL, 0., 20)
      CALL    SYMBOL(XTL, YTL, FHSTTL, 'TIME:       HR.',
     *              0., 15)
      CALL    NUMBER(XTN, YTL, FHSTTL, TIME, 0., 2)
      CALL    SYMBOL(XST, YST, FHSTTL, STATE1(K), 0., 8)
      CALL    SYMBOL(XLC, YST, FHSTTL, STATE2(K), 0., 8)
C
C  PLOT SCALES
C
      CALL    SYMBOL(XSL, YSL, FHSL, 'SCALE IN 1,000 FEET',
     *              0., 19)
      CALL    SYMBOL(XSVL, YSVL, FHSL,
     *              'VELOCITY SCALE IN FPS', 0., 21)
      CALL    SCAL( SCLNG3, SCLNG, XSS, YS1, YS2, YS3, YS4)
      CALL    SCAL( VRATIO,VSCLNG,XSVS,YSV1,YSV2,YSV3,YSV4)
      IF (YO .LT. YNMAX) GO TO 220
      CALL    PLOT(0., -FSBF, -3)
220   IF ( KPLOT(IK).NE.0 ) GO TO 30
C
C  STOP
C
990   CALL    ENPLT(4.+MMAX, 0.)
999   STOP
C
C  ERROR
C
3001  WRITE(6,9001)
9001  FORMAT(///' ???NCB EXCEEDED DIMENSION.???')
      GO TO 999
3002  WRITE(6,9002)
9002  FORMAT(///' ???NCP EXCEEDED DIMENSION.???')
      GO TO 999
3003  WRITE(6,9003)
9003  FORMAT(///' ???MMAX OR NMAX EXCEEDED DIMENSION.???')
      GO TO 999
3004  WRITE(6,9004)
9004  FORMAT(///' ???MMAX.GT.10???')
      GO TO 999
3032  WRITE(6,9032) K, MAXK
9032  FORMAT(///' ???K, MAXK =',2I5)
      GO TO 990
3040  WRITE(6,9040) TIME
9040  FORMAT(///' ???TIME =',F10.2)
```

```
      GO TO 990
C
C  FORMAT
C
6000  FORMAT(1X9A8)
6001  FORMAT(7F10.2)
6002  FORMAT(3I5)
6025  FORMAT(1X17I4)
6030  FORMAT(5A4/1X,F10.2)
6040  FORMAT(1X,10F6.3)
      END
C
C       *       *       *       *       *       *       *
C
      SUBROUTINE BRY(BX, BY, I, J1, NP)
C
      DIMENSION  BX(1), BY(1),     NP(1)
      COMMON/MB/  MAXNP, MAXNP2
C
      READ (1,6002) NPI
      WRITE(6,6002) NPI
      IF (NPI .GT. MAXNP) GO TO 3003
      IF (NPI.LE.0) GO TO 3003
      J1       =J1+MAXNP2
      J2       =J1+NPI-1
      READ (1,6001) (BX(J), J=J1,J2)
      WRITE(6,6001) (BX(J), J=J1,J2)
      READ (1,6001) (BY(J), J=J1,J2)
      WRITE(6,6001) (BY(J), J=J1,J2)
C
      J2        =J2+1
      BX(J2) =0.
      BY(J2) =0.
      J2        =J2+1
      BX(J2) =1.
      BY(J2) =1.
      NP(I)    =NPI
C
      RETURN
C
3003  WRITE(6,9003) NPI
9003  FORMAT(///' ???NPI EXCEEDED DIMENSION?  OR .LE. 0???'/
     1        ' NPI =', I10)
      STOP
C
6001  FORMAT(7F10.2)
6002  FORMAT(2I5)
      END
```

```
C
C       *       *       *       *       *       *       *
C
      SUBROUTINE SCAL( SCLNG3, SCLNG, A, YS1, YS2, YS3, YS4)
      COMMON/BMS/  VSCLU(4),       FHSN
      COMMON/MS/   QFHSN, XSS
      Z          =A+SCLNG
      CALL       PLOT(A, YS3, 3)
      CALL       PLOT(Z, YS3, 2)
      CALL       PLOT(Z, YS1, 2)
      X          =(Z-A)*2./3.+A
      CALL       PLOT(X, YS1, 3)
      CALL       PLOT(X, YS3, 2)
      X          =(X+A)*.5
      CALL       PLOT(X, YS3, 3)
      CALL       PLOT(X, YS1, 2)
      D          =(X-A)*.1
      DO 240 J=1,9
      X          =X-D
      CALL       PLOT(X, YS2, 3)
240   CALL       PLOT(X, YS3, 2)
      CALL       PLOT(A, YS3, 3)
      CALL       PLOT( A, YS1, 2)
      X          =XSS-QFHSN
      DO 260 J=1,4
      CALL       SYMBOL(X, YS4, FHSN, VSCLU(J), 0., 1)
260   X          =X+SCLNG3
      RETURN
      END
C
C       *       *       *       *       *       *       *
C
      BLOCK DATA
      COMMON/BMS/  VSCLU(4),       FHSN
      DATA  FHSN/.8/, VSCLU/'1', '0', '1', '2'/
      END
C
C       *       *       *       *       *       *       *
C
//GO.FT05F001 DD DSN=LECJ010.ECJ01.BASERUN.VEL.DATA,DISP=OLD
//GO.FT01F001 DD DSN=LECJ010.ECJ01.BOUNDARY.DATA,DISP=OLD
//GO.FT02F001 DD DSN=LECJ010.ECJ01.MAP.DATA,DISP=OLD
//GO.FT21F001 DD SYSOUT=X,
// DCB=(LRECL=504,BLKSIZE=3156,RECFM=VBS)
```